



Abdul Shakoor  
Kerry Cato *Editors*

# IAEG/AEG Annual Meeting Proceedings, San Francisco, California, 2018— Volume 2

Geotechnical and Environmental  
Site Characterization



 Springer

---

IAEG/AEG Annual Meeting Proceedings,  
San Francisco, California, 2018—Volume 2

---

Abdul Shakoor • Kerry Cato  
Editors

# IAEG/AEG Annual Meeting Proceedings, San Francisco, California, 2018—Volume 2

Geotechnical and Environmental Site  
Characterization



 Springer

*Editors*

Abdul Shakoor  
Department of Geology  
Kent State University  
Kent, OH, USA

Kerry Cato  
Department of Geological Sciences  
California State University  
San Bernardino, CA, USA

ISBN 978-3-319-93126-5      ISBN 978-3-319-93127-2 (eBook)  
<https://doi.org/10.1007/978-3-319-93127-2>

Library of Congress Control Number: 2018947486

© Springer Nature Switzerland AG 2019

This work is subject to copyright. All rights are reserved by the Publisher, whether the whole or part of the material is concerned, specifically the rights of translation, reprinting, reuse of illustrations, recitation, broadcasting, reproduction on microfilms or in any other physical way, and transmission or information storage and retrieval, electronic adaptation, computer software, or by similar or dissimilar methodology now known or hereafter developed.

The use of general descriptive names, registered names, trademarks, service marks, etc. in this publication does not imply, even in the absence of a specific statement, that such names are exempt from the relevant protective laws and regulations and therefore free for general use.

The publisher, the authors and the editors are safe to assume that the advice and information in this book are believed to be true and accurate at the date of publication. Neither the publisher nor the authors or the editors give a warranty, express or implied, with respect to the material contained herein or for any errors or omissions that may have been made. The publisher remains neutral with regard to jurisdictional claims in published maps and institutional affiliations.

Cover illustration: Golden Gate Bridge at night. Frederic Prochasson © 123rf.com

This Springer imprint is published by the registered company Springer Nature Switzerland AG  
The registered company address is: Gewerbestrasse 11, 6330 Cham, Switzerland

---

## Preface

The XIII IAEG Congress and 61st AEG Annual Meeting, San Francisco, USA, chose *Engineering Geology for a Sustainable World* as the theme for 2018. Based on the topical symposia and technical sessions, the proceedings are organized into six volumes and sub-categories as follows:

Volume 1: Slope Stability: Case Histories, Landslide Mapping, Emerging Technologies

Volume 2: Geotechnical and Environmental Site Characterization

Volume 3: Mining, Aggregates, Karst

Volume 4: Dams, Tunnels, Groundwater Resources, Climate Change

Volume 5: Geologic Hazards: Earthquakes, Land Subsidence, Coastal Hazards, and  
Emergency Response

Volume 6: Advances in Engineering Geology: Education, Soil and Rock Properties, Modeling

Participants of this joint meeting had the option to submit either a full paper or only an abstract. The editors would like to thank the authors for their valuable contributions. One hundred eighty-six full papers were submitted for review, and 153 papers successfully completed the process. Each paper submitted for the Proceedings was peer-reviewed by two reviewers. Authors revised their papers in accordance with reviewers' comments. The reviewers, from across the globe, included professional experts as well as authors of other papers. The editors greatly appreciate the help provided by the reviewers. A list of reviewers follows.

The editors are also very grateful to Karen Smith and Paisley Cato for their assistance throughout the review process.

Kent, OH, USA  
San Bernardino, CA, USA  
2018

Abdul Shakoor  
Kerry Cato

---

# Organization

## **General Meeting Chairs**

Sarah Kalika, Cornerstone Earth Group  
Gary Luce, Resource Concepts, Inc.  
Coralie Wilhite, United States Army Corps of Engineers

## **Field Course Chairs**

Chase White, California Geological Survey  
Drew Kennedy, Sage Engineers

## **IAEG Planning Committee Heads**

Scott Burns, Portland State University  
Jeffrey R. Keaton, Wood

## **Proceedings Editors**

Abdul Shakoor, Kent State University  
Kerry Cato, Cato Geoscience, Inc./California State University, San Bernardino

## **Editorial Assistants**

Karen Smith, Kent State University  
Paisley Cato, Cato Geoscience, Inc.

## **Short Course Chairs**

E. Morley Beckman, Kleinfelder  
Byron Anderson, Kleinfelder  
Chrissey Villeneuve, Shannon & Wilson, Inc.

## **Technical Program Committee**

Abdul Shakoor, Kent State University  
Kerry Cato, Cato Geoscience, Inc./California State University, San Bernardino  
William Godwin, Consulting Geologist  
Sarah Kalika, Cornerstone Earth Group

## **Symposium Chairs**

Robert E. Tepel, Retired Professional Geologist and Certified Engineering Geologist  
Brian H. Greene, United States Army Corps of Engineers  
Donald Bruce, Geosystems, L.P.  
Holly Nichols, California Department of Water Resources  
Keith Turner, Colorado School of Mines  
Fred Baynes, Consulting Engineering Geologist  
Kevin McCoy, Colorado Geological Survey

Hilary Whitney, Environmental Resources Management  
Michelle Sneed, United States Geological Survey  
Thomas Oommen, Michigan Technological University  
Julien Waeber, AECOM  
Ed Medley, Consulting Geological Engineer  
Mark Bailey, Asbestos TEM Labs  
Atiye Tugrul, Istanbul University, Avcilar Campus, Turkey  
Lindsay Swain, Dudek  
Ike Isaacson, Brierley Associates  
Mike Piepenburg, Aldea Services, LLC  
Bruce Hilton, Kleinfelder  
Anne Rosinski, California Geological Survey  
Steve Parry, Parry Engineering Geological Services  
Jan Novotny, Ceska Geologicka Sluzba, Czech Republic  
Xiaolei Liu, Shandong Provincial Key Laboratory of Marine Environment and Geological Engineering (Ocean University of China), China

### **Field Course Leaders and Contributors**

William Godwin, Consulting Geologist  
William McCormick, Kleinfelder  
Bradley Erskine, Kleinfelder  
Marina Mascorro, Langan  
Frank Rollo, Rollo & Ridley  
John Egan, Sage Engineers  
Ken Johnson, WSP  
John Wallace, Cotton, Shires and Associates, Inc.  
Ryan Seelbach, Geosyntec  
Tom Barry, California Department of Conservation, Division of Oil, Gas and Geothermal Resources  
John Wakabayashi, Fresno State University  
Greg Stock, Yosemite National Park  
Janet Sowers, Fugro  
Jim Lienkaemper, United States Geological Survey  
Keith Kelson, United States Army Corps of Engineers  
Carol Prentice, United States Geological Survey  
Gordon Seitz, California Department of Conservation  
Chris Madugo, Pacific Gas & Electric Company  
Mike Jewett, Miller Pacific Engineers  
Ray Sullivan, San Francisco State University  
George Ford, Geosyntec  
Wayne Akiyama, APTIM  
Ryan Coe, Terracon  
Kate Zeiger, AECOM  
John Murphy, California State Water Resources Control Board  
Jennifer Gomez, Syar Industries  
Mike George, BGC Engineering  
Nick Sitar, University of California, Berkeley  
Peter Holland, California Geological Survey  
Chris Hundemer, C2earth  
Jake Hudson, Holdrege & Kull/NV5  
Shane Cummings, Holdrege & Kull/NV5  
Chris Hitchcock, InfraTerra  
Roxanne Renedo, BSK Associates  
Tim Dawson, California Department of Conservation

Margaret Doolittle, Kleinfelder  
Kevin Clahan, Lettis Consultants  
Donald Wells, AMEC/Foster Wheeler  
Jennifer Dean, California State Water Resources Control Board  
Felix Desperrier, Lettis Consultants  
Karen Grove, San Francisco State University

**Guest Tour Chairs**

Alice Tepel  
Linda Upp

**Publicity Committee**

Nathan Saraceno, DiGioia Gray & Associates  
Courtney Johnson, Sage Engineers  
Maggie Parks, ENGEO

**Sponsorship Chair**

Courtney Johnson, Sage Engineers

**Technical Session Editing**

Bill Yu, Case Western Reserve University

**Guidebook App**

Clayton Johnson, Golder Associates  
Nathan Saraceno, DiGioia Gray & Associates

**Fed IGS**

Jean-Louis Briaud, Texas A&M University

**K-12 Teacher Workshop**

Cynthia Pridmore, California Geological Survey

**Special Event**

E. Morley Beckman, Kleinfelder

**AEG Meeting Manager**

Heather Clark, Association of Environmental & Engineering Geologists

**AEG Headquarters**

AMR Management



---

## List of Reviewers

David Abbott, USA  
Biljana Abolmasov, Serbia  
Okechukwu Aghamelu, Nigeria  
M. Farooq Ahmed, Pakistan  
Paolo Allasia, Italy  
Priyanthi Amarasinghe, USA  
Sofia Anagnostopoulou, Greece  
Pedro Andrade, Portugal  
Luis Bacellar, Brazil  
Marco Baldo, Italy  
Elizabeth Beckman, USA  
Zbigniew Bednarczyk, Poland  
Eduardo Bergillos Navarro, Spain  
David Bieber, USA  
Candan BiLen, Turkey  
Andrée Blais-Stevens, Canada  
Peter Bobrowsky, Canada  
Nana Bolashvili, Georgia  
James Borchers, USA  
Anika Braun, Germany  
Stephanie Briggs, USA  
Luke Brouwers, United Arab Emirates  
Brian Bruckno, USA  
Matthias Brugger, Germany  
Fintan Buggy, Ireland  
Domenico Calcaterra, Italy  
Michael Carpenter, USA  
Kerry Cato, USA  
Andrea Cevasco, Italy  
Hannah Chapella, USA  
Xiaoli Chen, China  
Sibonakaliso Chiliza, South Africa  
Jeff Coe, USA  
Mike Collins, USA  
Brian Conway, USA  
Jasper Cook, UK  
Isabela Coutinho, Brazil  
John Cripps, UK  
Balázs Czinder, Hungary  
Ranjan Kumar Dahal, Nepal  
Jerome De Graff, USA  
Rachael Delaney, USA  
Artem Demenev, Russia

---

Diego Di Martire, Italy  
Matthys Dippenaar, South Africa  
Angelo Doglioni, Italy  
Anastasia Dorozhko, Russia  
Peter Ellecosta, Germany  
Selman Er, Turkey  
Olga Eremina, Russia  
Georg Erharter, Austria  
Moises Failache, Brazil  
Andrew Farrant, UK  
Zhen Feng, China  
Clark Fenton, New Zealand  
Maria Ferentinou, South Africa  
Kenneth Ferguson, USA  
Isabel Fernandes, Portugal  
Paz Fernandez, Spain  
Mohammad Feruj Alam, Bangladesh  
Phil Flentje, Australia  
Yannis Fourniadis, UK  
Edwin Friend, USA  
Irina Galitskaya, Russia  
George Gaprindashvili, Georgia  
George Gardner, USA  
Jesus Garrido Manrique, Spain  
Eldon Gath, USA  
Ben Gilson, UK  
Daniele Giordan, Italy  
William Godwin, USA  
Robert Goldsmith, Australia  
Dick Gray, USA  
Brian Greene, USA  
James Hamel, USA  
Hans-Balder-Havenith, Belgium  
Greg Hempen, USA  
Egerton Hingston, South Africa  
Peter Hudec, Canada  
Matthew Huebner, USA  
Maria Ingunza, Brazil  
Upali De Silva Jayawardena, Sri Lanka  
Filipe Jeremias, Portugal  
Brendon Jones, South Africa  
Frank Jordan, USA  
Kumud Raj Kafle, Nepal  
Sarah Kalika, USA  
Efstratios Karantanellis, Greece  
Ekaterina Karfidova, Russia  
Hamza Karrad, Algeria  
Heiko Käsling, Germany  
Brian Katz, USA  
Katerina Kavoura, Greece  
Andrey Kazeev, Russia  
Jeffrey Keaton, USA  
Klaus-Peterkeilig, Germany  
Alexey Kindler, Russia  
Matheus Klein Flach, Brazil

Aliko Kokkala, Greece  
Goh Thian Lai, Malaysia  
Hana Lee, Austria  
Nkopane Lefu, South Africa  
Leticia Lescano, Argentina  
Cheng Li, China  
Wenping Li, China  
Qian Liu, Austria  
José Lollo, Brazil  
Silvina Marfil, Argentina  
Vassilis Marinos, Greece  
Milos Marjanovic, Serbia  
Kristofer Marsch, Germany  
Pedro Martins, New Zealand  
Flora Menezes, Germany  
Amira Merchichi, Algeria  
Olga Meshcheriakova, Russia  
Stuart Millis, Hong Kong  
Omar Mimouni, Algeria  
Oleg Mironov, Russia  
Matthew Morris, USA  
Tim Mote, Australia  
Elena Mraz, Germany  
Marcos Musso, Uruguay  
Masashi Nakaya, Japan  
Arpita Nandi, USA  
Marivaldo Dos Nascimento, Brazil  
Monique Neves, Brazil  
Holly Nichols, USA  
Vanessa Noveletto, Brazil  
Takehiro Ohta, Japan  
Kazuhiro Onuma, Japan  
Thomas Oommen, USA  
Rolando Orense, New Zealand  
Ibrahim Oyediran, Nigeria  
George Papathanasiou, Greece  
Steve Parry, UK  
Darren Paul, Australia  
Osni Jose Pejon, Brazil  
Giacomo Pepe, Italy  
Regina Pläskén, Germany  
Lindsay Poluga, USA  
Joaquim Pombo, Portugal  
Martin Potten, Germany  
Constantin Prins, Germany  
Mário Quinta-Ferreira, Portugal  
Rute Ramos, Portugal  
Emanuele Raso, Italy  
Liana Rocha, Brazil  
Valéria Rodrigues, Brazil  
Michael Rucker, USA  
Nicholas Sabatakakis, Greece  
Rosanna Saindon, USA  
Mahin Salimi, Iran  
Ligia Sampaio, Brazil

Paul Santi, USA  
Regiane Sbroglia, Brazil  
David Scarpato, USA  
Malcolm Schaeffer, USA  
William Schulz, USA  
Jorge Sfragulla, Argentina  
Sachin Shah, USA  
Abdul Shakoor, USA  
Timothy Shevlin, USA  
Anna Shidlovskaya, Russia  
Roy Shlemon, USA  
Zachary Simpson, South Africa  
Alessandra Siqueira, Brazil  
Young-Suk Song, South Korea  
Georg Stockinger, Germany  
Alexander Strom, Russia  
Wanghua Sui, China  
Valentina Svalova, Russia  
Debora Targa, Brazil  
Ashley Tizzano, USA  
Ákos Török, Hungary  
Emil Tsereteli, Georgia  
Ryosuke Tsuruta, Japan  
Atiye Tugrul, Turkey  
Alan Keith Turner, USA  
Anatiliï Tushev, Ukraine  
Resat Ulusay, Turkey  
Isabella Magalhães Valadares, Brazil  
Lazaro Valezuquette, Brazil  
J. Louis Van Rooy, South Africa  
Ioannis Vazaios, Canada  
Marlene Villeneuve, New Zealand  
Nicholas Vlachopoulos, Canada  
Yasuhiko Wakizaka, Japan  
Chester (Skip) Watts, USA  
Luke Weidner, USA  
Baoping Wen, China  
Charles Wilk, USA  
Stephen Wilkinson, UK  
John Williams, USA  
Louis Wong, Hong Kong  
Martin Woodard, USA  
Richard Wooten, USA  
Yang Yang, China  
Katherine Yates, New Zealand  
Julia Yeakley, USA  
Murat Yilmaz, Turkey  
Zelin Zhang, China

---

## Contents

<b>Pressuremeter Tests in Russia and Their Application</b> . . . . .	1
Anna Shidlovskaya, Anna Timchenko, and Jean-Louis Briaud	
<b>A Simple Method of Estimating Ground Model Reliability for Linear Infrastructure Projects</b> . . . . .	7
Darren Paul	
<b>A Case Study on the Microstructure of Fibrous Peat (West Lake, China)</b> . . . . .	15
Stephen Wilkinson, Chaofa Zhao, Zhongxuan Yang, and Kun Pan	
<b>Geomechanical Investigation of High Priority Geothermal Strata in the Molasse Basin, Bavaria, Germany</b> . . . . .	21
Martin Potten, Bettina Sellmeier, Elena Mraz, and Kurosch Thuro	
<b>The Potential Use of Residual Soil from Ribeira Valley (Brazil) in Mitigating Metal Contamination: A Geotechnical Characterization</b> . . . . .	27
Jéssica Pelinsom Marques, Valéria Guimarães Silvestre Rodrigues, Orencio Monje Vilar, and Edmundo Rogério Esquivel	
<b>New Approach to the Assessment of Buildings Vulnerability in Various Natural and Technogenic Urban Conditions</b> . . . . .	33
V. Burova and E. Karfidova	
<b>Geotechnical Characterization of Sands from the Portuguese Continental Shelf to Support the Design of Renewable Energy Converters Installation</b> . . . . .	39
Joaquim Pombo, Paula F. da Silva, and A. Rodrigues	
<b>Correlation Between CPT and Screw Driving Sounding (SDS)</b> . . . . .	47
Yasin Mirjafari, Rolando P. Orense, and Naoaki Suemasa	
<b>Litho-Structural Control on the Geotechnical Properties of Colluvial Deposits, Rio do Sul City, Santa Catarina, Brazil</b> . . . . .	55
Vanessa Noveletto, Marivaldo S. Nascimento, Murilo S. Espíndola, and Vitor S. Müller	
<b>Vadose Zone Characterisation for Hydrogeological and Geotechnical Applications</b> . . . . .	63
Matthys A. Dippenaar and J. Louis van Rooy	
<b>Evaluation of Geotechnical Parameters of Slopes at Blumenau, Santa Catarina, Brazil</b> . . . . .	69
L. E. C. Alves, M. Espíndola, Vitor S. Müller, M. Z. Broetto, R. L. Pizzolo, and V. F. Hickel	
<b>Engineering Geological Studies for the New Drainage Tunnels of Lisbon</b> . . . . .	75
Filipe Telmo Jeremias, Rute Ramos, and Laura Caldeira	

<b>Geological-Geotechnical Studies for the Ore Transport Railway Line “S11D—Sudeste do Pará”, Brazil</b> . . . . .	83
Priscilla H. P. Oliveira and Mário Quinta-Ferreira	
<b>Groundwater Nitrate Concentrations and Its Relation to Landcover, Buncombe County, NC</b> . . . . .	91
Adu Agyemang, Adela Beauty, Arpita Nandi, Ingrid Luffman, and Andrew Joyner	
<b>Land Change, Soil Degradation Processes, and Landscape Management at the Clarinho River Watershed, Brazil</b> . . . . .	99
José Augusto de Lollo, João V. R. Guerrero, Ana C. P. Abe, and Reinaldo Lorandi	
<b>Flooding Susceptibility Identification Using the HAND Algorithm Tool Supported by Land Use/Land Cover Data</b> . . . . .	107
José Augusto de Lollo, Alice N. Marteli, and Reinaldo Lorandi	
<b>Soil Mixing for Remediation of Contaminated Sites</b> . . . . .	113
Charles M. Wilk	
<b>Harry Ferguson’s Theory of Valley Stress Release in Flat-Lying Sedimentary Rocks</b> . . . . .	121
James V. Hamel	
<b>The Characterization of Tropical Peats for Potentially Toxic Metals Adsorption Purposes in an Abandoned Mine Area</b> . . . . .	129
Isabela Monici Raimondi, Jacqueline Zanin Lima, and Valéria Guimarães Silvestre Rodrigues	
<b>Carolina Piedmont Groundwater System—Existence of the Transition Zone Between Regolith and Bedrock</b> . . . . .	135
Malcolm F. Schaeffer	
<b>The Consequences of Pyrite Degradation During Construction—UK Perspective</b> . . . . .	143
M. A. Czerewko and J. C. Cripps	
<b>Measuring Fault Displacements Caused by Salt Tectonics Using Marine Geophysical Data</b> . . . . .	153
J. Yeakley, Abdul Shakoor, and W. Johnson	
<b>Environmental and Geological Characters and Stability Problems in the Historic Centre of Matera (South Italy)</b> . . . . .	161
Vincenzo Simeone, Angelo Doglioni, Rosa Maria Lacertosa, and Francesco Sdao	
<b>Naturally Occurring Asbestos in Argentina: A Compilation of Case Studies</b> . . . . .	169
Lescano Leticia, Locati Francisco, Marfil Silvina, Sfragulla Jorge, Bonalumi Aldo, and Maiza Pedro	
<b>Author Index</b> . . . . .	175

# Pressuremeter Tests in Russia and Their Application

Anna Shidlovskaya, Anna Timchenko, and Jean-Louis Briaud

## Abstract

A series of 12 preboring pressuremeter tests were performed for the foundation design of a tall building in St. Petersburg, Russia. The site is on the North shore of the Neva River Delta. The soil layers at the site consist of Quaternary soft saturated soils of marine, glacial-lake origin and hard Vendian clay. The test procedure was the one recommended by the Russian standard which calls for much longer pressure steps than the ASTM Standard. Modulus of deformation and limit pressure profiles were obtained for 24–40 m depth in the Vendian clay. Such pressuremeter test results are often used for the foundation design of tall buildings.

## Keywords

Pressuremeter • Modulus • Limit pressure

## 1 Introduction

A series of 12 preboring pressuremeter tests were performed for the foundation design of a tall building in St. Petersburg, Russia. The site is on the North shore of the Neva River Delta. The soil layers at the site consist of Quaternary soft saturated soils of marine, glacial-lake origin and hard Vendian clay. The test procedure was the one described in the Russian standard which calls for much longer pressure steps than the ASTM Standard. Modulus of deformation and limit

pressure profiles were obtained from depth of 24–40 m in the Vendian clay.

## 2 Background on the Pressuremeter

The idea of the pressuremeter is credited to Louis Menard who, as a student at the Ecole Nationale des Ponts et Chausees, proposed it as part of his graduation report in 1957. The pressuremeter gives an in situ stress strain curve for the material tested (see Fig. 1) from which many useful parameters can be derived including a modulus, a yield pressure, and a limit pressure. Briaud in 1978 developed a simpler version of Menard's pressuremeter now called the TEXAM (see Fig. 2). The TEXAM was the pressuremeter used for the tests reported here. The probe is monocellular and is inflated by forcing water out of a cylinder through a crank powered piston. The probe was inserted in a prebored borehole prepared by wet rotary drilling with injection of prepared drilling mud. The probe can be inflated in equal pressure steps or equal volume steps; the tests reported here were equal pressure steps tests. Each pressure step should be held for one minute according to the ASTM standard (2016) but until no noticeable increase in radius is detected according to the Russian standard (GOST 2012) which was followed for the tests reported here.

## 3 Site Geology

The two main strata in St. Petersburg (see Fig. 3) are surficial non-lithified saturated sand-with-clay deposits of Quaternary age which are about 400,000 years old underlain by an older lithified clay strata called the Vendian clay which is about 600 million years old. The Vendian clay was considered as the bearing layer for a foundation. The hard clay is found at the depth of 24 m. The Vendian clay is marine sediment. The sedimentation of the clay took place under placid tectonic conditions. The catagenic transformations of the clay were

A. Shidlovskaya (✉)  
St. Petersburg Mining University, St. Petersburg, Russia  
e-mail: shidanna2013@gmail.com

A. Timchenko  
LLC "Kanex Project", Moscow, Russia  
e-mail: timchenko.ann@gmail.com

J.-L. Briaud  
Texas A&M University, College Station, TX, USA  
e-mail: briaud@tamu.edu

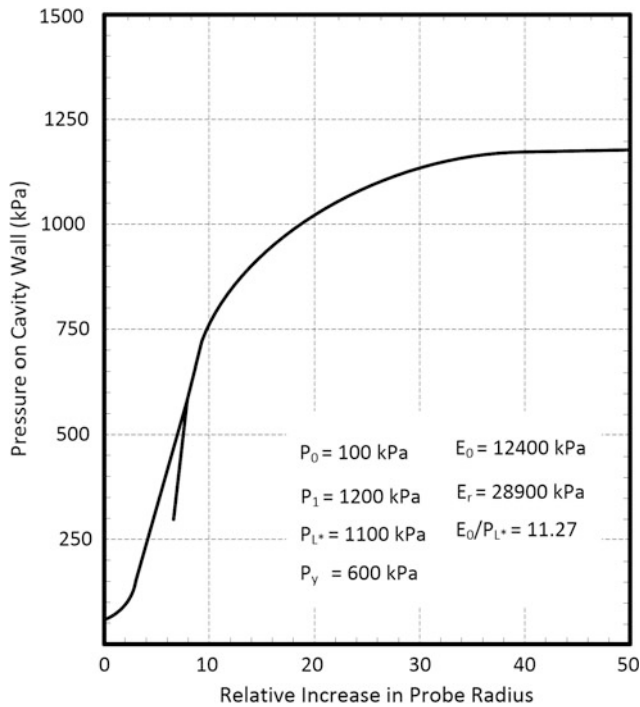


**Fig. 1** A pressuremeter curve

influenced by several processes: gravitational consolidation of the deposits through the pressure of overlays; tectonic activity at the junction of the Russian Plate and the Baltic Basement; and change in thermodynamic and physico-chemical conditions (Dashko 2003). The Vendian clay is fissured because of influence of tectonic and non-tectonic factors. The tectonic activity at the junction of the Russian Plate and the Baltic Basement manifests itself through



**Fig. 2** TEXAM pressuremeter

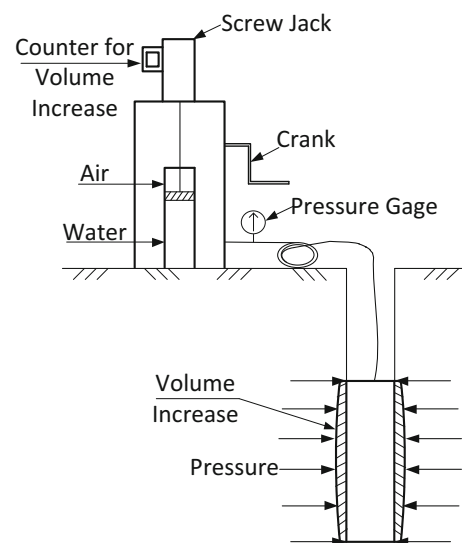
tectonic fissures within the clay that form two main systems of North-Western and North-Eastern course; there also are sublateral and submeridional tectonic fissures. Non-tectonic fissuring is largely typical for the upper zone of the clay section. In the upper zone of the clay regressive lithogenesis, formation of fissures of elastic reaction and of weathering in alternating temperatures and in crystallization of salts took place. In the glacial period the fissures were formed through glaciotectonics (wedges traced to the depth of 20–25 m) and through frost weathering (Dashko 2003).

#### 4 Soil Properties

Research on the Vendian clay done by Dashko (2003) shows that this clay should be considered as block fissured deposits (Dashko 2003). The clay properties are likely to be affected by fissuring and scale effect. Fissures are weakened mostly the strength and deformability of the clay. Table 1 shows features of macrostructure such as a block size of the clay and related water content. The index properties of the Vendian clay obtained at the site are shown in Table 2. The unit weight of solids was measured and averaged  $27.0 \text{ kN/m}^3$ .

#### 5 Pressuremeter Test Results in St. Petersburg

A series of 12 tests were performed at depth of 25–40 m below the surface. For each test, the pressure and the increase in volume of the probe was recorded. The data





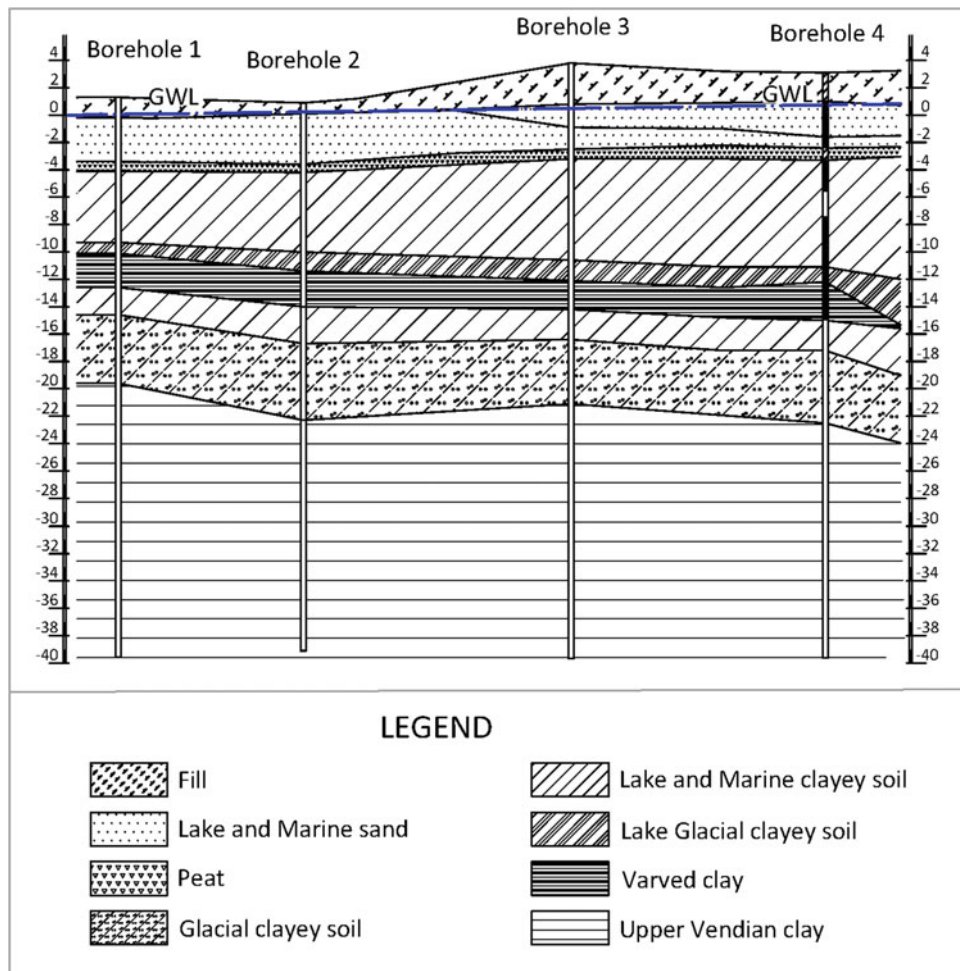


**Fig. 3** Stratigraphy of the site

**Table 1** Vendian clay structure and properties (Dashko 2003)

Zone No.	Layer No.	Depth from upper boundary (m)	Block size (m)	Water content (%)
I	1	0–20	0.1–0.5	12–23
	2	20–40	0.5–0.7	10–20
II	3	40–60	0.7–1.0	10–19
	4	60–75	1.2	10–17
	5	>75	>1.2	9–15

reduction included the data correction and then the development of a test curve such as the one shown on Fig. 1. From each curve, a set of PMT parameters were obtained including the first load pressuremeter modulus  $E_0$  (see Fig. 4), a yield pressure  $p_y$  (see Fig. 5), and a limit pressure  $p_L$  (see Fig. 6). In some of the tests and due to the limits of the equipment, it was not possible to expand the probe sufficiently to determine the yield

pressure and the limit pressure. In those cases, correlations based on the other tests where such data could be collected were used to estimate the missing parameters. These data points appear followed by question marks on Figs. 5 and 6. The yield pressure is used to check that the pressure under the foundation does not exceed  $p_y$ . The limit pressure  $p_L$  is used to calculate the ultimate bearing capacity of the foundation (Briaud 2013).

**Table 2** Index properties of the Vendian clay

PMT	Borehole #	Depth (m)	Grain size distribution			Unit weight (kN/m <sup>3</sup> )	Water content (%)	PI (%)	Void ratio (e)
			% clay particles	% silt particles	% sand particles				
1	1	25.5	23	43	34	20.6	19	18	0.560
3		30.4	32	50	18	20.8	15	17	0.500
4		32.9	38	49	13	21.2	14.5	16	0.460
5		35	20	52	28	21.8	14	16	0.413
6		40	25	50	25	22.0	13	17	0.385
7		2	26	36	51	13	20.6	19	18
8	28		18	51	31	20.8	16	19	0.508
9	32.5		34	40	26	21.0	15	18	0.475
10	36		22	48	30	21.9	14	17	0.406
11	40		27	38	35	22.2	12	17	0.363
12	3	25.5	30	30	40	20.6	18	19	0.525
13		28	30	48	22	20.8	16.5	19	0.508

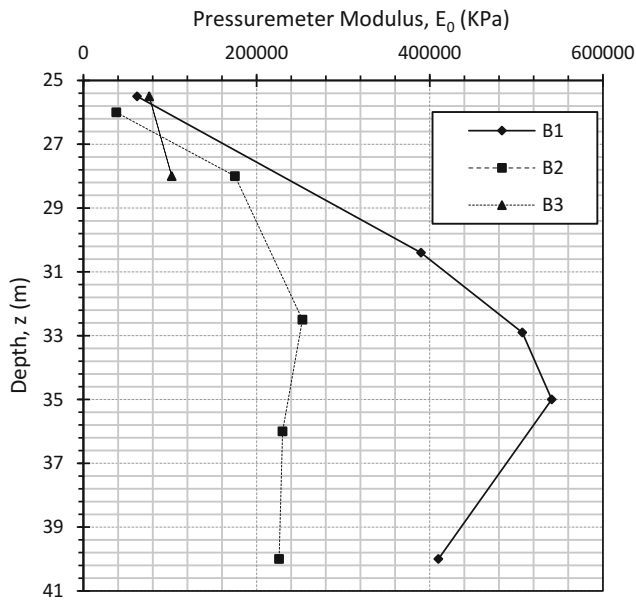


**Fig. 4** PMT first load modulus profiles

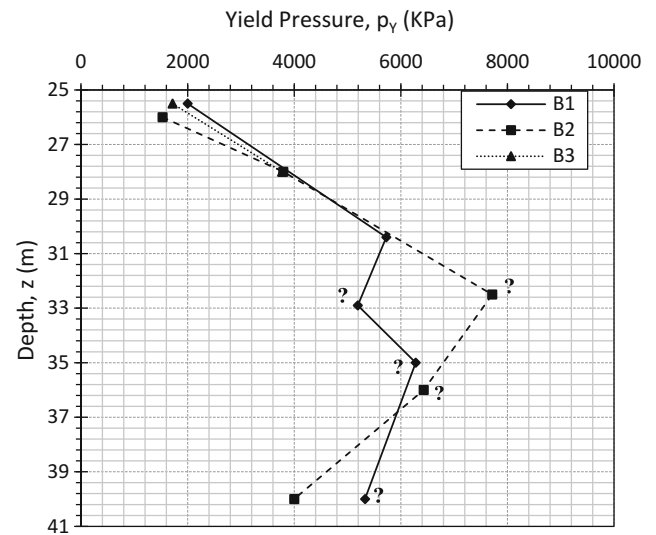


**Fig. 5** Yield pressure profiles

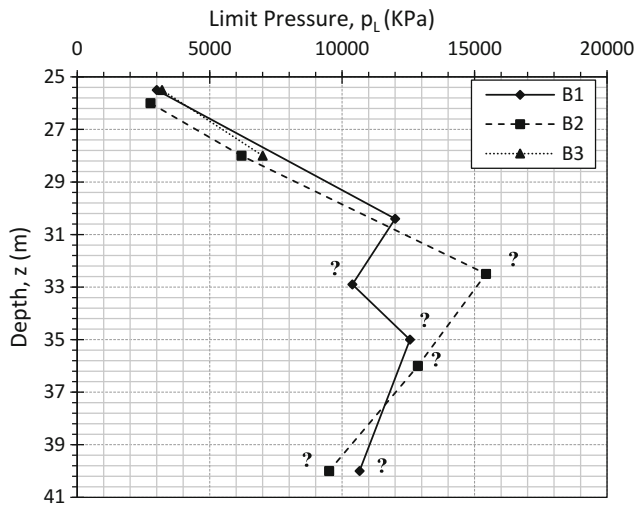


Fig. 6 PMT limit pressure profiles

## 6 Conclusions

This paper presents the results of a series of 12 pressuremeter tests performed for the foundation design of a tall building in St. Petersburg, Russia. The site geology and soil profile

consist of soft saturated soil underlain by a hard Vendian clay. The pressuremeter tests were performed in this hard Vendian clay. The test data was corrected and soil parameters were obtained for the foundation design. These parameters are the PMT modulus, the PMT yield pressure and the PMT limit pressure. The relationship between these parameters and depth was obtained. The modulus, yield pressure and limit pressure vary with depth and the profiles are presented. These parameters are useful in the calculation of the ultimate bearing pressure and the settlement of foundation.

**Acknowledgements** The authors wish to acknowledge the contributions of Denis Michailov for his help in performing the long PMT tests in St. Petersburg.

## References

- ASTM D4719-07. USA Standard Test Methods for Prebored Pressuremeter Testing in Soil. Withdrawn (2016). 10 p
- Briaud, J.-L.: Geotechnical Engineering: Unsaturated and Saturated Soils, 1000 p. Wiley (2013)
- Dashko, R.E.: Problems of geoecology in geotechnics. Reconstr. Historic Towns Geotech. Constr. **1**, 95–106 (2003)
- GOST 20276-12. Soil. Field methods for determining the strength and strain characteristics. NIIOSP, Moscow (2012). 89 p

# A Simple Method of Estimating Ground Model Reliability for Linear Infrastructure Projects

Darren Paul

## Abstract

The ground model is fundamental to any engineering project with ground structure interaction. Linear infrastructure projects have many forms of ground interaction and ground models are essential. All ground models are hypothetical. Interpolation or extrapolation from known data is required in order to form a prediction of the ground characteristics at any particular location. There is therefore inherent uncertainty in every ground model. The reliability of the ground model may be considered to be a function of (1) the accuracy or reliability of the data on which it based; (2) the quantity of data or ground information available; (3) the geological complexity of the ground from which the data has been obtained and (4) the complexity of the ground response to changes induced by the project. This paper presents a method of assessing ground model reliability for linear infrastructure projects based on an assessment of these four key factors. This method has been applied to three linear infrastructure projects in Australia, which are discussed.

## Keywords

Ground models • Geological uncertainty  
Geological reliability • Linear infrastructure

## 1 Introduction

Ground models are required over the full course of planning, design and construction of linear infrastructure projects. The typical progression of a ground engineering project would see the level of detail and certainty of the ground model increase over the course of the project as the ground model develops in parallel with the project and design

development. The uncertainty within the ground model would then generally reduce in parallel with the progression of the project. A challenge facing any geotechnical engineering project is in identifying how much uncertainty can be tolerated at any stage of the project. An assessment of the uncertainty in the ground model and its associated risks informs the investigation that needs to be undertaken over the course of the project and what risks must be accommodated in design.

Amongst other things, the usefulness of ground information used as input for developing a ground model depends on:

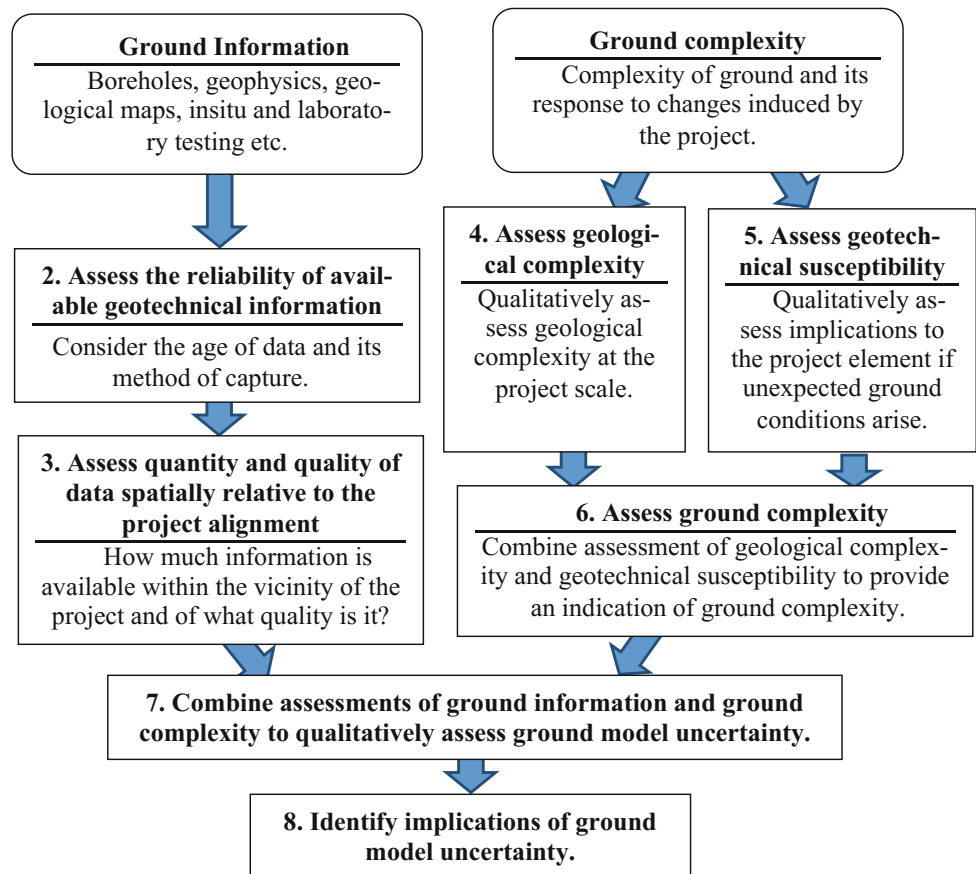
- the reliability that can be placed on the ground information;
- the quantity of information and its location or relevance to the project for which it is being assessed;
- the geological complexity and variability of the ground at the location of interest, and;
- the susceptibility of the project to ground conditions.

Assessing how much investigation should be undertaken at various stages throughout the project, requires an assessment of how much ground model uncertainty can be tolerated. A method is set out below which seeks to qualify the uncertainty associated with a ground model for linear infrastructure projects which can be applied throughout its various stages. The method proposed follows the process as set out in Fig. 1. Two key streams are considered: the available ground information (left column on Fig. 1) and the ground complexity (right column on Fig. 1). An assessment of each is undertaken and then qualitatively combined in order to assess ground model reliability.

This paper describes a qualitative process to assess ground model uncertainty which is similar to and draws inspiration from qualitative systems used to assess risk, for example the RTA system of slope risk assessment, Stewart et al. (2002). Each step of the qualitative process is described in this paper. The numbered headings may be cross-referenced to the numbers shown in the flow chart in Fig. 1.

D. Paul (✉)  
Golder Associates, Melbourne, Australia  
e-mail: dpaul@golder.com.au

**Fig. 1** Flow chart indicating steps in assessing ground model uncertainty. Numbered steps may be cross referenced to headings in this paper



## 2 Assess the Reliability of Available Geotechnical Information

The ground model at the concept or feasibility stage of a project is likely to be based on a desk study and informed by existing information that is unlikely to have been acquired specifically for the project. It may have been acquired to inform geotechnical aspects of other projects or for entirely unrelated, non-geotechnical purposes and therefore have varying relevance. For urban infrastructure projects for which the method set out in this paper was developed, the available information was predominantly historical borehole information and a method of assessing the quality of borehole information is set out here. Notwithstanding this, the methods set out here for boreholes could be adapted for map information, CPT, geophysics or any other relevant information.

In order to assess the reliability of boreholes, a semi-qualitative assessment can be made on a borehole by borehole basis. The method suggested here uses a similar approach to that used in rock mass classification systems such as RMR (Bieniawski 1989). Various attributes of the borehole are assessed and score is allocated for each attribute

as indicated in Table 1. The scores for each attribute are then summed with the score allocated to a borehole reliability category, 1–5. Although development of the borehole reliability score is semi-quantitative, it is important to note that the overall system presented here is qualitative and that the borehole reliability score is used to provide a qualitative input (borehole ranking) to the system. The attributes considered for boreholes are set out below.

**Drilling Method**—Boreholes with core drilling including an assessment of rock defects are more reliable than boreholes using washbore or hammer techniques.

**Survey**—Boreholes with recent ground survey are considered more accurate than those without survey and allow more reliable positioning in ground models.

**Sampling Frequency**—The greater the sampling frequency in the borehole, the more reliable the soil or rock description is considered to be.

**Age**—There is greater uncertainty around the provenance of older borehole logs.

**Depth**—Shallow boreholes are generally considered less relevant than deep boreholes, particularly for tunnel projects.

**Installation**—Boreholes with groundwater wells installed and groundwater measurements are considered more useful than boreholes without well installations.

**Table 1** Categories used to assess borehole reliability score

Borehole attribute	Category	Score
Drilling method	Washbore and coring	5
	Washbore or hammer only	2
Survey	Survey to modern coordinate system inc. RL	5
	Survey to modern coordinate system, RL estimated from topographical information OR Survey to modern coordinate system inc. RL	4
	Survey to modern coordinate system, RL estimated from topographical information OR No survey—georeferenced from site plan	3
	Converted from historical datum OR No survey—located using georeferenced aerial imagery and topographical information	2
Sampling frequency	<1.5m	10
	>1.5–3 m	6
	>3 m	2
Age	<5 years	5
	>5 to <10 years	4
	>10 to <20 years	3
	>20 years	2
Depth	>25 m	10
	>10 to <25 m	6
	>5 to <10 m	2
	<5 m	1
Installation	Piezometer or well installation	3
	No installation	0
In situ testing	SPT and packer, or pressuremeter testing	5
	SPT only	3
	No in situ testing	0

**In situ Testing**—Boreholes with in situ testing including SPTs, packer testing or pressuremeter testing provide information on engineering properties of the ground.

Note that the above criteria have been developed with a focus on urban tunneling projects but could be readily adapted to other forms of linear infrastructure projects or other types of projects.

The process of selecting suitable numbers for each category was one of trial and error. A borehole reliability assessment was undertaken for approximately 1000 boreholes and the scores assigned to each category varied until the output was considered reasonable. Judgement was exercised in undertaking this trial and error process. If required, it is a relatively simple process to vary the categories and numbers to include project or location specific attributes and weightings.

The reliability scores are then assigned to a category in accordance with Table 2 which can then be used as input to the qualitative assessment. Similar to the parameters used to

develop the reliability score, the category ranges have been developed through a trial and error process and can be tailored to the specific project and location. The implications of this borehole reliability ranking to future investigation and ground model development are set out in Table 2.

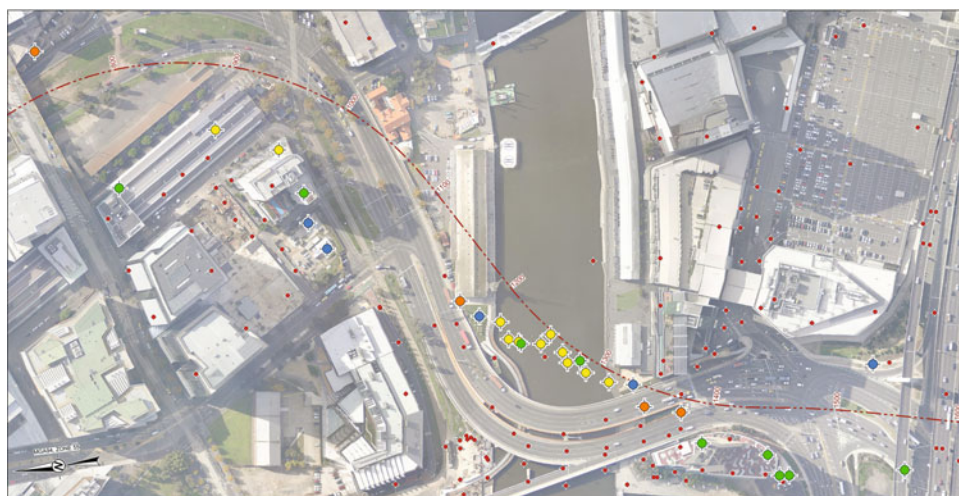
Boreholes ranked 1–3 would generally be used to inform ground model development, supplemented by boreholes with a lower ranking. Figure 2 provides an indication of the borehole reliability spatially along part a project assessed using the methods set out above.

### 3 Assess Quantity and Quality of Data Spatially Relative to the Project Alignment

To assess information quality and quantity, the borehole reliability ranking can be used in conjunction with an assessment of the density of boreholes relative to the proposed project alignment. Table 3 provides an example

**Table 2** Borehole reliability ranking

Borehole reliability score	Borehole reliability ranking	Implications
>34	1	Good, detailed information, known provenance, can be relied upon without need to undertake further investigation
29–34	2	Good information, but information needs to be supplemented or verified through further investigation
23–28	3	Information reliable, but shallow or lacking in detail. Supplemental investigation needed
16–22	4	Provides some useful information, but insufficient detail or uncertain provenance. Not to be relied upon. New investigation needed
<16	5	Minimal or no useful information, not to be relied upon. New investigation needed

**Fig. 2** Example of borehole reliability plotted on portion of linear infrastructure project**Table 3** Borehole information quality and quantity

Very poor	No intrusive investigation, or boreholes more than 100 m from the alignment, existing information limited to geological maps
Poor	Boreholes 50–100 m from the alignment
Fair	One or more boreholes within 50 m of the alignment, along a 100 m length. Borehole reliability ranking low, typically 4 or 5, some 3
Good	Up to 5 boreholes within 50 m of the alignment, along a 100 m length. Boreholes have a high borehole reliability ranking, 1 or 2
Very good	More than 5 boreholes within 50 m of the alignment. Boreholes have a high reliability ranking, 1 or 2

of how this was undertaken for an urban tunneling project in Melbourne, Australia where the assessment was undertaken over 100 m intervals along the proposed tunnel alignment.

#### 4 Assess Geological Complexity

Geological complexity refers to ground characteristics with complexity related to aspects such as variability of lithology, complexity of structure, stress field and tectonic history. It

might also be described as the degree of ground homogeneity at the scale of the project.

Table 4 presents a guideline for the assessment of geotechnical and geological complexity which was developed for an urban tunneling project in Melbourne.

For example, the geological complexity of normally to slightly overconsolidated Holocene sediment may be 'simple' because its depositional history and stress history are known and its engineering properties are relatively predictable. Conversely, a metamorphic rock mass with multiple phases of deformation and weathering would be

**Table 4** Assessment of geological complexity at scale of tunneling project

Very simple	Single material type, no deformation, regular or repeatable structure, no discernible weathering
Simple	Single material type, no deformation, predictable structure, some chemical or mechanical weathering
Intermediate	Multiple material types, single phase deformation, somewhat predictable structure, chemical and mechanical weathering
Complex	Multiple material types, single phase of deformation with unpredictable structures, multiple phases of chemical and mechanical weathering
Very complex	Many different lithologies, complex structure with multiple phases of deformation and metamorphism with complicated structure, multiple episodes of chemical and mechanical weathering

‘complex’. Note that geological complexity should be assessed at a scale relative to the projects zone of influence.

## 5 Assess Geotechnical Susceptibility

*Geotechnical susceptibility* refers to the susceptibility of the project or project element to ground uncertainty.

Table 5 presents a guideline for the assessment of geotechnical susceptibility which was used to qualitatively assess an urban tunnelling project in Melbourne.

Table 6 presents an example of the geotechnical susceptibility that might be estimated for various elements of an urban metro project.

**Table 5** Assessment geotechnical susceptibility

Very low susceptibility	Construction and structure proposed has a low susceptibility to uncertain or unexpected ground conditions. No significant consequences if unexpected ground conditions are encountered
Low susceptibility	Proposed design and construction has some susceptibility to unexpected ground conditions, but these can likely be mitigated or managed through design or pre-planned contingency
Intermediate susceptibility	Proposed design and construction is susceptible to unexpected ground conditions. There are expected to be implications if unexpected ground conditions are encountered during construction which may require design changes, remedial measures or delays during construction
High susceptibility	Proposed design and construction is susceptible to unexpected ground conditions with significant implications including project delays and cost overruns if unexpected ground conditions are encountered
Very high susceptibility	Proposed design and construction highly susceptible to ground variation or unexpected ground conditions with major implications if unexpected ground conditions are encountered. Project delays, cost overruns, health and safety risks and reputational damage likely if unexpected ground conditions are encountered

**Table 6** Estimated geotechnical susceptibility of various elements

Very low susceptibility	Shallow surface excavation Lightly loaded footings Lightly loaded pavements and track
Low susceptibility	Unsupported surface batter slopes
Intermediate susceptibility	Retained excavation TBM tunnels
High susceptibility	Deep retained excavation TBM tunnels close to existing underground assets with potential interaction effects or mixed face conditions
Very high susceptibility	Large span underground excavation (caverns) Deep retained excavation in close proximity to existing movement sensitive structures

## 6 Combine Assessments of Geological Complexity and Geotechnical Susceptibility to Assess Ground Complexity

The assessments of geological complexity are combined to arrive at an overall estimate of ground complexity. Table 7 provides a matrix which combines geological complexity and ground susceptibility. This matrix is biased towards geotechnical susceptibility. For example complex geological complexity and intermediate geotechnical susceptibility combines to intermediate.



**Table 7** Tool to assist in estimating ground complexity based on geological complexity and geotechnical susceptibility

Geological complexity	Geotechnical susceptibility				
	Very low	Low	Intermediate	High	Very high
Very simple	Very simple	Simple	Simple	Intermediate	Intermediate
Simple	Very simple	Simple	Intermediate	Intermediate	Complex
Intermediate	Simple	Simple	Intermediate	Complex	Complex
Complex	Simple	Intermediate	Intermediate	Complex	Very complex
Very complex	Intermediate	Intermediate	Complex	Complex	Very complex

## 7 Combine Assessments of Ground Information and Ground Complexity to Qualitatively Assess Ground Model Uncertainty

The assessments of ground information (step 3) and ground complexity (step 6) are combined using the matrix in Table 8, to arrive at an overall ground model reliability ranking. An example of how the ground model reliability may be communicated on a ground model, in this case a simple cross section, is presented in Fig. 3. The ground model uncertainty was superimposed over the ground model at project feasibility stage using desktop information.

## 8 Identify Implications of Ground Model Uncertainty

An indication of the implications of the estimated ground model reliability score is provided in Table 9.

This approach informs an assessment of where further investigation might be expected to provide the most value and can be refined multiple times as the project progresses and additional information becomes available.

**Table 8** Ground model reliability rating

Ground Information	Ground Complexity				
	Very Complex	Complex	Intermediate	Simple	Very Simple
Very Poor	Very Low	Very Low	Low	Low	Medium
Poor	Very Low	Low	Low	Medium	High
Fair	Low	Medium	Medium	High	High
Good	Medium	Medium	High	High	Very High
Very Good	High	High	Very High	Very High	Very High

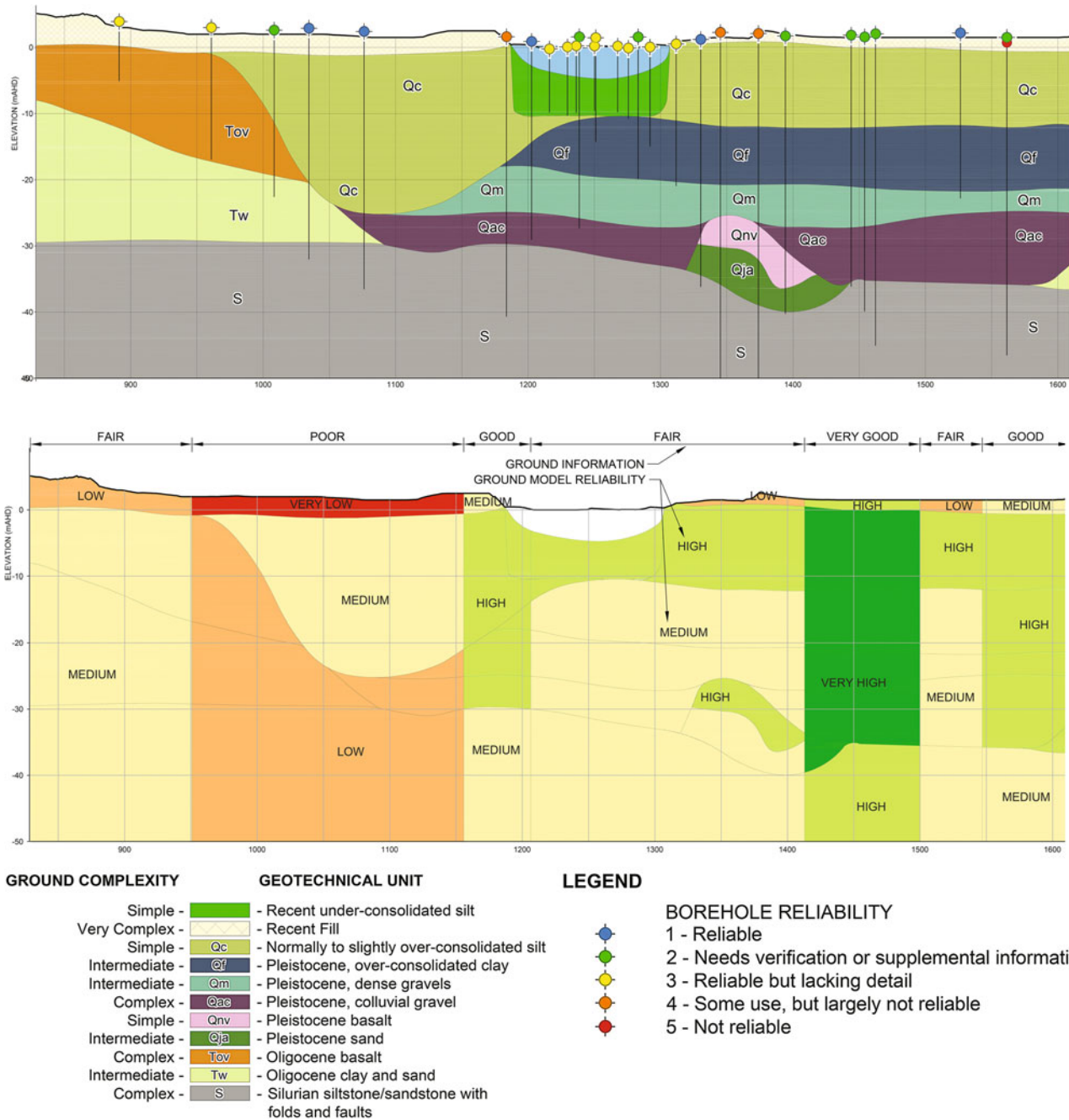


**Fig. 3** Example of cross section presenting ground model reliability for a tunneling project. Ground complexity for each geotechnical unit and ground information are combined to indicate Ground Reliability (lower section)

**Table 9** Implication of ground model reliability score

Very low (VL)	Available information insufficient given the geological complexity to develop a basic conceptual model. Indicative only.
Low (L)	Available information sufficient given the geological complexity to develop a basic conceptual ground model but not an observational model.
Medium (M)	Sufficient information given the geological complexity to develop an observational model. Significant residual uncertainty.
High (H)	Sufficient information given the geological complexity to develop an observational ground model. Some uncertainty remaining.
Very high (VH)	Able to develop detailed observational ground model. Sufficient information given the geological complexity to proceed with detailed design.

## 9 Conclusions

A method is set out here by which the reliability of a ground model may be assessed in a semi-quantitative manner. The methods described have been applied with success on three major tunneling projects in Melbourne, Australia. However, the methods described here are adaptable. The criteria and weightings assigned to criteria for borehole reliability assessment can be modified through a trial and error process and tailored to a specific project and geological setting.

Whilst the question of how much investigation is enough investigation cannot be answered directly using the technique described here, this method may inform identification of those areas where further investigation will add the most value.

## References

- Bieniawski, Z.T.: Engineering Rock Mass Classifications. Wiley, New York (1989)
- Stewart, I.E., Baynes, F.J., Lee, I.K.: The RTA guide to slope risk analysis, version 3.1. Aust. Geomech. **37**(2) (2002)

# A Case Study on the Microstructure of Fibrous Peat (West Lake, China)

Stephen Wilkinson, Chaofa Zhao, Zhongxuan Yang, and Kun Pan

## Abstract

The classification of peat soils involves a very large number of different types. From a descriptive perspective this is useful, however such a system generates too many options for engineering purposes. The behaviour of organic soils varies based on the quantity and type of organic material present within the soil. The effects of fibre content are particularly important. The West Lake in Hangzhou has been dredged many times during its history to maintain its beauty. During the most recent dredging the sludge from the lake was transported via a 4 km pipeline and deposited inside the Jiangyangfan Reservoir. The organic soil situated in Jiangyangfan Ecopark is a particularly interesting peaty material. The organic sludge was mixed and homogenised during the transportation process, and then settled out within the reservoir. This resulted in a more than 20 m thick peat layer deposited with an uneven surface. The Ecopark buildings were then constructed on top of this in 2008. A combined electron microscope and mechanical study of the microstructure and behaviour of the peat has been used to identify the engineering impact of the presence of relatively small number of fibres within the soil matrix. The fibres within the peat modify its behaviour such that it can no longer be understood within the typical critical state framework for soils. The peat starts to deform plastically under very small levels of applied stress. In addition, it does not

display a tension cut-off failure and, ultimately, fails in shear.

## Keywords

Peat • Classification • Microstructural imaging • Organic fibers • Microstructure assessment

## 1 Introduction

The West Lake (Xihu) in Hangzhou is recognised as a UNSECO World Heritage site due to its inspiration of Chinese painters and poets throughout history. The lake, originally a lagoon, on the banks of the Qiantang River, is fed by small rivers in the surrounding hills. Given its locality it is gradually being infilled by transported sediment and organic debris from the surrounding hillslopes. These natural processes have been resisted by human intervention in order to preserve the natural beauty of the site. The lake has been dug out several times in history. In fact, the first time the lake was referred to as “West Lake”, was in 1090 when the then governor Su Shi, also a well-known poet, made a request for soldiers to be sent to dig out the lake (Shi 1090). This long term history of dredging of the lake has produced deposits of peaty soil (which is a form of made ground) across the hills surrounding Hangzhou.

During one of the most recent engineering works to prevent the silting up of the West Lake, in 1999, a dredging method was employed. A 4 km long pipeline was built to transport dredged soil and organic debris from the lake across the hills to a small reservoir on the north bank of the Qiantang River. Due to the large quantities of peat the reservoir was almost completely filled with this debris (approximately 1,000,000 m<sup>2</sup> of sludge). After completion of the dredging work, the newly filled reservoir, known as the Jiangyangfan site, was allowed to settle under its own weight for five years (to 2008). Following which construction of an eco-park commenced on the site.

S. Wilkinson (✉)

University of Wolverhampton, Wolverhampton, WV1 1LY, UK  
e-mail: S.wilkinson4@wlv.ac.uk

S. Wilkinson

Formerly Department of Civil Engineering, Xi'an Jiaotong-Liverpool University, Suzhou, Jiangsu, China

C. Zhao

Formerly Department of Civil Engineering, Zhejiang University, Hangzhou, China

Z. Yang · K. Pan

Department of Civil Engineering, Zhejiang University, Hangzhou, China

Due to the sites anthropogenic depositional history the material within the Jiangyangfan eco-park is pretty unique. There is an 18 m thick sequence of rapidly deposited mixed organic and siliciclastic material. The soil constituents would have been very well mixed in the turbulent conditions present inside the pipeline. Any structures and layering of the peat sequence produced at Jiangyangfan would be generated by the movement of the dredging apparatus across the lake. It is thus anticipated that the amount of variation that this would produce in any layer would be minimal. The produced peat can be described as fibrous. However due to the transportation process the fibres tend to be short and well-distributed. This distribution of fibres allows this particular peat to exhibit intermediate behaviours (outlined later).

During the construction of the eco-park, as could be expected, issues with excessive settlement were encountered. Settlements of up to 0.7 m were measured during monitoring of the structures. This triggered an investigation into the behaviour of the peat, which was to contribute to mitigation works.

## 2 Peat Assessment

The classification methods available for peat are cumbersome, reflecting the broad variety of different materials identified as peat. Typically the classification of peat is carried out using one of two major classification systems, the Von Post (1922) system focusing on rural land management requirements, and the Radforth (1969) system focusing on the peats internal structure. The Radforth system splits peat into two major categories, amorphous and fibrous, with the fibrous category being subdivided into majority coarse and majority fine fibres. The Von Posts classification system is more extensive covering humification, water content, organic content, fine and coarse fibre content and wood content. Given this, the Von Post system provides a more rounded description of peats, however it lacks some important elements which could assist in understanding the engineering behaviour of peaty soils. Hobbs (1986) identified this lack and extended the Von Post system to include organic content, tensile strength in the vertical and horizontal directions, odour, plastic limit and acidity. The classification system produced in this way generates 245,760,000 unique

classifications for peat materials (Table 1). This provides too many options to be used practically to divide peats up into different behavioural systems for engineering purposes. It is however important to note that some of these options are not practically possible (i.e. a peat with high humification cannot also have fibres). Having said this, the description produced by this method is of great use in assessing the potential behaviours of the peat and providing a comparative identification of the layers within a peaty formation. An engineering focused classification system which identifies the range of behaviours of peat, while limiting the ultimate number of types would be more useful. However more recent analysis suggests that the variations in peat from region to region mean that it is unnecessary and indeed impossible to create a unified classification system (Landva et al. 1983). Given the variation in vegetation types that might act as a source for peat, locally driven systems may be the answer. However these must take account of, and allow for, broader correlations to be made. At present, the authors recommend the modified von Post system as an aid to description and that classification be carried out using a reduced locally focused system.

## 3 The West Lake Peat

The West Lake Peat has undergone a homogenisation process during transport within the pipeline to the Jiangyangfan site. The organic content has been mixed with large quantities of silt and the turbulent flow of this mixture within the pipeline would have resulted in a degradation of the quality and interconnectedness of the existing fibres. Using the modified von Post system, the peat is defined as a bryales moss peat, it has moderate humification, with intermediate water content, a high but non-dominant quantity of fine fibres with low coarse fibre content and no wood. Its organic content is low, it has moderate tensile strength in both the vertical and horizontal directions, it has a slight odour, a measurable plastic limit and is acidic.

In terms of its engineering behaviour, its fibre content being high but not dominant is important as is its low organic content (Yang et al. 2016). The peats engineering behaviour is discussed further below.

As part of the investigation into the behaviour of the West Lake Peat a scanning electron microscope (SEM) assessment

**Table 1** The number of options for each sub classification in the von Post classification system for peat, as extended by Hobbs (1986)

Parameter	Plant type	Humification	Water content	Fine fibre content	Coarse Fibre content	Wood remnants	Shrub remnants	Organic content	Vertical tensile strength	Horizontal tensile strength	Odour	Plasticity	Acidity	Total
Number of options	10	10	5	4	4	4	4	5	4	4	4	2	3	245,760,000

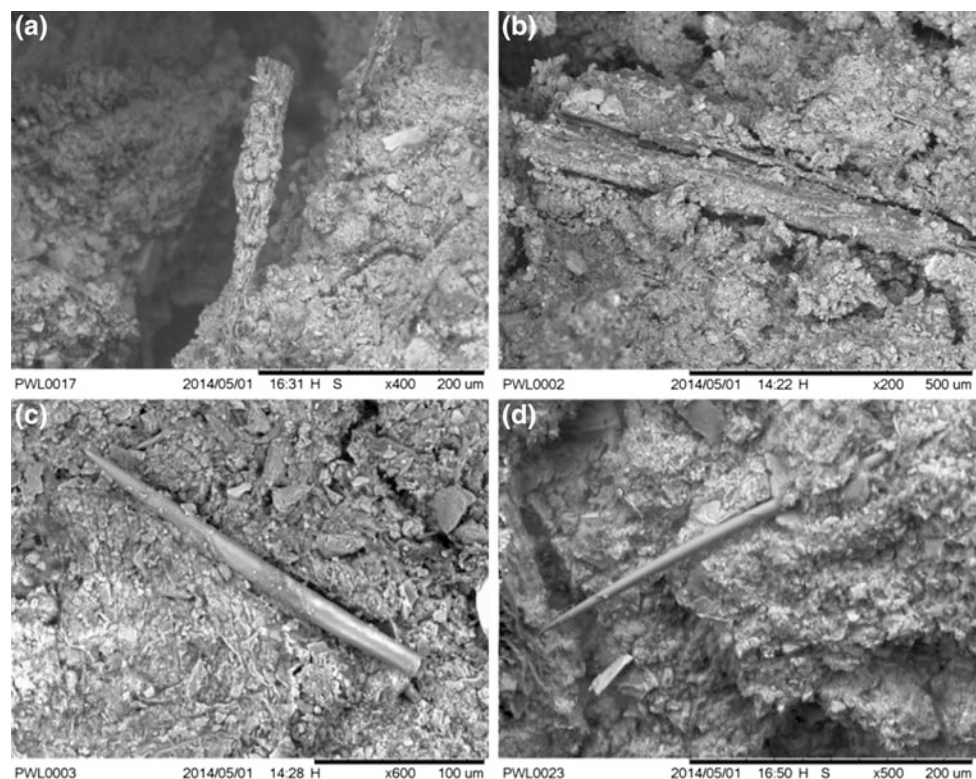
was carried out using the Hitachi TM300 tabletop microscope imaging facility at Xi'an Jiaotong Liverpool University. One key feature identified in the SEM analysis was the relative lack of fibres and fibrous matter in comparison to most peats (Fig. 1). Much of the groundmass of the peat is siliciclastic in origin. However, the reasonable tensile strength of the peat is an indicator the presence of fibrous material, and although sparse several types of fibre were identified within the peat. Multi-strand fibres were identified (Fig. 1a, b). In some instances, these fibres displayed evidence of resisting the tensile force used to generate the broken surface for imaging (Fig. 1a). In addition, several smoother fibres (root like) were identified. These would provide less frictional resistance and thus have a lower contribution to the tensile stresses (Fig. 1c, d). Different types of fibres and fibre structures can also be observed at the smaller scale (Fig. 2). These vary from fairly rigid and well-structured microfibrils with rough surfaces (Fig. 2a), to more ductile less structured rough fibres (Fig. 2b), and to smoother root structures (Fig. 2c).

In addition, the variability of the West Lake Peat is also displayed in its microscale particles and structures. Pyritic framboids typically form post deposition (during burial) and are indicative of a reducing environment (Fig. 2d). Diatoms may have been present in the sludge at the base of the lake, or may have been sucked directly from the lake water (Fig. 2e).

Leaf structures were observed in multiple locations, forming a large proportion of the organic matter in the peat (Fig. 2f).

As a part of the geotechnical assessment of the soil a range of classification and mechanical test of the West Lake Peat were carried out (Yang et al. 2016). The key observed behaviours of the West Lake Peat are: the soils angle of friction was high, however it did not reach the tension cut-off criteria, and so failed in shear (Fig. 3). The majority of fibrous peats fail in tension, so this is unusual behaviour. It is clear that the presence of a quantity of fibres has enhanced the peats strength (angle of friction), but that the fibres do not dominate the peats behaviour. These test results match well with the SEM observations, that the fibres are present, but are well separated.

**Fig. 1** Examples of fibres (fine) found within the West Lake Peat. **a** Rough fibres that have been pulled during the formation of the broken surface for imaging. **b** Rough fibres embedded in the matrix of the peat showing distinct separation between the fibre and the surrounding soil. **c**, **d** Examples of smoother fibres within the peat matrix



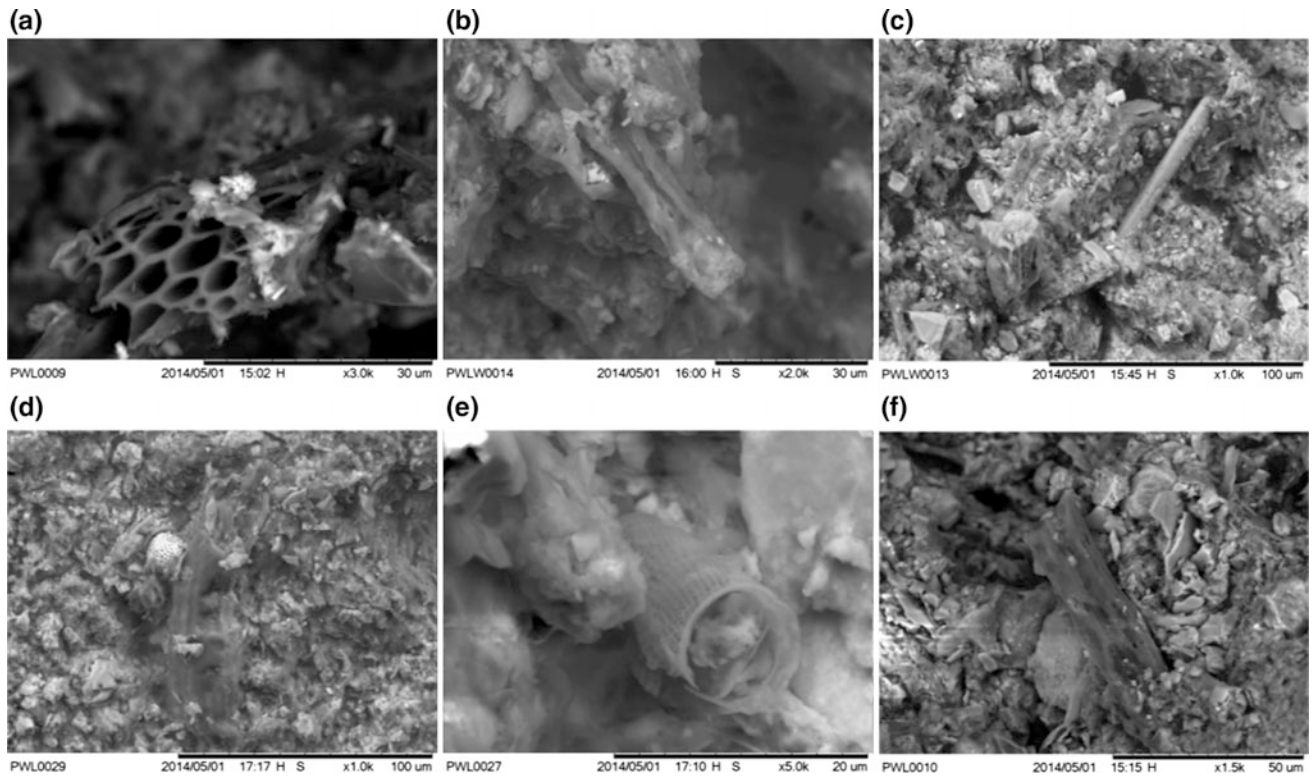
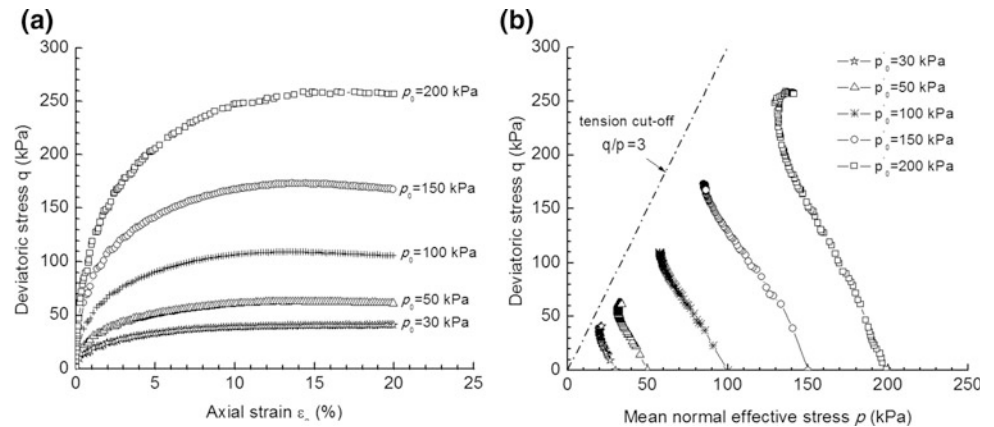


**Fig. 2** Examples of small scale structures within the West Lake Peat **a** sections of plant fibres showing xylem and phloem, **b** crumpled and degraded plant fibres, **c** granular matrix of the peat and small fibrous structures, **d** pyritic framboid and leaf like structures, **e** diatom from the West Lake, **f** crumpled leaf like structures

**Fig. 3** Triaxial compression results for the West Lake Peat. Modified from Yang et al. (2016)



## 4 Conclusions

Classification systems for peat produce a very large number of different possible outcomes. This is a result of the inclusion of the wide range of parameters that would be important for geotechnical engineering, and it is clear that having such information in the description of the soil is very important. But attempts to use such systems for classification in order to make correlations between sites (or even samples)

to compare engineering behaviour will be problematic. The utilisation of local classification systems to allow local correlations with less chance for confusion is recommended.

The West Lake Peat due to its unique geological history, had an unusual structure, with fibres present and clearly influencing the engineering behaviour of the soil. But the peat still failed in shear rather than in tension. This interesting result highlights the variability of peat systems and indicates the importance of evolving peat models to include more elements of its behaviour.

**Acknowledgements** The research was funded by the Natural Science Foundation of China (Grant Nos. 51578499).

---

## References

- Hobbs, N.B.: Mire morphology and the properties and behaviour of some British and foreign peats. *Q. J. Eng. Geol.* **19**, 7–80 (1986)
- Landva, A.O., Korpijaakko, E.O., Pheeney, P.E.: Geotechnical classification of peats and organic soils. Testing of peat and organic soils, STP 820, ASTM, West Conshohocken, pp. 37–51 (1983)
- Radforth, N.W.: Classification of muskeg. In: MacFarlane, I.C. (ed.) *Muskeg Engineering Handbook*. Canadian Building Series. University of Toronto Press (1969)
- Shi, S.: The request of dredging West Lake in Hangzhou. [http://www.blog.sina.com.cn/s/blog\\_500bc46501012fe3.html](http://www.blog.sina.com.cn/s/blog_500bc46501012fe3.html) (1090) (in Chinese)
- von Post, L.: Sveriges Geologiska Undersöknings torvinventering och nogra av dess hittills vunna resultat (SGU peat inventory and some preliminary results). *Svenska Mosskulturforeningens Tidskrift*, Jonkoping, Sweden **36**, 1–37 (1922)
- Yang, Z.X., Zhao, C.F., Xu, C.J., Wilkinson, S.P., Cai, Y.Q., Pan, K.: Modelling the engineering behaviour of fibrous peat formed due to rapid anthropogenic terrestrialization in Hangzhou, China. *Eng. Geol.* **215**, 25–35 (2016)



# Geomechanical Investigation of High Priority Geothermal Strata in the Molasse Basin, Bavaria, Germany

Martin Potten, Bettina Sellmeier, Elena Mraz, and Kuroschi Thuro

## Abstract

Due to the increasing use of geothermal energy in Bavaria, Germany, over the last years, the practical experience in geothermal plant operation for heat and power generation has shown an evident need for research. Especially questions related to deep geothermal energy need to be answered, and the risk of geothermal exploration in the Molasse Basin and the crystalline rocks in the northern part of Bavaria should be reduced to optimize reservoir engineering. The Molasse Basin, extending along the northern flank of the Alps, represents an alpine foreland basin. Situated south of Munich, the basin offers ideal conditions for the use of hydrothermal geothermal energy. The petrothermal potential in crystalline rock is focused in the northern part of Bavaria. The development and use of this future technology initially requires extensive research but has outstanding future potential. In this context, the determination of rock mechanical parameters is indispensable for the subsequent modelling of hydrothermal and petrothermal reservoirs. For this purpose, laboratory tests were conducted using drilling samples as well as analogue samples from quarries. Based on the results of these experiments a database has been created. This database improves the knowledge of the mechanical properties of representative rock types. Furthermore, the database improves the knowledge about detection of a local stress field, which has major impact on the hydraulic system of the geothermal reservoir. The outcome of this research should increase profitability and minimize risk of geothermal projects.

## Keywords

Geomechanic • Molasse basin • Geothermal research

## 1 Deep Geothermal Energy in Bavaria

### 1.1 Research Gap: Geomechanical Parameter Characterization

The local stress field has a major impact on the hydraulic system of a geothermal reservoir. An extensive and precise knowledge of the reservoir properties is necessary to complete a geothermal project successfully. Understanding the local stress field and the fractures around the bore hole is the key to an improving inflow from the reservoir into the exploration well. Since Barton et al. (1995) found that critical fractures are more often hydraulically active than uncritically stressed fractures, the geomechanical reservoir parameters describing the field of tension are important for the exploration of geothermal projects. The quality of these parameters depends on the identification of the deposit properties of the period and cost-intensive exploratory drillings. Due to the high costs, there are not enough. Deep core holes typically reach depths of several thousand meters. Because it is very expensive to drill them. The existing deep core holes were created during the course of the hydrocarbon exploration. Most of the data pool is limited to rock formations that were relevant for the oil industry. The database for geothermal host rock formations is very small.

In order to complete this database, various studies by Clauser and Huenges (1995), Clauser et al. (2002), Koch et al. (2007, 2009) have provided characteristic rock parameters. However, the geomechanical parameters describing the local stress field around the borehole, were not covered sufficiently. Homuth (2014) first published geomechanical rock mass parameters on analogue samples from different outcrops. Due to the small number of available samples, his general statement about the geomechanical reservoir characteristics was not useful.

The aim of this work is to fill the database with geomechanical parameters of analogue and drilled core samples. The parameters will therefore improve the understanding of

M. Potten (✉) · B. Sellmeier · E. Mraz · K. Thuro  
Technical University of Munich, Arcisstr. 21,  
80333 Munich, Germany  
e-mail: martin.potten@tum.de

the hydraulic inflow to the reservoir. This work will reduce the geothermal exploration risk in the north Alpine foreland basin (so-called Molasse Basin) and will optimize the reservoir engineering in the northern part of Bavaria in crystalline rock.

## 2 High Priority Geothermal Strata

### 2.1 Molasse Basin: Upper Jurassic Carbonates

The target formations of the geothermal reservoirs in the Molasse Basins are the Upper Jurassic carbonates (Malm) (Fig. 1). These rocks are underlain by Permo-Carboniferous troughs and Variscan crystalline complex (Lemcke 1988). The basin is filled with Cenozoic sedimentary rocks, which are alternating sequences of sandstone with claystone (Meyer and Schmidt-Kaler 1989). Due to alpine tectonics and the formation of the Molasse Basin as a typical wedge-shaped foreland basin, synsedimentary fracture and fault zones influenced the Upper Jurassic carbonates (Büchi et al. 1965).

An epicontinental sea, connected to the northern part of the Tethys, was the deposit environment of the Upper Jurassic carbonates. The Upper Jurassic is composed of alternating sequences of limestone, marl and dolomites (Meyer and Schmidt-Kaler 1989).

In southern Germany, the Upper Jurassic is separated in a massive and bedded facies. The massive facies, also called reef facies, is built by reef and reef-like organisms. This

facies, can be dolomitized influencing the behavior of the carbonate rocks. The limestones were partially carstified by the uncovering and eroding of the Upper Jurassic limestones during the Cretaceous period (Koschel 1991).

Situated south of Munich, the basin offers ideal conditions for the use of hydrothermal geothermal energy. The requirement for the hydrothermal geothermal energy is the presence of a water-bearing formation, the Upper Jurassic carbonates. In a hydrothermal circuit, the hot water is pumped to the surface where the essential part of its heat energy is available via a heat exchanger to a secondary power plant circuit. The cooled thermal water is then traced back into the subsoil via a second borehole (injection borehole).

These carbonates exist there at depths between 3500 and 6000 m b.l.s. with host fluid temperatures between 65 and 120 °C. The thickness of the Upper Jurassic reservoirs can reach up to 400 m (Pomoni-Papaioannou et al. 1989). The Molasse Basin has a typical dip of 5° (Clauser et al. 2002) in the south-east direction, which results in an outcrop area north of the Basin (Fig. 2). The outcrops of this area (Swabian and Franconian Alb) reflect the properties of the geothermal reservoirs.

### 2.2 Northern Part of Bavaria: Crystalline Rock

The target formation of the northern part of Bavaria consist of different granite types of the Variscan basement. These rocks build the basement of the Franconian Basin,

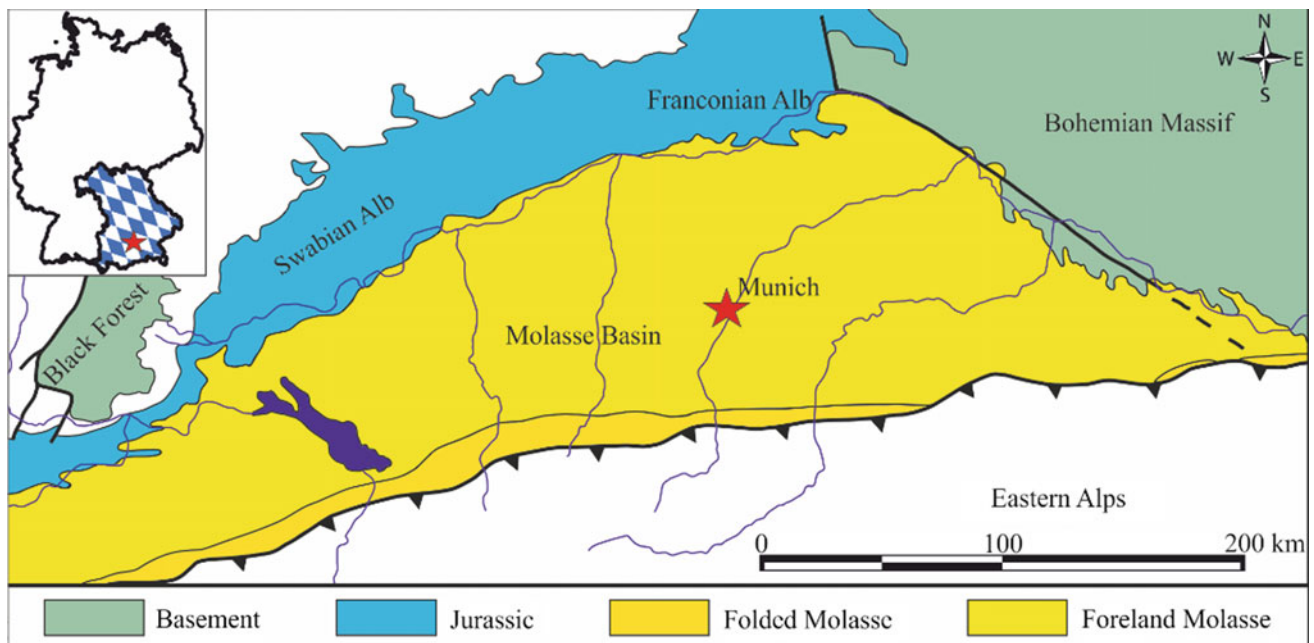


**Fig. 1** Geological overview map of the Molasse. According to Walter (2007)

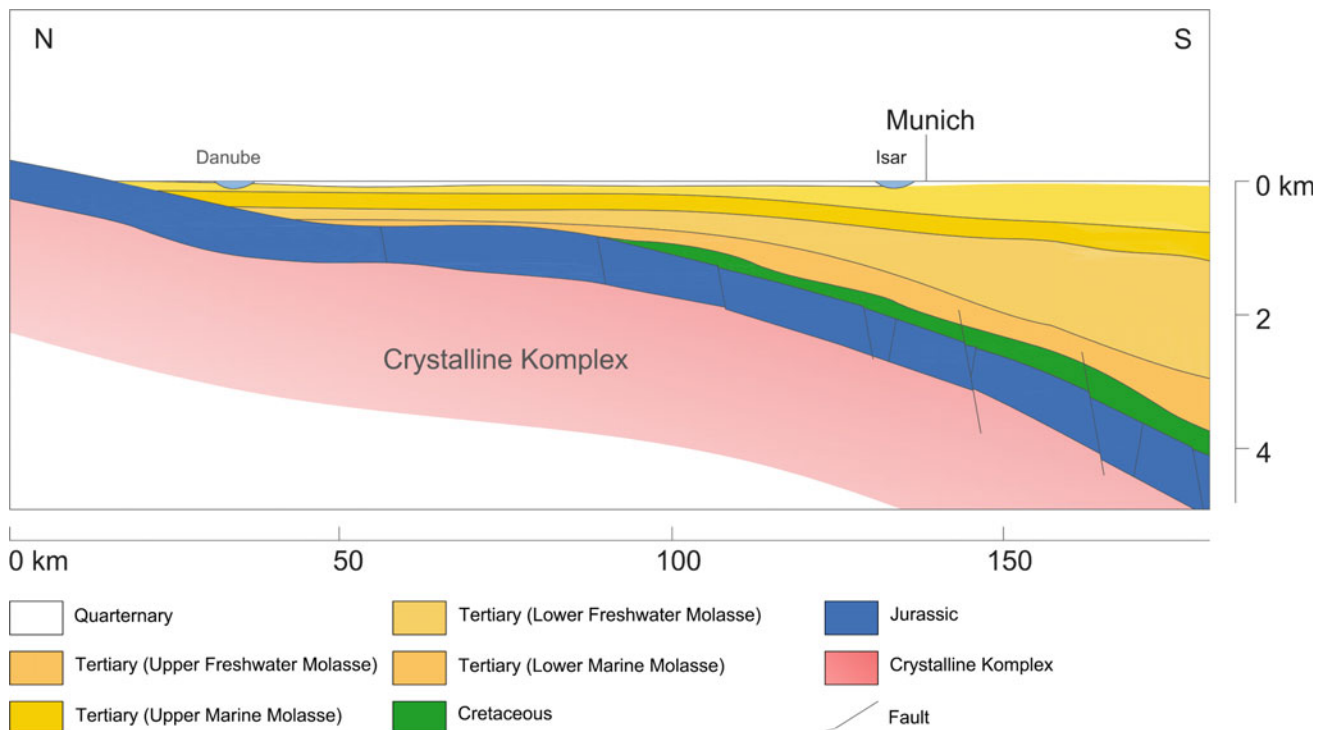


**Fig. 2** Geological cross-section of the Molasse Basin. Modified after Lemcke (1988)

a Permo-Mesozoic sedimentary platform. The sediments consist of sandstones, pelites, limestone and marls (Scharfberg et al. 2016).

The development of the Franconian basin begins with the end of the Variscian orogenesis. The Variscian Orogen has been subjected to uplift and erosion since the lower Carboniferous (Welzel 1991). The post-variscan development, characterized by a crustal collapse and an extension of the lithosphere, led to the formation of half trenches and ditches in the Upper Carboniferous. These intramontane basins locally covered over 2500 m sediments of the variscian mountain range (Bauer 2000).

During the Upper Carboniferous period, magma penetrated overlapping rocks and formed extensive granite plutons. These granites built subsurface granite bodies, which provide potential heat sources for the petrothermal geothermal energy. In contrast to the hydrothermal systems, petrothermal systems use the heat energy of the crystalline rock. In petrothermal systems, crystalline rock with a low permeability are used as a heat source. It should be noted that “petrothermal systems” include all geothermal reservoirs that have been influenced by engineering measures, either chemical or hydraulic stimulation (Stober and Bucher 2014). This stimulation enhances the permeability in the borehole area.

In Germany, about 95% of the geothermal energy potential is attributable to this technology (VBI 2013).

According to the zoning of the variscian orogen of Kossmat (1927), the field of interest (Franconian Basin) is situated within the saxothurian zone (Fig. 3; Riemer 2011). The first signals for increased underground temperatures were found during a drilling campaign in the 1970s and 1980s (Gudden 1981). In 2000 Bauer (2000) identified a regional geothermal anomaly. This local anomaly is located north of Bayreuth in the area of the Franconian Basin, in the spreading extension of the granite of the Fichtelgebirge. In this anomaly, the geothermal gradients reach up to 5 °C/100 m (Riemer 2011). In the Fichtelgebirge, the outcrops display properties of geothermal reservoirs. The Fichtelgebirge includes four different types of granite, which will be analyzed as analogue samples.

### 3 Materials and Methods

To carry out a geomechanical reservoir characterization of high priority geothermal strata, drill cores from Bavaria were already searched for in the existing database of the geothermal information system (GeotIS). The discovered wells, which were drilled in Bavaria, are compared with the Lower Saxony Soil Information System (NIBIS). This information system contains the cored boreholes (Müller and Waldeck 2011). The samples have been selected from different depths of the drillings in order to characterize the high

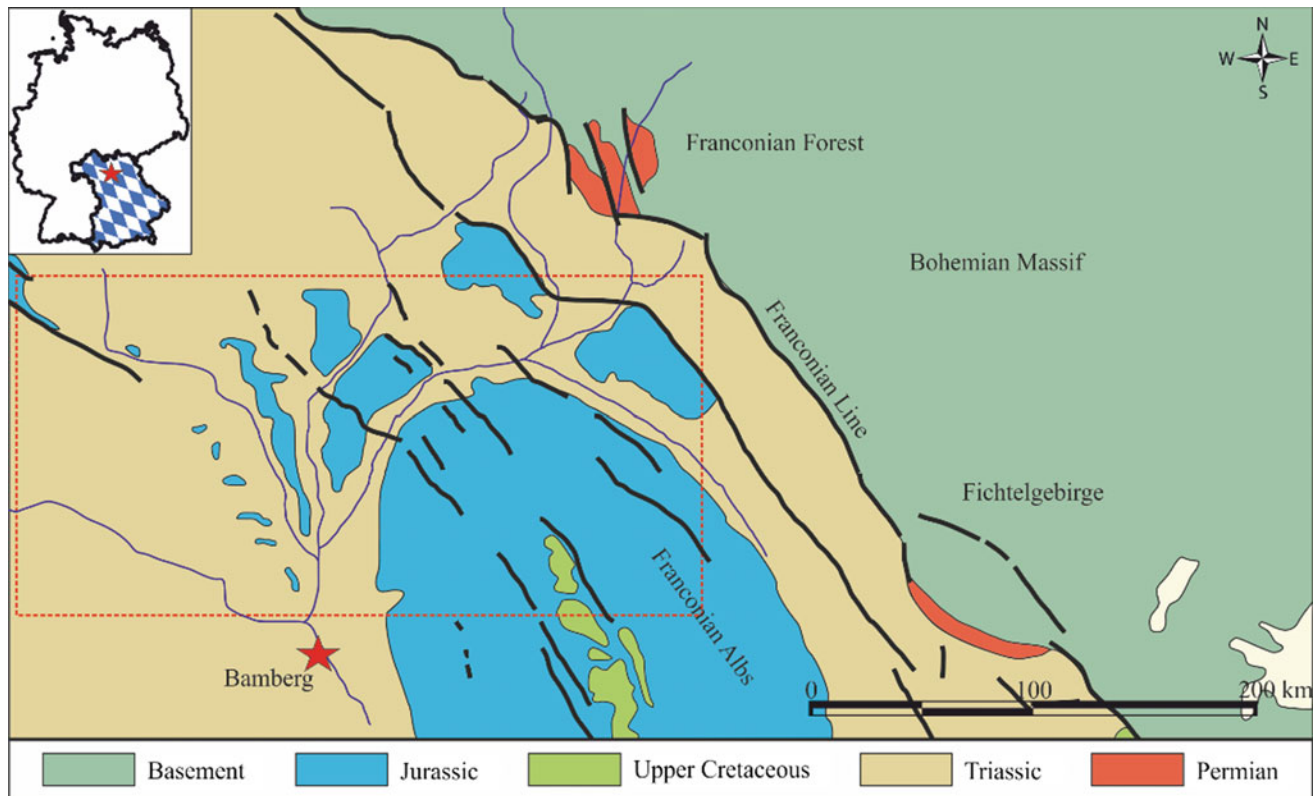


**Fig. 3** Geological overview map of the target area (marked area) (Riemer 2011)

geothermal strata completely geomechanically. Historically not all companies release the cores for sampling, so analogue samples of outcrops from quarries are also taken (Alber and Backers 2015). The analogue samples have the advantage that they are available in large quantities and are therefore easy to sample. Together with the core samples of former oil drillings, they form the material for this research.

The analogue samples should originate from the same rock formations (stratigraphy, lithology, facies) as the samples of the drillings to characterize the respective reservoir aquifer (Philipp et al. 2007). The core drillings and quarries are present in all parts of Bavaria so that the aquifer can be studied throughout the region. In order to characterize the reservoir in a geomechanical manner, a large number of samples is required.

After the core samples from drillings and analogue samples from quarries have been collected, laboratory tests are carried out on these samples.

After the drilling cores have been overcored or the analogue samples have been drilled, they are cut to length and prepared with an end face grinder. To measure the geomechanical properties of the samples, and to create reproducible results, the samples are dried at 105 °C to mass constancy and then cooled to 20 °C in an exsiccator. For the statistical

validation of the measured values, 5–10 individual measurements of the respective characteristic values are carried out.

The laboratory program includes the following tests:

- (1) Ultrasonic tests (US)/non-destructive tests

The US tests are carried out according to DIN EN ISO 16810. The P-shaft serves as an indicator of porosity. The transversal shaft (S-shaft) combined with the P-shaft determine the dynamic modulus of elasticity ( $E_{dyn}$ ) and the Poisson's ratio.

- (2) Uniaxial Compressive Test

The UCT tests are carried out according to the test recommendation of the DGGT (2004) in order to determine the rock strength and to correlate the strength with its other properties. In addition, knowing determined strength, statements can be made about the depth of the loosening and thus the prevailing stress conditions (Hoek and Martin 2014). The deformation modulus, the Young's Modulus transverse expansion destruction work according to Thuro (1996) have been determined.

### (3) Tensile Test (Brazilian Test)

The tensile strength of the test specimen is determined indirectly by the tensile splitting strength. The relevant tests are carried out in accordance with the recommendation of DGGT (2008).

### (4) Triaxial Compressive Test

The triaxial compression tests are carried out according to DIN 18137-2. To measure under simulated geothermal reservoir conditions a Thermo-Triax-Cell simulating have been used. The Mohrian voltage circuits determine the following parameters: Angle of internal friction and the Cohesion.

In order to get a prognosis of tool wear during drilling, two different abrasiveness tests are carried out. These results complete the geomechanical database.

### (5) Cerchar Abrasivity Test

The Cerchar Abrasiveness Index (CAI) assesses the abrasive properties of the samples by scratching (Cerchar 1986, recommendation 23 according to DGGT 2016).

### (6) LCPC Abrasivity Test

The LCPC abrasiveness test determines the abrasiveness of the rock, in the form of the LCPC abrasiveness coefficient LAK, by grinding (AFNOR 1990; Thuro et al. 2006; Thuro and Käsling 2009).

All results serve as input parameters for geomechanical reservoir simulations.

## 4 Objectives and Research Questions

Two areas in Bavaria are unique in terms of their geothermal potential, the Upper Jurassic carbonates in the South Molasse Basin and the crystalline rock in North East Bavaria. The geomechanical characterisation is an important criterion for the characterization of crystalline and sedimentary geothermal aquifers. However, there are still considerable uncertainties regarding the minimization of the exploration risk and the safe development of the geothermal potential.

In order to reduce these uncertainties, the following research questions will be addressed:

1. Which geomechanical parameters have
  - (a) the project-relevant Upper Jurassic carbonates and
  - (b) the project-specific granite of Northern Bavaria?
2. Which local stress situation exists around the borehole?

3. Which failure mechanisms can be deduced and which stress redistributions can be identified?

The intended research aims answer the posed questions and contribute to the geomechanical characterization of the rock of the geothermal drillings.

## 5 Summary

Analogue studies offer the possibility to generate a comprehensive data base of geothermal rock parameters in a cost-efficient way. This is also of particular interest if there is not a sufficient number of deep core drillings, which is currently the case in the Molasse Basin area. The results of the geomechanically investigations will present a data set of previously unachieved quality and quantity.

The suggested database will enable an improved prognosis with a quantification of the uncertainty of rock properties. A successful reservoir exploration, modelling and management directly depends on the quality of the input data and the general understanding of the system. The database obtained within the scope of this research will be applied in future projects to assure a sustainable data basis.

**Acknowledgements** Funding came from the Bavarian State Ministry of Education, Science and the Arts in the frame of the project Geothermal-Alliance Bavaria.

## References

- Alber, M., Backers, T.: Erforschung der Mechanismen und Simulation hydraulisch induzierter Risse in geklüfteten Gesteinen für die Optimierung des Aufschlusses geothermischer Lagerstätten. In: Abschluss zum Verbundprojekt des BMWi mit dem Förderkennzeichen 0325279A & 0325279B, 136 p (2015)
- Barton, C.A., Zoback, M.D., Moos, D.: Fluid-flow along potentially active faults in crystalline rock. *Geology* **23**, 683–686 (1995)
- Bauer, W.: Geothermische Verhältnisse des Fränkischen Beckens (Nordbayern/Südthüringen). Lehr- und Forschungsbereich Hydrogeologie und Umwelt, Würzburg, 186 p (2000)
- Büchi, U., Lemcke, K., Wiener, G., Zimdars, J.: Geologische Ergebnisse der Erdölexploration auf das Mesozoikum im Untergrund des schweizerischen Molassebeckens. *Bulletin der Schweizerischen Vereinigung von Petroleum-Geologen und Ingenieuren* **15**, 7–38 (1965)
- Clauser, C., Deetjen, H., Höhne, F., Rühaak, W., Hartmann, A., Schellschmidt, R., Rath, V., Zschocke, A.: Erkennen und Quantifizieren von Strömung: Eine geothermische Rasteranalyse zur Klassifizierung des tiefen Untergrundes in Deutschland hinsichtlich seiner Eignung zur Endlagerung radioaktiver Stoffe. In: Endbericht zum Auftrag 9X0009-8390-0 des Bundesamtes für Strahlenschutz (BfS), Applied Geophysics and Geothermal Energy E.ON Energy Research Center, 159 p, Aachen (2002)
- Clauser, C., Huenges, E.: Thermal conductivity of rocks and minerals. In: Ahrens, T.J. (ed.) *Rock Physics and Phase Relations: A*

- Handbook of Physical Constants, AGU Reference Shelf, 3, pp. 105–126. American Geophysical Union, Washington (1995)
- DGGT: Empfehlung Nr. 10 des Arbeitskreises 3.3 “Versuchstechnik Fels” der Deutschen Gesellschaft für Geotechnik e. V.: Indirekter Zugversuch an Gesteinsproben – Spaltzugversuch. Bautechnik **85** (9), 623–627, Ernst & Sohn, Berlin (2008)
- DIN 18137-2: Baugrund, Untersuchung von Bodenproben - Bestimmung der Scherfestigkeit - Teil 2: Triaxialversuch, Beuth Verlag, Berlin (2011)
- DIN EN ISO 16810: Zerstörungsfreie Prüfung – Ultraschallprüfung – Allgemeine Grundsätze (ISO 16810:2012), Beuth Verlag, Berlin (2014)
- Gudden, H.: Über Thermal-Mineralwasser-Bohrungen im Coburger Umland. Jahresberichte und Mitteilungen des Oberrheinischen Geologischen Vereins **63**, 229–252 (1981)
- Hoek, E., Martin, C.D.: Fracture initiation and propagation in intact rock—a review. *J. Rock Mech. Geotech. Eng.* **6**, 287–300 (2014)
- Homuth, S.: Aufschlussanalogstudie zur Charakterisierung oberjurasischer geothermischer Karbonatreservoirs im Molassebecken. Dissertation Technische Universität Darmstadt, Darmstadt, 314 p (2014)
- Käsling, H. & Plinninger, R.: Empfehlung Nr. 23 des Arbeitskreises 3.3 “Versuchstechnik Fels” der Deutschen Gesellschaft für Geotechnik e. V.: Bestimmung der Abrasivität von Gesteinen mit dem CERCHAR-Versuch. Bautechnik **93**(6), 409–415, Ernst & Sohn, Berlin (2016)
- Koch, A., Hartmann, A., Jorand, R., Mottaghy, D., Pechinig, R., Rath, V., Wolf, A., Clauser, C.: Erstellung statistisch abgesicherter thermischer und hydraulischer Gesteinseigenschaften für den flachen und tiefen Untergrund in Deutschland (Phase 1 – Westliche Molasse und nördlich angrenzendes Süddeutsches Schichtstufenland). In: Schlussbericht zum BMU-Projekt FKZ 0329985, Aachen, 220 p (2007)
- Koch, A., Jorand, R., Arnold, J., Pechinig, R., Mottaghy, D., Vogt, C., Clauser, C.: Erstellung statistisch abgesicherter thermischer und hydraulischer Gesteinseigenschaften für den flachen und tiefen Untergrund in Deutschland (Phase 2 – Westliches Nordrhein-Westfalen und bayerisches Molassebecken). In: Abschlussbericht zum BMU-Projekt FKZ 0329985, Aachen, 174 p (2009)
- Koschel, G.: Geologischer Überblick–Hydrogeologische Randbedingungen, München, Freiburg i. Br (1991)
- Kossmat, F.: Gliederung des varistischen Gebirgsbaues. Abhandlungen der sächsischen geologischen Landesanstalt. 1, 1–39, Leipzig (1927)
- Lemcke, K.: Das Bayerische Alpenvorland vor der Eiszeit: Erdgeschichte, Bau, Bodenschätze. Geologie von Bayern I. Schweizerbart, Stuttgart (1988)
- Meyer, R.K.F. & Schmidt-Kaler, H.: Paläogeographischer Atlas des süddeutschen Oberjura (Malm). Bundesanstalt für Geowissenschaften und Rohstoffe und den Geologischen Landesämtern in der Bundesrepublik Deutschland, Hannover, 77 p (1989)
- Mutschler, T.: Neufassung der Empfehlung Nr. 1 des Arbeitskreises “Versuchstechnik Fels” der Deutschen Gesellschaft für Geotechnik e. V.: Einaxiale Druckversuche an zylindrischen Gesteinsprüfkörpern. Bautechnik **81**(10), 825–834, Ernst & Sohn, Berlin (2004)
- Müller, U. & Waldeck, A.: Auswertungsmethoden im Bodenschutz: Dokumentation zur Methodenbank des Niedersächsischen Bodeninformationssystems (NIBIS®). In: GeoBerichte 19, Landesamt für Berbau, Energie und Geologie (LBEG), 416 p, Hannover (2011)
- N F (NORMALISATION FRANÇAISE) P18-579 (AFNOR): Granulats - Détermination des coefficients d’abrasivité et de broyabilité. Paris: AFNOR Association française de normalisation, AFNOR (1990)
- Philipp S.L., Gudmundson A., Oelrich A.R.I.: How structural geology can contribute to make geothermal projects successful. In: European Geothermal Congress 2007, Unterhaching, 10 p (2007)
- Pomoni-Papaioannou, F., Flügel, E., Koch, R.: Depositional environments and diagenesis of Upper Jurassic subsurface sponge- and tubiphytes reef limestones: Altensteig 1 well, western Molasse Basin, Southern Germany. *Facies* **21**, 263–283 (1989)
- Riemer, A.: Kluff- und Störungssysteme im westlichen Oberfranken und Eigenschaften des Temperaturfeldes mit Fokus auf die Mürsbacher Temperaturanomale. Unveröffentlichte Diplomarbeit, Geozentrum Nordbayern, 86 p (2011)
- Scharfenberg, L., de Wall, H., Bauer, W.: In situ gamma radiation measurements on Variscan granites and inferred radiogenic heat production, Fichtelgebirge, Germany. *Zeitschrift der Deutschen Gesellschaft für Geowissenschaften* **167**(1), 19–32 (2016)
- Stober, I., Bucher, K.: Geothermie, 2nd edn. Springer, Heidelberg, 306 p (2014)
- Thuro, K.: Bohrbarkeit beim konventionellen Sprengvortrieb - Geologisch-felsmechanische Untersuchungen anhand sieben ausgewählter Tunnelprojekte. *Münchner Geologische Hefte* **1**, 149 (1996)
- Thuro, K., Singer, J., Käsling, H., Bauer, M.: Abrasivitätsuntersuchungen an Lockergesteinen im Hinblick auf die Gebirgslösung. In: Deutsche Gesellschaft für Geotechnik: Beiträge zur 29. Baugrundtagung 27. - 29. Sept. 2006, Bremen, pp. 283–290 (2006)
- Thuro, K., Käsling, H.: Classification of the abrasiveness of soil and rock. *Geomechanik und Tunnelbau*, **2**(2), 179–188 (2009)
- VBI (Verband Beratender Ingenieure): VBI-Leitfaden Tiefe Geothermie. Schriftenreihe der VBI **21**, 108 (2013)
- Walter, R.: Geologie von Mitteleuropa. 7 edn. Schweizerbart, Stuttgart, 511 p (2007)
- Welzel, B.: Die Bedeutung von K/Ar-Abkühlaltem an detritischen Muskoviten für die Rekonstruktion tektonometamorpher Einheiten im orogenen Liefergebiet - ein Beitrag zur Frage der varistischen Krustenentwicklung in der Böhmisches Masse. *Göttinger Arbeiten zur Geologie und Paläontologie* **49**, 61 (1991)

# The Potential Use of Residual Soil from Ribeira Valley (Brazil) in Mitigating Metal Contamination: A Geotechnical Characterization

Jéssica Pelinsom Marques<sup>✉</sup>, Valéria Guimarães Silvestre Rodrigues<sup>✉</sup>,  
Orencio Monje Vilar<sup>✉</sup>, and Edmundo Rogério Esquivel<sup>✉</sup>

## Abstract

The incorrect disposal of hazardous waste causes serious problems around the world. For instance, mining waste is one of the main sources of potentially toxic metals in the environment. In the Ribeira Valley region of Brazil, residues generated during lead ore smelting were improperly deposited in the Ribeira de Iguape River and on the soil's surface without protection. An alternative solution for mitigating local contamination is verifying whether a local residual soil is appropriate to use as a mining waste landfill liner. The soil is sandy silty clay, with a plasticity index of 24%, an optimum water content,  $w_{opt}$ , of 26.3% and a maximum dry density,  $\rho_{dmax}$ , of 1.515 g/cm<sup>3</sup> from the Standard Proctor test. Specimens molded at an optimum compaction condition showed hydraulic conductivity of 10<sup>-9</sup> m/s and effective shear strength parameters of  $c' = 22$  kPa and  $\phi' = 26.8^\circ$ . The soil is acidic (pH 4.6), exhibits low CEC (41.4 mmol<sub>c</sub>/dm<sup>3</sup>) and presents a predominance of negative charges on the particle surface (PZSE 3.6 < pH), favoring cation retention. The hydraulic and mechanical characteristics together with the chemical properties suggest that this soil is a candidate for use as a liner. Further studies are underway to characterize its chemical contaminant retention and to complete the analysis about its suitability for the desired purpose.

## Keywords

Tropical soil • Liner • Metal contamination

## 1 Introduction

Inadequate disposal of hazardous waste causes serious problems around the world. Substances present in such waste can be released into the environment and affect its quality. For instance, potentially toxic metals can be absorbed by and accumulate in various lifeforms and persist for decades in the environment (Lester 1987; Alloway 1995).

Potentially toxic metals originate in natural or anthropic processes, and their toxic effects depend on the quantity of the ions available for cation exchange (Sparks 1995; Sposito 1984). One of the main sources of metals in the environment is the incorrect disposal of mining waste that contains these elements. In the Ribeira Valley of Brazil, residues generated during the lead (Pb) ore smelting process were improperly deposited in the Ribeira de Iguape River. Between 1991 and 1995, waste was deposited directly onto the soil surface without base or cover protection. Thus, the river and soil were contaminated by metals such as Pb and cadmium (Cd) (Kasemodel et al. 2016).

An alternative to minimize mining waste contamination is the deposition of residues in a waste containment facility with liner and cover systems. A liner's function is waterproofing and contaminant retention (Daniel 1993; Rowe et al. 1995). Besides low hydraulic conductivity and adequate shear strength, the material selected for the construction of a sealant barrier must have favorable characteristics to retain the contaminants, and resistance to chemical elements and to the erosive process (Bradl 2004). In the context of the Ribeira Valley problem, an alternative is the use of local soil as a liner. It's a residual soil formed under tropical climate, for which there is still little information related to its contaminant retention ability. Thus, the purpose of the current study is to characterize a residual soil collected in the Ribeira Valley, to verify whether it presents suitable properties to be used as a sealant barrier in mining waste containment facilities.

J. P. Marques (✉) · V. G. S. Rodrigues · O. M. Vilar · E. R. Esquivel

São Carlos School of Engineering, University of São Paulo, São Carlos, SP 13566-590, Brazil  
e-mail: jessica.pelinsom.marques@usp.br

V. G. S. Rodrigues  
e-mail: valguima@usp.br

## 2 Materials and Methods

The studied soil is a residual soil from the municipality of Eldorado Paulista, in the Ribeira Valley of Brazil. Figure 1 shows an overview map of the region.

The soil was collected in the superficial portion of the profile (0–40 cm). It was a highly weathered pink and white colored soil. It is a residual soil resulted from shale rock alteration. The soil was collected in the coordinates S 24° 31' 12" e W 48° 04' 37". The samples were shade dried, quartered and homogenized. This study includes measuring soil geotechnical properties and characteristics. The properties and characteristics considered were particle size distribution, according to Brazilian standard NBR 7181/2016 (ABNT 2016); consistency limits [NBR 6459/1984 from ABNT (1984) and NBR 7180/1984, also from ABNT (1984)]; and Standard Proctor compaction test [NBR 7182/1986 from ABNT (1986)]. Subsequently, three compacted cylindrical specimens of 5 cm in diameter and 10 cm in height were prepared under the optimum conditions for measuring hydraulic conductivity and shear strength. The hydraulic conductivity tests were conducted using triaxial cells as flexible wall permeameters (Head 1998). Shear strength tests were consolidated undrained (CU) with consolidation stresses,  $\sigma'_3$ , of 50, 100 and 200 kPa. The failure was indicated by the peaks in the curves  $\sigma'_1/\sigma'_3$  against axial strain. Mohr-Coulomb criterion yielded shear strength parameters

for both total and effective stresses, according to Eqs. (1) and (2), respectively:

$$\tau = c + \sigma \cdot \tan(\varphi) \quad (1)$$

$$\tau = c' + \sigma' \cdot \tan(\varphi') \quad (2)$$

In these equations,  $c$  and  $\varphi$  are the total cohesion and shear strength angle,  $c'$  and  $\varphi'$  are the effective cohesion and shear strength angle.

The study also included soil chemical tests following geotechnical tests. Soil pH measurement were taken in distilled water and in KCl solution as described by the Brazilian Agricultural Research Corporation (EMBRAPA) (Empresa Brasileira de Pesquisa Agropecuária 2011). The procedure was performed in triplicate and the pH readings were taken with a Digimed DH21 pHmeter with a glass electrode. The results allowed for the calculation of  $\Delta\text{pH}$  ( $\text{pH}_{\text{KCl}} - \text{pH}_{\text{H}_2\text{O}}$ ), providing information about the surface electrical charges of the particles.

The PZSE—Point of Zero Salt Effect was measured through a potentiometric titration (Alleoni et al. 2016). HCl was used as an acid, NaOH as a base and KCl as the electrolyte.

The organic matter (OM) content was determined through oxidation with a potassium dichromate solution in the presence of sulfuric acid (Camargo et al. 2009). Cation exchange capacity was obtained through the sum of the bases method (Embrapa 1997).

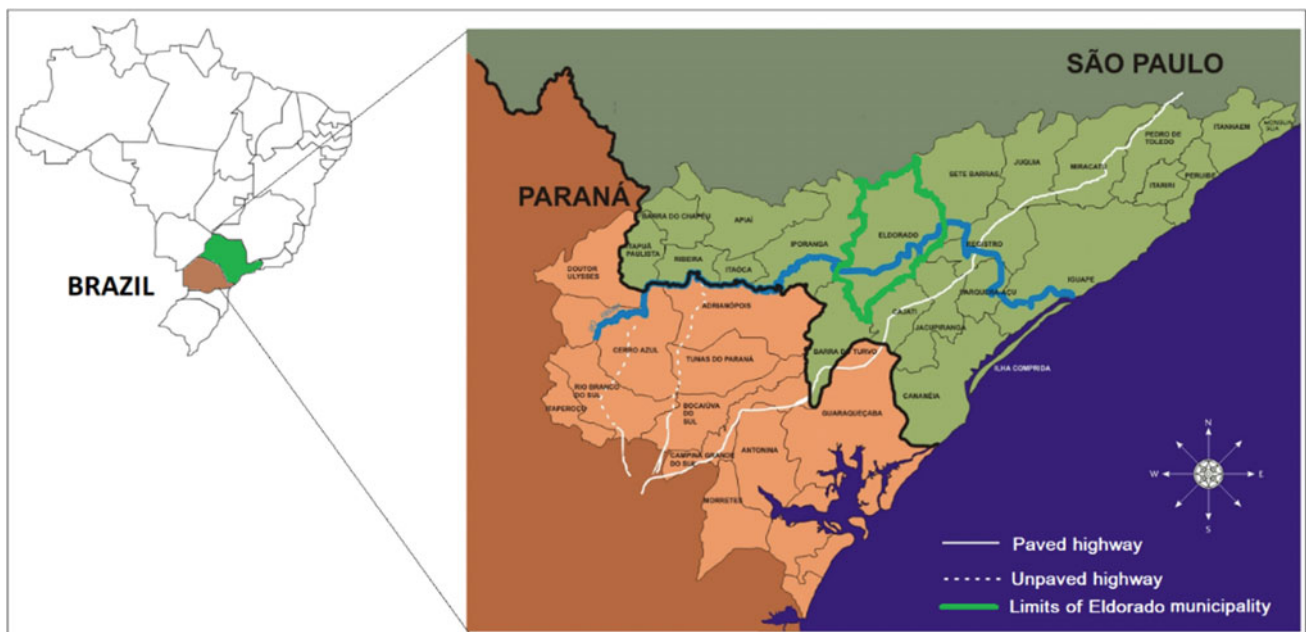


**Fig. 1** Overview map of the Ribeira Valley region, highlighting Eldorado municipality. Adapted from Vale do Ribeira Program, Federal University of Paraná (UFPA)



### 3 Results and Discussion

Table 1 shows the results from soil geotechnical characterization tests. A predominance of fines (54.5% clay and 20.4% silt) was observed, which is a favorable characteristic, since the natural materials adsorption capacity is strongly influenced by its surface area exposed to reactions and therefore by the particle size (Langmuir 1997). Also, these proportions satisfy the recommended literature suggestions for the use of clayey soil as liners that are a minimum of 20% clay (Rowe et al. 1995) and 30% fines (silt + clay) (Benson et al. 1994).

Also from Table 1, the soil LL is 58% and the PI is 24% that classifies the soil as CL in the Unified Soil Classification System (American Society for Testing and Materials 2000), i.e., an elastic clay of low plasticity, lean clay. PL and PI values obtained for the residual soil comply with the literature recommendations for a good performance as sealant barrier, since typical recommendations indicate a minimum PL of 20% and a minimum PI of 7% (Benson et al. 1994).

Figure 2 shows the compaction curve of the soil that presented an optimum water content,  $w_{opt}$ , of 26.3% and a maximum dry density,  $\rho_{dmax}$ , of 1.515 g/cm<sup>3</sup> through a Standard Proctor test. Table 2 shows the conditions of the compacted specimens used in the hydraulic and triaxial shear tests. The hydraulic conductivity was  $6.5 \times 10^{-9}$  m/s. This result is in the same order of magnitude of the recommendations found in literature about soils to be used as liners (Daniel 1993; Rowe et al. 1995; Benson et al. 1994; United States Environmental Protection Agency 1989).

Figure 3 shows the shear strength envelopes. For total stress, cohesion was 34 kPa and the friction angle was 13.5°. Effective parameters were cohesion of 22 kPa and friction angle of 26.8°, figures consistent to those typically observed for soils classified as CL in the Unified Soil Classification System (Carter and Bentley 1991).

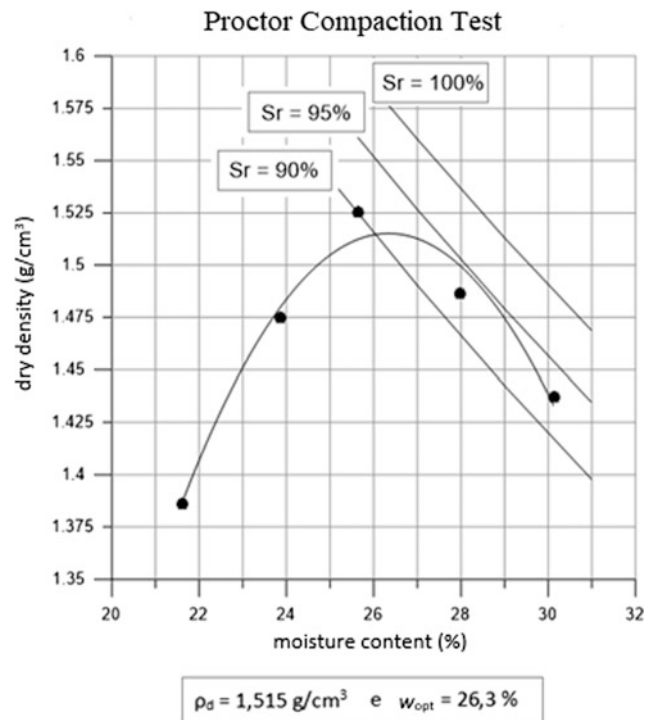


Fig. 2 Proctor compaction curve of the Ribeira Valley soil

Table 3 summarizes the results of hydraulic conductivity and shear strength tests.

Finally, Table 4 gathers the chemical test results. The soil CEC is 41.4 mmol<sub>c</sub>/dm<sup>3</sup>. CEC demonstrates a soil's ability to retain and exchange positively charged ions on the colloidal surface. Therefore, it is important in soil characterization, mainly for studying contaminant retention. The CEC value obtained for the studied soil suggests a predominance of low activity non-expansive clay minerals such as kaolinite, and a possible presence of Fe oxides. The typical range of CEC values for kaolinite is 50–150 mmol<sub>c</sub>/dm<sup>3</sup>,

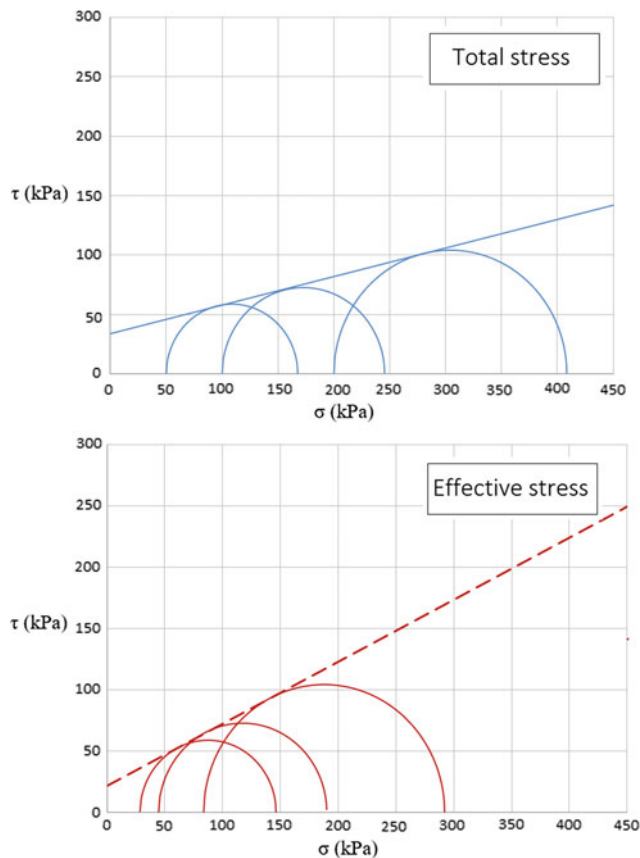
**Table 1** Geotechnical characteristics of the Ribeira Valley residual soil

Parameter	Unit	Average value
Clay content	%	54.4
Silt content	%	20.4
Fine sand content	%	13.4
Medium sand content	%	7.0
Coarse sand content	%	3.8
Gravel content	%	1.0
Liquid limit LL	%	58
Plastic limit PL	%	34
Plasticity index PI	%	24
Optimum water content $w_{opt}$	%	26.3
Maximum dry density $\rho_{dmax}$	g/cm <sup>3</sup>	1.515

**Table 2** Conditions of the compacted specimens used in the triaxial shear tests

Specimen	$w_m$	$w_m - w_{opt}$	$\rho_d$ (g/cm <sup>3</sup> )	RC	e	$\eta$ (%)	Sr (%)
1	25.8	-0.5	1.514	99.9	0.799	44.4	87.9
2	25.7	-0.6	1.513	99.9	0.800	44.4	87.5
3	24.9	-1.4	1.526	100.7	0.785	44.0	86.4

Obs.:  $w_m$ —molding water content; RC =  $100 \cdot \rho_d / \rho_{dmax}$ —Relative compaction; e—void ratio; n—porosity; Sr—degree of saturation

**Fig. 3** Determination of strength parameters of the soil from Ribeira Valley (Brazil) by Mohr-Coulomb failure criterion

and for Fe oxides is 20–50 mmol<sub>c</sub>/dm<sup>3</sup> (de Mello et al. 1983). Kaolinite and Fe oxides are common in intensely weathered soils formed in tropical environments, especially in near the surface (Fookes 1997).

The soil's organic matter content is 9 g/kg. Soil organic matter plays an important role in its metal retention capacity.

The pH of the soil measured in water is 4.6. This condition favors metal mobility because it allows the metals to remain free in the solution (Sparks 1995). In addition, pH influences the surface charge of Al, Fe, Mn and Si oxides and hydroxides, and clay minerals like kaolinite (Langmuir 1997). The soil pH measured in the KCl solution is 3.7. Thus,  $\Delta pH$  is -0.9, a negative value that indicates a predominance of negative charges on the surface of colloidal particles of soil. PZSE also provide information about the

**Table 3** Results of hydraulic conductivity and shear strength tests

Parameter	Unit	Average value
Hydraulic conductivity, k	m/s	$6.5 \times 10^{-9}$
Total cohesion c	kPa	34
Total shear strength angle $\phi$	°	13.5
Effective cohesion c'	kPa	22
Effective shear strength angle $\phi'$	°	26.8

**Table 4** Parameters obtained from the Ribeira Valley residual soil characterization tests

Parameter	Unit	Average value
CEC	mmol <sub>c</sub> /dm <sup>3</sup>	41.4
OM	g/kg	9
pH <sub>H<sub>2</sub>O</sub>	–	4.6
pH <sub>KCl</sub>	–	3.7
$\Delta pH$	–	-0.9
PZSE	–	3.6

charge of soil particles. The soil PZSE is 3.6. The value is lower than the pH measured in water. This is more evidence that the particles' surface charges are predominantly negative. These negative charges favor the retention of cations, such as potentially toxic metals (Sparks 1995; Sposito 1984).

## 4 Conclusion

The predominance of negative charges at the soil surface and the geotechnical characteristics suggest that this is a soil appropriate for composing a landfill liner, considering its texture, low permeability, low clay activity (indicating non-expansive clay) and shear strength. Thus, the use of the local soil as a liner to mitigate contamination is a feasible alternative for the recuperation of the region. For this reason, complementary chemical tests are underway to address the contaminant retention capacity of this tropical soil.

**Acknowledgements** The authors would like to thank the São Paulo Research Foundation (FAPESP) for funding through a master's degree grant (2016/17894-2) and research grant (2014/07180-7), and the National Council for Scientific and Technological Development (CNPq) for a research productivity grant (305096/2015-0).

## References

- Alleoni, L.R.F., Mello, J.W.V., Rocha, W.S.D.: Electrochemistry, adsorption and ion exchange in soils. In: Melo, V.F., Alleoni, L. R.F. (eds.) *Soil Chemistry and Mineralogy—Part II—Applications*. Sociedade Brasileira de Ciência do Solo, Viçosa (2016) (in Portuguese)
- Alloway, B.J.: *Heavy Metals in Soils*, 2nd edn. Blackie Academic & Professional, London (1995)
- American Society for Testing and Materials (ASTM): ASTM D2487. Standard Classification of Soils for Engineering Purposes (Unified Soil Classification System). ASTM International, West Conshohocken (2000)
- Associação Brasileira de Normas Técnicas (ABNT): NBR 7181. Standard test method for granulometric analysis of soils. ABNT, Rio de Janeiro (2016) (in Portuguese)
- Associação Brasileira de Normas Técnicas (ABNT): NBR 6459. Standard test method for liquid limit. ABNT, Rio de Janeiro (1984) (in Portuguese)
- Associação Brasileira de Normas Técnicas (ABNT): NBR 7180. Standard test method for plastic limit. ABNT, Rio de Janeiro (1984) (in Portuguese)
- Associação Brasileira de Normas Técnicas (ABNT): NBR 7182. Standard test method for soil compaction. ABNT, Rio de Janeiro (1986) (in Portuguese)
- Benson, C.H., Zhai, H., Wang, X.: Estimating hydraulic conductivity of compacted clay. *J. Geotech. Eng.* **120**(2), (1994)
- Bradl, H.B.: Adsorption of heavy metal ions on soils and soil constituents. *J. Colloid Interface Sci.* **277**, 1–18 (2004)
- Camargo, O.A., Moniz, A.C., Jorge, J.A., Valadares, J.M.A.S.: Methods of chemical, mineralogical and physical analysis of soils - Instituto Agronômico de Campinas. *Boletim Técnico* **106** (2009)
- Carter, M., Bentley, S.P.: *Correlations of Soil Properties*. Pentech Press, London (1991)
- Daniel, D.E.: *Geotechnical Practice for Waste Disposal*. Chapman & Hall, London (1993)
- Embrapa: *Manual of methods of soil analysis*. Centro Nacional de Pesquisa de Solos. Rio de Janeiro (1997) (in Portuguese)
- Empresa Brasileira de Pesquisa Agropecuária (EMBRAPA): *Methods of Soil Analysis* (in Portuguese) (2011)
- Federal University of Paraná (UFPA): Vale do Ribeira Maps. Available in: <http://www.valedoribeira.ufpr.br/mapas.htm> (in Portuguese)
- Fookes, P.G. (ed): *Tropical Residual Soils: A Geological Society Engineering Group. Working Party Revised Report*. The Geological Society, London (1997)
- Head, K.H.: *Manual of Laboratory Testing*, vol. 3, 2nd edn. Wiley, Chichester (1998)
- Kasemodel, M.C., Lima, J.Z., Sakamoto, I.K., Varesche, M.B.A., Trofino, J.C., Rodrigues, V.G.S.: Soil contamination assessment for Pb, Zn and Cd in a slag disposal area using integration of geochemical and microbiological data. *Environ. Monit. Assess.* **188**(698)
- Langmuir, D.: *Aqueous Environmental Geochemistry*. Prentice Hall, New Jersey (1997)
- Lester, J.N.: Heavy metals in waste water and sludge treatment process, vol. 2. In: *Treatment and Disposal*. CRC Press, Boca Raton, FL (1987)
- Rowe, R.K., Quigley, R.M., Brachman, R.W.I., Booker, J.R.: *Clayey Barrier Systems for Waste Disposal Facilities*. Chapman & Hall, London (1995)
- Sparks, D.L.: *Environmental Soil Chemistry*. Academic Press, London (1995)
- Sposito, G.: *The Surface Chemistry of Soils*. University Press, Oxford (1984)
- United States Environmental Protection Agency.: *Requirements for hazardous waste landfill design, construction and closure*. Seminar publication EPA (1989)
- de Mello, F.A., Brasil Sobrinho, M.O.C., Arzolla, S., Silveira, R.I., Cobra Neto, A., de Kiehl, J.C.: *Soil Fertility*. Nobel, São Paulo (1983) (in Portuguese)

# New Approach to the Assessment of Buildings Vulnerability in Various Natural and Technogenic Urban Conditions

V. Burova and E. Karfidova

## Abstract

This paper proposes a new approach for assessing the vulnerability of buildings using relative economic indicators that correspond to the standards and costs for inspection of the technical condition of a building. The total (cumulative) for carrying out works to measure and inspect the building are taken as the main indicator characterizing vulnerability. The analysis allowed identifying the main components forming total costs: category of building complexity, location of the building in engineering-geological conditions, category of work complexity, category of the technical condition of the building (normative/operable/limited operational condition), the number of inspections and inspection prices. Seven different scenarios of cumulative inspection costs that are most characteristic for large cities were considered. The value of total costs for the entire period is equal to the unit of relative economic vulnerability. The approach to assessing the relative economic vulnerability of buildings takes into account the metric, engineering and economic characteristics of the building and the engineering-geological conditions of its location, and is universal, operational and readily available.

## Keywords

Relative cumulative costs • Technical condition of building • Vulnerability • Scenario

## 1 Introduction

The vulnerability of a building of a certain type (material, design, number of floors, durability and other characteristics) can be estimated based on an assessment of the engineering

and geological conditions of the urbanized territory where the building is located. In assessing the engineering and geological conditions of the territory, a combination of natural and technogenic conditions is taken into account (Osipov et al. 2015, 2017). At the same time, a building vulnerability assessment is linked with the regulation of building maintenance safety. The regulatory framework for safety of buildings is defined in the Federal Law “Technical Regulations on the Safety of Buildings and Structures”. Federal regulations relating to health, safety and quality in the construction industry became necessary for purposes of technical regulation, town planning activities and fire safety (2009) (Federal Law of the Russian Federation 2009). The basic concepts introduced by this law, which play a decisive role in resolving the problem of natural risk and in assessing the vulnerability of buildings during their operation are as follows: Accident, Impact, Lifecycle of the Building or Structure, Engineering Protection, Mechanical Safety, Natural Hazards. Another basic standard is the interstate standard “Buildings and Structures. Rules of Inspection and Monitoring” (2011) (Interstate standard 2010). This standard is meant to be applied in the construction field in inspecting and monitoring the technical condition of buildings and structures, developing orders for project design, inspection and monitoring of buildings (structures) and in developing project documentation. Terms and definitions given in this standard: safety of a building (structure); complex inspection of the technical condition of a building (structure); inspection of the technical condition of a building (structure); technical condition category; general monitoring of the technical condition of buildings and structures.

The subject of the inspection is the building and its natural foundation (subgrade). The normative frequency and cost of inspection depend on three factors: (1) location in normal/unfavorable engineering and geological conditions, (2) complexity of the building and (3) complexity of the inspection work, which depends on the category of the technical condition of the building. These assumptions provide a basis for a method of assessing economic

V. Burova · E. Karfidova (✉)  
Institute of Environmental Geoscience RAS, Moscow, Russia  
e-mail: e.karfidova@yandex.ru

vulnerability of a building based on the calculation of cumulative relative costs.

## 2 Data Sources

Information support is based on the methodological provisions on engineering geological zoning (Golodkovskaya and Lebedeva 1984; Osipov et al. 2012), assessments of the vulnerability of capital-construction assets in Moscow (Osipov et al. 2017) and the general methodology for assessing natural risks (Osipov et al. 2017).

Sources of information for the method of assessing buildings vulnerability are:

- The map of engineering geological zoning of Moscow territory (Osipov et al. 2012);
- Categories of technical condition of buildings;
- Complexity of the building (Table 1);
- Complexity of the inspection work (Table 2);
- Prices for inspection work (Collection of basic prices ... 2013);
- Real Estate Cadastre of Moscow—information about the building: year of commissioning, material of load-bearing structures, number of floors/underground floors, etc.; <https://pkk5.rosreestr.ru/>;
- Information about location of the building in normal/unfavorable engineering geological conditions;
- Life cycle of the building (GOST 2010).

The map of engineering geological zoning of Moscow territory defines three hazard zones: low (green color), medium (yellow color) and high (pink color) and delineates engineering geological massifs with an index of a hazardous process. Hazardous processes are indexed as follows: 1—flooding, 2—shallow landslides, 3—potential karst-suffusion, 4—karst-suffusion, 5—deep landslides, 6—technogenic soils, 7—weak soils.

There are 4 categories of technical condition of buildings:

1. Normative
2. Operable
3. Limited operational
4. Emergency condition (not considered in the method).

**Table 1** Categories of building complexity

Category	Category characteristics	Technical condition of the building
I	Depth of foundations: no more than 1.5 m; no groundwater in the pits; 1–2 masonry types. Wall material: 1 type. Floor structures with a simple structural design, symmetrical loads, rectangular load areas	Normative
II	Depth of foundations: 1.5–3.0 m; a moderate inflow of water into the pits with periodic dewatering as necessary; 3 masonry types. Wall material: 2 types. Floor structures with a complex structural design, load areas of various shapes. Different types of rooms within a floor	Normative
III	Depth of foundations: more than 3.0 m; an abundant inflow of water into the pits; 4 or more masonry types. Wall material: 3 or more types. Floor structures: beamless; frame or braced frame design. Prefabricated reinforced concrete elements are prestressed. Bending elements are multi-span with asymmetrical loads and unequal spans. The building underwent reconstruction with the rebuilding of a part of the main load bearing structures	Normative, operable, limited operational

**Table 2** Categories of inspection work complexity

Category	Category characteristics	Technical condition of the building
I	Visual technical expert inspection of buildings. Preparation of technical passports of buildings with issuance of drawings, charts, plans and cross-sectional views	Normative
II	Visual technical expert inspection of buildings, including identification of the composition, structural layouts and junctions of structures and their elements, recording of structural defects and preparation of drawings	Normative
III	Visual expert technical inspection of buildings, including identification of the composition, structural design and junctions of structures and their elements, recording of structural defects and preparation of drawings. Study of operational documentation. Identification of emergency and the most dangerous places in the building to develop emergency prevention measures. Instrumental inspection of the building structures with preparation of drawings (locations where collapse, rot and damage occurred)	Normative, operable, limited operational

According to standards, the inspection frequency is every 10 years, or every five years if the building is located in adverse engineering-geological conditions (that is, if there is a hazardous process).

Additional inspections are required:

- (1) two years after commissioning,
- (2) two years after a major overhaul,
- (3) at the end of the life cycle.

In accordance with the standard, additional inspections are also required after fortuitous events: extreme situations, extremely high precipitation, floods, but the associated relative costs are not taken into account in the calculations.

The cost of inspection work depends on:

- the category of technical condition of the building,
- complexity of the building,
- complexity of the inspection work.

The price of inspection work of complexity category I per cubic meter of a building up to 15 m high, in the normative technical condition and belonging to complexity category I is taken as 1 (Fig. 1).

The approach considers brick and panel buildings. The period under consideration is 1.25 of the building's life cycle (which is 150 years for a brick building and 88 years for a panel building).

### 3 Methods

Seven different scenarios of cumulative costs for inspection work that are most characteristic for large cities were considered. In each subsequent scenario, the conditions are

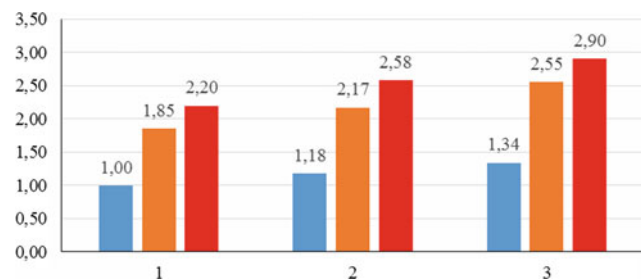


**Fig. 1** Diagram of price ratio for inspection works (Golodkovskaya and Lebedeva 1984). The color denotes the building's complexity—blue (complexity category I), brown (II), red (III). The lowest cost of inspection work is for facilities in buildings of complexity category I with inspection work of complexity category I— $C_{\min} = 1$ , the highest cost of inspection work is for facilities in buildings of complexity category III with inspection work of complexity category III— $C_{\max}$ , relative ratio =  $C_{\max}/C_{\min} = 2.9$

consistently worsening. Let us look at the proposed scenarios.

1. The first scenario assumes the most optimistic change in the building's condition, when at the end of its life cycle the category of the technical condition of the building changes from 'normative' to 'operable' (от нормативного технического состояния к работоспособному), as well as the associated minimal change in prices. Building complexity category: I, inspection work complexity category: I.
2. The second scenario is similar to the first one, but the building is located in unfavorable engineering geological conditions.
3. The categories of the technical condition of the building are the same as in the first scenario, but the building and the inspection work fall into complexity category II.
4. The scenario is similar to the third one, but the building is located in unfavorable engineering geological conditions.
5. The categories of the technical condition of the building are the same as in the first scenario, but the building falls into complexity category II and the inspection work complexity category increases over the above-mentioned normative life cycle and becomes III.
6. The sixth scenario is similar to the fifth one, but the building is located in unfavorable engineering geological conditions.
7. The scenario is similar to the sixth one, but over the above normative life cycle the category of the technical condition of the building becomes 'limited operational'.

The conditions are consistently worsening in each subsequent scenario. The seventh scenario is the worst case. The use of such houses with very high costs involved becomes economically unprofitable/inexpedient.

Graphs of relative vulnerability for brick and panel buildings were calculated using the formula below:

$$Y_t = RC_t/RC_{mat} \quad (1)$$

where

$t$  = year of the life cycle,  $Y_t$  = relative vulnerability in year  $t$ ;  $RC_t$  = relative costs in year  $t$ ;  $RC_{mat}$ —maximum costs for the entire period under scenario 7.

Then a graph of increase in relative vulnerability for brick five-storey houses is plotted (Fig. 2); trend lines are calculated in Excel as a function  $y = f(t)$ , where  $t$  is the year of the building's life cycle.

The same calculations were made for a panel building. A graph showing relative vulnerability of brick and panel buildings under the worst case scenario 7 is presented in Fig. 3.

The graph shows that the relative vulnerability is increasing much faster during the period beyond the life

**Fig. 2** Graph of increase in cumulative costs of inspection work for brick five-storey houses. The x-axis indicates the building's operation period (years), and the y-axis indicates the building's vulnerability (relative shares)

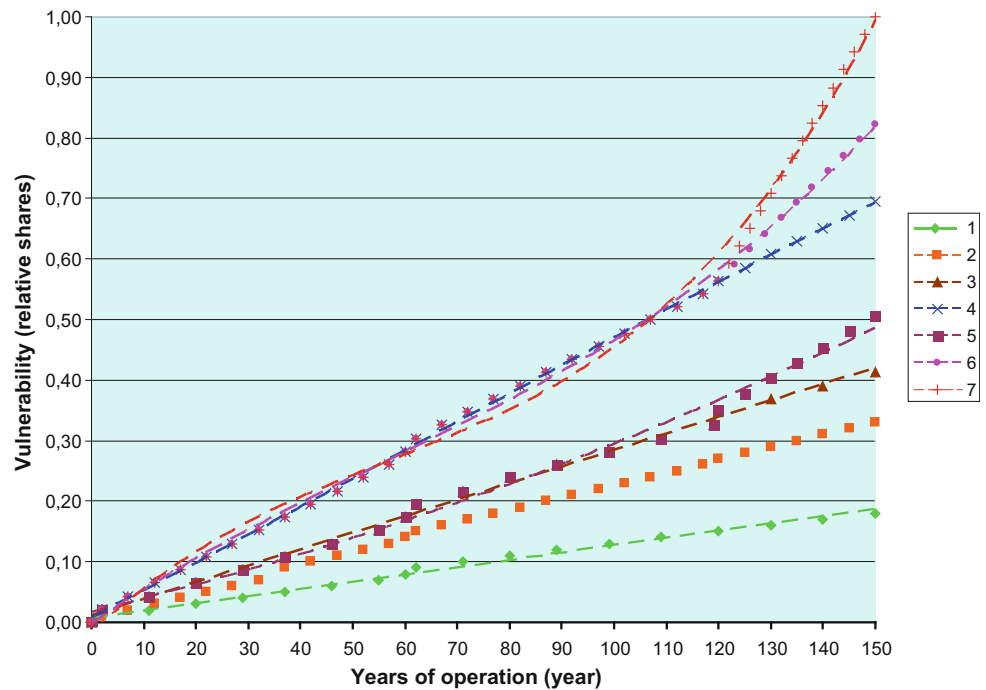
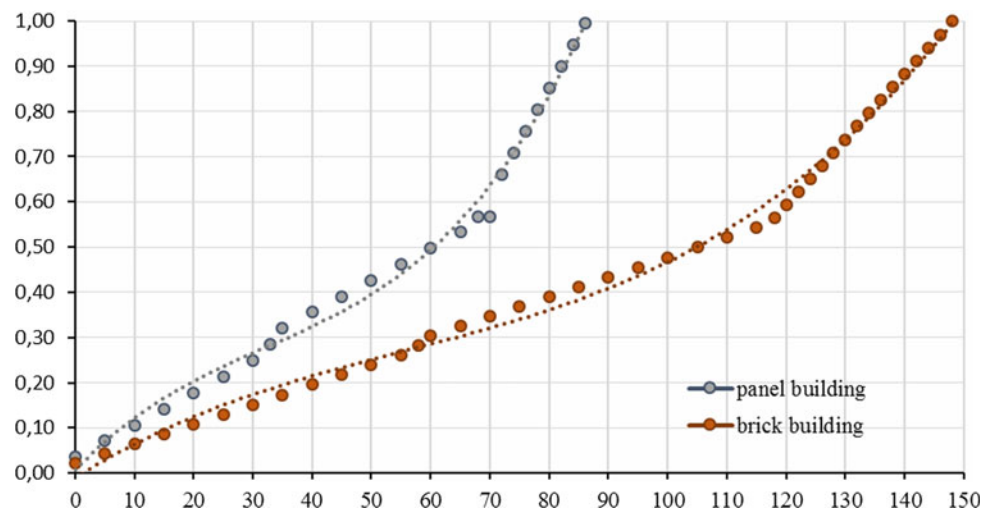


**Fig. 3** Graph of relative vulnerability for brick and panel buildings under worst-case scenario 7 (the building is located in unfavorable engineering geological conditions). The x-axis indicates the building's operation period (years), and the y-axis indicates the relative vulnerability of the building (relative shares)



cycle boundaries than during the life cycle period (both for panel and brick buildings) and that the relative vulnerability of panel buildings is increasing much faster than that of brick buildings.

## 4 Results and Discussions

The calculated trend line equations and the annual increases in costs under the 7 scenarios for brick and panel houses are presented in Table 3. In scenarios 1 to 4, the calculated trend

lines are linear equations, in scenario 5—second degree polynomials, and in scenarios 6 and 7—third degree polynomials. The coefficient of determination of the trend line is quite representative— $R^2 > 0.95$ .

The analysis of the graphs of total costs under the 7 scenarios showed that:

1. When the engineering geological conditions are unfavorable, total costs increase by 1.6–1.8 times over the entire period;

**Table 3** Estimated trend line equations and annual increase in costs for normative inspection works

No	Trend line equation	Annual increase over the life cycle		
	Brick building	Panel building	Brick building	Panel building
I	$y_1 = 0.1198t + 0.7404$	$y_1 = 0.1346t + 0.4488$	0.13	0.14
<b>II</b>	<b><math>y_2 = 0.2196t + 0.5653</math></b>	<b><math>y_2 = 0.2229t + 0.5863</math></b>	<b>0.23</b>	<b>0.23</b>
III	$y_3 = 0.2732t + 1.0984$	$y_3 = 0.2922t + 0.9738$	0.29	0.31
<b>IV</b>	<b><math>y_4 = 0.4574t + 0.1867</math></b>	<b><math>y_4 = 0.4776t + 0.7683</math></b>	<b>0.47</b>	<b>0.49</b>
V	$y_5 = 0.0007t_2 + 0.207t + 1.8328$	$y_5 = 0.0009t_2 + 0.2494t + 1.1175$	0.29	0.31
<b>VI</b>	<b><math>y_6 = 0.00002t_3 - 0.0031t_2 + 0.5922t - 0.224</math></b>	<b><math>y_6 = 0.00005t_3 - 0.0051t_2 + 0.6063t + 0.15</math></b>	<b>0.47</b>	<b>0.49</b>
<b>VII</b>	<b><math>y_7 = 0.00005t_3 - 0.0085t_2 + 0.8232t - 1.8515</math></b>	<b><math>y_7 = 0.0001t_3 - 0.0141t_2 + 0.8276t - 0.6393</math></b>	<b>0.47</b>	<b>0.49</b>

\*Bold font is used for scenarios with unfavorable engineering geological conditions

- When the complexity of inspection work increases, total costs increase by 1.2 times;
- If both factors are changed, total costs increase by 2.3–2.4 times.

From this follows that the value of cumulative costs is most affected by engineering geological conditions. Similar calculations of relative vulnerability are made for any buildings and conditions, which allow us to quickly assess vulnerability and move on to further estimates of the risk of losses.

## 5 Conclusion

The approach to assessing the relative economic vulnerability of buildings takes into account the metric, engineering and economic characteristics of the building and the engineering geological conditions of its location. Buildings of complexity categories I and II account for more than 85% of the buildings in Moscow, unique buildings or buildings after reconstruction fall into complexity category III, so the method covers all possible construction options. All possible changes in the technical condition of the building are accounted for by an increase in the complexity of inspection works. The estimated trend line equations of buildings vulnerability allow calculating the building's vulnerability for any year of operation. The proposed regulatory documents are public and available for use. So, the approach is universal, operational and readily available.

**Acknowledgements** This research was supported by the Russian Science Foundation, project no. 16-17-00125.

## References

- Collection of basic prices for work involving inspection and monitoring of the technical condition of building structures and engineering equipment of buildings and structures, including subway facilities, within areas impacted by construction projects, which is funded from the Moscow city budget. MPP 3.2.05.06-12. Pricing system in the Moscow construction sector (2013)
- Federal Law of the Russian Federation No. 384: "Technical Regulations on the Safety of Buildings and Structures"—the electronic resource of the legal reference system. ConsultantPlus, 30 Dec 2009. <https://www.consultant.ru/online/>
- Golodkovskaya, G.A., Lebedeva, N.I.: Engineering Geological Zoning of Moscow City Territory. *Inzhenern. Geol.* no. 3, 87–102 (1984)
- ISO 2394:1988 General principles on reliability for structures (NEQ)/StandardInform, Moscow (2011)
- Interstate standard 53778-2010.: "Buildings and Structures. Rules of Inspection and Monitoring of Technical Condition"—the electronic resource of the legal reference system. ConsultantPlus. <https://www.consultant.ru/online/>
- Osipov, V.I., Burova, V.N., Karfidova, E.A.: Formation of information on geoeological conditions within the boundaries of the cadastral division of the territory of the city of Moscow/Sergeev readings. In: *Engineering and Geological and Geoeological Problems of Urban Agglomerations*, pp. 76–82. Moscow, 23–24 March 2015
- Osipov, V.I., Burova, V.N., Karfidova, E.A.: Methodological principles of geo-hazard vulnerability evaluation of capital construction assets in urbanized areas. *Soil Mech. Found. Eng.* **53**(6), 421–425 (2017). <https://doi.org/10.1007/s11204-017-9422-z>. ISSN 0038-0741/17/5306-0420
- Osipov, V.I., Burova, V.N. et al.: A map of large-scale (detail) engineering geological zoning of Moscow territory. *Water Resour.* **39**(7), 737–746 (2012). Print ISSN 0097-8078. <https://doi.org/10.1134/S0097807812070093>
- Osipov V.I., Larionov V.I., Burova V.N. et al.: *Nat Hazards* **88**(Suppl 1): 17 (2017). Print ISSN 0921-030T. <https://doi.org/10.1007/s11069-017-2780-z>



# Geotechnical Characterization of Sands from the Portuguese Continental Shelf to Support the Design of Renewable Energy Converters Installation

Joaquim Pombo, Paula F. da Silva, and A. Rodrigues

## Abstract

Projects for the installation of offshore renewable energy converters usually require the in situ characterization of the marine soils due to the high variability of marine environments, which is caused by the constant interplay between sediments and physical agents. In this regard, the safety of the foundations of these devices is a mandatory issue and it must predict adverse meteorological and oceanographic conditions. This article is part of a geotechnical characterization study of a small sector of the Portuguese continental shelf, very close to a designated area for the installation of offshore renewable energies devices. In order to investigate the mechanical and the physical properties of poorly graded sands (SP) and poorly graded sands with silt (SP-SM), triaxial compression tests (CK<sub>0</sub>D) were performed on undisturbed samples. The effective friction angles for those sands were 35.2° and 34.5°, respectively.

## Keywords

Triaxial tests • Geotechnical studies • Marine sediments • Offshore renewable energies

## 1 Introduction

The meteo-oceanographic conditions on the Portuguese coast are suitable for the production of renewable energies in the marine environment (wave and offshore wind). In addition to the energetic potential, the shoreline concentration of the main population groups increase the demand for this

energetic resources, being the development of industry and infrastructure facilities, such as modern ports and shipyards with tradition in metal-mechanics, secondary goals, highly supported by the Portuguese state.

In the last decade, the Portuguese offshore has been sought for testing and technological demonstration of devices (Pelamis, Waveroller, Windflot, Demogravi3) for the use of renewable energies. These projects have associated specific needs regarding the geotechnical characterization of the marine soils, as their adequate foundation in the open sea is essential for the feasibility and risk management of the whole project. In this sense, and due to the lack of CPT equipment in Portugal for the offshore characterization of the sedimentary stratigraphy and estimation of geotechnical parameters of the marine soils of the targeted area, the authors selected good quality sampling and alternative laboratory tests to characterize the soils, namely triaxial compression tests. This more traditional approach also allowed the acquisition of real, non-empirical, geotechnical parameters (opposite of those derived from the CPT), which were integrated with geologic information allowing the foundation design for the study area.

This is because, until now, there are no studies that characterize the sedimentary deposits of the Portuguese offshore from the geotechnical point of view. Thus, the present study intends to fulfill the gap in the knowledge of the mechanical characteristics of marine soils and proposes a multidisciplinary alternative to execute the basic geotechnical description of marine sites, necessary to any foundation at the sea bottom. The selected approach is based on the implementation of a geotechnical model, by investigating the mechanical proprieties of the most favorable geological units.

J. Pombo (✉) · A. Rodrigues  
Instituto Hidrográfico, 49, Lisbon, Portugal  
e-mail: joaquim.pombo@netcabo.pt

P. F. da Silva  
GeoBioTec and Department Earth Sciences, FCT, NOVA  
University of Lisbon, Caparica, Portugal

## 2 The Site

### 2.1 Location and Background Geology

The site is located 4 km off the village of S. Pedro de Moel, in the northern Portuguese continental shelf, between 30 and 60 m water depths (Fig. 1). It comprises an area of about 15 km<sup>2</sup> with a very smooth morphology with no major outcrops. Despite the general gentle slope (about 0.3%), a morphologic structure is recognized at 55 m deep, consisting in a 1 m vertical displacement of the sea bottom. This feature marks the transition of a fine sedimentary deposit (between 30 and 55 m deep) to a coarser one (between 55 and 60 m deep). In the remainder of the studied area no morphological features were recognized.

Seismic profiles, acquired with a boomer and sub-bottom profiler systems, allowed the definition of a geophysical model of the studied site, based on the description three seismic units (U1, U2 and U3 from the bottom to the top of the seafloor) with different acoustic characteristics (Pombo 2016).

According to Rodrigues (2004), Unit 1 (U1) corresponds to a very deformed and dolomitized carbonate rocks. The basal sedimentary unit (U2), a coarser deposit (sandy gravel sediments), covers the bedrock and is exposed in the deepest area, below 55 m deep. The more recent unit (U3), covering the coarser deposit, was identified in the shallow area, being composed by sandy sediments. According to Pombo (2016), the sandy deposit increases its thickness towards the coast line, from 0.5 to 7 m, while the sandy-gravelly deposit, despite the difficulty in the basal delimitation, seems to be a thicker unit (5–13 m, also increasing eastward).

## 3 Methods

Once in the laboratory, the corers were submitted to several tests using international normalized methods: namely, grain size distribution (NP EN 933-1:2014 and ISO 13320-1:2009), particle density, specific weight and water content (ISO/TS 17892-1, 2, 3:2004a, b, c) and triaxial tests.

Triaxial compression tests with CK<sub>0</sub>D anisotropic consolidation, with seismic wave (P and S) measurements, were carried out on six undisturbed samples. These tests were performed with monotonic increase of vertical stress. For the triaxial tests, adequate preparation of the test specimens according to Part 2 of Eurocode 7 (EN 1997-2: 2007) was required, all of which performed as described below, in compliance with ISO/TS 17892-9: 2004d.

The specimens tested were approximately 70 mm in diameter and 140 mm in height and were previously extruded from the core samplers (Table 1).

After assembly in the triaxial chamber, ‘water’ was percolated to eliminate the soil air bubbles, followed by saturation with increasing back pressure up to 500 kPa, maintaining the effective confinement of 10 kPa; to ensure the saturation, the Skempton’s B parameter value (>0.95) was controlled. Initial isotropic consolidation was then carried out at an effective stress followed by anisotropic consolidation to the condition of  $K_0 = 0.5$  and maintaining this anisotropic condition for 24 h.

Five discharge-charge cycles were carried out for the determination of the modulus of elasticity ( $E_{dr}$ ), followed by increasing vertical compression,  $\sigma_1$ , in drained conditions with volume change variation readings; throughout this final compression stage, the applied axial strain rate to

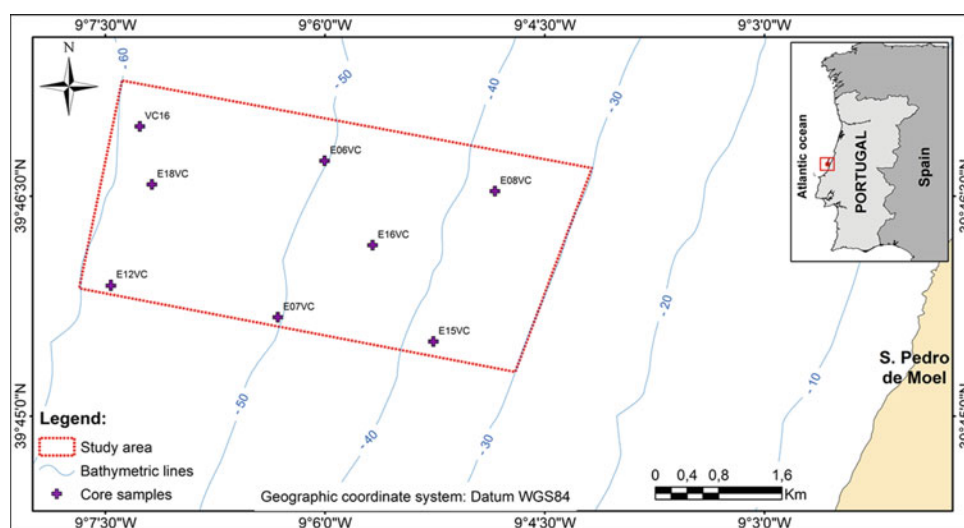


**Fig. 1** The studied marine site and vertical sediments sampling

**Table 1** Identification of specimens analyzed

Specimen	Core samples	Samples depth (m)
P5	E06VC	0.72–0.89
P8		1.30–1.30
P9		1.48–1.66
P10	E08VC	0.74–0.92
P11		0.92–1.10
P12		1.10–1.28

the test specimen remained unchanged. These compression trajectories followed the required condition: that  $\sigma_3$  was constant. At the end of those cycles, the velocities of S and P waves were measured using bender-extender elements.

It should be noted that the percolated and the injected water (for back pressure) inside the specimen during the saturation phase used natural saline deaired water from the studied area.

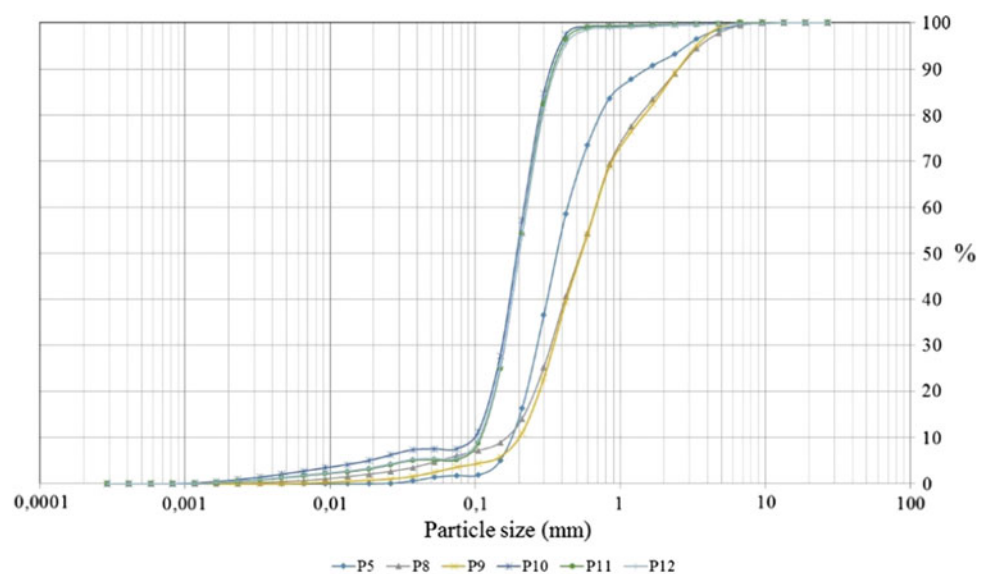
## 4 Results

According to the site investigation and testing, the U3 seismic unit, with an average thickness of 3 m, encompasses poorly graded sands, SP, and poorly graded sands with silt, SP-SM (Pombo 2016). The characteristics of the test specimens of these types of sands are summarized in Table 2, and the grain size distribution curves in Fig. 2.

**Table 2** Summary of the specimen properties

Specimen	Gravel	Sand	Silt	D <sub>10</sub>	D <sub>50</sub>	C <sub>u</sub>	C <sub>c</sub>	G <sub>s</sub>	$\gamma_d$ (kN/m <sup>3</sup> )	CaCO <sub>3</sub> (%)	USCS
	%			mm							
P5	6.8	91.4	1.8	0.15	0.31	2.51	0.94	2.66	17.6	4.2	SP
P8	10.9	84.2	4.9	0.13	0.45	4.26	1.02	2.69	17.3	5.0	SP
P9	11.0	85.4	3.6	0.16	0.45	3.48	0.90	2.64	17.4	5.0	SP
P10	0.4	92.1	7.6	0.08	0.16	2.33	1.15	2.66	15.4	4.2	SP-SM
P11	0.4	94.4	5.18	0.09	0.17	2.08	1.03	2.68	15.6	5.0	SP-SM
P12	0.5	93.9	5.6	0.09	0.17	2.13	1.02	2.64	15.9	5.0	SP-SM

**Fig. 2** Grain size distribution of the U3 seismic unit soils tested

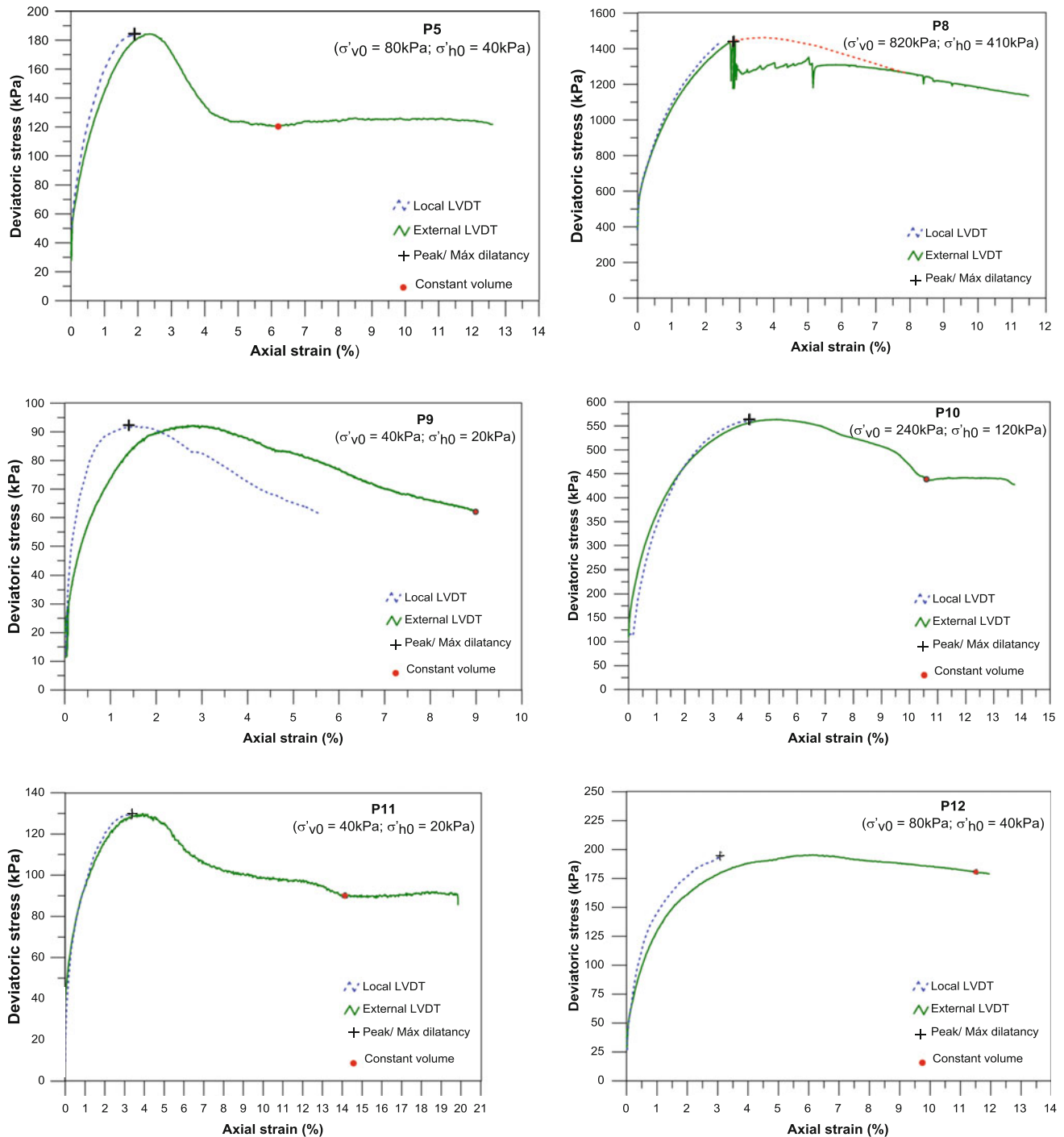


According to the results three specimens (P5, P8 and P9) correspond to poorly graded medium sands (SP) and the other three specimens (P10, P11 and P12) correspond to poorly graded fine sand with silt (SP-SM).

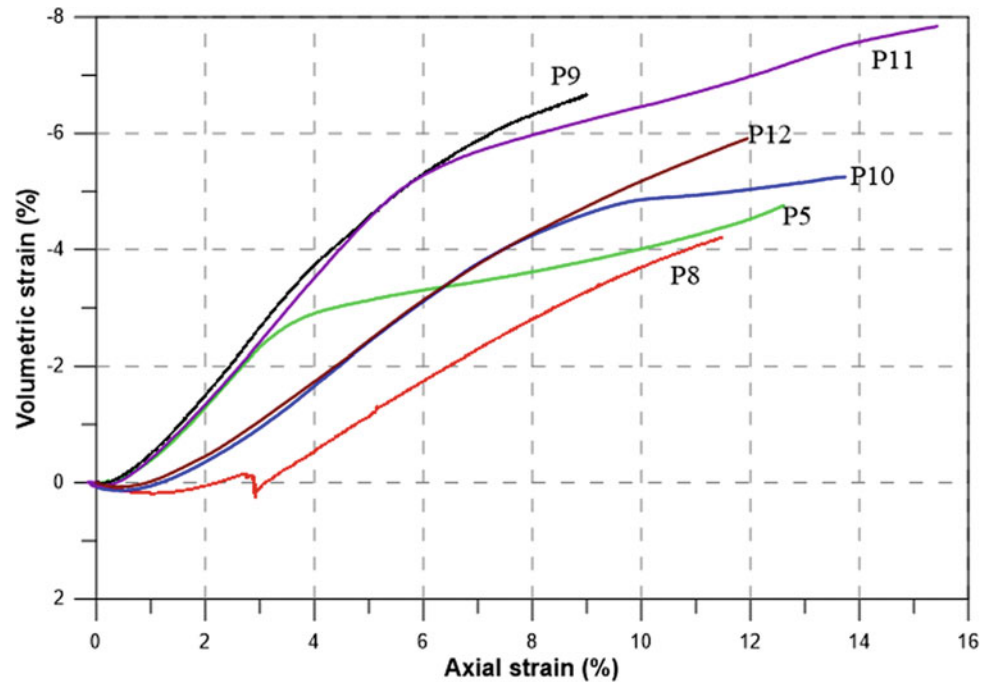
The dry weight of the SP sediments ranges from 17.3 to 17.6 kN/m<sup>3</sup>, while for the SP-SM sediments it varies between 15.4 and 15.9 kN/m<sup>3</sup>. Both group of soils have

low carbonate contents, around 5%, and their particles densities are around 2.65, which are indicative of quartz particles.

To evaluate the mechanical behavior of these soils, tri-axial tests were performed, and the deviatoric stress—axial strain curves and the volumetric strain—axial strain of each test specimen are presented in Figs. 3 and 4.



**Fig. 3** Deviatoric stress—axial strain curves for the six specimens tested

**Fig. 4** Volumetric strain—axial strain for the specimens tested

The deviator stress vs axial strain curves (Fig. 3) show that, in general, there is a common tendency to all triaxial tests analyzed: the stress-deformation behavior of the tested marine sediments seems to be initially rigid, apparently linear, to a well-defined yield point, from which the soil undergoes increasing plastic deformations until rupture. The behavior after failure is characterized by a more intense and rapid deviatoric stress drop in the test specimens P5 and P11, and by the existence of a critical state, where the deviatoric stress approaches a stable residual value, for increasing axial deformations. The tested sands present a hardening behavior.

Figure 4 shows the volumetric strain vs axial strain variation for all specimens tested at different consolidation

stresses. It is observed that both groups of test specimens present an initial compression followed by a strong expansion until rupture, which coincides with the maximum dilatation and increase in volume. After this point, the expansion gradient decreases, leaning at the end to a constant value.

The behavior described above is typical of medium to dense sands.

Table 3 presents the obtained rupture values, peak deviatoric stress  $(\sigma_1 - \sigma_3)_p$  and residual deviatoric stress  $(\sigma_1 - \sigma_3)_{cv}$ , for the test specimens and the discharge-charge (pseudo-elastic) modulus,  $E_{dr}$ , calculated between the vertices of hysteresis of the five cycles centered on the value of  $K_0 \cong 0.5$ .

**Table 3** Elastic modulus, peak and constant volume strength of the specimens tested

Specimen	$\sigma'_{c0}$ (kPa)	$\sigma'_{v0}$ (kPa)	$E_{dr}^*$ (MPa)	$(\sigma_1 - \sigma_3)_p$ (kPa)	$\epsilon_p$ (%)	$(\sigma_1 - \sigma_3)_{cv}$ (kPa)	$\epsilon_{cv}$ (%)
P5	$\sigma'_{c0} = 40$	$\sigma'_{v0} = 80$ $\sigma'_{h0} = 40$	226.6	184.4	1.9	120.4	6.2
P8	$\sigma'_{c0} = 410$	$\sigma'_{v0} = 820$ $\sigma'_{h0} = 410$	692.7	1439.2	2.7	**	**
P9	$\sigma'_{c0} = 20$	$\sigma'_{v0} = 40$ $\sigma'_{h0} = 20$	258.7	92.3	1.4	61.5	9.1
P10	$\sigma'_{c0} = 120$	$\sigma'_{v0} = 240$ $\sigma'_{h0} = 120$	253.4	563.4	4.3	438.4	10.9
P11	$\sigma'_{c0} = 20$	$\sigma'_{v0} = 40$ $\sigma'_{h0} = 20$	100.3	129.9	3.9	90.0	14.2
P12	$\sigma'_{c0} = 40$	$\sigma'_{v0} = 80$ $\sigma'_{h0} = 40$	124.7	195.3	3.1	180.7	11.5

\* Modulus for  $\sigma'_h = 0,5\sigma'_{v0}$  ( $K_0 \cong 0,5$ ); \*\* Did not reach constant volume

**Table 4** S and P waves at end of discharge-charge cycles

Specimen	Ø (mm)	Height (mm)	Volume (cm <sup>3</sup> )	w (%)	γ <sub>dry</sub> (kN/m <sup>3</sup> )	e <sub>0</sub>	End of cycles	
							V <sub>P</sub> (m/s)	V <sub>S</sub> (m/s)
P5	70.14	139.72	539.84	19.8	17.7	0.529	2029	180
P8	68.81	140.36	522.00	31.1	17.9	0.827	2239	383
P9	69.75	139.60	533.42	25.3	17.5	0.641	2032	194
P10	71.97	134.99	549.13	31.6	15.4	0.844	2027	229
P11	69.84	140.19	537.05	32.3	15.7	0.866	2117	152
P12	69.45	139.62	528.98	32.2	16.0	0.863	2096	197

**Table 5** Strength parameters of the sands

Specimen	USCS	φ' <sub>p</sub>	φ' <sub>cv</sub>	c' <sub>p</sub> (kPa)	Ψ
P5, P8 e P9	SP	39	35.2	9.0	6.0
P10, P11, P12	SP-SM	44	34.5	2.3	15.6

Analyzing the data in Table 3, it can be registered that the modules determined between the vertices of the discharge-charge cycles ( $E_{dr}$ ) are very variable and are related to the properties of each specimen and the initial consolidation stress. Regarding the deviatoric stresses, it can be concluded that they are also directly related to the type of material of each specimen and to the effective consolidation stresses applied.

Table 4 presents the values obtained in the calculation of acoustic wave propagation velocities for each of the test specimens. These values are used to determine the dynamic deformability of the soil, the Poisson coefficient and the distortion modulus, and can be compared with the values of the same parameters determined in static conditions. However, dynamic modules generally give higher values because deformations involved are very small.

The results of the effective peak ( $\phi'_p$ ) and residual ( $\phi'_{cv}$ ) friction angles, cohesion ( $c'$ ) and dilation angle ( $\Psi$ ) of the SP and SP-SM samples tested in this investigation (Table 5) are overall consistent with those published in reference works (Schanz and Vermeer 1996; Lee 2003).

It is also worth mentioning that the angles determined by the graphs  $q-p'$  show an excellent statistical correlation ( $r > 0.98$ ) and agree with the stipulate in EN 1997-2: 2006.

According to Bolton (1986), the angle of shear strength in the critical state mainly reflects the sediment mineralogy. In the specimens analyzed by this research (Table 5), it is verified that the friction angles for SP and SP-SM soils are 35.2° and 34.5°, respectively, very close to the one reported

by Bolton (1986) for specimens composed of quartz particles (33°).

## 5 Conclusions

This paper presents the results of part of the geotechnical investigation carried out at a small site of the Portuguese continental shelf, mainly characterized by poorly graded sands (SP) and poorly graded sands with silt (SP-SM). The strength parameters of these soils, through triaxial compression tests (CK<sub>0</sub>D), were calculated to support the foundation design for renewable energy offshore floating structures.

The results of the triaxial tests, performed on the SP and SP-SM soils, presented a typical behavior of medium to dense sands showing, while shearing, a hardening behavior with an initial compaction followed by dilation and increase in volume. The effective friction angles for the two types of sands tested were 35.2° and 34.5°.

The results obtained for both physical and mechanical properties are in accordance with the benchmark values presented in literature for the same type of siliceous sands.

This was the first case study for the Portuguese offshore, where no strength parameters had ever been determined. Further researches should be carried out to complement the presented results.

**Acknowledgements** Paula Silva's research was supported by UID/GEO/443 04035/2013.

## References

- ASTM D2487: Standard for classification of soils for engineering purposes (Unified Soil Classification System) (2006)
- Bolton, M.D.: The strength and dilatancy of sands. *Geotechnique* **36**(1), 65–78 (1986)
- EN 1997-2: Eurocode 7: Geotechnical design—Part 2: Design assisted by laboratory testing. IPQ, Lisbon, Portugal (2007)
- FEUP: Application of piezoelectric transducers in the determination of the velocity of seismic waves in specimens. FEUP, Porto (2003). <http://www.fe.up.pt/sgwww/labgeo>
- ISO/TS 17892-1: Geotechnical investigation and testing—Laboratory testing of soil—Part 1: Determination of water content. ISO 2004. Switzerland (2004a)
- ISO/TS 17892-2: Geotechnical investigation and testing—Laboratory testing of soil—Part 2: Determination of bulk density. ISO 2004. Switzerland (2004b)
- ISO/TS 17892-3: Geotechnical investigation and testing—Laboratory testing of soil—Part 3: Determination of particle density. ISO 2004. Switzerland (2004c)
- ISO/TS 17892-9: Geotechnical investigation and testing—Laboratory testing of soil—Part 9: Consolidated triaxial compression tests on water-saturated soil. ISO 2004. Switzerland (2004d)
- ISO 13320-1: Particle size analysis—Laser diffraction methods. ISO 2009. Switzerland (2009)
- Lee, W.-F. Applications of dilative behavior in marine soil. In: *Proceedings of the Thirteenth International Offshore and Polar Engineering Conference*, pp. 366–371. International Society of Offshore and Polar Engineers, Honolulu, Hawaii, USA (2003)
- NP EN 933-1: Ensaio das propriedades geométricas dos agregados. Parte 1: Análise granulométrica. Método da peneiração. IPQ 2014. Portugal (2014)
- Pombo, J.: Geotechnical Studies for the anchoring of offshore Wave Energy Converters. Ph.D. in Geological Engineering, Faculty of Sciences and Technology, New University of Lisbon, 221 pp. (in Portuguese) (2016)
- Rodrigues, A.: Tectono-estratigrafia da plataforma continental setentrional portuguesa. Documentos Técnicos do Instituto Hidrográfico, no 35. Lisboa (2004)
- Schanz, T., Vermeer, P.A.: Angles of friction and dilatancy of sand. *Géotechnique* **46**(1), 145–151 (1996)

# Correlation Between CPT and Screw Driving Sounding (SDS)

Yasin Mirjafari, Rolando P. Orense, and Naoaki Suemasa

## Abstract

Cone penetration test (CPT) is probably the most popular in situ testing method in the world today. Various design parameters, such as undrained strength and relative density, as well as indices for liquefaction assessment, can be derived from the CPT. However, the use of CPT in many roading projects and in subdivision developments may be constrained by the number of tests or project cost; hence, alternative in situ testing technique to supplement the CPT is necessary. Screw Driving Sounding (SDS) is a new in situ test in which a machine drills a screw point into the ground in several loading steps while the attached rod is continuously rotated. During the test, a number of parameters, such as torque, load, speed of penetration and friction, are measured at every rotation of the rod; these provide a robust way of characterising soil stratigraphy. In this paper, the principle of SDS testing is described. SDS tests were performed at various sites in New Zealand where CPT data are available. Then, a side-by-side comparison between CPT and SDS is performed to derive correlations between the CPT tip resistance ( $q_c$ ), sleeve friction ( $f_s$ ) and soil behavior type index ( $I_c$ ) and the SDS parameters. Based on the results, it is observed that  $q_c$  correlates well with the penetration energy in SDS while  $f_s$  and  $I_c$  are related to the average torque and change in torque, respectively. The good correlation obtained between CPT and SDS indicates that SDS can supplement CPT results for a more cost-effective geotechnical investigation.

## Keywords

In situ testing • Cone penetration test • Screw driving sounding

## 1 Introduction

Accurate estimation of soil properties is necessary in order to determine the required input parameters in the design of geotechnical structures. For this purpose, in situ testing has been the preferred approach over the more tedious soil sampling and laboratory testing and geotechnical properties are empirically correlated with the measured in situ parameters. Among the various in situ testing techniques currently available, the cone penetration test (CPT) has been gaining popularity because of its many advantages. However, the requirement for large equipment, open space and skilled operators, not to mention cost, is prohibitive for small-scale residential house construction and for some roading projects.

In Japan and other European countries, the Swedish Weight Sounding (SWS) test is a popular alternative as the apparatus used does not occupy a large space and the implementation is simpler compared to other methods. However, SWS has been observed to have low accuracy in terms of soil classification, and rod friction has a significant effect on the test results.

The Screw driving sounding (SDS) is a new in situ testing technique developed in Japan. It is an advanced version of SWS and it takes into account the rod friction in the measurements and monitors more parameters. As SDS is simpler, faster to implement, more economical than CPT and more accurate than SWS, it can be a good alternative in situ test for soil/site characterisation; hence, it can be a good supplement to CPT especially when applied to projects extending over wide areas, such as roading works.

This paper attempts to correlate CPT and SDS parameters by performing SDS tests at sites where CPT data are available and conducting side-by-side comparison between CPT and SDS. The results indicate a good correlation between the two, suggesting that SDS can supplement CPT results for the most cost-effective geotechnical investigation.

Y. Mirjafari · R. P. Orense (✉)  
University of Auckland, Auckland, 1142, New Zealand  
e-mail: r.orense@auckland.ac.nz

N. Suemasa  
Tokyo City University, Tokyo, 158-8557, Japan



## 2 Principle of SDS and Test Procedure

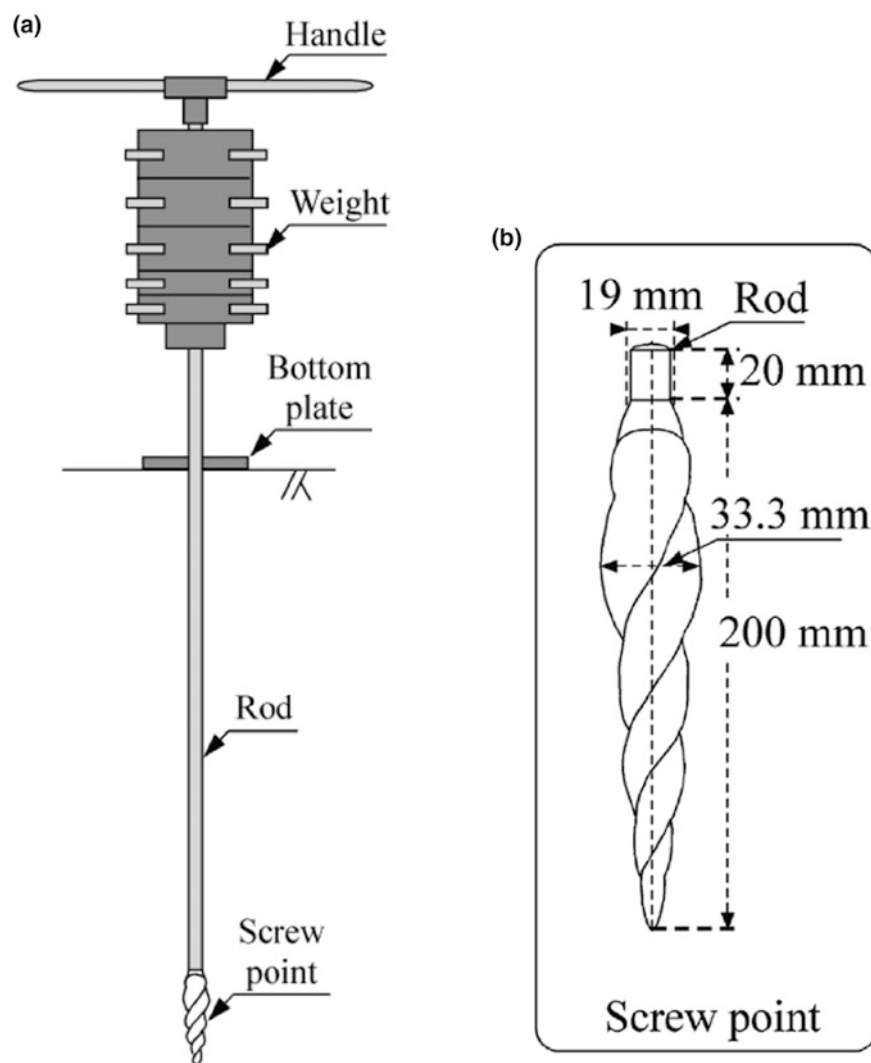
### 2.1 Swedish Weight Sounding (SWS) Method

Before discussing the principle behind the SDS method, it is worthwhile to provide a background of the SWS technique (Tsukamoto et al. 2004; Tsukamoto 2013). The apparatus consists of a screw point, sounding rods, a rotating handle and six pieces of weights making a total of 100 kgf (980 N), as shown in Fig. 1. The field test comprises two phases: (1) static penetration; and (2) rotational penetration. In the static penetration phase, the screw-shaped point attached to the tip of the rod (weighing 49 N or 5 kgf) is statically penetrated by loading several weights (10, 10, 25, 25, 25 kgf)

on top of the rod in stepwise increments until the total load is equal to 980 N (100 kgf). At each load increment, the depth of static penetration is measured and the total weight is denoted as  $W_{sw}$  (kN). If the screw point cannot penetrate under the maximum load, static penetration is ceased and rotational penetration is conducted. The horizontal handle attached to the top of the rod is rotated, and the number of half turns necessary to penetrate the rod through 25 cm is denoted as  $N_a$ . The values of  $N_a$  are then multiplied by 4 and are converted to the number of half turns per metre,  $N_{sw}$ .

Although the SWS test is highly portable and simpler than other sounding tests, this test has some disadvantages, such as the results being fairly influenced by rod friction. In cases where the soil contains gravel, the required load to

**Fig. 1** a Equipment used for Swedish weight sounding (SWS); and b details of screw point (Tsukamoto 2013)



penetrate, the number of half-turns and, consequently, the soil resistance from the SWS tends to be overestimated as the rod friction becomes large.

Suemasa et al. (2005) investigated the interaction between the torque and the vertical load during SWS implementation and proposed an analogy model based on plasticity theory and the results of SWS miniature test results. Based on these, they noted that the coefficient of yield locus,  $c_y$  (which relates the normalised torque and normalised weight applied) and the coefficient of the plastic potential,  $c_p$  (which relates the normalised half-turns and the torque on the rod), vary depending on the soil type; i.e. clay, loam, medium sand or dense sand; hence, they proposed that soil can be classified based on the data obtained from SWS tests if the torque can be measured. This resulted in further refinement of the SWS method in terms of operating system, which led to the development of the SDS method.

## 2.2 Screw Driving Sounding (SDS) Method

**Test Procedure.** A new system for conducting the SWS method has been recently developed in Japan to minimise the disadvantages of the SWS method and to incorporate a procedure to measure the rod friction. Such method is referred to as the Screw driving sounding (SDS) test. For this purpose, a small portable machine is used to apply the load monotonically in seven steps (250 N, 375 N, 500 N, 625 N,

750 N, 875 N, and 1000 N), i.e. the load is increased at every complete rotation of the rod until a 25 cm penetration is reached. During this time, the rod is always rotated at a constant rate (25 rpm). The process is repeated at every 25 cm of penetration. The parameters measured during the test are the maximum torque ( $T_{max}$ ), the average torque ( $T_{ave}$ ), and the minimum torque ( $T_{min}$ ) on the rod for each applied load, the penetration length ( $L$ ), the penetration velocity ( $V$ ) and the number of rotations ( $N$ ) of the rod. These parameters are measured at every complete rotation of the rod. Note that after each 25 cm of penetration in the SDS method, the rod is lifted up by 1 cm and then rotated to measure the rod friction. Then it is moved down 1 cm back to its original position and the process is repeated. Tanaka et al. (Tanaka et al. 2012) derived a way to correct the torque and load to take into account friction. The procedure in performing the SDS test is outlined in Fig. 2a.

While the SWS method is usually performed manually (i.e. application of weights and rotation of rods are done with human effort), the need for measurement of torque and velocity requires the use of a machine. A machine originally used for the SWS test has been improved to be suitable for the SDS application. Figure 2b illustrates the small-scale machine used in the SDS test, which can be disassembled for ease in transport and handling. With the test capable of measuring more parameters, a better insight of the soil profile and penetration resistance of the layers can be obtained.

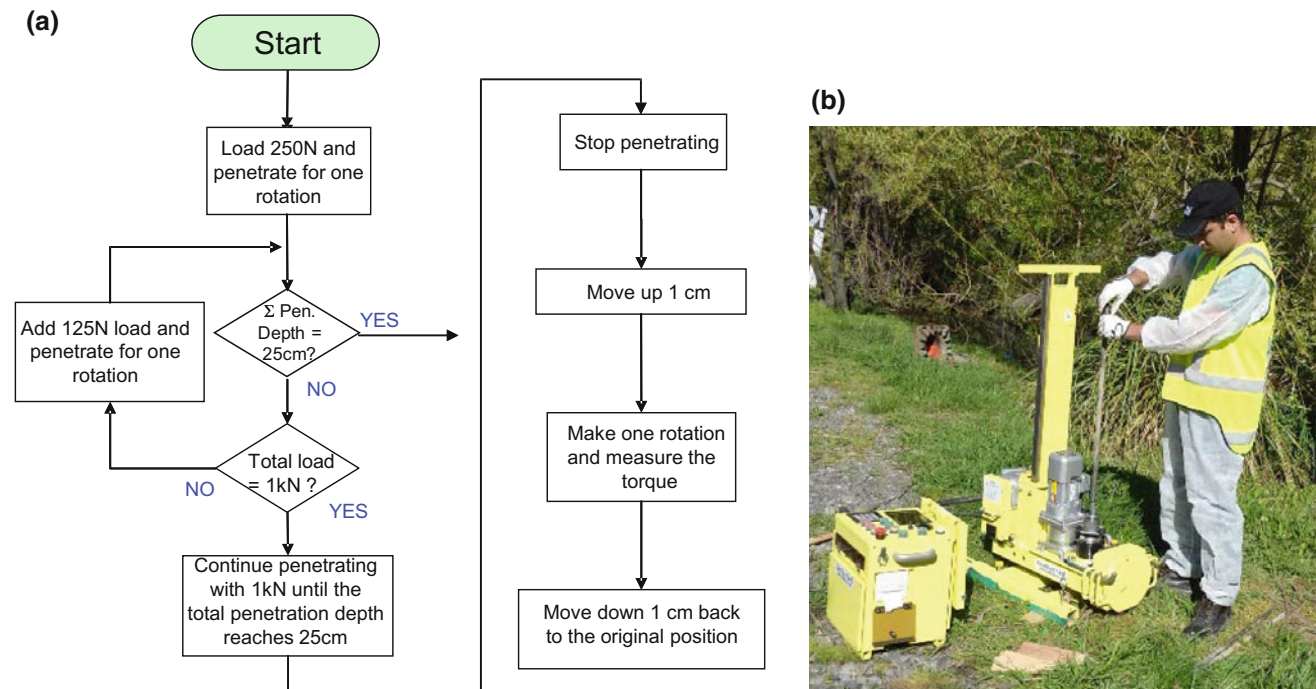


**Fig. 2** a Procedure in performing SDS test; b SDS equipment

**SDS-derived parameters.** More information can be obtained by processing the measured data from SDS tests (Mirjafari 2016). For example,  $N_{SD}D$  is the normalised half-turns obtained by multiplying the number of half-turns for every 25 cm of penetration ( $N_{SD}$ ) by the outer diameter of the screw point ( $D$ ). This number gives an indication of the level of torque required to twist the rod. Another parameter,  $\pi T/WD$ , represents the normalised torque and is defined using the torque ( $T$ ), the weight applied ( $W$ ) and the outer diameter of the screw point ( $D$ ). Other SDS-derived parameters include the following:

$$\text{Ave}(\delta T) = \frac{1}{n-1} \sum_{i=1}^{n-1} (T_{i+1} - T_i) \quad (1)$$

$$c_p'' = \frac{1}{n} \sum_{i=1}^n \left( \frac{N_{SD}D}{\pi T/WD} \right)_i \quad (2)$$

where  $\delta T$  is the change in torque,  $T$ , at each step of loading,  $i$ ;  $n$  ( $= 7$ ) is the number of loading; and  $c_p''$  is the modified coefficient of plastic potential.

During the SDS test, both load and torque are applied to the rod at the same time. The combined effect of the applied load and torque can be expressed in terms of energy, i.e., the

incremental work done,  $\delta E$ , by the torque and vertical force for a small rotation can be calculated as (Suemasa et al. 2005):

$$\delta E = \pi T \delta n_{ht} + W \delta s_t \quad (3)$$

where  $\delta n_{ht}$  is the number of incremental half turns and  $\delta s_t$  is the incremental settlement caused by the load. The specific energy,  $E_s$ , is defined as the amount of energy for complete rotation,  $E$ , divided by volume of penetration:

$$E_s = \frac{E}{L \cdot A} \quad (4)$$

where  $L$  is the depth of penetration and  $A$  is the maximum cross-sectional area of the screw point.  $E_s$  is taken as the average of the specific energies calculated at different steps of loading at each 25 cm of penetration. Based on this definition, it is clear that as the difficulty in penetrating the layer increases,  $E_s$  also increases.

**Comparison with other in situ methods.** A comparison between the SDS method and conventional in situ testing techniques is summarised in Table 1. As observed from the table, the SDS method has many advantages, such as simpler system, faster procedure, lighter reaction weight and better cost

**Table 1** Comparison between SDS method and conventional sounding methods (Orense et al. 2014)

		SDS	SWS (automatic)	SPT	CPT
Basic data	Penetration type	Static <b>and</b> rotational penetration	Static <b>or</b> rotational penetration	Dynamic penetration	Static penetration
	Penetration ability	SPT $N$ value of around 10	SPT $N$ value of around 10	High	Based on load ability
	Obtained information	3 components: load, torque, and penetration depth	One component: load or half turns	One component: number of blows (soil type)	3 components: penetration resistance, friction, and pore pressure
	Estimated information	Soil type, firmness, etc.	$N$ value, $q_u$	Firmness	Soil type, strength, liquefaction, and consolidation
Workability	Efficiency	Good	Good	Bad	Acceptable
	Working space	Applicable to constricted space	Applicable to constricted space	Equivalent to two vehicles	A little wide
	Installation effort	Easy	Easy	Scaffolding and water supply are required	Anchor casting
	Required skill	Not very high	Not high	High	High
	Environmental impact	Quiet	Quiet	With noise and vibration	Quiet
Cost	Low	Low	High	Slightly high	
Remarks	Currently only JHS	Lacks reliability. Widely used for residential houses in Japan	Physical testing is available; Widely used in Japan	Difference in apparatus is observed. Widely used in Europe and America	

efficiency than other sounding tests. It has a lot of potential in terms of application especially to residential houses.

### 3 Correlation with CPT

#### 3.1 SDS Application in New Zealand

The authors have taken the opportunity to use the SDS method at various sites in New Zealand for three purposes: (1) by comparing the SDS results with available data from adjacent CPT/SPT sites or borehole logs, provide further data to characterise sites in New Zealand and determine their geotechnical properties; (2) add data to the existing database of Japanese soils in order to improve the applicability of SDS method; and (3) explore the possibility of correlating SDS results with those of CPT and SPT.

Overall, 260 SDS tests have been performed at various soil sites in New Zealand. All of the tests were conducted at sites where borehole data and/or CPT data are available. From the database created, soil classification charts (Mirjafari et al. 2016) as well as liquefaction potential charts (Mirjafari et al. 2015, 2016) have been developed making use of SDS test results.

A typical SDS result showing the depth profile of specific energy,  $E_s$ , is shown in Fig. 3. The test was performed within 2 m of a CPT site and borehole. Also shown in the

figure is the CPT profile available, where it is seen that the variation of the  $E_s$  with depth is similar to the variation of the CPT tip resistance,  $q_c$ , along the soil profile.

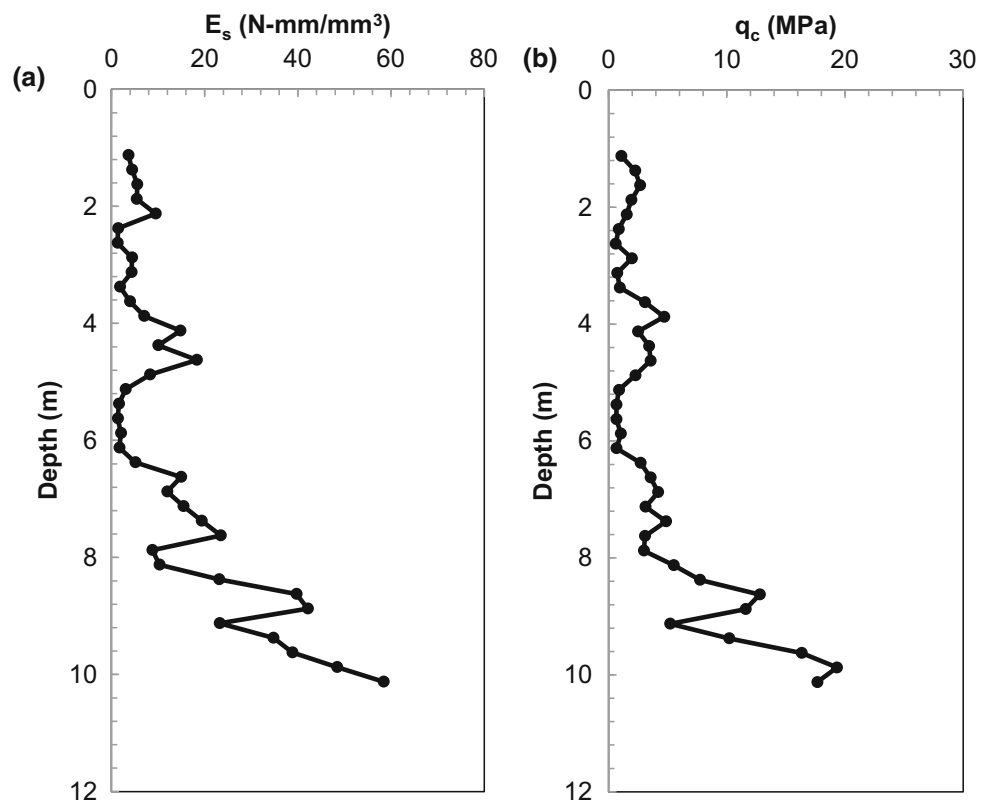
#### 3.2 SDS Correlation with CPT

**Correlation with  $q_c$ .** Using the results of all the SDS tests conducted adjacent to CPT sites, a correlation was made between the specific energy and the cone tip resistance. Figure 4 illustrates the relationship between  $E_s$  and  $q_c$  for all soils with different fines content ( $FC$ ). The values of  $FC$  were estimated from the SDS data (Mirjafari et al. 2017).

It can be observed that for deposits consisting of clean sands (fines content,  $FC \leq 5\%$ , there is a good correlation between  $E_s$  and  $q_c$ , although the data is scattered. However, for silty sands with  $5\% < FC < 35\%$ , the correlation appears to be better (with higher correlation coefficient). For soils with high  $FC$ , the relation can be divided into two: soft clayey soils ( $c_p'' \leq 0.9$ ) and stiff clayey soils ( $c_p'' > 0.9$ ). Note that high  $c_p''$  is an indication of highly plastic clay or stiff clay.

**Correlation with  $f_s$ .** Attempts were made to correlate SDS parameters with the CPT sleeve friction,  $f_s$ . In order to facilitate the correlation,  $f_s$  was combined with  $q_c$  in terms of the parameter  $P$ :

**Fig. 3** Typical variation with depth of **a**  $E_s$  from SDS test; and **b**  $q_c$  from CPT test



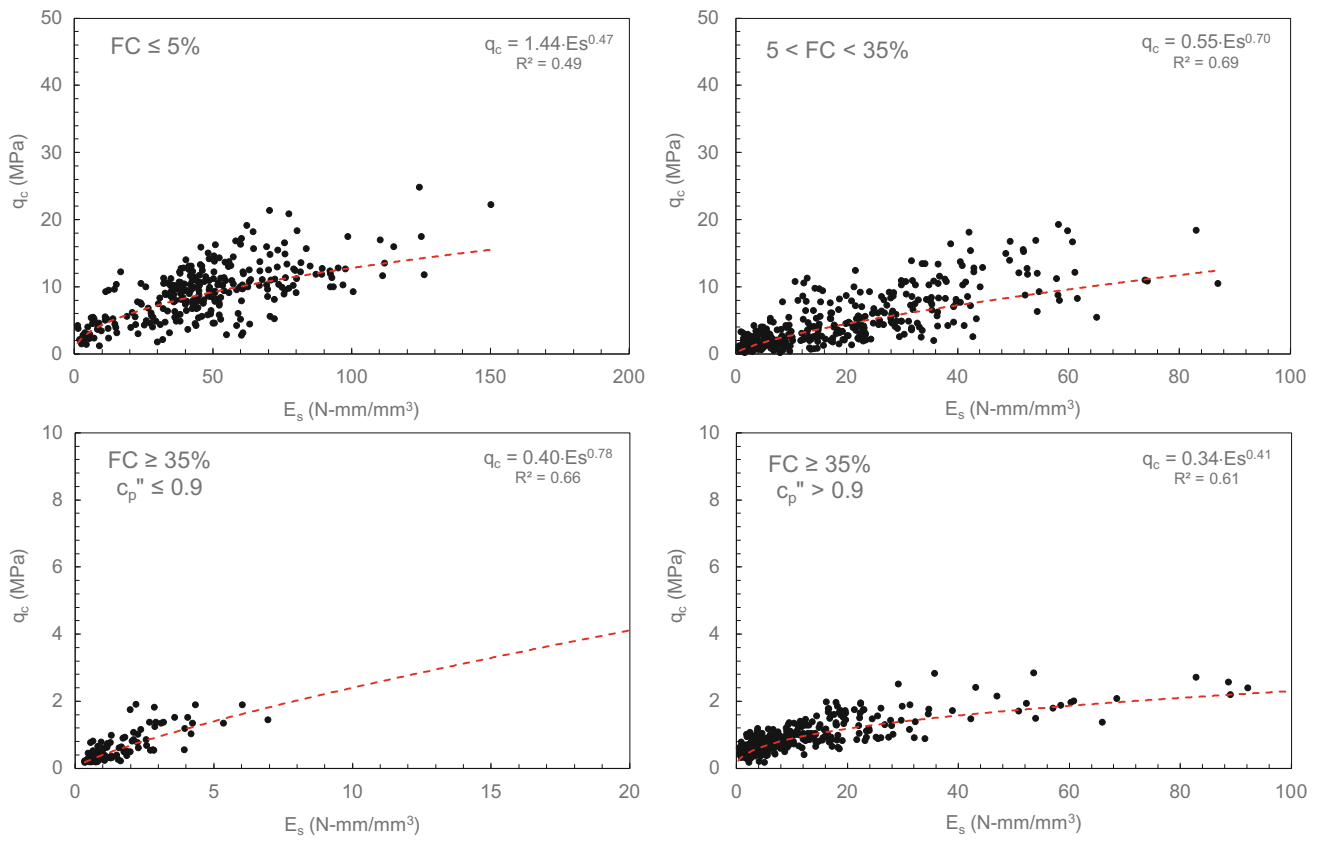
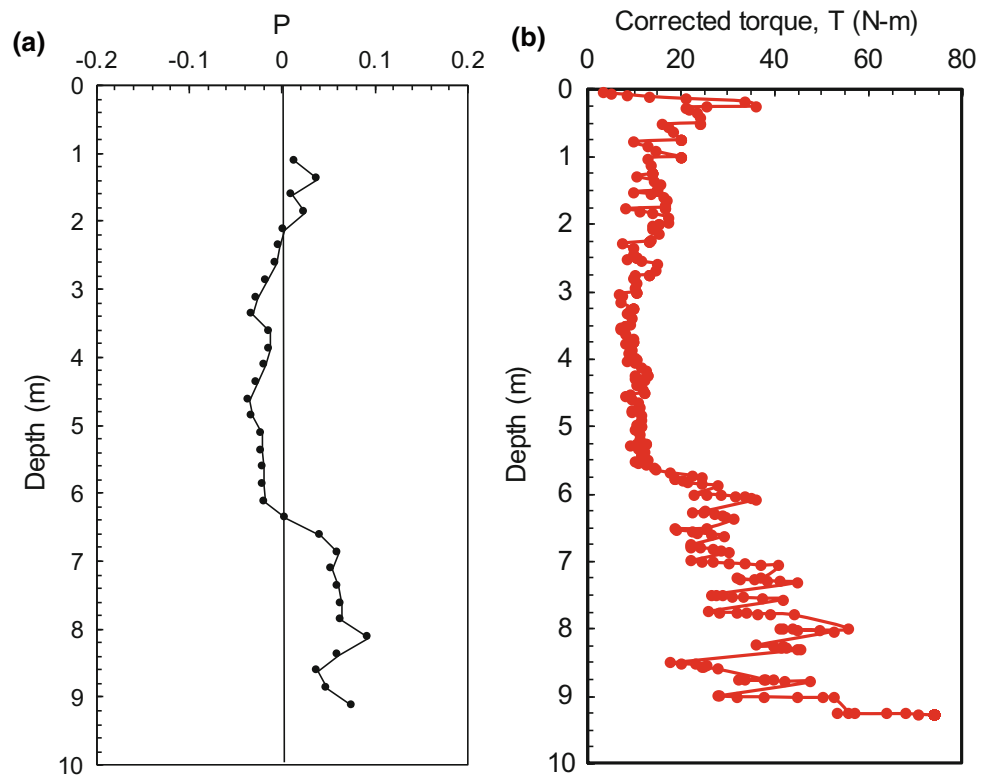


**Fig. 4** Correlation between  $q_c$  and  $E_s$

**Fig. 5** Typical variation with depth of: **a**  $P$  from CPT test; and **b** corrected  $T$  from SDS test



$$P = \frac{\log q_c}{\log F_r + 10} \quad (5)$$

where  $F_r = (f_s / (q_c - \sigma_{v0})) \times 100\%$  and  $\sigma_{v0}$  is the total vertical pressure (Robertson 1990). By analysing the SDS results obtained, it was determined that  $P$  correlates well with the corrected torque,  $T$ . A typical depth profile comparison between  $P$  and  $T$  is given in Fig. 5, where a good agreement is obtained.

The correlation between  $P$  and the average torque,  $T_{ave}$ , is shown in Fig. 6. It can be seen from the figure that with the

relatively good value of the coefficient of determination,  $R^2$ , there is good correlation between the two parameters. Thus,  $f_s$  at any given point can be estimated from  $T_{ave}$  and  $P$  correlation, and then through Eq. (5).

**Correlation with  $I_c$ .** Finally, SDS parameters were correlated with the soil behaviour type index,  $I_c$ , which is essentially the radius of the concentric circles delineating boundaries between soil types in the soil behavior chart (Robertson and Wride 1998). Figure 7 shows the correlation between  $I_c$  and  $Ave(\delta T)$ ; again, good correlation can be observed.

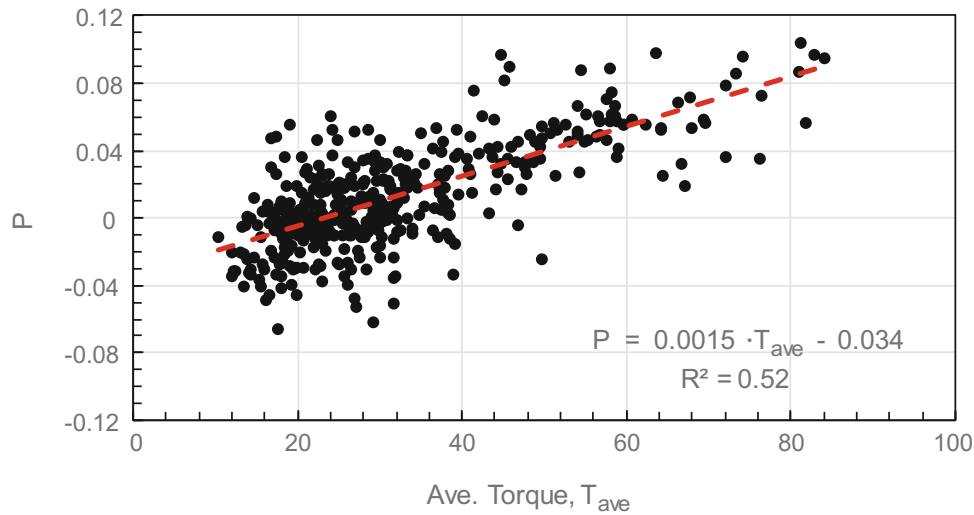


**Fig. 6** Correlation between  $P$  and  $T_{ave}$

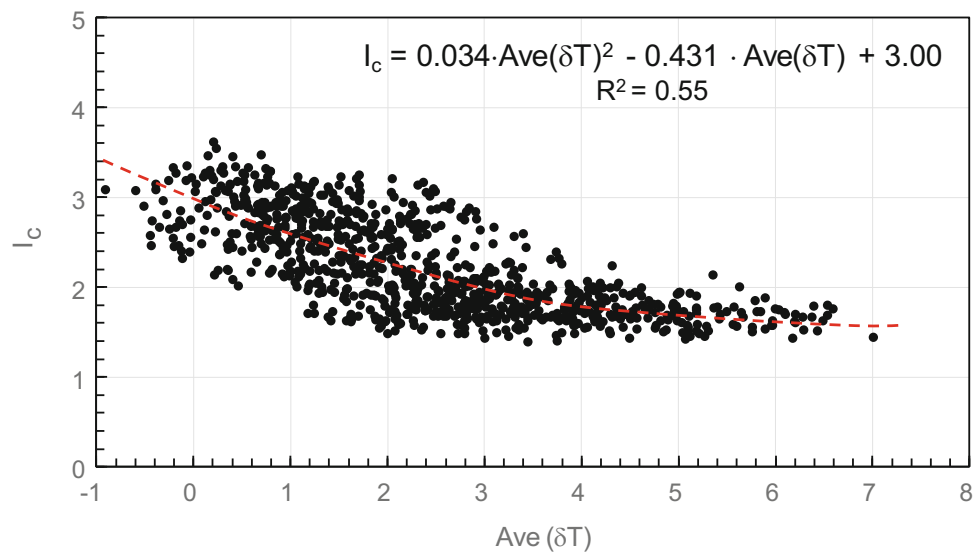


**Fig. 7** Correlation between  $I_c$  and  $Ave(\delta T)$

## 4 Concluding Remarks

A new in situ testing method, referred to as the Screw driving sounding (SDS) method, has been recently developed. As an improved version of the conventional Swedish weight sounding (SWS) method, more parameters can be measured during the SDS tests, such as the torque, load and penetration velocity. Additional parameters can be derived by processing the measured SDS data. Based on a number of tests conducted adjacent to CPT sites in New Zealand, attempts were made to correlate various SDS parameters with the tip resistance, sleeve friction and soil behavior type index in CPT.

With the relatively good correlations obtained, it was then possible to estimate the CPT strength profile from SDS. As SDS is simpler, faster and more economical test, the results suggest that SDS can supplement CPT results for a more cost-effective geotechnical investigation.

**Acknowledgements** The authors would like to acknowledge Nitto Seiko Company for providing the SDS machine for use in NZ and the Japan Home Shield (JHS) Company for providing assistance for this research. We also would like to thank the New Zealand Geotechnical Database (NZGD) for providing the borehole data and CPT records, as well as the various city councils for providing access to the test sites.

## References

- Mirjafari, S.Y.: Soil characterization using Screw Driving Sounding (SDS) data. Ph.D. Thesis, University of Auckland (2016)
- Mirjafari, Y., Orense, R.P., Suemasa, N.: Assessment of in-situ liquefaction resistance of soils using Screw Driving Sounding. In: Proceedings of 6th International Conference on Earthquake Geotechnical Engineering, Christchurch, NZ, 8p (2015)
- Mirjafari, Y., Orense, R.P., Suemasa, N.: Soil classification and liquefaction evaluation using Screw Driving Sounding. In: Proceedings of 5th International Conference on Geotechnical and Geophysical site Characterisation, Gold Coast, Australia, 6p (2016)
- Mirjafari, Y., Orense, R.P., Suemasa, N.: Soil type identification and fines content estimation using the Screw Driving Sounding (SDS) data. In: Proceedings of 20th New Zealand Geotechnical Society Geotechnical Symposium, Napier, NZ (2017)
- Orense, R., Mirjafari, Y., Suemasa, N.: Geotechnical site characterisation using Screw driving sounding method. In: Proceedings of New Zealand-Japan Workshop on Soil Liquefaction during Recent Large-scale Earthquakes, Auckland, NZ, pp. 11–20 (2014)
- Robertson, P.K.: Soil classification using the cone penetration test. *Can. Geotech. J.* **27**(1), 151–158 (1990)
- Robertson, P.K., Wride, C.E.: Evaluating cyclic liquefaction potential using the cone penetration test. *Can. Geotech. J.* **35**(3), 442–459 (1998)
- Suemasa, N., Shinkai, K., Suzawa, T., Tamura, M.: A plasticity model for Swedish weight sounding test. In: Proceedings of 4th Japan—Philippines Workshop on Safety and Stability of Infrastructure against Environmental Impacts, University of Philippines, pp. 169–177 (2005)
- Tanaka, T., Suemasa, N., Ikegame, A.: Classification of strata using screwdriver sounding test. In: Proceedings of 22nd International Offshore and Polar Engineering Conference, Rhodes, Greece, pp. 851–856 (2012)
- Tsukamoto, Y.: Integrating the use of Swedish weight sounding tests for earthquake reconnaissance investigations. In: Proceedings of International Conference on Earthquake Geotechnical Engineering: From Case History to Practice, Istanbul, Turkey, 21 pp. (2013)
- Tsukamoto, Y., Ishihara, K., Sawada, S.: Correlation between penetration resistance of Swedish weight sounding tests and SPT blow counts in sandy soils. *Soils Found.* **44**(3), 13–24 (2004)

# Litho-Structural Control on the Geotechnical Properties of Colluvial Deposits, Rio do Sul City, Santa Catarina, Brazil

Vanessa Noveletto, Marivaldo S. Nascimento, Murilo S. Espíndola, and Vitor S. Müller

## Abstract

Mountain regions are characterized by high instability and geodynamic processes which result in a wide variety of mass movement, rockfalls and debris flow or avalanches. Mass movement constitutes one of the major hazard in the Rio do Sul city, northeast Santa Catarina state, Brazil. This work investigates the relationship between lithology, tectonic structures, geotechnical properties and landslides processes in the study area. Results showed that lithological control is expressed in alteration grade of different rocks and materials, which is evident by the higher susceptibility of shales and colluvial deposits to weathering, as well as in clay content, which is primarily represented by illite in the stratigraphic units. Structural control is marked by two failures and fractures sets that affect all stratigraphic units, with NE–SW as the major strike and NW–SE as the subordinate one. Colluvial deposits present in the study area are the result of landslides processes. Geotechnical properties and shear resistance parameters showed a good correspondence between granulometric texture, which is related with mineral composition of parent rock as well as with weathering and erosion processes. Therefore, it is possible to assume that landsliding in the Rio do Sul city can be explained and predicted by the nature of the geological

framework and geotechnical behavior of the rocky masses and soil.

## Keywords

Geology • Geotechnic • Colluvial deposit • Santa Catarina

## 1 Introduction

Geological and structural setting of slopes are the main factors controlling dynamic mass movement's development. Bedding, tectonic structures, stratigraphic contact between rocks with different geotechnical properties, and weathering grade are some factors that control the slope stability (Wu and Sidle 1995). This paper presents mineralogical, structural and geotechnical data from sedimentary rocks of the Rio do Sul Formation, volcanic rocks of the Serra Geral Formation (Milani et al. 2007), and colluvial deposits in the Rio do Sul city, Santa Catarina (Schneider et al. 1974) (Fig. 1). The Rio do Sul Formation is a lithostratigraphic unit of Itararé Group and represents the Permo-Carboniferous glacial sedimentation in the Paraná Basin (Milani 1997). Dark gray to black shales, rhythmites, mudstones, silty-argillaceous matrix diamictites and fine-grained sandstones are the main lithology (Lima et al. 2015). The Serra Geral Formation encompasses Mesozoic volcanic sequences of the Paraná Basin, related to the evolution of the South Atlantic Ocean. Tholeiitic basalts and basaltic andesites represent the main lithology, while the subordinate lithology comprises rhyolites and rhyodacites (Peate et al. 1992).

## 2 Materials and Methods

Stratigraphic units were characterized by faciologic and architectural analysis (Reading and Levell 1996). Petrographic characteristics of units were obtained with optical

V. Noveletto (✉) · M. S. Nascimento · M. S. Espíndola  
V. S. Müller  
Federal University of Santa Catarina, Santa Catarina State,  
88040-900 Florianópolis, Brazil  
e-mail: vanessa.noveletto@gmail.com

M. S. Nascimento  
e-mail: nascimento.marivaldo@gmail.com

M. S. Espíndola  
e-mail: muriloespindola@gmail.com

V. S. Müller  
e-mail: vitor@mullergeo.com

V. Noveletto · M. S. Nascimento  
Basin Analysis and Characterization of Reservoir Group (ANBA),  
Florianópolis, Brazil



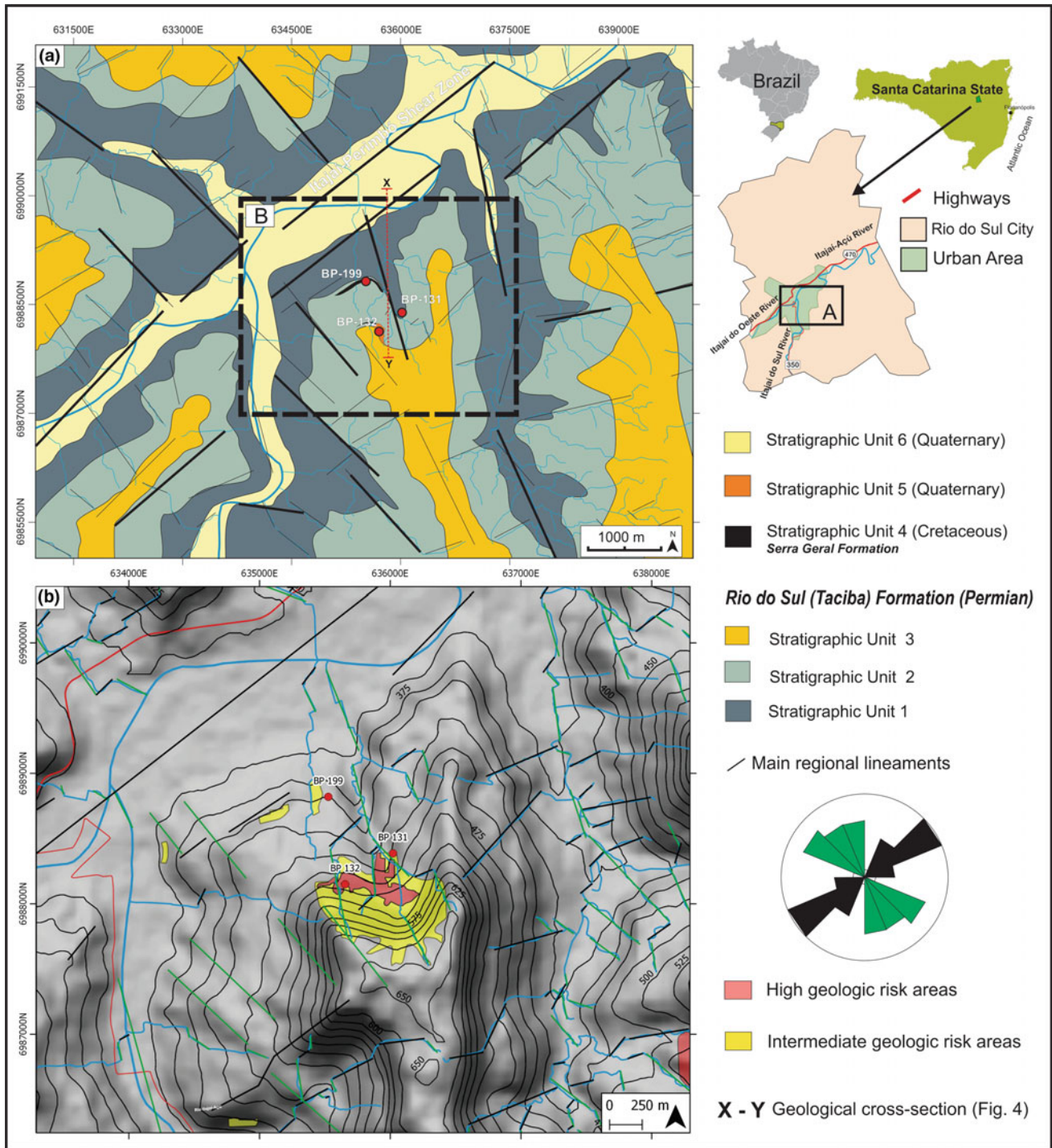


**Fig. 1** Geological and structural context of the study area: **a** Geological map of the main stratigraphic units with location of the outcrops; and **b** Geomorphological map with high- to intermediate geologic risk areas, as defined by (Cenad—Defesa Civil Do ... 2013). Note The main

microscopic description at Laboratory of Sedimentary Basin Research and Reservoir Characterization (LABAC), and scanning electron microscopy (SEM) at Central Laboratory of Electronic Microscopy (LCME) of the UFSC. Mineral compositional analysis was performed by energy-dispersive

structural lineaments NE–SW are associated with Itajaí-Perimó Shear Zone (IPSZ), while small lineaments reflect the subordinate structural pattern NW–SE

X-ray spectroscopy (EDX) at LCME and X-ray diffraction (XRD) at Laboratory of Minerals and Rocks Analysis (LAMIR) of the Federal University of Paraná State. Structural lineaments were extracted from shaded relief mesh with NE–SW, NS and NW–SE illuminations. Shaded relief

maps were generated from digital elevation maps (DEM) provided by EPAGRI/CIRAM (Environmental Resources and Hydrometeorology Information Center of Santa Catarina State). Granulometry, soil moisture content, and specific gravity of soil solids tests, followed the Brazilian Standards NBR 7181 (Associação Brasileira de Normas Técnicas 1984b), NBR 6457 (Associação Brasileira

de Normas Técnicas 1986) and NBR 6508 (Associação Brasileira de Normas Técnicas 1984a), respectively. Mechanical behavior was obtained from consolidated and drained direct shear test following ASTM D3080 standard (American Society for Testing and Materials 2003). The normal strains used at the consolidation stage were 50, 150 and 250 kPa.

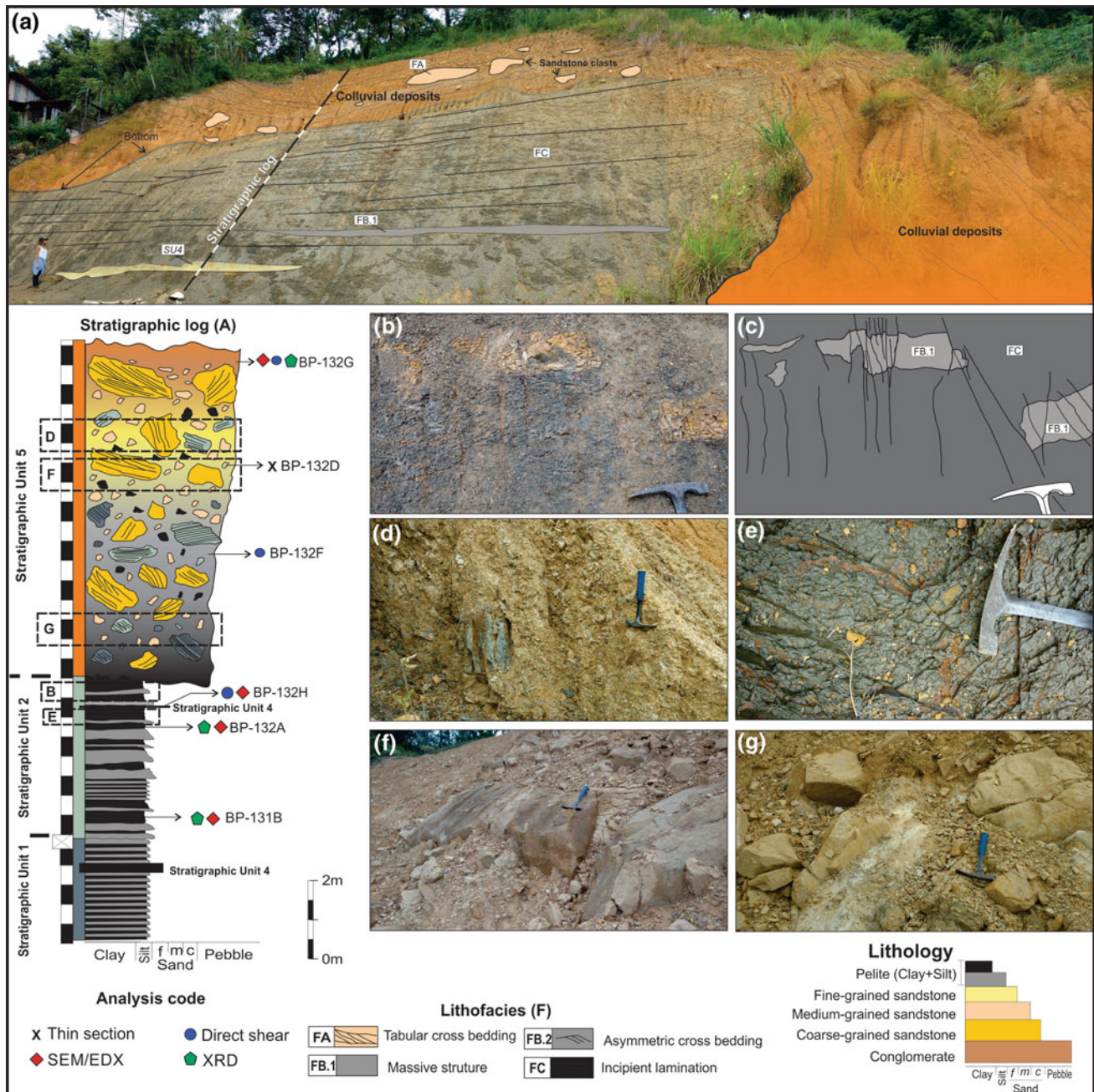


**Fig. 2** Faciologic and architectural aspects of the studied stratigraphic units: **a** Panoramic view of the outcropping (BP-132) with stratigraphic log; **b** Dark-gray shale (FC) and displaced silty layers (FB.1); **c** Vertical and subvertical fractures and faults, with two direction patterns: 130-135Az and 195-215Az; **d** Colluvial deposit, with chaotical and

massive structure, composed of shale clasts; **e** Dark-gray shales with incipient lamination (FC), highly fractured and friable; **f** and **g** Sandstone boulders (FA) of the SU3 immersed in an argillaceous to-arenitic-argillaceous matrix

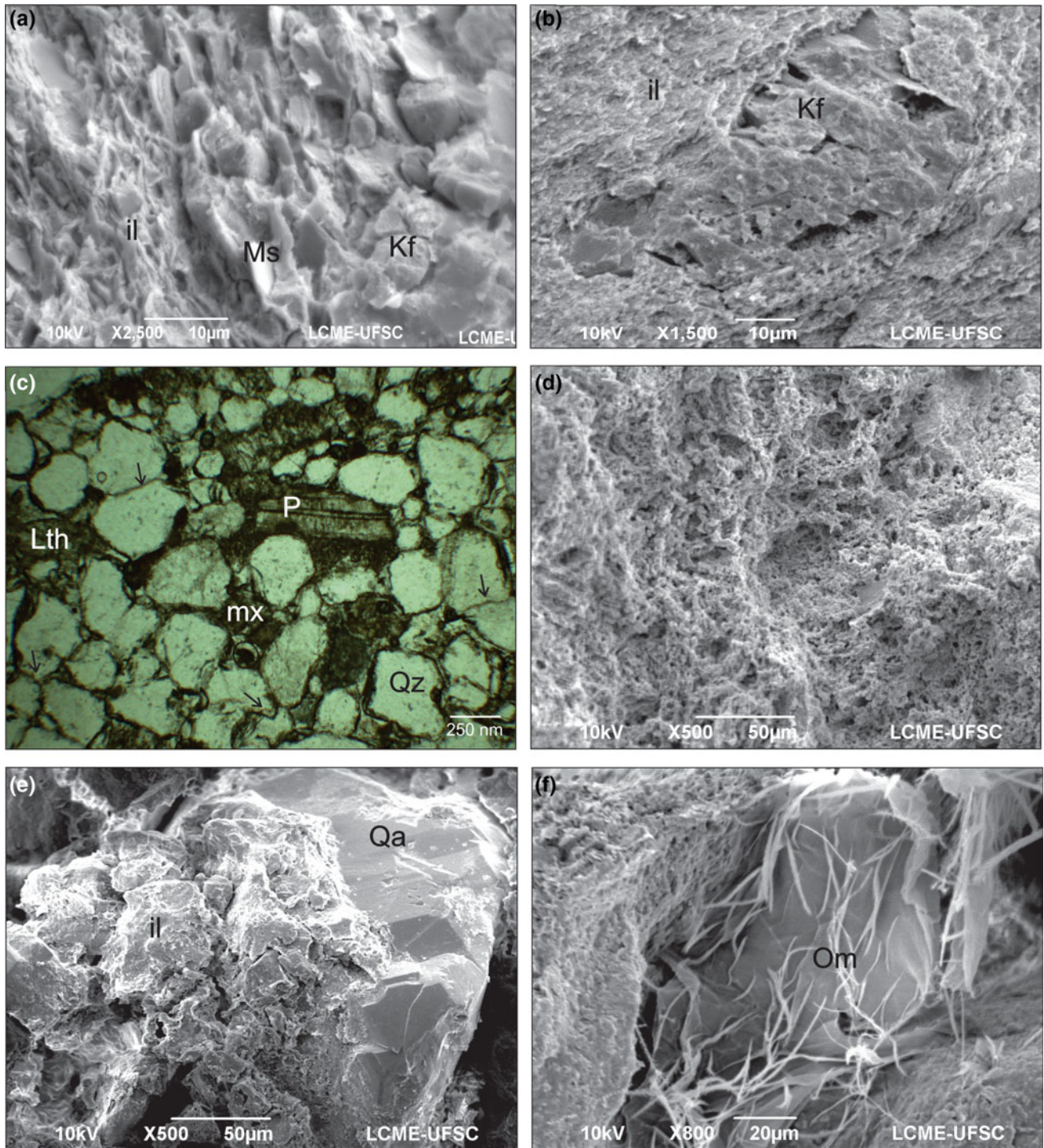


**Fig. 3** Petrographic characteristics of the stratigraphic units: **(a and b)** Detrital grains of feldspar (Kf) and muscovite (Ms), and detrital k-feldspar with dissolution feature and illite (il) coating of SU1 and SU2; **(c)** Sandstone of SU3 with quartz (Qz), k-feldspar, plagioclase (P) and lithic (Lth) grains, clay minerals from matrix and authigenic

quartz (Qa) (thin section under polarized light); **(d)** Highly porous structure from SU4; **(e)** Particles of colluvial soil of SU5 cemented mainly by clay minerals, as illite, and locally by authigenic quartz. **(f)** Organic matter (Om) filaments of SU5

### 3 Results and Discussions

#### 3.1 Stratigraphic Units and Tectonic Structures

In the study area were described five stratigraphic units (SU) named as: SU1, SU2, SU3, SU4 and SU5. The SU1 comprises tabular and fine-laminated dark gray shales with aggradational pattern of facies (Fig. 2). This stratigraphic unit has abrupt contact with the SU2. The SU2 includes a rhythmic succession of silty-shale with aggradational and fining upward patterns of facies. The lithofacies FB2 occurs as a tabular layer with current ripples. In the outcropping BP132, shale and silty clay-stones present blocky texture and joint fractures (Fig. 2b, c) favorable to the erosional processes. The SU3 includes tabular medium to coarse-grained feldspathic sandstones, with planar and cross-bedding, which represents the uppermost portion of the stratigraphic units in the studied area (Fig. 2a, f, g). The SU4 consist of volcanic rock sills (3 m thick) between the bedding of shales and rhythmities. It presents weathered massive structure and brownish color (BP-199). The sill has a pattern with vertical fractures with directions 240–245 Az, and a sub vertical fracture pattern with direction 335 Az. This unit also occurs as a lenticular layer 3.5 cm thick, with planar bedding and whitish-yellow color. At this site, the sill differs from the rest of rocks due to its high weathering grade, low density and the existence of dissolution pores. Furthermore, the adjacent silty claystone layers are more compact, and when they crack, they have conchoidal fracture, which represent the influence of the heat generated by sill intrusion. The SU5 includes matrix-supported colluvial deposits that occurs as a talus on the SU2 (Figs. 2, 3 and 4), and consists of poorly sorted sub angular boulders of sandstones from SU3 and shales chaotically immersed in a matrix. There are remarkable changes towards the top of unit: the matrix grades from argillaceous to arenitic-argillaceous; the size and number of shale clasts decrease, while the sandstone clasts increase; and the color grades from medium-gray to reddish. The SU5 content allows interpreting that this deposit represents the product of SU2 and SU3 weathering, which was eroded and accumulated above SU2.

The influence of tectonic context is also expressed through lineaments (Fig. 1b), interpreted at 1:50,000 and 1:250,000 scale. The main pattern is characterized by bigger lineaments with NE–SW direction, which control the course

of the main rivers, and represent the fractures and joints system associated with Itajaí-Perimbó Shear Zone (IPSZ) (Silva 1981). The subordinate small and more disperse lineaments NW–SE are related to the Mesozoic reactivations of IPSZ (Rostirolla 2003). This same fractures and joints systems were recorded on stratigraphic units in the study area (Noveletto et al. 2016).

#### 3.2 Mineral Composition

Shales and rhythmities (SU1 and SU2) are composed of subangular to subrounded feldspar and muscovite grains (Fig. 3a, b). Illite is the main clay mineral which occurs as flaky authigenic aggregates coating on the detrital feldspar grains (Fig. 3a, b). XRD analysis showed the likely presence of smectite and kaolinite (Fig. 4).

Well to- moderate-sorted sandstones (SU3) have framework composed of quartz (Qz), potassic feldspars (Kf), plagioclase (Pl) and lithic fragments (Lt) (Fig. 3c). The grains contact are mainly long to- concave-convex. Quartz grains are mainly monocrystalline and exhibit parallel to—undulose extinctions. Subhedral potassic feldspars and plagioclase grains are slightly bigger than quartz grains. Detrital and authigenic clay minerals are the main constituents of the matrix, and authigenic quartz occurs cementing the grains. Weathered volcanic rocks (SU4) has a highly porosity (Fig. 3d). Colluvial soil (SU5) is mainly composed of clay minerals as illite, as well as authigenic quartz, and filaments of organic matter (Fig. 3f). XRD analysis showed the likely presence of kaolinite and smectite (Fig. 4). These deposits present highly porosity and well aggregated particles.

#### 3.3 Geotechnical Properties of Colluvial Deposit (SU5)

The geotechnical properties of colluvial deposit (SU5) were obtained from two different portions, represented by the matrix (BP132F) that involves the shale and sandstone clasts, and by the colluvial soil (BP132G; Table 1). Effective angles of internal friction with higher values are typical of granular materials. However, in this case the authors estimate that the dispersion of angles of internal friction were influenced by the deposit heterogeneity.

**Table 1** Geotechnical properties of colluvial deposit

Sample	Wnat (%)	$\gamma_s$ (kPa)	e	n (%)	Sr (%)	Granulometry (%)			Angle of internal friction (°)	Cohesion (kPa)
						sand	silt	clay		
Matrix	11.68	26.60	0.50	35.40	60.10	23.05	59.09	15.37	29	10.50
Colluvial soil	8.40	28.60	0.65	39.31	38.46	76.52	17.96	4.15	54.70	0

Notes Wnat natural moisture;  $\gamma_s$  solid particles density; e void ratio; n porosity; Sr saturation

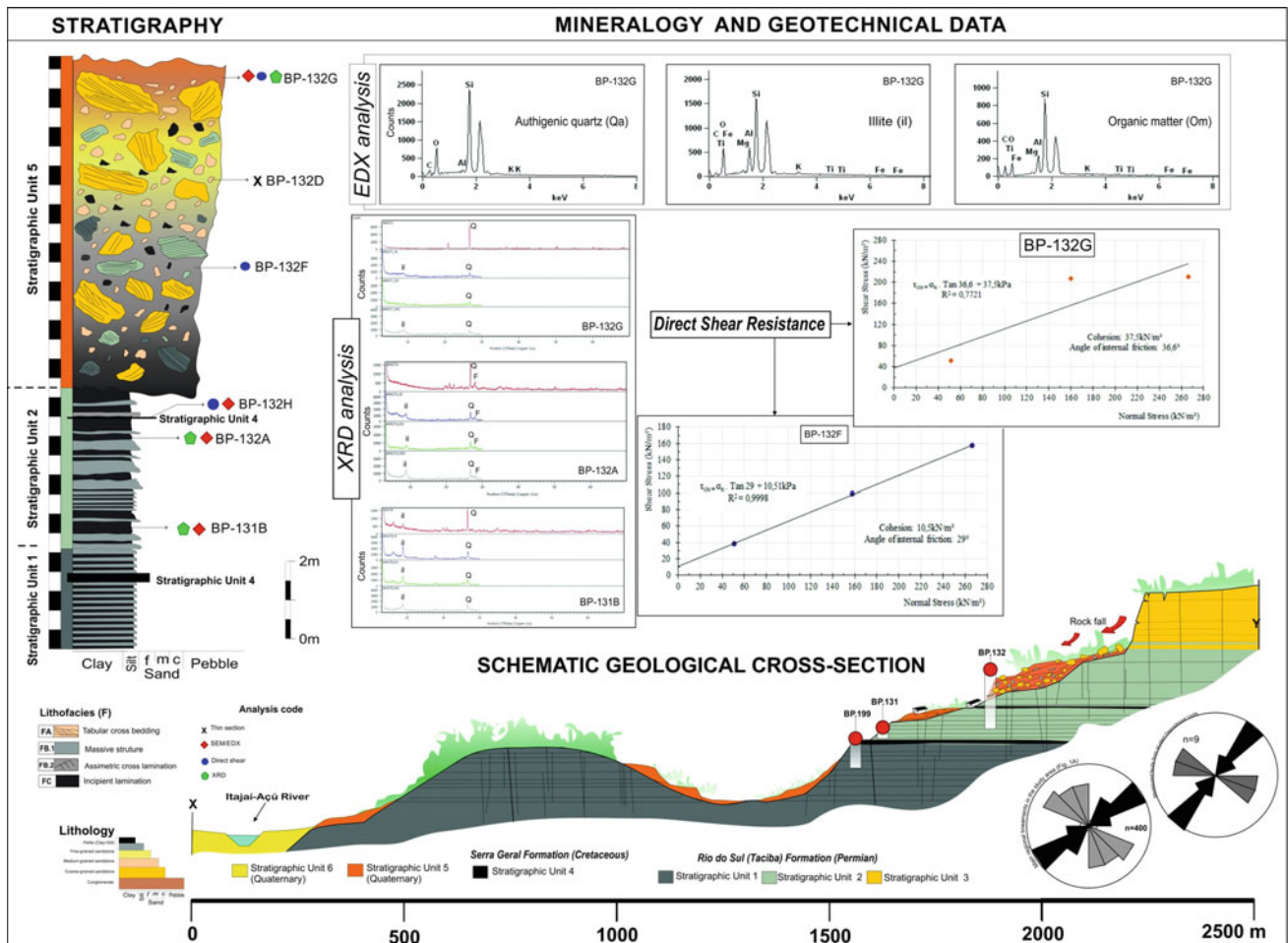


**Fig. 4** Graphical abstract with integrated mineralogical, structural and direct shear resistance data: The stratigraphy in the area includes the stratigraphic units SU1, SU2 and SU3 (Rio do Sul Formation); SU4 (Serra Geral Formation), and SU5 (colluvial deposit). The presence of sandstone and shale clasts composing the colluvial deposit, along with local geomorphology, enable the interpretation that these deposits are the product of weathering and erosion of SU2, SU3, and SU5. Detrital illite (muscovite) (il) and feldspar grains (F), and a small amount of smectite (il/s) and kaolinite compose shales and silty clay stones.

## 4 Conclusions

The geological and geotechnical controls on the landslides in a specific area of the Rio do Sul city were investigated mainly from the viewpoint of integration of mineralogical, structural and direct shear resistance data (Fig. 4). A comprehensive mineralogical and geotechnical investigation is discussed to derive the contribution of parameters involved in the occurrence of landslides. The stratigraphy in the area includes five stratigraphic units: SU1, SU2 and SU3 (Rio do Sul Formation); SU4 (Serra Geral Formation); and SU5 (colluvial deposit). The SU5 matrix-supported colluvial deposit with boulders of sandstones (from SU3) and shale

Quartz, feldspar and lithic fragments, matrix with detrital clay and quartz cements compose sandstones (SU3). Illite is the main mineral constituent of the colluvial deposits. Interpreted lineaments show NE-SW as the main structural pattern, associated with Itajaí-Perimbó shear zone. The direct shear resistance parameters show that the highest cohesion and the lowest angle of internal friction are associated with the matrix of SU5, while colluvial soil has cohesion equivalent to 0 kPa and the highest angle of internal friction

clasts (from SU1 and SU2) deposited as debris flow and rock fall on the slopes.

The mineralogical analysis indicate that shales and silty clay stones are composed mainly of detrital illite (muscovite) and feldspar grains, and a small amount of smectite and kaolinite. Sandstones (SU3) are composed mainly of monocrystalline quartz, feldspar and lithic fragments, and matrix with detrital clay and quartz cements. Illite is the main mineral constituent of the colluvial deposits, where SEM micrographs showed skeletal matrix aggregation with high porosity.

Lineaments observed in shaded relief map, as well as faults and fractures measured at field, showed two structural patterns: NE-SW and NW-SE. The main structural pattern

NE-SW, represented by bigger lineaments are concordant with NE/SW Itajaí-Perimbó shear zone (Schneider et al. 1974). These tectonic structures represent weakness surfaces, which provide an increase of water access and, consequently, an increase of weathering rate. A higher content of water might also reflect an increment of pore pressure inside the colluvial deposit, which means another variable that contributes to the mass movement. Weathering influence is evident by the presence of alteration minerals, like illite coating, and by dissolutions features.

The direct shear resistance parameters showed a good correspondence with granulometry. Matrix, the final material, has the highest cohesion and the lowest angle of internal friction. Otherwise, colluvial soil, which has the highest content of sand, showed cohesion equivalent to 0 kPa and the highest angle of internal friction. The dispersion of points in Mohr's circle from colluvial soil (BP132G) can be justified by the heterogeneity of colluvial deposit. The origin process of deposit itself can explain this dispersion, hence coarse fragments tend to be accumulated upstream (where BP132G was collected), and they might reflect in different shear strains for the same sample.

## References

- American Society for Testing and Materials: D3080: Standard Test Method for Direct Shear Test of Soils Under Consolidated Drained Conditions. West Conshohocken, ASTM International (2003)
- Associação Brasileira de Normas Técnicas: NBR 6508: Grãos de solo que passam na peneira de 4,8 mm—Determinação da massa específica, 8 p (1984a)
- Associação Brasileira de Normas Técnicas: NBR 7181: Solo—Análise Granulométrica, 13 p (1984b)
- Associação Brasileira de Normas Técnicas: NBR 6457: Solo—Preparação para ensaios de compactação e ensaios de caracterização, 9 p (1986)
- Cenad—Defesa Civil Do Brasil—Ministério Da Integração Nacional Relatório Consolidado Sobre As Intervenções No Município: Local: Rio Do Sul—Sc Contrato No 04/2013 GeoEnvi—Geologia e Meio Ambiente LTDA. Florianópolis, 30 de Setembro de 2013
- Lima, J.H.D., Netto R.G., Corrêa, C.G, Lavina, E.L.C.: Ichnology of deglaciation deposits from the Upper Carboniferous Rio do Sul Formation (Itararé Group, Paraná Basin) at central-east Santa Catarina State (southern Brazil). *J. S. Am. Earth Sci.* **1**(63), 137–148 (2015)
- Milani, E.J.: Evolução tectono-estratigráfica da Bacia do Paraná e seu relacionamento com a geodinâmica fanerozóica do Gondwana Sul-ocidental. Doctoral dissertation, Federal University of Rio Grande do Sul, Porto Alegre, 255 pp (1997)
- Milani, E.J. et al.: Cartas Estratigráficas: Bacia do Paraná. *Boletim de Geociências da Petrobras* **2**(15), 265–287 (2007) (Rio de Janeiro)
- Novelletto, V., Nascimento, M.S., Parizoto, D.G.V., Pellerin, J.R.G.M., Manna, M.O.: Aspectos Geológicos e a Susceptibilidade a Movimentos de Massa no Perímetro Urbano Norte de Ituporanga, Santa Catarina. In: XLVIII Congresso Brasileiro de Geologia, Sociedade Brasileira de Geologia, Porto Alegre, vol. 1, p. 5101 (2016)
- Peate, D.W., Hawkeswort, C.J., Mantovani, M.S.M.: Chemical stratigraphy of the Paraná lavas (South America): classification of magma types and their spatial distribution. *Bull. Volcanol.* **55**, 119–139 (1992)
- Reading, H.G., Levell, B.K.: Controls on the sedimentary record. In: Reading, H.G. (ed.). *Sedimentary Environments: Processes, Facies and Stratigraphy*, 5–36 pp. Blackwell Science, Oxford (1996)
- Rostirolla, S.P.: Structural styles of the intracratonic reactivation of the Perimbó fault zone, Paraná basin, Brazil. *J. S. Am. Earth Sci.* **16**, 287–300 (2003)
- Schneider, R.L., Mühlmann, H., Tommasi, E., Medeiros, R.A., Daemon, R.F., Nogueira, A.A.: Revisão estratigráfica da Bacia do Paraná. In: XXVIII Congresso Brasileiro de Geologia, vol. 1, 41–65 pp, Sociedade Brasileira de Geologia, Porto Alegre (1974)
- Silva, L.C., Dias, A.A.: Projeto Timbó-Barra Velha, Brasil. Convênio DNPM/CPRM, Porto Alegre, 282 pp (1981)
- Wu, W., Sidle, R.C.: A Distributed Slope Stability Model for Steep Forested Basins, vol. 31, 2097–3110 pp. AGU Publications, Water Resources Research (1995)



# Vadose Zone Characterisation for Hydrogeological and Geotechnical Applications

Matthys A. Dippenaar and J. Louis van Rooy

## Abstract

Rapid urbanization is resulting in increased vertical development and use of anthropogenic materials. Geotechnical site investigation is well established in assessing ground conditions, and moisture specifically is a standard descriptor in soil profile logging and is addressed through a variety of laboratory tests. However, changing moisture conditions, occurring in the vadose zone between land surface and the groundwater table, results in highly variable conditions. Noting the presence and variability in moisture is not sufficient to ensure longevity of engineering structures and protection of water resources. Water at partial saturation is proposed to impact the infrastructure and the vadose zone moisture budget as: (A) perching above lower permeability (lower-k) materials; (B) perching as waterlogged lower-k materials above capillary barriered higher-k materials; both resulting in (C) possible imbibition into less saturated low-k materials; or, under further wetting, resulting in (D) lateral interflow under a hydraulic gradient; (E) gravity-driven percolation breaching capillary barriers and resulting in translatory downward flow; or (F) unsaturated fracture flow. All these mechanisms combine to result in complex moisture implications on infrastructure during project lifecycle, as well as on recharge and contaminant transport rates above the phreatic surface. These are further exacerbated by anthropogenic materials (e.g. made ground) replacing natural materials and infringing on the natural and pre-development subsurface water cycle, as well as climate change, and more elaborate engineering development. Contrary to saturated systems, unsaturated systems

result in alternating wetting-drying cycles causing continuous changes in effective stress and redox conditions. The paper addresses some key findings and examples from experiments and case studies.

## Keywords

Unsaturated flow • Fracture flow • Partial saturation  
Engineering hydrogeology

## 1 Introduction

Knowledge worldwide is rapidly expanding with reference to the management of runoff, stormwater, water sensitive design and urban hydrogeology. Infrastructure development, mining, and disruption of the geological environment are changing how water influences our development and how we alter the water cycle in the present and the future.

Consequences of (i) non-revenue water losses, misappropriation, overexploitation and improper management of urban waters and (ii) influences of water on infrastructure development are progressively becoming more noteworthy, and improved assessment, management, monitoring, design and long-term planning are due.

In addressing contributions to variably saturated flow and its implications on engineering geology and hydrogeology, experimental studies (examples shown in Fig. 1) conducted by the authors are discussed here with application to the influence of vadose zone conditions on engineering development. Vadose zone conditions relate to variably saturated conditions, ranging between dry and saturated, and incorporating hysteresis, whereas engineering development relates to any proposed change in current conditions and those during and following change induced through development.

The influence of water on development relates typically to the presence or absence of water itself, notably also the

M. A. Dippenaar (✉) · J. L. van Rooy  
Department of Geology, University of Pretoria, Pretoria,  
South Africa  
e-mail: matthys.dippenaar@up.ac.za; madippenaar@gmail.com

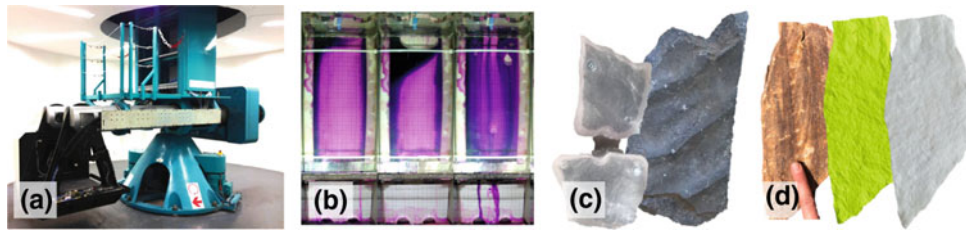


**Fig. 1** a The geotechnical centrifuge used to scale some models; b horizontal and vertical acrylic fractures mimicking unsaturated flow at intersections; c actual and resin-cast fractures for variable roughness

profiles; d actual, scanned and 3D-printed fractures for variable roughness profiles

alternating cycles of wetter or drier state due for instance to seasonality, as well as the influence(s) of said water quality. The set of experiments cited are extensively described in the relevant literature. This review of the published results aims to contribute not to the experimental methodologies, but to the collation of the combined findings, thus contributing to our understanding of variably saturated flow through complex systems.

## 2 The Vadose Zone in Urban Areas

The vadose zone is well understood to imply the variably saturated zone of the ground profile between land surface and the phreatic surface (groundwater table) where pore water pressure is predominantly below atmospheric pressure. It is characterised by highly variable saturation between unsaturated and locally saturated zones, but behaving in its entirety as an unsaturated system governed by the forces of capillarity and gravity (e.g. Dippenaar 2014a, b).

The vadose zone falls within a complex framework involving numerous disciplines such as soil science, soil mechanics, hydrology and hydrogeology (e.g. Dippenaar 2012; Ehlen 2005). However, the implications of the vadose zone far exceed these and vadose zone hydrology becomes imperative in studies pertaining to any land use change or urban development, given the likely interaction between construction and subsurface waters, and the increased possibility of contamination.

Urbanisation is known to alter urban water cycles distinctly in terms of its quantity (through imports, leakages construction altering flow paths) and quality (through contamination and reticulation of chlorinated water). This is well described (e.g. Attard et al. 2015; Lerner 2002; Vásquez-Suñe et al. 2005). Apart from the obvious influences of the phreatic zone, changes in moisture content and water quality of the vadose zone are becoming increasingly important in planning urban development.

## 3 Engineering Hydrogeology

In establishing a subdiscipline in Engineering Hydrogeology, incorporation of both the phreatic and vadose zones and their relationships with surface water need to be understood. This section aims to shed light on recent advances regarding the application of hydrogeology of fully and variably saturated systems to engineering geology.

### 3.1 Hydraulic Considerations

#### Phreatic and permanently waterlogged systems

Classically, permanently saturated systems have received significant attention and are mostly mitigated with dewatering practices. As permanently saturated systems are governed by (i) flow along a hydraulic gradient and (ii) mostly chemically reducing conditions, the focus of this paper will be on variably saturated systems where hydraulic gradients and redox conditions are more complex and less understood.

#### Variably saturated systems

When moisture conditions change seasonally or periodically, hysteresis plays an important role in defining the relationship between soil suction (or pore water pressure) and hydraulic conductivity (or intrinsic permeability). Imbibition of water into pore spaces occurs more readily than removal of the same water during drainage. Subsequently, the same degree of water saturation results in higher suction during wetting of an initially dry soil than when draining an initially wet soil.

Moisture thresholds such as field capacity will furthermore govern whether water will gravitate, imbibe, or remain as adhesive water attracted to mineral surfaces. In such variably saturated systems, altering the ground during construction inevitably alters this moisture regime and the



associated hydraulic properties. Perched systems may develop, water may imbibe into foundations, or basements and excavations may be flooded due to altering the unsaturated flow regime, subsequently highlighting the need to understand these systems as well as the influence of induced change. Case studies addressed at the hand of shallow perched and interflow systems by Dippenaar (2014a, b) and Dippenaar and Van Rooy (2016) detail the development of such systems, most notably with the perched and interflow systems forming periodically on the weathered bedrock interface. Further work by Brouwers (2017) and Brouwers and Dippenaar (2018) evaluates the reason for capillary barriered systems to even occur in soil above open fractures, implying that the development of these systems is not solely due to lower permeability basal horizons, but also due to higher permeability basal horizons.

Variably saturated systems are furthermore prone to clogging as wetter conditions mobilise fines and dissolved matter, resulting in deposition or precipitation as saturation decreases (e.g. Dippenaar and Van Rooy 2016). This translocation of materials can further alter the hydrological behaviour during project life cycle.

Further to this, certain other heterogeneities and anisotropies require consideration (e.g. Dippenaar and Van Rooy 2014). The co-occurrence of soil and rock at unsaturated state creates further complexity at the soil-rock interface, notably with respect to dispersion plumes developing in soils over fractures, until the moisture breaches the fracture and gravity-driven flow is induced (e.g. Brouwers 2017; Brouwers and Dippenaar 2018). Unsaturated flow in fractures of different geometries and orientations, as well as their intersections, result in complex flow mechanisms, where it has been shown that horizontal fractures tend to saturate to higher degree than their vertical counterparts (e.g. Jones et al. 2017a; b).

It becomes important, also, to define the reason for the occurrence of moisture in the profile. The competent geologist or engineer is able to deduce the hydrological system of whether water is imbibing upwards or laterally, or moving down a gradient on a lower-permeability barrier, or gravitating vertically downwards. The ground (soil and rock) profile description (notably the moisture and colour descriptors, together with any indication of porosity or permeability, noting that the latter two are not inherently related) alone can contribute to this knowledge, provided that description is detailed and cognisant of the implications.

### 3.2 Water Quality Considerations

#### Corrosivity and aggressiveness

In variably saturated systems, redox conditions are continuously changing. The air-water system in soils, notably

when organic, acidic and/or contaminated, increase aggressiveness of soils and soil moisture to cement in concrete and steel. Due to altering the flow system during construction and using other imported materials, the aggressiveness of site conditions may be changed and, apart from water affecting infrastructure through seepage and imbibition, soil moisture may also behave in a more corrosive manner.

Combining readily available information such as grading, field descriptors of moisture conditions, pH and electrical conductivity, a very good preliminary estimation of corrosivity can be deduced as different metals corrode at different rates based on soil type, soil moisture, pH and temperature (e.g. van Allemann 2017; Van Allemann et al. 2018).

#### Contaminated land and water

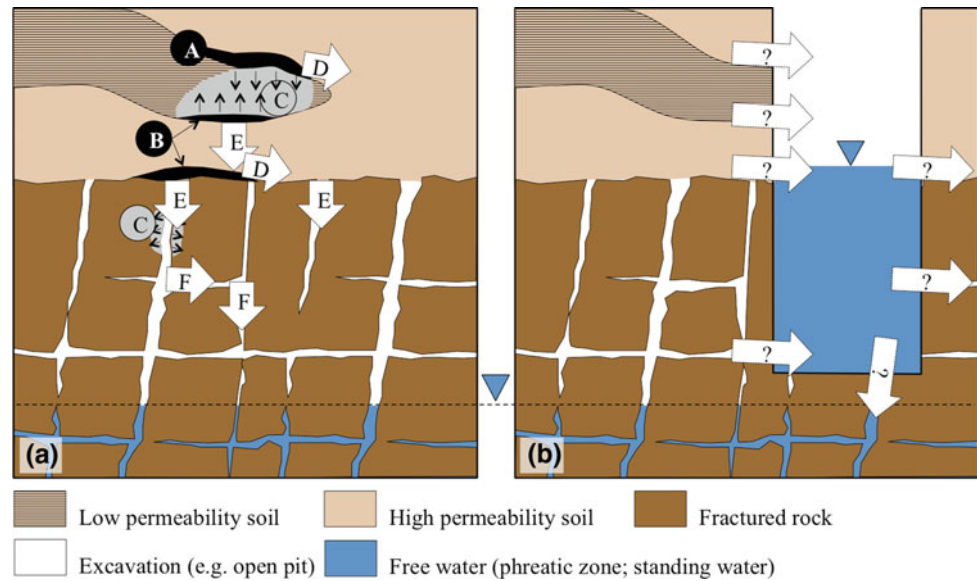
Depending on the type, disposition, persistence and bioaccumulation, different contaminants can have different influences on infrastructure. Organics (such as petroleum hydrocarbons) will behave very differently in the vadose zone to saline waters or brines, or high acidity waters, and so forth. This will also influence the use of the contaminated soils for engineering purposes, as contaminants may result in blistering, loss of strength, reactions between cement or bitumen with materials, and so forth. Where possible, an indication of the water quality of soil water is always beneficial.

## 4 Conclusions

Through the set of experiments, six scenarios were identified describing the most fundamental occurrences of water in the vadose zone that affects development (Fig. 2):

- (A) Normal perching: moisture can perch and disperse on lower permeability horizons due to the high suctions in small void spaces and the effort required to breach those suctions for water entry.
- (B) Capillary-barriered perching: moisture can perch and disperse on higher permeability horizons due to excessive adhesion and suction in fine-grained materials retaining moisture above larger voids or fractures, thus not allowing water entry.
- (C) Imbibition: moisture can imbibe laterally or vertically into finer-grained lower-permeability materials (soil or primary porosity of rock) due to suction, especially at fairly low moisture contents.
- (D) Shallow interflow: perched water can be mobilised as cohesion (water-water attraction) dominates and interflow ensues on lower permeability materials.

**Fig. 2** **a** Proposed occurrence of water at partially saturated state in the vadose zone, and **b** the uncertainty in apportioning the source of water flooding a hypothetical excavation with potential new flow paths indicated



- (E) Percolation: perched water at high or total saturation in the vadose zone can mobilise as cohesion dominates, and gravity-driven percolation or drainage results.
- (F) Unsaturated fracture flow: seepage at partial saturation through fracture intersections and networks.

Each of these occurrences of water in the vadose zone will affect infrastructure differently. When excavating and/or replacing in situ materials, these flow occurrences will be altered, resulting in, for instance, flooding of excavations (even at partial saturation) or increased aggressiveness to construction materials. Identifying these changes aids in mitigating damage to infrastructure and increased construction cost.

In achieving improved characterisation, it is recommended to improve the evaluation of these water occurrences. Noting whether moisture contents and mottling increase or decrease in certain directions (vertically in a profile, or spatially between profiles) already provide very sensible initial indications of flow systems. Understanding that porosity governs the storage of water, but that it effectively has very little influence on permeability (as void size rather than abundance governs the latter) explains the development of certain flow systems, or the relationship between water being retained versus water available for flow.

Most development occurs in the vadose zone. Resilience in planning during construction and project life requires improved incorporation of ground hydraulics. The data are

already being acquired through conventional site investigation; it now becomes merely a matter of interpreting data accordingly.

## References

- Attard, G., Winiarski, T., Rossier, Y., Eisenlohr, L.: Review: impact of underground structures on the flow of urban groundwater. *Hydrogeol J* (2015). <https://doi.org/10.1007/s10040-015-1317-3>
- Brouwers, L.B.: Geotechnical centrifuge modelling of variably saturated flow at the soil-rock interface. MSc Dissertation, (unpub.). University of Pretoria (2017)
- Brouwers, L.B., Dippenaar, M.A.: Partially saturated flow from sand into a discrete smooth open vertical fracture at the soil-rock interface: experimental studies. *Bull. Eng. Geol. Env.* (2018). <https://doi.org/10.1007/s10064-018-1258-x>
- Dippenaar, M.A.: How we lose ground when earth scientists become territorial: defining “soil”. *Nat. Resour. Res.* **21**(1), 137–142 (2012)
- Dippenaar, M.A.: Towards hydrological and geochemical understanding of an ephemeral palustrine perched water table “wetland” (Lanseria Gneiss, Midrand, South Africa). *Environ. Earth Sci.* **72** (7), 2447–2456 (2014a)
- Dippenaar, M.A.: Towards a multi-faceted Vadose Zone Assessment Protocol: cemetery guidelines and application to a burial site located near a seasonal wetland (Pretoria, South Africa). *Bull. Eng. Geol. Environ.* **73**(4), 1105–1115 (2014b)
- Dippenaar, M.A., Van Rooy, J.L.: Review of engineering, hydrogeological and vadose zone hydrological aspects of the Lanseria Gneiss, Goudplaats-Hout River Gneiss and Nelspruit Suite Granite (South Africa). *J. Afr. Earth Sc.* **91**, 12–31 (2014)
- Dippenaar, M.A., Van Rooy, J.L.: On the cubic law and variably saturated flow through discrete open rough-walled discontinuities. *Int. J. Rock Mech. Min. Sci.* **89**, 200–211 (2016)

- Ehlen, J.: Above the weathering front: contrasting approaches to the study and classification of weathered mantle. *Geomorphology* **67**, 7–21 (2005)
- Jones, B.R., Brouwers, L.B., Dippenaar, M.A.: Partially to fully saturated flow through smooth, clean, open fractures: qualitative experimental studies. *Hydrogeol. J.* (2017a). <https://doi.org/10.1007/s10040-017-1680-3>
- Jones, B.R., Brouwers, L.B., van Tonder, W.D., Dippenaar, M.A.: Assessing geotechnical centrifuge modelling in addressing variably saturated flow in soil and fractured rock. *Environ. Sci. Pollut. Res.* **24**, 13203–13223 (2017b)
- Lerner, D.N.: Identifying and quantifying urban recharge: a review. *Hydrogeol. J.* **10**, 143–152 (2002)
- Van Allemann, S.T.: A laboratory simulation of the potential groundwater contamination associated with Burial Materials. MSc dissertation (unpub.), University of Pretoria (2017)
- Van Allemann, S.T., Oliver, J., Dippenaar, M.A.: A laboratory simulation of the pollution of formaldehyde in cemeteries (South Africa). *Environ. Earth Sci.* (2018). <https://doi.org/10.1007/s12665-017-7219-z>
- Vásquez-Suñé, E., Sánchez-Vila, X., Carrera, J.: Introductory review of specific factors influencing urban groundwater, an emerging branch of hydrogeology, with reference to Barcelona, Spain. *Hydrogeol J.* **13**, 522–533 (2005)



# Evaluation of Geotechnical Parameters of Slopes at Blumenau, Santa Catarina, Brazil

L. E. C. Alves , M. Espindola , Vitor S. Müller , M. Z. Broetto ,  
R. L. Pizzolo , and V. F. Hickel 

## Abstract

The state of Santa Catarina, Brazil, has climatic, biological, geomorphological and geological characteristics that contribute directly to the occurrence of landslides. From the geological point of view, colluvial materials resulting from landsliding deposited in the lower parts of the slopes are denominated as hillslope deposits although they do not necessarily originate from the same rock. This study evaluated the geotechnical parameters of the slopes at Blumenau, where intense rainfalls and potentially unstable soils are present on steep hillsides and give rise to unstable colluvial slopes below. These factors resulted in a large number of slopes covered by colluvial deposits. However, in geotechnical mapping these kinds of materials are treated as “hillslope deposits” units with similar behaviors even though they have different geological-geotechnical evolutions and have experienced distinct processes of pedogenesis. The paper covers the classification as colluvial soils and landslides, as well as the use of geotechnical laboratory tests and geotechnical mapping. Evaluation of the geotechnical behavior of the soils was based on geotechnical characterization tests and drained direct shear tests in which parameters of cohesion and internal friction angle were obtained. Thus, the goal of this study was to understand the variability of the geotechnical parameters of these colluvial soils that

formed as “hillslope deposits” units according to Davison Dias (1995) methodology, so that they could be classified based on their lithotypes. The study results will help in urban planning in Blumenau and contribute to safety and predictability of areas subject to possible landslides.

## Keyword

Colluvial soils • Residual soils • Geotechnical parameters • Blumenau • Brazil

## 1 Introduction

Natural disasters related to landslides are important processes to geomorphological and dynamic evolution of hillsides. In urban areas, besides gravity, it is possible to cite the anthropic activities (bad management of water resources, unplanned landfills, poorly executed slope cuts or vegetation cover removal) as factors for the occurrence of landslides. In Brazil, landslide is related to intense rainy seasons, which results in national disasters when it happens in big Brazilian cities (de Castro 2003).

The development of Geotechnical engineering in Santa Catarina state, southern Brazil, has been constant. In 2008, the region known as Itajaí Valley was affected by several landslides and the socioeconomic impacts were significant, causing civil and governmental interest on the subject. In total, 60 cities and 1.5 million people were affected by landslides and floods. However, due to disorderly urban planning many occupations are in sites with a higher incidence of landslides.

Blumenau, situated in Itajaí Valley and this paper’s study area, is highly susceptible to the occurrence of landslides, where factors include high rainfall weak soils and hill-sides. These factors resulted in the presence of slopes filled by colluvial deposits that may be directly associated to colluvial deposits occurrence.

L. E. C. Alves (✉) · M. Espindola · Vitor S. Müller · M. Z. Broetto  
R. L. Pizzolo · V. F. Hickel  
Federal University of Santa Catarina, Florianópolis, SC  
88040-900, Brazil  
e-mail: lucas\_card.as@hotmail.com

M. Espindola  
e-mail: murilo.espindola@ufsc.br

Vitor S. Müller  
e-mail: vitor@mullergeo.com

M. Z. Broetto  
e-mail: mateuszani7@gmail.com

R. L. Pizzolo  
e-mail: renatapizzolo@gmail.com

In subtropical climate regions, the intense and prolonged rain results in the development of residual soil profiles of great thickness and provides enough material to the remobilization and, consequently, colluvial deposits formation on the hillsides (Vitte 2005). The residuals soils are consequence of the weathering from their places of origin. Soil with small particles are found in soil surface and the grain size increases according to the analyzed depth (Das 2011). According to Lacerda and Sandroni (1985), colluvium is “a deposit consisting of blocks and/or grains of any diameters, carried by gravity and accumulated at the foot or in a short distance from slopes or rocky cliffs”. Two processes work like a trigger to colluvium, and both are related to intense and prolonged rainy seasons. The first one is the accumulation of soil in lower regions as result of slipping. The second is the movement of residual soil on the hillside itself. In this last case, the deposit can be found as disaggregated (Lacerda 2002).

This study was done following the methodology of geotechnical mapping proposed by Davison Dias (1995), one of the most applied methodologies in Brazil. However, in this methodology, the colluvial deposits are treated as if they all had the same behavior, although they have different geological-geotechnical evolutions and have been submitted to distinct processes of pedogenesis. Therefore, the main objective of this paper was to evaluate the geotechnical parameters of colluvial soils of the different lithologies and define whether lithology should be a factor in the Davison Dias’ classification of colluvial deposits.

## 2 Description of Study Area

Blumenau is located in Santa Catarina state, southern Brazil, and occupies an area of 519.837,000 m<sup>2</sup>, where approximately 40% represents urban area. The city is 150,000 km away from the state capital, Florianopolis. This region is characterized by occurrence of natural disasters such as landslides and floods, especially in rainy seasons.

The combination of the intertropical and polar air masses has direct influence in the state’s climate, which is defined as subtropical. In Köppen’s climate classification, the most widely used in the world, Blumenau is characterized for being a city of humid mesothermal climate with well-distributed rains and hot summer.

There are four geological units in Blumenau’s area: the Santa Catarina Granulite Complex, Brusque Metamorphic Complex, Itajaí Basin and Quaternary Deposits. Blumenau’s relief is characterized by the presence of steep mountains which represent the main units (SCGC, BMC and IB) of the city. The alluvial deposits correspond to the central portion of the city and are cut by the Itajaí-Açu River.

## 3 Methodology

The pre-fieldwork activity follows the methodology of geotechnical mapping proposed by Davison Dias (1995). In which the geological and pedological maps are overlapped. Thus, a new geotechnical map is created and from this map, via aerial images, the sampling points are chosen for each geotechnical unit delimited.

Disturbed and undisturbed samples of 8 different lithologies were taken from 13 locations (Fig. 1) in both colluvial and residual soils. Disturbed samples were subjected to geotechnical characterization tests, whereas the undisturbed samples, which were taken in metal molds (Fig. 2), were subjected to direct shear tests. The sampling points are shown in Table 1.

Characterization tests follows the Brazilian Association of Technical Standards. The soil’s physical properties analysis and grain size analysis were performed to characterize the materials. The physical characterization test of the soil measured its water content, solid specific weight, void ratio, porosity and degree of saturation. The grain size test performed adopted the NBR 6502/95 standard. According to which the grain size distribution can be divided into gravel (>2.0 mm), coarse sand (2.0–0.6 mm), medium sand (0.6–0.2 mm), fine sand (0.2–0.06 mm), silt (0.06–0.002 mm) and clay (0.002–0 mm).

Metal molds that measure 104.04 cm<sup>2</sup> and 0.2 cm in height were used for the direct shear tests, both in drained and natural humidity conditions, under normal stresses of 33, 78 and 128 kPa. The shear speed was 0.307 mm/min. In each soil it was possible to define the Mohr-Coulomb envelope, as well as the internal friction angle and cohesion.

## 4 Direct Shear Tests in Colluvial and Residual Soils of Brazil

Some results for maximum shear stress from colluvial and residual soils of previous studies are presented in Table 2.

## 5 Results and Discussions

This chapter presents the results and discussions about the geotechnical characterization and direct shear test.

### 5.1 Geotechnical Characterization and Grain Size Analysis

The geotechnical characterization results and grain size analysis data are presented in Tables 3 and 4. The characterization

**Fig. 1** Localization map and lithological map of Blumenau

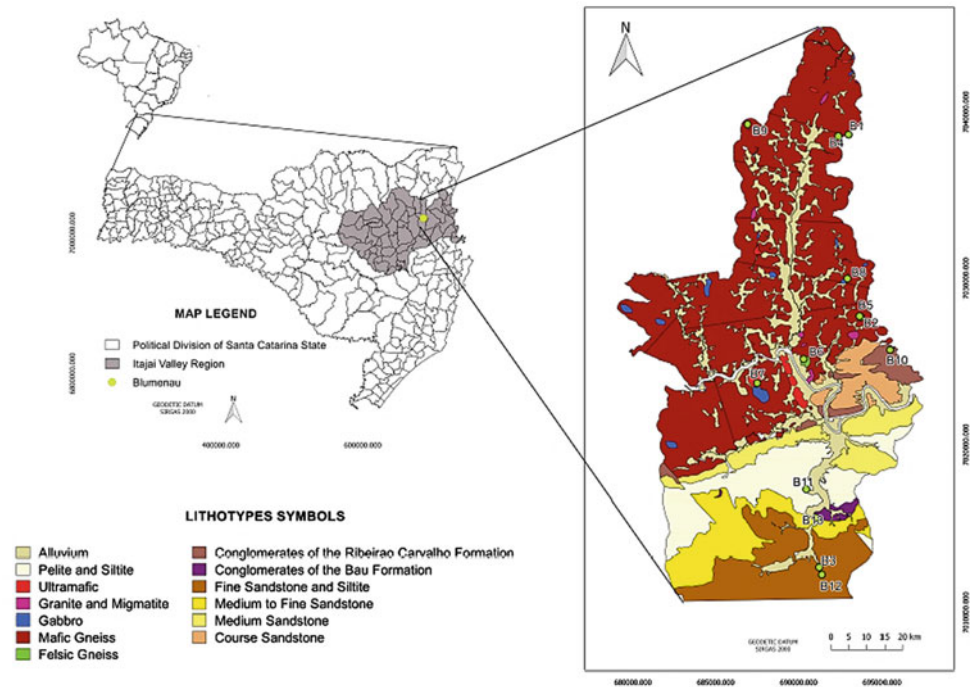


**Fig. 2** Metal molds to the drained shear test

defined soil physical characteristics as solid specific weight ( $\gamma_s$ ), water content ( $w$ ), void ratio ( $e$ ), porosity ( $n$ ) and degree of saturation ( $S_w$ ).

In colluvial soils (B1, B2 and B3), the variation in grain size was expected due to the heterogeneous of grain sizes, according to Lacerda and Sandroni (1985). The grain size distribution in colluvial soils presented a high silt and clay content, ranging from 54.63 to 67.18%. In addition, the sand content ranged from 29.94 to 38.93%.

In residual soils it is necessary to highlight the amount of gravel at point B9. This may be related to the sampling depth, close to the bedrock.

## 5.2 Direct Shear Test

To define the Mohr-Coulomb envelope at least three tests were necessary under normal stresses of 33, 78 and 128 kPa. Thus, it was possible to define the parameters of cohesion and internal friction angle.

The direct shear test results in inundated conditioning are shown in Table 5.

In colluvium materials, the lowest and highest cohesion value (5.9 and 19.4 kN/m<sup>2</sup>) were obtained in soils developed in mafic gneiss (B1) and fine-grained sandstone and siltite (B3), respectively. In the meantime, the lowest and highest angle of internal friction (21.0° and 30.7°) were obtained at points B3 and B1, respectively.

In residual soil the lowest cohesion value (8.1 kN/m<sup>2</sup>) was obtained in residual soil from mafic gneiss (B5). The highest (23.9 kN/m<sup>2</sup>) was obtained in residual soil from granite and migmatite (B9) (Figs. 3 and 4).

**Table 1** Description of the sampling points

Point	Description
B1–M117	Colluvial soil developed in mafic gneiss
B2–M128	Colluvial soil developed in mafic gneiss
B3–M126	Colluvial soil developed in fine-grained sandstone and siltite
B4–M118	Residual soil from mafic gneiss
B5–M129	Residual soil from mafic gneiss
B6–M120	Residual soil from felsic gneiss
B7–M121	Residual soil from ultramafic
B8–M119	Residual soil from gabbro
B9–M116	Residual soil from granite and migmatite
B10–M122	Residual soil from conglomerate
B11–M124	Residual soil from pelite and siltite
B12–M125	Residual soil from fine-grained sandstone and siltite
B13–M127	Residual soil from medium to fine-grained sandstone

**Table 2** Compilation of maximum shear stress results in colluvium and residual soils (Perazzolo 2003)

Reference	Soil	c' (kPa)	$\phi$ (°)
Fonseca et al. (2002)	Colluvial soil developed in mafic gneiss and granitic rocks	6–8	36.2–26.5
Soares et al. (2001)	Residual soil from mafic gneiss	0 a 16.7	26.4–30.6
Soares e Politano (1997)	Colluvial soil developed in mafic gneiss and granitic rocks	10–98	38–48
Avelar e Lacerda (1997)	Colluvial and residual soils developed in mafic gneiss and granitic rocks	22.3	26.4
Campo et al. (1997)	Colluvial and residual soils developed in migmatite	1.5–2.9	32.4–32.8
Abramento e Pinto (1993)	Colluvial soil	0	38–40
Brugger et al. (1993)	Colluvial and residual soils developed in mafic gneiss and granitic rocks	0–85	25–40
Clementino e Lacerda (1992)	Colluvial soil developed in and granitic rocks	38.8–42.9	19–32

**Table 3** Soil physical characterization results

Point	Solid specific weight (kN/m <sup>3</sup> )	W (%)	e	n	S <sub>w</sub> (%)
B1	27.6	38.89	1.68	0.63	63.77
B2	27.1	41.70	1.34	0.57	85.18
B3	26.3	23.94	0.85	0.46	65.93
B4	26.3	20.43	0.64	0.39	83.55
B5	26.9	37.06	1.26	0.56	79.20
B6	27.6	35.83	1.07	0.52	91.64
B7	26.5	29.70	0.93	0.48	83.98
B8	26.8	42.23	1.65	0.62	69.70
B9	26.9	7.76	0.44	0.31	46.12
B10	26.7	16.28	0.60	0.37	72.55
B11	26.7	29.88	0.85	0.46	93.31
B12	26.2	21.24	0.77	0.43	71.87
B13	25.5	26.28	0.87	0.47	76.56

**Table 4** Grain size results

Point	Grain size distribution					
	Gravel (%)	Course sand (%)	Medium sand (%)	Fine sand (%)	Silt (%)	Clay (%)
B1	6.44	4.15	13.42	21.36	36.21	18.42
B2	0.82	3.59	13.78	12.57	53.80	15.45
B3	1.09	0.66	8.86	22.21	19.46	47.72
B4	1.44	9.91	29.99	23.27	28.85	6.54
B5	0.00	0.42	10.88	15.91	47.24	25.56
B6	0.10	1.22	4.58	4.16	51.18	35.75
B7	0.91	6.23	13.93	17.87	37.48	23.82
B8	0.44	3.97	17.52	12.72	52.75	12.59
B9	9.60	21.82	37.18	13.31	13.83	4.26
B10	0.60	8.37	33.54	11.14	25.87	20.47
B11	0.04	2.02	3.59	5.79	59.63	28.94
B12	0.00	0.07	15.49	20.09	36.22	28.13
B13	0.74	3.19	4.22	5.36	67.21	19.28

**Table 5** Direct shear test results

Point	Cohesion—c' (kN/m <sup>2</sup> )	Angle of internal friction—φ (°)	R <sup>2</sup>
B1	5.9	30.7	0.9999
B2	13.8	26.4	1.0000
B3	19.4	26.0	0.9799
B4	13.8	33.6	0.9719
B5	8.1	28.0	0.9651
B6	23.5	26.0	0.9412
B7	23.7	24.5	0.9349
B8	12.8	25.1	0.9834
B9	23.9	41.4	0.8900
B10	20.3	23.0	0.9669
B11	11.8	32.0	0.9907
B12	15.8	22.7	0.9900
B13	10.8	21.3	0.9822

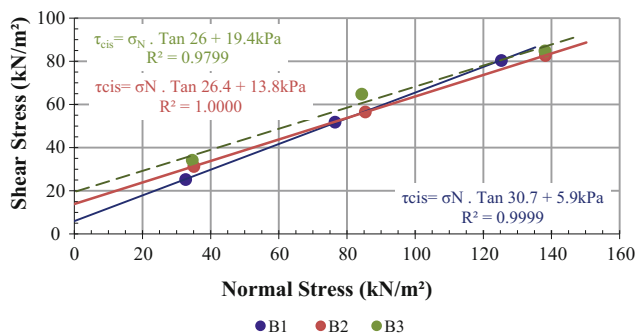


**Fig. 3** Colluvial soils from B1, B2 and B3 points

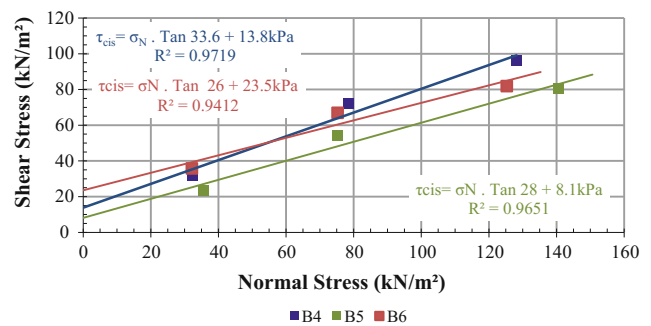


**Fig. 4** Residual soils from mafic gneiss



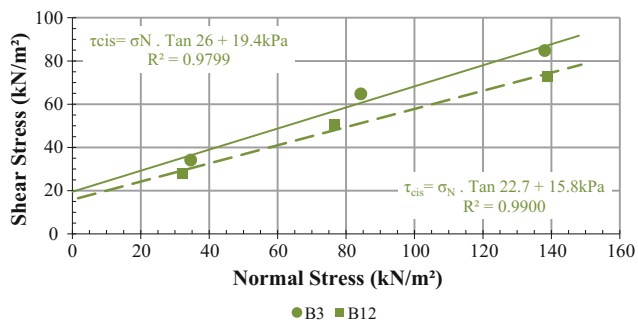


**Fig. 5** Residual and colluvial soils from fine-grained sandstone and siltite

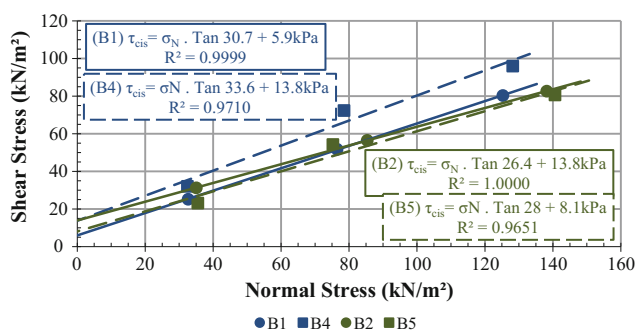


**Fig. 6** Residual and colluvial soils from mafic gneiss

The residual soils are represented by squares and dashed lines in Figs. 5 and 6. While colluvial soils are represented by circles and solid lines. Equal colors represent colluvial and residual soil sampled at nearby points, as with points B1 and B4, for example.

## 6 Conclusions

When comparing the granulometric compositions and direct shear results of the colluvial soils and their respective residual soils, such as B1–B4, B2–B5 and B3–B12, no similar compositions or trends are found, whereas the behavior of the colluvial soils relates to the grain sizes presents.

For the colluvial materials the soil's behavior is directly regulated by the granulometric composition. It is verified that the highest cohesions are associated with the finer materials (B2 and B3). Meanwhile, the course-grained material (B1) is the one with the highest effective internal friction angle.

Residual materials also tend to behave according to their granulometric compositions. However, points such as B5, B9 and B11 do not follow this trend and show discrepancy according to the granulometric criterion. The lithotypes of these materials are associated with metamorphic processes and sedimentary structures, which may have influenced cohesion and internal friction angle.

There are no trends related to shear strength parameters ( $c'$  and  $\phi$ ), either between the colluvium and residual soils with same lithotype or among colluvial soils with different lithotypes. Thus, it is possible to conclude that colluvial deposits should be treated as independent geotechnical units in Davison Dias' (1995) methodology.

## References

- de Castro, A.C.C.: Manual de Desastres, 1st edn. Ministério da Integração Nacional, Brasília (2003)
- Das, B.M.: Fundamentos de Engenharia Geotécnica, 7th edn. Cengage Learning, São Paulo (2011)
- Davison Dias, R.: Proposta de metodologia de definição de carta geotécnica básica em regiões tropicais e subtropicais. Revista do Instituto Geológico, 51–55 (1995)
- Lacerda, W.A., Sandroni, S.S.: Movimentos de Massa Colúviais. In: Conferência brasileira de estabilidade de encostas, 1–19. Clube da Engenharia, Rio de Janeiro (1985)
- Lacerda, W.: Comportamento geotécnico de massas colúviais. In: Simpósio de Prática de Engenharia Geotécnica da Região Sul, Joinville (2002)
- Perazzolo, L.: Estudo geotécnico de dois taludes da Formação Serra Geral, RS. 2003
- Vitte, A.C.: Relações entre a estratigrafia de rampas de colúvios e a evolução das vertentes na bacia do Ribeirão Juncal, município de Salto de Pirapora, SP. In: Anais do X encontro de geógrafos da América Latina, São Paulo (2005)

# Engineering Geological Studies for the New Drainage Tunnels of Lisbon

Filipe Telmo Jeremias, Rute Ramos, and Laura Caldeira

## Abstract

The municipality of Lisbon is currently planning the construction of two drainage tunnels in order to control the periodic flooding that occurs in the city during the winter. The first tunnel is 5 km long with DN5500 diameter, crossing the downtown in a NW-SE direction, and probably will be constructed by TBM. The second tunnel is located in the north part of Lisbon. This tunnel is 1 km long and is planned to be constructed by TBM or by NATM. The first tunnel crosses volcanic rocks and calcareous rocks from the Cretaceous and then detrital and calcareous rocks from Miocene. The second tunnel only intersects Miocene detrital and calcareous rocks constituted mostly by sand, silty sand, clay and biocalcarenite. For engineering geological characterization of alignments of tunnels, a site investigation program was planned and carried out that included boreholes, in situ (SPT, self boring pressumeters tests, packer tests, pumping tests and crosshole test) and laboratory tests (index, oedometer and triaxial compression tests). An integrated analysis of the data obtained from the site investigation works was performed in order to define the engineering geological conditions along the alignments of the tunnels.

## Keywords

Site investigation • Engineering geological characterization • Drainage tunnels

## 1 Introduction

Municipality of Lisbon is currently planning the construction of two drainage tunnels with the aim of controlling the floods that periodically occur in Lisbon during the rainy

F. T. Jeremias (✉) · R. Ramos · L. Caldeira  
Laboratório Nacional de Engenharia Civil, Av. Do Brasil, 101  
Lisbon, Portugal  
e-mail: ftelmo@lneec.pt

season. The main tunnel designated as TM crosses through a NW-SE trend the central area of Lisbon and it is 5 km long with DN5500 diameter (Hidra/Engidro 2017). The second tunnel designated as TCB is planned to be constructed at the eastern part of Lisbon with an extension of about 1 km. The TCB's alignment is approximately perpendicular to Tagus River bank. Both tunnels end at Tagus River bank at sites several kilometers apart (see Fig. 1).

TM tunnel crosses a heavy density urban area with several constrains and it mostly probably being constructed using a TBM machine. In relation of TCB tunnel its alignment crosses an open urban area without strong constrains. For this tunnel construction solutions by TBM (DN5500 diameter section) or by NATM (4.85 × 6.20 m section) are possible (Hidra/Engidro 2017).

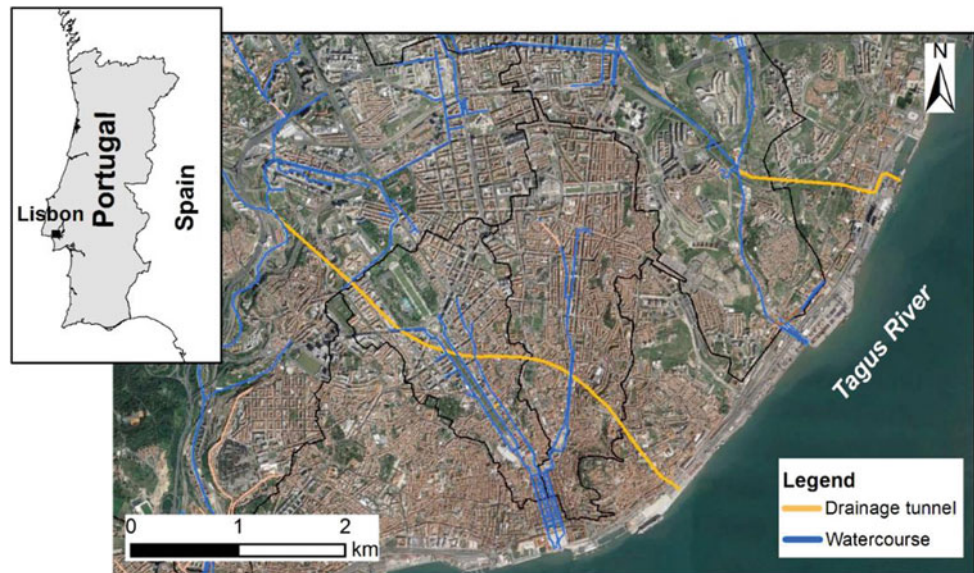
Site investigation works for the international trend for basic project concept designs were planned taking into account both the general requirements of the tunnels alignments and the geological conditions of the sites. The methods and techniques of site investigation were selected accordingly and aiming at giving a full account of the site conditions and to provide the engineering geological data deemed pertinent in this phase for the engineering design (LNEC 2016).

The site investigation program carried out along the proposed tunnel alignments consisted of drilling, sampling, in situ testing (standard penetration test, self boring pressumeter test, packer test, pumping test and crosshole test) and laboratory testing on both rock and soil samples.

## 2 General Geological Setting

TM tunnel crosses obliquely the central area of Lisbon between Campolide in the middle on the city and Tagus River, approximately through a NW-SE trend. Topographically, from the upstream point towards the Tagus River, the alignment of this tunnel crosses three hills with elevations of 116, 70 and 95 m. These hills are separated by two valleys

**Fig. 1** Location of TM and TCB tunnels, (Hidra/Engidro 2017)



existing in central area of Lisbon city with elevations of 30 and 25 m where the tunnel alignment intersected.

The first hill which corresponds approximately to half part of the total extension of TM tunnel is constituted by volcanic rocks mainly pyroclastic rocks and basaltic rocks of neo Cretaceous age and by calcareous rocks of Bica and Caneças Formations of Cretaceous age (Cenomanian). The upper unit, Bica Formation, is mostly constituted by compacted limestone, sometimes, with flint nodules. The Caneças Formation is formed mainly by marly limestone, marls, limestone and dolomitic limestone. This hill formed an anticlinal structure elongated in the NE-SW direction occurring in the core the Caneças Formation rocks and at the East and West limbs the Bica Formation and volcanic rocks (INETI 2006).

The second and the third hills crossed by the TM tunnel alignment are constituted by detrital and calcareous formations of Miocene age. These formations are chiefly formed by sandstone, claystone, sand, silty sand, silty-clayey sand, clay and biocalcarenite. The Miocene rocks forming a regular monoclinical structure dipping lesser than  $10^\circ$  to East towards the estuary of Tagus River (Antunes et al. 2000).

TCB tunnel planned to be located in the eastern part of Lisbon develops approximately perpendicular to the right bank of Tagus River through a W-E direction. This tunnel only crosses Miocene formations whose units are younger than those of Miocene age crossed by TM tunnel. The Miocene units are mainly constituted by sandstone, biocalcarenite, claystone and silty sand, forming a monoclinical structure gently dipping to East beneath the alluvial deposits of Tagus River in the eastern part of Lisbon (Antunes et al. 2000).

Superficial deposits constituted by fills and alluvial soils of Tagus River were recognized on both tunnels. The first ones are associated with the earthworks carried out for civil and road infrastructures of Lisbon city. The alluvial deposits occurring close to the Tagus River bank over the Miocene units. The fills are constituted by heterogeneous and heterometric materials often reflecting the bedrock composition showing mainly sandy and silty-clayey composition. The alluvial deposits consist mainly of organic silty-clayey and sandy soils.

Different hydrogeological systems are presented in Lisbon area. Miocene hydrogeological system is constituted by a sequence of sediments which stratigraphically apart formations with different hydrogeological behaviour producing cyclic interlayered sequences of aquifers, aquitards and aquicludes. This multi-layered aquifer system allows recharge by vertical leakage between beds. Thus, the hydrogeological behaviour of this aquifer system is mostly controlled by the lithological features of the occurring geological formations. In the basaltic layers and calcareous rocks, the groundwater flow is controlled by the interconnection and characteristics of the discontinuities occurring in rock mass. In general basalts layers have low discharges.

Lisbon area is crossed by several faults which interested mainly the Mesozoic formations. These structures with NE-SW, NW-SE, N-S and E-W directions have lengths range from several hundreds of meters to 6 km long, dipping, in general, more than  $70^\circ$  (INETI 2006). The alignment of TM tunnel is crossed at the beginning and at the end by faults with NE-SW direction, which have no sismogenic character, corresponding to singular discontinuities that

materialize mechanical characteristics weaker than rock mass.

Lisbon seismicity is ruled by two generation zones located the first one at African and EuroAsiatic plates' border and the second inside the Iberian Peninsula, where interplate and intraplate earthquakes occurred, respectively. The most important neotectonic structure close to project area is the Lower Tagus Valley Fault Zone (LTVFZ) which is responsible by the regional seismicity in Lisbon area. As the geometry, depth, activity and average recurrence of this seismogenic structure are unknown, it was considered, besides its importance in the regional seismicity, that there was no need to be specifically taken into account in the definition of design earthquakes. Accordingly, the zonation proposed for intraplate and interplate design earthquakes in the Eurocode (NP-EN 1988-1 2010) (IPQ 2010) for the Lisbon area will be adopted for tunnels design studies.

### 3 Site Investigations

#### 3.1 Planning

The site investigation program concerned the needs of engineering geological information for the initial project design and conception. As in this stage only a preliminary definition of the main characteristics of the project was available, the site investigation program was design to give a global characterization of ground conditions along the tunnels rather to detail specific site conditions which will require a much greater number of works, being assumed that they will be performed in the further stages of the undertaken. Taken into account this aspect and after the analysis of the existing geological and geotechnical data collected, a large distance between site investigation points and a higher concentration of the works at the shafts sites were adopted.

For the assessment of the engineering geological information required the following objectives were established:

- composition and thickness of the superficial deposits occurring at the shafts and at open cuts of upstream and downstream ends of the tunnels;
- reconnaissance of the stratigraphic sequence and geological structure of the bedrock;
- determination of index properties and hydromechanical and environmental characterization of soils;
- determination of index and mechanical properties of rocks;
- in situ static and dynamic characterization of the alluvial and bedrock units;
- hydrogeological characterization of the bedrock units.

In order to achieve the previous objectives a set of site investigations were proposed which are described in Sect. 3.2.

#### 3.2 Site Investigations Works

Site investigation works were carried out along the alignments of TM and TCB tunnels with 5 and 1.6 km, respectively. Site investigation works consisted of drilling, sampling and monitoring of water level and in situ tests, namely standard penetration test (SPT), self boring pressumeter test (SBP), packer test, crosshole test and pumping test, as well as laboratory tests on rock samples and on disturbed and undisturbed soil samples (LNEC 2017a, b).

##### Drilling

Shaft boreholes were put down using core drilling. Between shaft boreholes the borings were first drilled using destructive techniques and coring on a length of 18 m centred at the depth of the axis of the tunnel. Twenty-three and eleven boreholes were drilled along the alignments of TM and TCB tunnels, respectively. In general boreholes locations were spaced at 200–300 m intervals. Boreholes were drilled to a maximum depth of 98.5 m and the use of bentonite during drilling was not allowed as packer tests will be carried out. Boreholes were drilled in order to recognize the sequence, lithological composition and geological structure, sampling, in situ testing and at the end of all works groundwater level monitoring. Undisturbed samples were collected using 86 mm diameter triple-tube core barrels.

##### In situ testing

In situ testing was performed in order to provide data on the engineering geological characterization of soil and rock units. Packer tests were performed on all boreholes of TM and TCB tunnels at two different depths. In TM and TCB tunnels nine and five boreholes locations were selected to carry out self boring pressumeter tests, respectively. Cross-hole tests were performed in both tunnels on two locations and pumping tests were carried out on six and two locations selected on TM and TCB tunnels alignments, respectively. In shaft boreholes test depths were selected according with the geological characteristics of the terrains drilled. In the boreholes between shafts in situ tests were carried according to the depths shown in the scheme presented in Fig. 2.

The concentration of in situ tests at the same location allowed an easier interpretation of different site investigation methods and helped very much to establish correlations between the results obtained. The in situ tests performed were as follows.

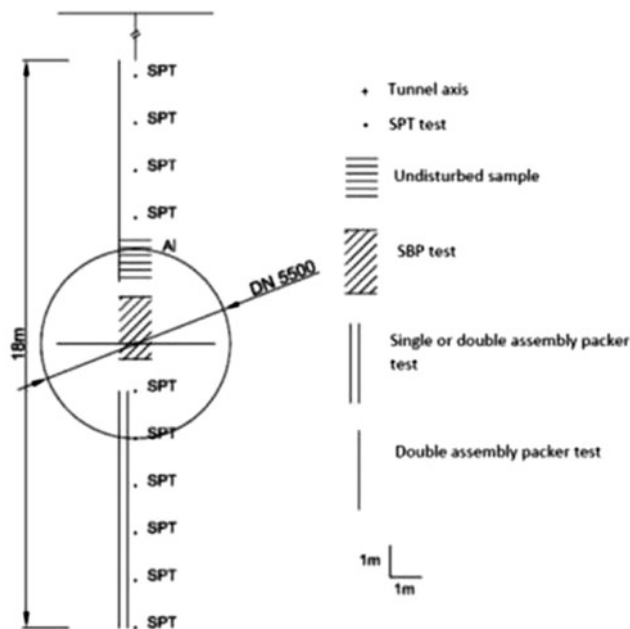


**Fig. 2** Vertical sequence of the in situ tests on boreholes of TM and TCB tunnels

- Standard penetration tests were carried out in the boreholes constituted by soil units spaced at 1.5 m intervals over the full depth in shaft borings and in borings between shafts only in coring length drilled. The SPT's data provided data on the in situ density and/or consistency of soils units.
- Packer tests were carried out in all boreholes of TM and TCB tunnels using single or double packer assembly. Lugeon type tests were carried out in rock and Lefranc type tests were performed in soil in order to determine the hydraulic conductivity of the ground.
- Self boring pressurimeter tests were performed to a maximum depth of 57.4 m, allowing the computation of in situ horizontal stress, unload-reload modulus and undrained shear strength.
- Pumping tests were carried out in six selected locations of TM tunnel borings and on two locations of TCB tunnel aiming to cover different geological formations. Aquifer parameters as hydraulic conductivity, transmissivity and coefficient of storage were determined.
- Crosshole tests were performed in order to provide data on the dynamic parameters of the alluvial deposits occurring close to the Tagus River bank and the underlying bedrock. Tests were carried out to a maximum depth of 29 m, between borings 5 m apart. Determination of longitudinal and shear wave velocities at depths spaced 1 m allowed to compute the dynamic shear modulus and the dynamic Young modulus.

### Laboratory testing

Laboratory tests were carried out on rock samples and on disturbed and undisturbed soil samples. Rock composition was determined by micropetrographic and X-ray diffraction analyses and rock index properties were evaluated through the determination of porosity, density, swelling, uniaxial compressive strength (with and without the determination of Young's modulus and Poisson's ratio), Brazilian tensile strength and sound velocity (longitudinal and shear waves). Soil index properties were evaluated through the determination of particle size analysis, Atterberg limits and methylene blue index. Environmental analysis on alluvial organic silty-clayey soils to evaluate according with Ontario criteria (Ontario 2011) the occurrence of volatile organic compounds (VOC) and metals were performed. On undisturbed soil samples oedometer and triaxial compression and extension tests were also carried out.

### Groundwater monitoring

Simple or double piezometers were installed in all boreholes. Open standpipe piezometers of 1½" diameter was used for rock and high to medium permeability soils, while for low permeability soils (silty-clayey) a porous tip was installed. Installing depths were selected according with the geological conditions recognized during the drilling. In general, one piezometer was installed above the tunnel's roof depth. Piezometric level readings were performed immediately after piezometer installation, 24 and 48 h, one week, one month and then every 3 months during one year (or six months after the end of site investigation works).

## 4 Engineering Geological Interpretation

An extensive engineering geological data collection was provided from site investigations works carried out. For alluvial deposits and for Miocene, Volcanic and Cretaceous formations the composition and physical, mechanical and hydraulic properties are presented in Table 1. Taken into account the volume of data obtained a range of values for some properties are presented.

Alluvial deposits are not interested in tunnels works, but on the open excavations at the end of tunnels' alignments at Tagus River right bank. Alluvial deposits are constituted by interstratified layers of sandy, medium to very dense, with percentages of fines of about 40% of low plasticity, and by very soft to soft, organic silty-clayey soils, with high percentage of fines of moderate plasticity.

Miocene formations interested in both tunnels are constituted by several lithostratigraphic units. However, and in spite of their differences at a small scale, the geotechnical

**Table 1** Composition and physical, mechanical and hydraulic properties of geological formations crossed by TM and TCB tunnels

Geological formation		Composition		Physical properties							
		USCS/MC		% Fines	PI (%)	MBI (g)	n (%)	$\varepsilon (\times 10^{-4})$			
AID	SL	SM		42–45	8–11	1.5	–	–			
	CL	CL		53–77	11–14	2.0–4.0	–	–			
M (TM)	SL	SM		19–46	NP–7	0.2–1.5	–	–			
	CL	CL, CH, ML, MH		60–100	9–40	0.6–8.0	–	–			
	B	Calcite, quartz, feldspar		–	–	–	15–22	0.08–37.2			
M (TCB)	SL	SM		9–47	NP–16	0.2–0.8	–	–			
	CL	CL, ML		55–98	10–23	1.0–5.7	–	–			
V	BR	Plagioclase, pyroxene, iron oxides, smectite		–	–	–	1.6–2.1 6–24*	0.43–1.25 12.3–333*			
	PR	Quartz, pyroxene, iron oxides, smectite		–	–	–	–	174–452			
C	L	Calcite, dolomite		–	–	–	>1–2	0.42–2.09			
	BL	Calcite, dolomite		–	–	–	2.9–8.1	4.5–20.8			
	ML	Calcite, dolomite, quartz		–	–	–	18.4–30.7	0.55–101			
Geological formation		Mechanical properties									
		$N_{SPT}$	$K_0$	$C_u$ (kPa)	$G_i$ (MPa)	$\phi'_p$ (°)	$\phi'_c$ (°)	$\sigma_c$ (MPa)	E (GPa)	$\sigma_t$ (MPa)	$V_p/V_s$ (m/s)
AID	SL	15–60	–	–	–	21.4	19.1	–	–	–	–
	CL	02/abr	–	–	–	–	–	–	–	–	–
M (TM)	SL	15–60	0.28–1.41	1280–1408	34.8–86.3	–	–	–	–	–	2000–3000
	CL	60	0.26–2.68	787–2949	44.3–223	40.5–35.5	23.3–32.3	–	–	–	300–600
	BC	–	–	–	–	–	–	7.3–20.4	8.7–18.0	2.0–3.6	–
M (TCB)	SL	10–>60	0.58–0.96	676–6094	35–150	–	–	–	–	–	2000–2700
	CL	15–>60	0.28	4292	110	38.8–51.1	33.3–35.1	–	–	–	350–700
V	BR	–	–	–	–	–	–	94.9–135.2 15.1–56.1*	63.7–77.2 4*	10 2.5*	–
	PR	–	–	–	–	–	–	2.3–20.5	0.07–7.4	1.26	–
C	L	–	–	–	–	–	–	81.9–95.4	63.8	7.0–9.4	–
	BL	–	–	–	–	–	–	>10	21.5	3.0–4.8	–
	ML	–	–	–	–	–	–	11.9–71.9	6.3–28.7	1.4–4.4	–
Geological formation		Hydraulic properties									
		Lefranc test		Lugeon test	Pumping test			Oedometer test		Triaxial compression test	
		k (m/s)	k (m/s)	k (m/s)	T (m <sup>2</sup> /s)	S	$C_v$ (m <sup>2</sup> /s)	k (m/s)	k (m/s)		
AID	SL	–	–	–	–	–	–	$6.10^{-8}$ – $8.10^{-8}$	$1.10^{-10}$	$7.10^{-7}$ – $2.10^{-6}$	
	CL	–	–	–	–	–	–	$6.10^{-8}$ – $1.10^{-7}$	$2.10^{-10}$	$9.10^{-8}$	
M (TM)	SL	$2.10^{-8}$ – $2.10^{-5}$	–	$1.10^{-7}$ – $2.10^{-7}$	$4.10^{-7}$ – $5.10^{-7}$	–	–	–	–	–	
	CL	$6.10^{-10}$ – $4.10^{-9}$	–	$4.10^{-7}$ – $7.10^{-7}$	$4.10^{-6}$ – $7.10^{-6}$	–	–	$6.10^{-8}$ – $2.10^{-7}$	$7.10^{-11}$ – $7.10^{-10}$	$1.10^{-8}$ – $3.10^{-7}$	
	B	$5.10^{-10}$ – $2.10^{-5}$	–	$8.10^{-6}$ – $1.10^{-5}$	$4.10^{-5}$ – $8.10^{-5}$	–	–	–	–	–	
M (TCB)	SL	$1.10^{-7}$ – $2.10^{-6}$	–	$5.10^{-5}$ – $2.10^{-4}$	$4.10^{-4}$ – $2.10^{-3}$	$3.10^{-3}$ – $1.10^{-2}$	–	–	–	–	
	CL	$3.10^{-9}$ – $5.10^{-10}$	–	$1.10^{-7}$	$7.10^{-7}$	–	–	$8.10^{-8}$ – $1.10^{-7}$	$5.10^{-11}$ – $2.10^{-10}$	$5.10^{-8}$ – $4.10^{-6}$	
V	BR	$3.10^{-9}$ – $1.10^{-8}$ *	$2.10^{-9}$ – $1.10^{-5}$	$1.10^{-7}$ – $6.10^{-7}$	$1.10^{-7}$ – $6.10^{-7}$	$2.10^{-2}$	–	–	–	–	
	PR	$3.10^{-8}$ – $8.10^{-7}$	–	$6.10^{-8}$ – $3.10^{-7}$	$4.10^{-7}$ – $4.10^{-6}$	$6.10^{-4}$	–	–	–	–	

(continued)

**Table 1** (continued)

Geological formation		Hydraulic properties							
		Lefranc test	Lugeon test	Pumping test			Oedometer test	Triaxial compression test	
		k (m/s)	k (m/s)	k (m/s)	T (m <sup>2</sup> /s)	S	C <sub>v</sub> (m <sup>2</sup> /s)	k (m/s)	k (m/s)
C	L	–	3.10 <sup>-9</sup> –6.10 <sup>-7</sup>	–	–	–	–	–	–
	ML	1.10 <sup>-9</sup> –1.10 <sup>-6</sup>	1.10 <sup>-7</sup> –2.10 <sup>-6</sup>	5.10 <sup>-8</sup> –9.10 <sup>-8</sup>	4.10 <sup>-7</sup> –7.10 <sup>-7</sup>	–	–	–	–

*AID* Alluvial deposits; *M* Miocene; *V* Volcanic; *C* Cretaceous; *USCS* Unified soil classification system; *MC* Mineral composition; *PI* Plastic index; *MBI* Methylene blue index; *n* Porosity; *ε* Swelling; *SL* Sandy layers; *CL* Clay layers; *BC* Biocalcareite; *BR* Basaltic rocks; *PR* Pyroclastic rocks; *L* Limestone; *BL* Brechified limestone; *ML* Marly limestone; *N<sub>SPT</sub>* Number of blows (from standard penetration test) *K<sub>0</sub>* In situ earth pressure coefficient (from SBP tests); *C<sub>u</sub>* Undrained shear strength (from load cycle of SBP tests); *G<sub>i</sub>* Initial modulus (from SBP tests); *φ<sub>p</sub>* Peak friction angle (from triaxial compression tests); *φ<sub>c</sub>* Critical state friction angle (from triaxial compression tests); *σ<sub>c</sub>* Uniaxial compressive strength; *σ<sub>t</sub>* Brazilian tensile strength; *E* Young's modulus; *V<sub>p</sub>/V<sub>s</sub>* Longitudinal and shear velocities (from crosshole seismic tests); *k* Hydraulic conductivity; *T* Transmissivity; *S* Storage coefficient; *C<sub>v</sub>* Coefficient of consolidation

\*Weathered basalt

properties of these formations may be interpreted as a complex composed by interstratified layers of sand, clay and biocalcareite (weak rock). Sandy layers are composed by yellowish, greyish and brownish, medium to very dense, with 9 to < 50% of fines, non-plastic or with low plasticity, SM (USCS) soils. Hydraulic conductivity values range from 10<sup>-7</sup> to 10<sup>-4</sup> m/s as function of the percentage of fines and degree of cementation. Silty-clayey layers are constituted by greyish, greenish, brownish, yellowish and blackish, medium to hard, with percentages of fines up to 100%, with moderate to high plasticity, mostly CL (USCS) soils. Low to very low hydraulic conductivity values between 10<sup>-10</sup> and 10<sup>-7</sup> m/s were determined, which are in accordance with the silty-clayey composition of these soil layers. Strength characteristics (*C<sub>u</sub>*, *φ<sub>p</sub>* and *φ<sub>c</sub>*) are slightly higher in TCB units than those crossed by TM alignment. Biocalcareite is constituted by yellow and grey fossiliferous layers with variable degree of cementation, showing high porosity and very low swelling values. High swelling values were obtained for long saturation periods as a consequence of textural features of these rocks composed sometimes by heterogeneous layers. Biocalcareite layers are characterized as low strength and high deformability rocks (weak rock). Biocalcareite layers present hydraulic conductivity values range from 10<sup>-9</sup> to 10<sup>-5</sup> m/s. This depends on pore space is interconnected as consequence of cementation degree.

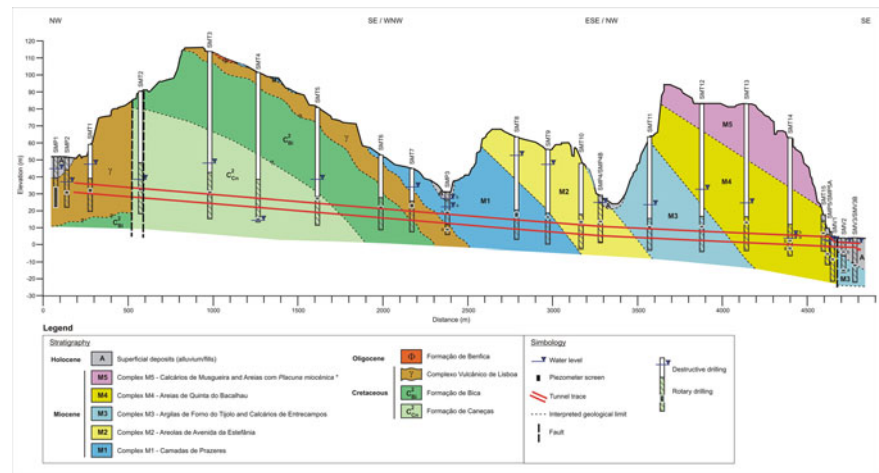
Volcanic formations occurred in TM tunnel under the Miocene formations and above the Cretaceous units and they are formed by interlayered basaltic and pyroclastic rocks. These layers may reach a few decimetres to several meters in thickness. At upper part grey-greenish weathered/decomposed basaltic rocks occur. In depth medium to dark grey moderately to slightly weathered/sound basaltic rocks

occur. Moderate (20–60 cm) to very close spaced (2–6 cm) discontinuities and RQD values of about 80% characterize the sound basaltic rock mass. Discontinuities are often filled with argillaceous material and calcite which also occurred as nodules. High and low values, of porosity and swelling were achieved on weathered and fresh rock, respectively. Sound basalts are high strength and low deformability rocks, while weathered basalts have poor mechanical characteristics. Hydraulic conductivity values ranging from 10<sup>-9</sup> to 10<sup>-5</sup> m/s depends on the characteristics of discontinuities (spacing, aperture and infills).

Pyroclastic rocks occur mostly as subhorizontal fine layers of volcanic tuffs. These rocks present variable degree of welding. They are reddish, fine-grained and friable showing often nodules and veins of calcite. These rocks present high swelling values and strength and deformability characteristics similar to those of soils, *i.e.* *E* < 1 GPa and *σ<sub>c</sub>* < 10 MPa as well as low hydraulic conductivity values between 10<sup>-8</sup>–10<sup>-7</sup> m/s.

Cretaceous Bica and Caneças Formations occurred in TM tunnel beneath the volcanic rocks. The Bica Formation is constituted by white, subcrystalline with nodules of grey flint of compacted limestone and by whitish, brechified limestone. High degree of fracturing and karst processes were recognized mostly for compacted limestone showing zones and discontinuities filled by red argillaceous material (*terra rosa*). Moderate to wide (60–200 cm) spaced discontinuities and RQD values between 50 and 100% characterize the brechified limestone rock mass. Unweathered compacted limestone is characterized by very low porosity and swelling values (<1) and high strength and low deformability. Brechified limestone presents moderate to high values for porosity and swelling, and low to medium

**Fig. 3** Geological cross section of TM tunnel



strength and high deformability. Hydraulic conductivity values of Bica Formation rocks ranging from  $10^{-9}$  and  $10^{-6}$  m/s depends on the characteristics of discontinuities (spacing, aperture and infills).

Caneças Formation is composed by an interstratified sequence of light to medium grey marly limestone, sandy limestone and marl layers. Very close to moderate spaced discontinuities and RQD values in general not higher than 50% characterized the Caneças Formation rock mass. Very high porosity and swelling values and low strength and high deformability (weak rock) characterize these carbonate rocks.

The interpretation of geological data was synthesized in geological cross-sections along the alignments of the tunnels TM and TCB. In Fig. 3 the geological units, their thicknesses and spatial arrangement as well as an interpreted average value of piezometric levels monitored for each borehole for TM tunnel cross section are presented.

## 5 Final Remarks

The global objectives of the planned site investigation were reached, main difficulties were found at the interpretation level related with problems of systematization and generalization of data, concerning the identification of units and the assumptions of validity of the engineering geological properties determined for each unit, given the considerable distance of several hundred meters between site investigation locations.

After the stage of initial project conception, a complementary site investigation program is being planned to assist the final design project. Once the type of structure, its location and constructive solutions are defined, the site

investigation program will be directed towards the investigation of site specific ground conditions to allow checking and completing the existing knowledge of engineering geological conditions along the alignments of both tunnels.

The site investigation program in this preliminary stage for such long linear works was planned by LNEC as compromise between the needs of geological and engineering data for the initial project conception and the time needed for site investigation works. Taken into account the estimate cost of the project of about 100 M€, the total cost of site investigation at this stage was about 0.5% of that figure, however this amount will be fully recovered considering the benefits of site investigation on the optimization of better proposals in terms of design and, consequently of bill of quantities of the works that will be presented for tunnel alignments.

**Acknowledgements** The authors thank Project Team of General Drainage Plan 2016–2030 of Lisbon Municipality for allowing the publication of the data.

## References

- Antunes, M.T.; Legoinha, P.; Cunha, P.P.; Pais, J.: High resolution stratigraphy and miocene fácies correlation in Lisbon and Setubal Peninsula (Lower Tagus basin, Portugal). *Ciências da Terra* (UNL), 14, pp. 183–190 (2000)
- Hidra/Engidro: Processo de concurso para a empreitada dos túneis de drenagem da cidade de Lisboa e intervenções associadas. Volume II - Túneis de Monsanto - Sta. Apolónia e de Chelas – Beato. Tomo 2 - Peças desenhadas (2017)
- INETI: Carta Geológica de Portugal na escala 1:50 000 Folha 34-D (Lisboa). Instituto Nacional de Engenharia, Tecnologia e Inovação, Departamento de Geologia (2006)



- IPQ: Eurocódigo 8. Projeto de estruturas para resistência aos sismos. Parte 1: Regras gerais, acções sísmicas e regras para edifícios. NP-EN 1988-1: 2010 (2010)
- LNEC: Lisbon General Drainage Plan. Site investigation programme. Report 36/2016 – DG/NGEA (2016)
- LNEC: Lisbon General Drainage Plan. Geological-geotechnical studies. Monsanto/S.ta Marta/S.ta Apolónia. Report 264/2017-DG-NGEA (2017a)
- LNEC: Lisbon General Drainage Plan. Geological-geotechnical studies. Chelas/Beato. Report 262/2017-DG-NGEA (2017b)
- Ontario: Soil, ground water and sediment standards for use under Part XV.1 of the environmental protection act. Ministry of the Environment (2011)

# Geological-Geotechnical Studies for the Ore Transport Railway Line “S11D—Sudeste do Pará”, Brazil

Priscilla H. P. Oliveira and Mário Quinta-Ferreira 

## Abstract

In Brazil, the railway transport of iron ore moves large quantities and needs to overcome huge distances between the mining areas and the shipping harbors. As the Brazilian railway network requires renewal and expansion, sound procedures to conduct suitable engineering geology studies are needed. The objectives, methodology, and study phases are presented, focusing on the geological and geotechnical constraints of the terrains crossed by the railway line. These constraints may increase the costs, cause construction delays, or generate difficulties during construction or operation. The new iron ore railway project, “S11D—Ramal Ferroviário Sudeste do Pará” in Brazil, is used as a case study. It is 100 km in length, connecting the new S11D mine to the existing Carajás railway, and hauls the iron ore to a shipping port, the Ponta da Madeira Maritime Terminal. The geological-geotechnical studies developed for the design, and utilized during construction along the S11D railway branch line, are presented and discussed. Several unusual aspects of the engineering geology studies for an excavation, an embankment, a bridge, a tunnel, and for the location of natural granular materials for sub-ballast and ballast layers are presented. It is concluded that continuous improvement of the engineering geology studies is desirable to increase the efficiency of the design, construction, and operation of a railway.

## Keywords

Geological-geotechnical studies • Railways • Iron ore transport

P. H. P. Oliveira  
Mining and Geological Engineering, Geosciences Center,  
University of Coimbra, Coimbra, Portugal  
e-mail: hamada.pri@gmail.com

M. Quinta-Ferreira (✉)  
Geosciences Center, University of Coimbra, Coimbra, Portugal  
e-mail: mqf@dct.uc.pt

## 1 Introduction

Ore transport railway lines are designed with the only purpose of transporting ore between the mine and the shipping harbor, presenting significant differences from other railway lines, e.g. high-speed railway lines or mixed passenger and cargo railway lines. Their main characteristics are: usually single track with crossing yards; speed generally not exceeding 80 km/h; horizontal curve radius above 400 m; longitudinal gradient below 2.5%; use of long trains with hundreds of wagons; heavy static loads and high dynamic loads; and a large number of simultaneously circulating trains.

Topographic aspects and the properties and behavior of the geological materials are of the greatest importance, due to the need to adjust the design to the local conditions, requiring construction of large embankments, excavations, and bridges or tunnels. This makes these projects very complex, time-consuming, and costly. A fairly important aspect of a geological-geotechnical investigation is understanding the contribution of geology to ensure the safety of all the engineering solutions related to excavations, embankments, bridge foundations, tunneling, ground treatment, and the location of natural construction materials, mainly for ballast. The railway needs to be adjusted to the encountered geomorphology, geology, and geotechnical characteristics. The possibility of the occurrence of geohazards such as landslides, unstable soils, and flooding, within the railway route corridor, must also be evaluated. For a successful project implementation, it is important to avoid or overcome all the adverse geological and geotechnical aspects, which may increase costs and delays during construction, or generate work stoppages during the railway line operation that would create serious constraints and quite significant costs.

## 2 The S11D Railway Branch Line and the Carajás Railway

The iron ore mined in Carajás is destined for export and hauled to Ponta da Madeira Maritime Terminal, along 900 km of the Carajás railway, using some of the longest and most heavily-loaded railway trains in the world. The Carajás trains consist of up to 330 wagons and four locomotives of 4,400 hp, totaling 3.3 km in length, carrying more than 40,000 tons of iron ore and imposing individual axle loads of 30 tons onto the railway track, which has a gauge of 1.60 m. The Carajás railway has 35 trains running simultaneously in continuous operation, and carries more than 120 million tons of iron per year.

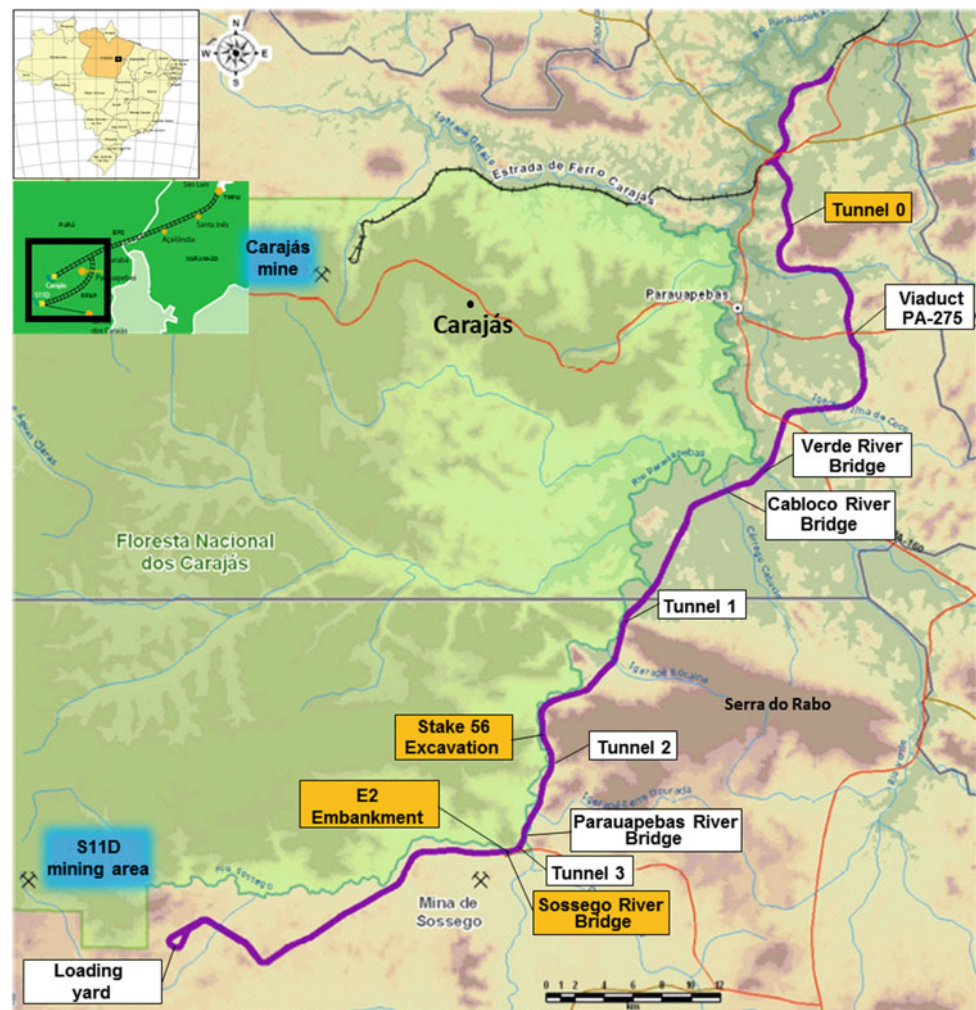
The S11D railway branch line links the S11D project to the Carajás railway, and started operations in 2016, increasing the iron ore production capacity up to a total of 230 million tons of iron ore per year. Other main features of the S11D railway branch are: single line, 100 km long (Fig. 1); one connecting yard with the Carajás railway, six

crossing yards and one loading yard; maximum ramp of 0.4% in the direction of export and 1.0% in the direction of import; minimum curve radius of 859 m; four tunnels, four railway bridges, two railway viaducts and two road viaducts; earthmoving volumes: 14.9 Mm<sup>3</sup> of excavation (12.4 Mm<sup>3</sup> of soil, 1.5 Mm<sup>3</sup> of rippable material, and 1.0 Mm<sup>3</sup> of rock material) and 12.0 Mm<sup>3</sup> of embankment; sub-ballast: 325,712 m<sup>3</sup> and ballast: 496,713 m<sup>3</sup>; trains with an empty weight of 7650 tons and a loaded weight of 41,970 tons; running speed of 80 km/h empty and 70 km/h loaded; capacity for up to 14 pairs of trains per day.

## 3 Geological-Geotechnical Studies

The general objective of geological-geotechnical studies is to understand and quantify the ground conditions and material properties that can affect the feasibility, design, construction, and operation of a project. It is quite important to implement the project according to the geological,

**Fig. 1** Location of the S11D railway line, with the main works indicated, and the works analyzed later on in more detail highlighted. Modified from Arcadis (2011)



geotechnical, and geoenvironmental conditions, selecting the most favorable routes, identifying stability problems and geological risks, and determining the geotechnical properties necessary for the design and construction of the structures (Luis et al. 2002). Directing efforts immediately to subsurface investigations at an early stage of a project is not the best approach, because changes in the alignment required by ongoing design inevitably results in wasted site investigation works, requiring additional expensive subsurface investigations. In this way, engineering, geological, and geomorphological mapping are far less expensive and far more productive, because they are more likely to provide relevant information (Baynes et al. 2005). An effective way to implement any engineering project is based on the thorough understanding of the complete geological and geomorphological history of the project area and the associated engineering implications (Baynes et al. 2005). For railways, a reasonable balance between expenditure on the investigations and the resulting benefit of the information obtained is

considered to have been met when the geological mapping is able to generate reliable geological models for all cuts, the embankment foundation conditions are characterized, all sources of construction materials have been located and their performance characterized, all geohazards have been identified, and a reasonable design of the complete rail line is completed, allowing the development of a complete bid package for construction (Baynes et al. 2005).

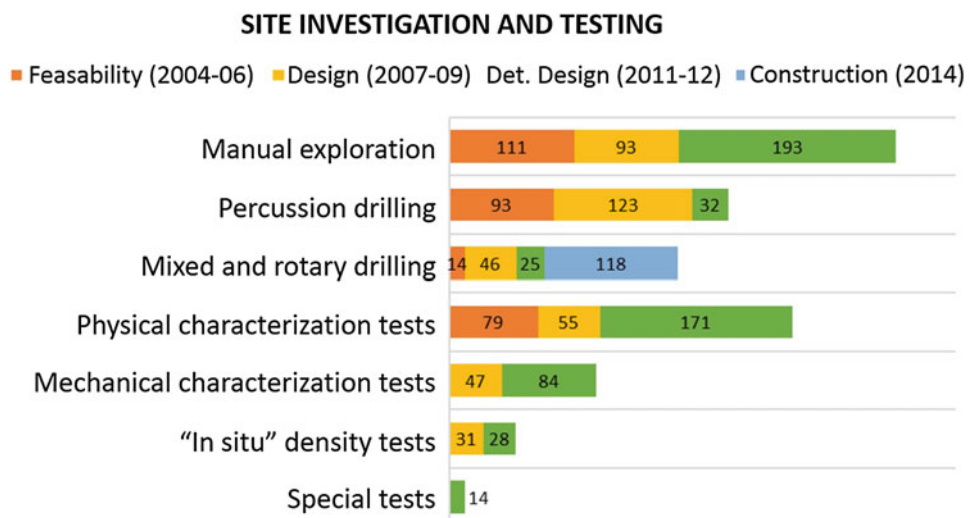
The geological-geotechnical investigations for railway projects are usually done in stages (Table 1). The geological-geotechnical studies of the S11D were carried out over nine years, in distinct stages (Fig. 2). Different companies were involved, being responsible for the Conceptual Phase Minerconsult Engenharia (2004) and for the design and detailed design stages Vega Engenharia e Consultoria (2009, 2012, 2013, 2014a, b; c; 2015).

At the **feasibility stage**, the collection of low-cost information involves desk studies, analysis of aerial photographs, site reconnaissance, general mapping, and site inspection.

**Table 1** Summary of geological-geotechnical investigations for railway projects, by stages (Luis et al. 2002; Baynes et al. 2005; Oliveira 1979; Rodrigues et al. 1998)

Stage	Feasibility	Design	Detailed design	Construction	Operation
Objectives	Geological reconnaissance of the possible routes, identify geohazards and sources of construction materials	Design alignment, assess construction requirements, identify engineering geology formations	Engineering geology zoning, constructive solutions for geotechnical risks, construction materials description	Confirm ground conditions and perform necessary adjustments	Ensure the safety and efficiency of railway operation
Activities	Review of existing geological information, aerial photo and satellite imagery interpretation, site reconnaissance	Geo-mapping, geophysical exploration, test pits and boreholes, in situ and laboratory tests	Detailed mapping, test pits, boreholes, in situ and laboratory tests	Collection and registration of excavation and fill works data, additional exploration	Preventive periodic inspection, reduction of risks and accidents
Report	Preliminary report	Interim report	Final report	Complementary report	Operation reports

**Fig. 2** Geotechnical investigations and testing along the S11D, by stages. Modified from Vega (2012)



The preliminary geological reconnaissance is important for the initial definition of alternative routes; it provides information on the characteristics and quality of the terrain crossed by the railway, and on the viability of the project.

The level of knowledge should progressively increase throughout the development of the **design**, using progressively more elaborate and time-consuming methods and techniques (Luis et al. 2002; Baynes et al. 2005; Oliveira 1979; Rodrigues et al. 1998) to obtain information that is adequate to support the decisions that must be taken. Investigations involving detailed mapping, test pitting, drilling boreholes, and laboratory testing are far more expensive and would be done when the route has been selected and greater detail is required for design. During the design stage, it was necessary to perform changes to 35% of the route length, due to occupations by the Movement of the Landless (MST) or because of a lack of permits from the Brazilian environmental agency (IBAMA) to perform site investigations in protected Amazon forest areas.

The **detailed design** is based on engineering geological mapping, in situ geophysical prospection, mechanical exploration investigations, and in situ and laboratory tests. The work is divided into several projects in order to optimize the design for the excavations, embankments, bridges, viaducts, and tunnels. The work specifications and the preparation of the technical reports with all the geological and geotechnical information of the project, suitable for construction, are prepared.

In the **construction stage**, special attention should be paid to the engineering geological model validation, in order to carry out the engineering geology mapping of the exposed surfaces to verify the ground conditions and identify possible differences with respect to the design. This is needed in order to be able to perform the necessary adjustments, especially in tunnels where the discrepancy between the data obtained in the design studies and those obtained during the construction stage may be large. During construction of the S11D railway branch, it was also necessary to perform complementary site investigation for four bridges, one viaduct and one tunnel, and adaptations of the project based on the encountered conditions. Most of the mixed and rotary drilling were completed during the construction stage, because the site investigation for a long viaduct was insufficiently developed during the design. All the project surveys would represent an average of one survey location for each 200 m of the railway line.

Table 1 presents the proposed methodology for the geological-geotechnical studies and in situ investigations, summarizing the objectives, the main activities, and the type of report issued in each project stage. A comprehensive approach is intended to be tailored to the specificities of each

type of work (excavations, embankments, bridges, or tunnels). All the activities carried out during the geological-geotechnical studies must be aimed at avoiding the occurrence of geotechnical problems, which affect the safety of workers and infrastructure, the construction time, and the operation costs of the railway.

As the studies and projects were developed by several companies, which in turn subcontracted the surveys and tests, the information is dispersed among many different sources. There was no systematic information processing, such as a database that could gather all project information, maps, and profiles incorporating the results of the several site investigation and testing campaigns. If the information generated during the studies were included in a single database and represented in a GIS environment, such as the work done by the Geological Survey of Brazil for the High Speed Train project, there would be greater efficiency due to easier access to information, and a better use of all data and information for decision making. Despite this, the data obtained was fundamental and quite useful for the development of the project.

---

#### 4 Geological-Geotechnical Units

The tropical humid climate (Arcadis 2011a) with an annual precipitation around 1800 mm, average temperature range from 23 to 24 °C, with a maximum of around 30 °C, where the S11D railway branch line is located, significantly influences the geotechnical properties of the terrain, mainly outcropping soils developed by the weathering processes.

The extensive office and field work, and laboratory testing, allowed eight geological-geotechnical units crossed by the S11D railway branch to be defined (Arcadis 2011a; Vega 2009):

- **Granitic Suites:** comprises the Anorogenic Granite Formations and Plaquê Suite. At the surface they mainly present as sandy-clay and silt-sandy saprolite. They weather down to 15 m. The soils are highly susceptible to erosion and have suitable bearing capacity. The Anorogenic Granite occur from the beginning of the railway branch until Tunnel 0. The Plaquê Suite are elongated bands interspersed in the Xingu Complex, from Sossego Mine until the end of the railway line. This is the only unit that has the right conditions for the installation of quarries;
- **Rio Novo Unit:** this is an amphibolite enclave in the Xingu Complex, composed of volcano-sedimentary rocks, with a predominance of metabasic/amphibolite, schist, and associated iron formations. The outcrops are

red residual clay soils, sometimes with fragments of hard relic rock, with medium to high expansiveness. The susceptibility to erosion is medium and has low to medium bearing capacity. This unit occurs from Tunnel 0 (km 4.7) to the vicinity of the viaduct over the PA-275 (km 16.1);

- **Gneiss Complexes Unit:** this covers the lithologies of the Xingu Complex and the Estrela Granitoids, and is composed of granoblastic gneisses, migmatites, and anisotropic granite-gneisses, with milonitized bands. It has weathering soils of 15 to 20 m, showing high susceptibility to erosion and satisfactory bearing capacity. This unit occurs: (a) from the viaduct over the PA-275 highway (km 16.1) to the vicinity of the Verde River (km 30.9); (b) from the Sossego River (km 65.75) to the loading yard (km 96.2), interspersed with the unit Granites Suites (Plaquê Suite);
- **Águas Claras Unit:** this is composed of conglomerate metarenites, siltstones, and rhythmic subordinate argillites. The resulting soils have small thickness, and are silty sand and occasionally gravel and clayey soils. This unit occurs from the vicinity of the Verde River (km 30.9) to Tunnel 1 (km 45.4);
- **Parauapebas unit:** this consists of intensely fractured metabasic, metadacite, metariorite, and amphibolitized rocks. The relief is strongly undulating to hilly. The soils produced by weathering are clayey silts, often covered by laterized clayey soils and crusts. Soils are poorly susceptible to erosion, and have low bearing capacity. This unit occurs from Tunnel 1 (km 45.4) to the Sossego River (km 65.75) and constitutes the segment with the greatest restrictions on the implementation of the railway;
- **Lateritic-detritic unit:** this is the soil covering the other units, and is composed of iron concretions and carapaces in an arenaceous matrix, oolites and ferruginous pisolites,

pebbles, and reworked quartz gravel. The relief has smooth, undulating surfaces. The soils are only 2 to 3 m thick, silty sand with gravel and concretions (A-1-b). It is susceptible to erosion and has a good to optimum bearing capacity, and is easily compacted. This is the unit that can supply the stabilized soils required for the sub-ballast layer of the railway and the primary coating of service roads;

- **Alluvium unit:** composed of sandy sediments, with few intercalations of clay lenses and rare occurrences of organic matter. It has low susceptibility to erosion and good bearing capacity when associated with surface drainage. It is associated with the Águas Claras and Gneiss Complex units (after the Sossego River at km 65.75);
- **Colluvium unit:** composed of residual soils occurring in the Serra do Rabo and in less rugged terrain, as in the Granitic Suites, Gneiss Complexes and Águas Claras units, confused with the surfaces of the lateritic-detritus unit.

Table 2 presents a statistical summary by soil groups along the S11D railway branch, showing the predominance of clayey soils of type A-7-5 and A-7-6, represented by plastic clays with the presence of organic matter (high compressibility) and A-6, represented by medium plastic silty clays with little or no expansible material (low compressibility). According to the American Association of State Highway Transportation Officials (AASHTO) classification, these clayey soils have a weak to poor behavior; however, by the Departamento Nacional de Infraestrutura de Transportes (DNIT) specification (2015), these soils can be used in the embankment bodies, as they have a California Bearing Ratio (CBR) > 5, and expansion  $\leq 2\%$ . They can also be used in the reinforcement of the subgrade (last 60 cm), because they have CBR  $\geq 8$  and expansion  $< 2\%$ .

**Table 2** Statistical summary by soil groups of the S11D railway branch (Vega 2012)

AASHTO classification	Frequency (%)	% passing n° 200#	Max. dry density (kgf/m)	Expansion (%)	CBR (%)	Natural moisture (%)	Optimal moisture (%)
A-7-5	44.0	64.0	1635	0.8	14.4	16.9	20.8
A-6	20.9	62.9	1662	1.3	8.6	17.5	14.4
A-7-6	13.3	59.8	1638	0.7	13.9	16.9	19.2
A-2-4	9.4	28.4	1881	0.1	18.2	7.4	11.2
A-4	4.3	46.8	1736	0.6	15.0	–	15.7
A-1-b	3.6	20.4	2028	0.1	27.9	–	9.9
A-2-6	2.5	29.3	1915	0.6	22.1	15.0	12.4
A-2-7	2.5	33.2	1722	0.2	21.2	15.7	19.2

## 5 Comments on a Cut, a Bridge, an Embankment, and a Tunnel

In the analysis of some specific examples of the geological-geotechnical studies of the S11D, a cut, a bridge, an embankment, a tunnel and the occurrences of natural materials for sub-ballast and ballast were selected to be commented upon. A few proposals for improvement and omissions to the extensive and successful work carried out are summarized below.

- In the **stake 56 excavation** (km 56.00) the execution of mixed drill reaching the bedrock, only in the construction stage, implied the loss of previously developed projects based on quite short drills only intersecting superficial soils. For the new design, other methods could be used for evaluating the shear strength parameters of the terrain, such as laboratory tests (direct shear and triaxial) and in situ tests (e.g. Standard Penetration Test - SPT), or using geomechanical classifications like the Rock Mass Rating (RMR) (Bieniawski et al. 1989) and the Slope Mass rating (SMR) (Romana and Serón 2003) for better guidance on the stabilization methods.
- For the **Sossego River bridge** no geological-geotechnical longitudinal section was available at the time of construction, nor any test reports that would allow the strength and deformability of the soil to be defined, nor any explanation of why some piles were of the continuous auger type. The foundation ground was also simplified in the finite element modeling, and no static load tests were performed on piles to check the failure load.
- In the **embankment of the bridge over the Sossego River**, it would be advisable to include in the design specification an allusion to the need to perform experimental embankments to define the constructive aspects of the rockfill embankment, such as the cord deposition technique, and to the construction quality control method, macro testing, and precision leveling.
- The early identification of geological-geotechnical problems in the **southern portal of tunnel 0** and the modification of the design allowed an increase in stability in the portal construction and in the first meters of the tunnel excavation. The quality of the geological-geotechnical profile, the cartography of the excavation fronts, the use of the RMR and Q geomechanical classifications, and the instrumentation ensured the success of the excavation by the NATM method, without any

substantial difference in relation to the design (Vega 2016);

- In the study of the occurrence of natural materials for the sub-ballast layers, the standards used for characterization should be mentioned, and the characteristic values of the Liquidity Limit (LL) and the Plasticity Index (PI) of tested samples should be presented. For the stone material for ballast, the only suitable lithology was granite.

## 6 Final Considerations

The primary objective of the engineering geology studies is to understand the nature and the geotechnical behavior of the terrain that will receive the new railroad, a linear infrastructure, crossing diverse geological formations and variable topography, where, in addition to the earthworks, it will be necessary to build special works requiring specific studies, which must be quite detailed and diversified.

All the activities carried out during the engineering geology studies must be aimed at avoiding the occurrence of geotechnical problems, increasing safety, and optimizing the construction schedule and costs, as well as the efficient operation of the railway.

As the railway was completed in December 2016, it is now very important to ensure the safety and efficiency of the operation of the railway. To achieve this objective, it is necessary to carry out periodic preventive inspections and to propose solutions to problems or anomalies that may develop and generate risks or accidents. Monitoring and interpretation of the instrumentation installed along the railway line must be systematically carried out, and the trends assessed to evaluate the stability of soil and rockfill embankments, cuts, and structures.

For the rockfill shoulder of the Sossego River bridge, it is recommended that the settlements be periodically measured, and that the behavior of the embankment be monitored, as it is located in a region with high and concentrated rainfall that can induce deformations in the rockfill (Oliveira 2017).

Adequate compilation and additional interpretation of the site investigation, of the design, of the construction and of the operation of the railway can improve the geotechnical knowledge and behavior of the railway, allowing the investments made to be optimized, a good performance of the infrastructure to be ensured, and to serve as a basis for more efficient development of new ore transport railway projects.

**Acknowledgements** The authors would like to thank VALE mining company for the authorization to publish the data from the S11D project (Ramal Ferroviário do Sul do Pará). This work was supported by FCT (Fundação para a Ciência e a Tecnologia, I.P.), through Portuguese funds, in the research project UID/Multi/00073/2013 of the Geosciences Center of the University of Coimbra.

## References

- Arcadis. Environmental impact report of the southeast railway branch of Pará, São Paulo: Arcadis Tetraplan S.A., 112 pages. (2011). (In Portuguese)
- Arcadis. Environmental impact study of the southeast railway branch of Pará, São Paulo: Arcadis Tetraplan S.A., 1,280 pages. (2011). (In Portuguese)
- Baynes, F.J., Fookes, P.G., Kennedy, J.F.: The total engineering geology approach applied to railways in the Pilbara, Western Australia. *Bulletin of Engineering Geology and the Environment* **64** (1), 67–94 (2005). <https://doi.org/10.1007/s10064-004-0271-4>
- Bieniawski, Z.T.: *Engineering rock mass classifications*. John Wiley and Sons (1989)
- DNIT. *Railway Service Instruction: Geotechnical Studies*. Brazil: Directorate of Railway Infrastructure (DIF), ISF-207, National Department of Transport Infrastructure, 44 pages. (2015). (In Portuguese)
- González de Vallejo, Luis, I., Ferrer, M., Ortuño, L., Oteo, C. *Ingeniería Geológica*. Madrid: Pearson Educación (2002)
- Minerconsult. Report on geological and geotechnical studies. Belo Horizonte: Minerconsult Engenharia Ltda (currently SNC-Lavalin), Memorial describing the conceptual phase, 38 pages. (2004). (In Portuguese)
- Oliveira, R.: Engineering geological problems related to the study, design and construction of dam foundations. *Bull. Int. Assoc. Eng. Geol.* **20**, 4–7 (1979)
- Oliveira, P.H.: Geological-geotechnical studies of railway cargo works. The Southeast of Pará Railway Branch (Brazil). MSc Thesis in Mining and Geological Engineering. University of Coimbra, Portugal (2017). (In Portuguese)
- Rodrigues, R., Lopes, J.A.U. *Rodovias.*: In: Oliveira, A.M.S., Brito, S. N.A. (eds.) *Geologia de Engenharia*. São Paulo: ABGE, cap. 25, 419–430. (1998). (In Portuguese)
- Romana, M., Serón, J., Montalar, E.: SMR Geomechanics classification: Application, experience and validation. *ISRM 2003–Technology roadmap for rock mechanics*, South African Institute of Mining and Metallurgy, 4 p (2003)
- Vega. Containment project for the cut of the 56 km massif. São Paulo: Vega Engenharia Ambiental S.A., railway branch southeast of Pará, Technical report, 292 pages. (2015). (In Portuguese)
- Vega. Execution of landfill in material of 3rd category. São Paulo: Vega Engenharia Ambiental S.A., railway branch southeast of Pará, Technical report on earthworks, 3 pages. (2014c). (In Portuguese)
- Vega. Geological and geotechnical studies of the southeastern railroad branch of Pará, São Paulo: Vega Engenharia Ambiental S.A., descriptive memorial of the detailed project, 153 pages. (2012). (In Portuguese)
- Vega. Geotechnical studies of the southeastern railway branch of Pará, São Paulo: Vega Engenharia Ambiental S.A., Descriptive memorial and justification of the basic project, 55 pages. (2009). (In Portuguese)
- Vega. Memories of calculation of the stakes of the bridge on the river Sossego, São Paulo: Vega Engenharia Ambiental S.A, southeast railway branch of Pará. (2014b). (In Portuguese)
- Vega. Technical report on surveys. São Paulo: Vega Engenharia Ambiental S.A., Railroad southeast of Pará, 13 pages. (2014a). (In Portuguese)
- Vega. Tunnel 0—Topographic plant and geotechnical profile. São Paulo: Vega Engenharia Ambiental S.A., Railway Branch Southeast of Pará, Drawing of As Built. (2016). (In Portuguese)
- Vega. Tunnel Project—Tunnel 0. São Paulo: Vega Engenharia Ambiental S.A., Memorial descriptive of the detailed project, 51 pages. (2013). (In Portuguese)





# Groundwater Nitrate Concentrations and Its Relation to Landcover, Buncombe County, NC

Adu Agyemang, Adela Beauty, Arpita Nandi, Ingrid Luffman, and Andrew Joyner

## Abstract

High concentrations of nitrate ( $\text{NO}_3$ ) in groundwater can be harmful to human health if ingested, and the primary cause of blue baby syndrome, among other health impacts. In this study, the spatial distribution of  $\text{NO}_3$  in groundwater for 610 private drinking water wells in Buncombe County, North Carolina was modeled. While  $\text{NO}_3$  concentration in the sampled wells did not exceed the 10 mg/L limit established by the United States Environmental Protection Agency, some wells had  $\text{NO}_3$  concentrations approaching this limit (as high as 8.5 mg/L). Kriging interpolation was implemented within a Geographic Information System to predict  $\text{NO}_3$  concentrations across the county, and a cokriging model using land cover type. Cross validation statistics of root mean square and root mean square standardized for both models were compared and the results showed that the predicted  $\text{NO}_3$  map was improved when land cover type was integrated into the model. The cokriging interpolated surface with land cover as a covariate had the lowest root mean square (0.979) when compared to the kriging interpolated surface (0.986), indicating a better fit for the model with land cover.  $\text{NO}_3$  concentrations equal or greater than 2 mg/L were concentrated in 37% hay/pasture land, 34% developed open space, and 29% deciduous forest. The study did not reveal any statistically significant difference in the presence of high  $\text{NO}_3$  concentration between these landcover types, indicating they all relate to high  $\text{NO}_3$  content.

## Keywords

Nitrate • Spatial statistics • Kriging

## 1 Introduction

Groundwater provides about 80% of usable water storage in the world. The quality of groundwater is as important as that of its availability and quantity because it represents our main source of drinking water (Rahman 2008). Groundwater is an important source of water supply because of its low susceptibility to pollution compared to surface water (U.S. Environmental Protection Agency 1995). Groundwater is vulnerable to pollution from underlying bedrock, human activities, and sewage discharge from industrial and agricultural sites (Rahman 2008; Babiker et al. 2004). Nitrate ( $\text{NO}_3$ ) is a widespread pollutant that enters the groundwater through the surface and is not naturally contained in the groundwater. Predicting areas that are likely to contain high levels of  $\text{NO}_3$  may help to prevent the use of  $\text{NO}_3$  contaminated water, and provide developers and planners with information about areas in need for additional testing.

Nitrogen is a primary component of fertilizers based on its ability to boost the productivity of crops. Global increase in the use of nitrogen fertilizer over the last few decades has led to increased  $\text{NO}_3$  in groundwater, threatening water quality (Burow et al. 2010). When nitrogen in fertilizer exceeds the demand of plants and the ability of the soil to retain it, nitrogen leaches into groundwater in the form of  $\text{NO}_3$  through infiltration of precipitation, irrigation, and other processes (Shamrukh et al. 2001). Agricultural areas are susceptible to high levels of  $\text{NO}_3$  concentrations due to the use of  $\text{NO}_3$  rich fertilizers (Zhang et al. 1996; Thorburn et al. 2003). Factors that affect  $\text{NO}_3$  concentration in groundwater include land use operations, shallow water table, water chemistry like redox potential and pH, and subsurface clay thickness (Townsend and Young 1995). Increased concentration of  $\text{NO}_3$  in groundwater may represent a loss of fertility in the overlying soil, cause eutrophication from the discharge of groundwater into surface water, and become a health hazard to animals and humans (McLay et al. 2001). Environmental Protection Agency (EPA) has

A. Agyemang · A. Beauty · A. Nandi (✉) · I. Luffman · A. Joyner  
Department of Geosciences, East Tennessee State University,  
Johnson City, TN 37614, USA  
e-mail: nandi@etsu.edu

established a maximum contaminant level of 10 milligrams per Liter for drinking water NO<sub>3</sub> level beyond which could be harmful to human health (U.S. Environmental Protection Agency 1995).

### 1.1 NO<sub>3</sub> Concentrations in North Carolina

NO<sub>3</sub> concentrations in groundwater in the United States are highest in shallow, oxygenated groundwater (Burow et al. 2010), most typically in areas beneath agricultural land with well-drained soils. In North Carolina, more than 25% of the population relies on private wells for drinking water, located outside municipal water supply systems. A state-wide study by North Carolina Health and Human Services between 1998 and 2010 reported concentrations of NO<sub>3</sub> in private well water that ranged from 0.5 to 20 mg/L (NCDHHS 2014). A study in the southeastern plains of North Carolina indicated that high levels of NO<sub>3</sub> concentrations are related to wastewater treatment residuals and localized animal feeding operations (Messier et al. 2014). Excess nutrient and fertilizer loadings in eastern North Carolina have degraded overall water quality (Burkholder 2006). A study in North Carolina concluded that both agricultural and urban sites contributed to high percentages of NO<sub>3</sub> point sources in central and eastern North Carolina (Hardin and Spruill 2000). Excess NO<sub>3</sub> concentration in groundwater and its health implications has raised concerns, resulting in the need for further research to locate areas with high NO<sub>3</sub>. The objectives of this study are to: (1) analyze the spatial distribution of NO<sub>3</sub> in groundwater wells in Buncombe County, North Carolina, and (2) evaluate the extent to which NO<sub>3</sub> concentrations in groundwater relate to land cover type.

This study was performed in Buncombe County, North Carolina (Fig. 1). Buncombe County is located in western North Carolina in the Blue Ridge Physiographic province. The county is bordered to the north by Madison and Yancey counties, to the south by Henderson County, to the east by Rutherford and McDowell counties and to the west by Haywood County. The county also shares a border with the Appalachian Mountains to the west and the Black Mountains to the east. The county covers a total area of 660 square miles, of which 657 square miles is land and 3.5 square miles is water. The average annual temperature of Buncombe County is 55.83 °F, and average annual precipitation is 40.92 inches. Physiographically, Buncombe County consists of high, smooth-rounded mountains surrounded by streams flowing in narrow valleys and underlain by bedrock consisting of igneous, meta-igneous, and sedimentary rocks. Aquifers in Buncombe County are mostly found in the crystalline metamorphic and igneous rocks (Trapp and Horn

1997) where fractures in the crystalline bedrock serve as the primary storage for groundwater (Drever 1997). Wells located in valleys typically have shallow water tables and are more susceptible to contamination than wells located in hilly areas.

## 2 Methods

### 2.1 Data Development and Geocoding

Two different spatial variables were used in this study: NO<sub>3</sub> concentration in groundwater wells, and land cover. Wells data were acquired from the North Carolina Division of Water Resources in spreadsheet form. Data included well owner's identification number, well permit number, first and last name, well location addresses (including city, state, zip code), GPS coordinates (longitude and latitude), and collection date. The forested areas, and the urban areas located in the central part of the county did not have records of private drinking wells. Well data containing no spatial information were discarded from the dataset. The remaining dataset was geocoded using ArcGIS Online World Geocode Service to create a well location point map in ArcGIS 10.3. A total of 610 wells were matched during the geocoding process, and were subsequently used for analysis. Additionally, the National Land Cover Dataset, available from the Multi-Resolution Land Characteristics Consortium stored at Geospatial Gateway (USDA NRCS 2008) at a resolution of 30 X 30 m<sup>2</sup>, was used (Fig. 2). The county has over 60% of its land covered by deciduous forests followed by developed open space (14%) and hay/pasture (13%). Emergent herbaceous wetland is the least represented land cover type within the county.

### 2.2 Exploratory Statistics

Per USEPA statistical protocol, all NO<sub>3</sub> concentration data below minimum detection limits (0.5 mg/L) were selected. Half of the values were kept at 0.5 mg/L while the rest were assigned a concentration value of 0.25 mg/L. Descriptive statistics (mean, standard deviation, and range) were performed on the variables using Statistical Package for the Social Sciences, IBM SPSS statistics 23 (George and Mallery 2016). Exploratory analysis was also conducted to test for normality and correlation among the variables: NO<sub>3</sub> concentration, and land cover.

To understand how NO<sub>3</sub> concentrations within each well compare with the different land cover types, a buffer radius surrounding the groundwater well was used to extract land

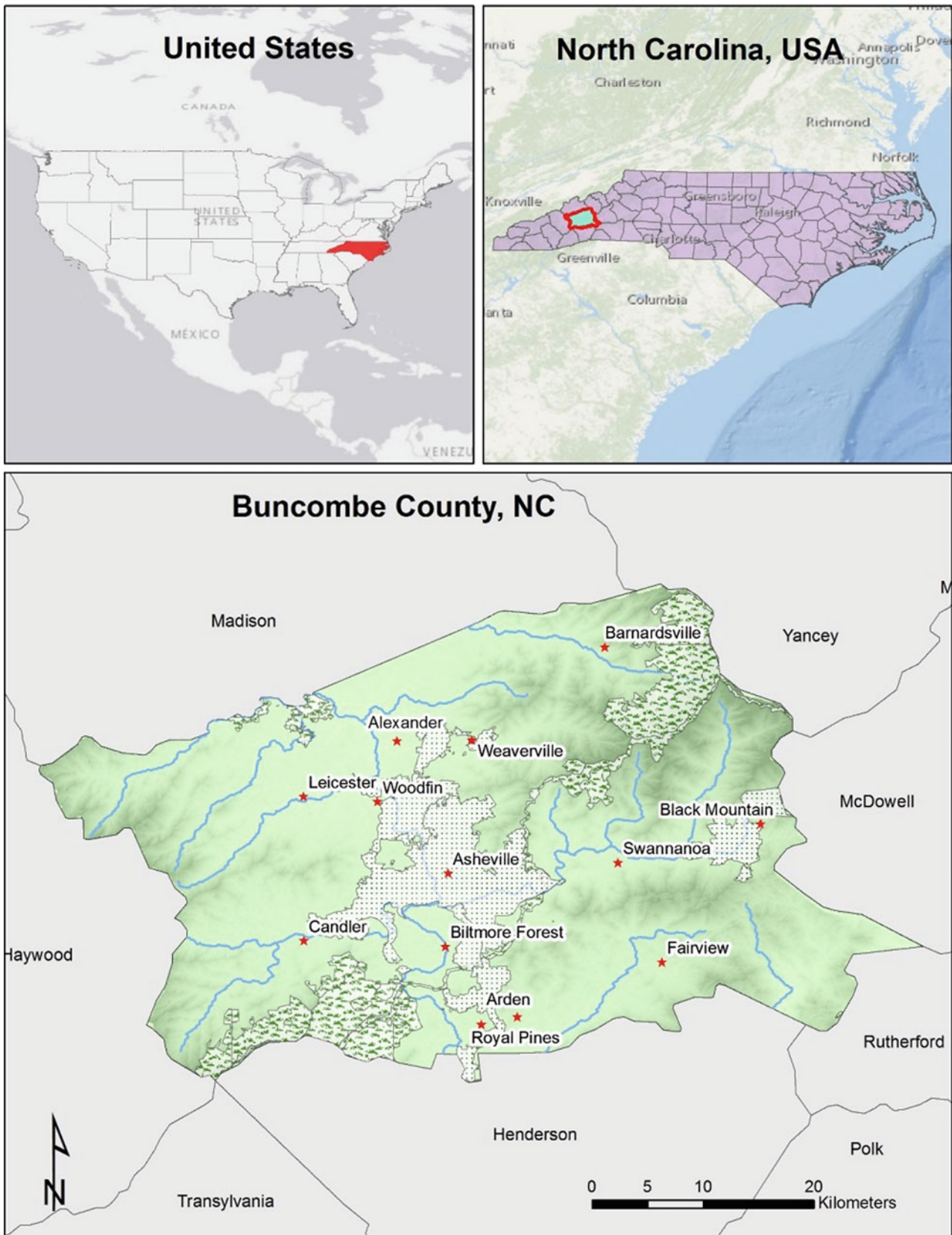
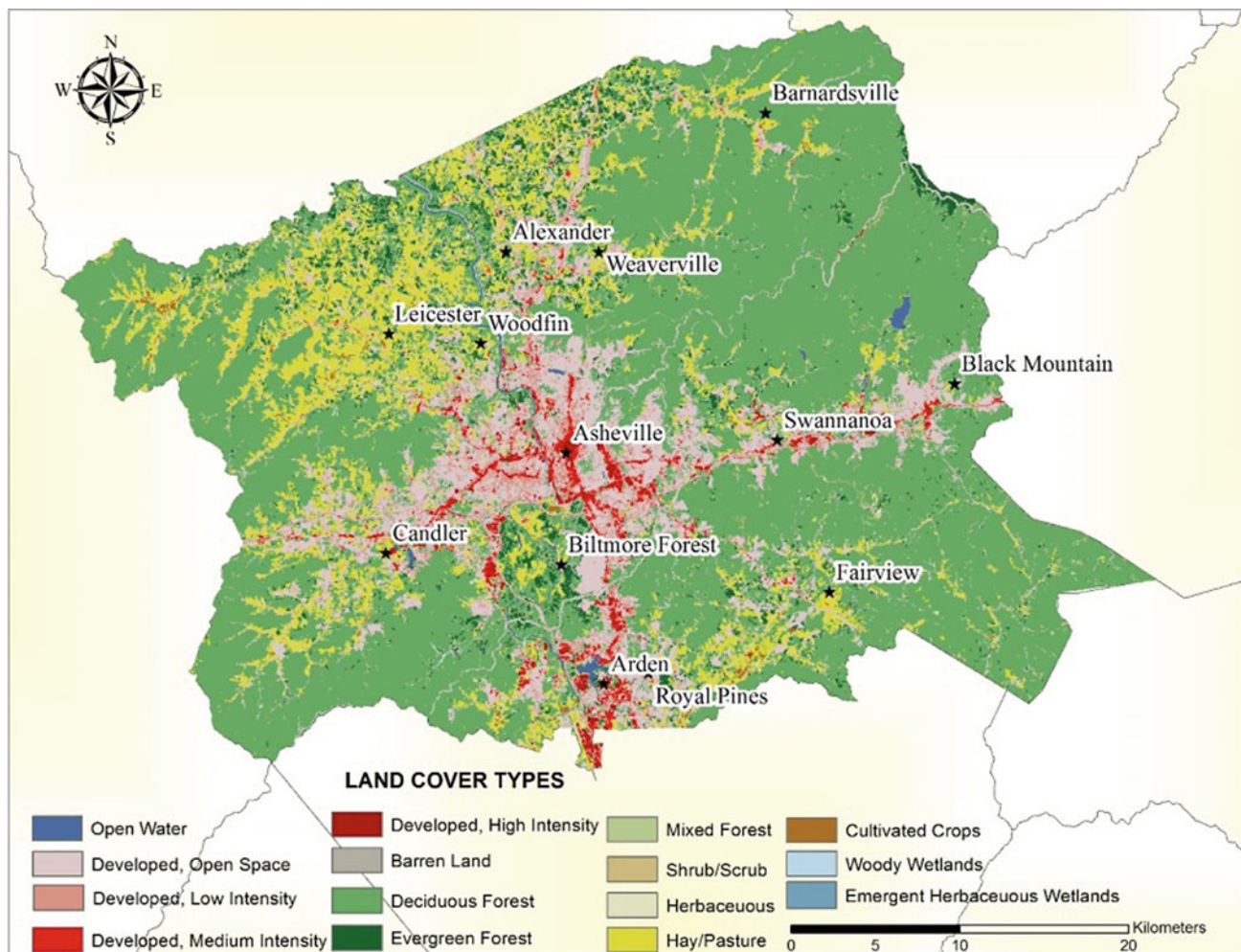


Fig. 1 Study area map of Buncombe County, North Carolina, US



**Fig. 2** Landcover data of Buncombe County, NC

cover data. Several studies have used different buffer radii ranging from 250 to 1000 m (Barringer et al. 1990). The land cover in each well location within the 500 m buffer area was extracted using zonal histogram and the majority land cover was assigned to each well. Based on the test of normality, Spearman's correlation coefficient was calculated to measure the statistical dependence of  $\text{NO}_3$  on land cover. Additionally, one-way Analysis of Variance (ANOVA) was performed to compare the presence of high  $\text{NO}_3$  content in different landcover types.

The existence of spatial dependency in the  $\text{NO}_3$  was examined with GeoDa 1.8.14 (Anselin et al. 2006). GeoDa is a software package used for spatial data analysis, data visualization, spatial autocorrelation, and spatial modeling. Spatial autocorrelation was examined in this study to check spatial dependency in the  $\text{NO}_3$ . The result from this check served as the basis for further analysis in ArcGIS environment. Global and Local Moran's I statistical tests were then conducted to detect the presence of spatial autocorrelation in the  $\text{NO}_3$  data.

### 2.3 Spatial Statistics Using Kriging and Cokriging

Kriging presumes that there is autocorrelation in the data, which was examined in the previous section (Sect. 2.2). In this study, ordinary kriging interpolation was used to create a predicted  $\text{NO}_3$  concentration map from the  $\text{NO}_3$  point data to examine the variation and spatial extent of  $\text{NO}_3$  contamination in Buncombe County.

Landcover data was used as covariate in a cokriging approach to further improve the  $\text{NO}_3$  concentration prediction surface. A cross validation comparison was performed for the kriged  $\text{NO}_3$  surface and the cokriged  $\text{NO}_3$  surfaces based on models diagnostics. The mean standardized error (ME), root mean square error (RMS), root mean square standardized error (RMSSE), and average standard error (ASE) of each interpolation were used to assess the model's performance. A model is said to be best if it has a ME nearest to zero, a small RMS, an ASE closest to the RMS, and a RMSSE closest to one. The  $\text{NO}_3$  concentrations for the

kriged/cokriged surface were grouped into six categories using geometric classification. Geometric classification is generally used for classifying continuous data and visualizing predicted surfaces that are not normally distributed.

### 3 Results

#### 3.1 Wells Location and Exploratory Statistics

NO<sub>3</sub> contaminated wells in Buncombe County had concentration values ranging from 0.25 to 8.5 mg/L. These wells were distributed across the county except the north-eastern corner, Biltmore, and the forest zones (Fig. 3). There were 43 drinking water wells with concentrations of 2.0 mg/L and above, and these were in the northern, northwestern, central, and southeastern part of the county.

The Shapiro-Wilk Test of normality indicated that the NO<sub>3</sub> was not normally distributed. The wells with high NO<sub>3</sub> content (2.0 mg/L) indicated correlation with landcover data (Spearman's rho = 0.24 at  $p = 0.04$ ). High level of NO<sub>3</sub> (2 mg/L) was concentrated near hay and pasture land (37%), developed urban open space (34%), and deciduous forest (29%). The result from ANOVA did not find any significant difference in NO<sub>3</sub> content between developed urban open space, deciduous forest, and hay and pasture land. the mentioned land cover types.

Local Moran's I using LISA (Local indicators of spatial association) statistics identified 54 wells with high NO<sub>3</sub> values close to other high NO<sub>3</sub> values, and 79 wells with low NO<sub>3</sub> values close to other low NO<sub>3</sub> values. The results of the analysis using GeoDa showed the existence of spatial autocorrelation in the NO<sub>3</sub> therefore provided the basis for further analysis with Kriging and Cokriging.

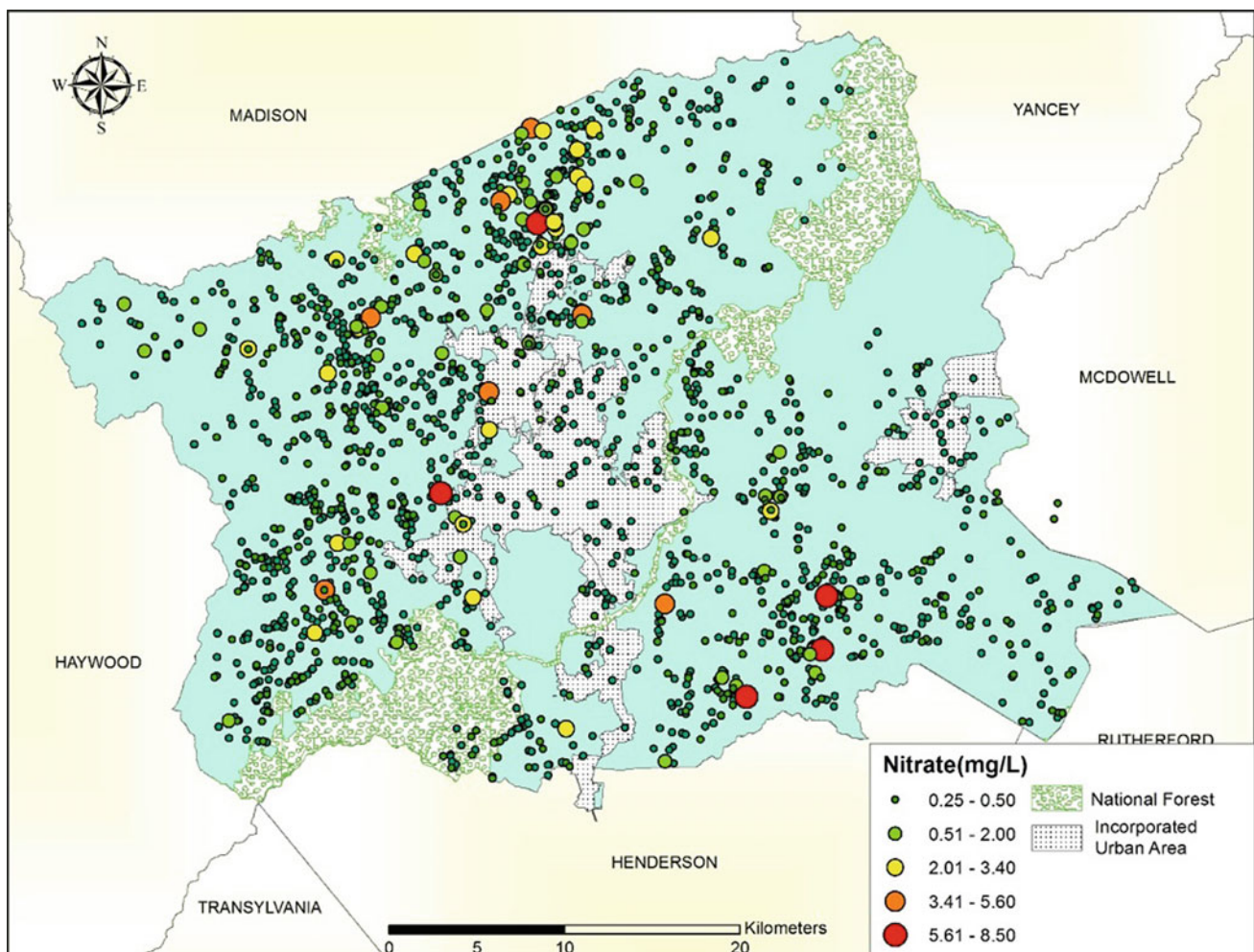


**Fig. 3** Nitrate contaminated wells in Buncombe County, NC

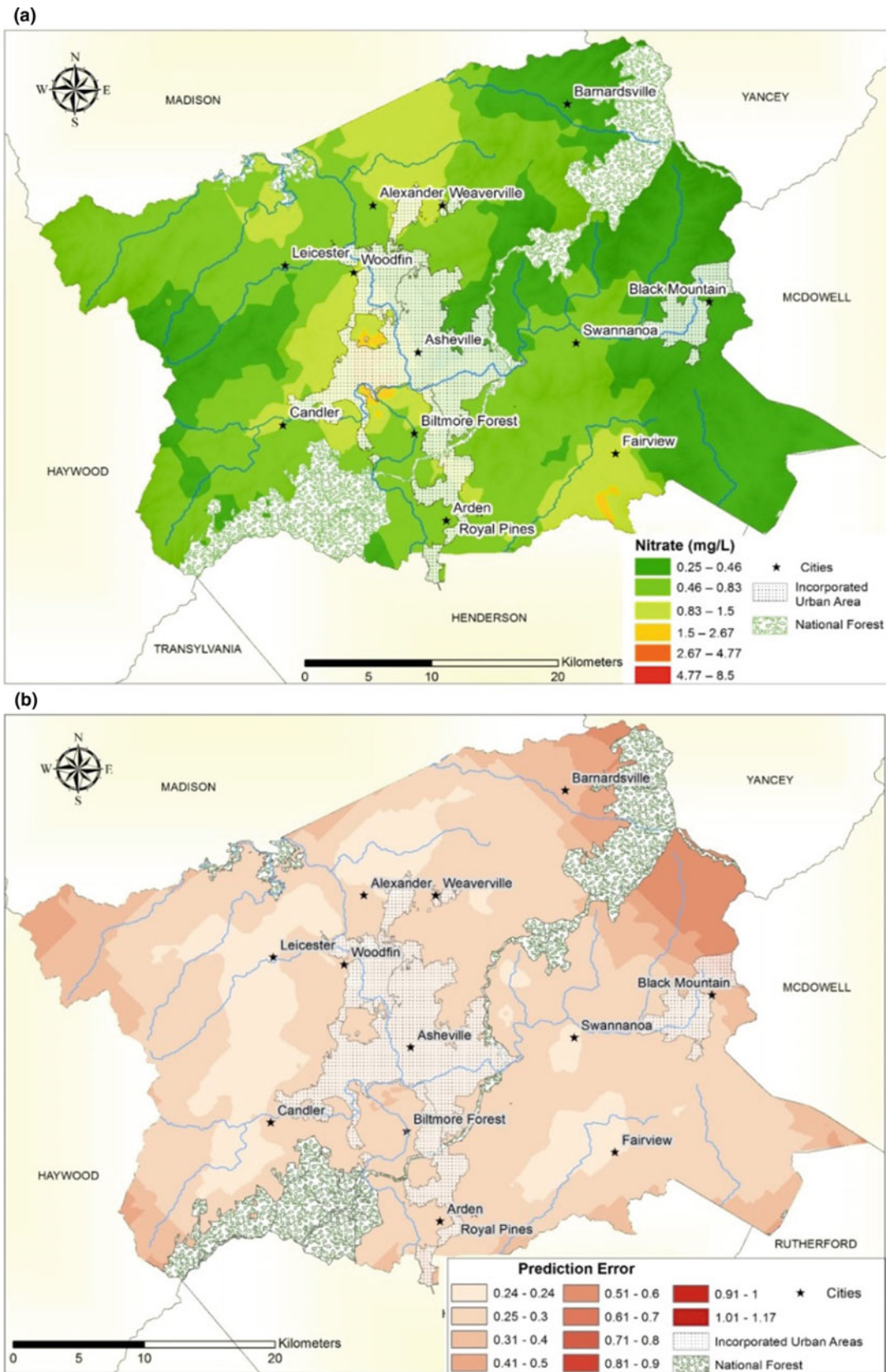


**Fig. 4** Prediction map of NO<sub>3</sub> concentrations cokriged with landcover (a), Prediction error map of NO<sub>3</sub> cokriged with landcover (b)

**Table 1** Comparison of cross validation statistics of kriging and cokriging

Prediction errors	NO <sub>3</sub>	NO <sub>3</sub> + Landcover
ME	-0.0047	-0.0044
RMS	0.979	0.986
RMSSE	0.8956	0.9469
ASE	1.0941	1.0390

### 3.2 Spatial Statistics—Kriging and Cokriging

The cross-validation matrix for the kriging and cokriging were compared to determine the best model. The model produced from cokriging was better in terms of models accuracy metrics compared to the kriging model. A summary of the accuracy metrics of NO<sub>3</sub> concentration from kriging/cokriging is given in Table 1. For both models, mean error (ME) was centered around zero with a range from -0.0044 to -0.0047. Nitrate/land cover however, had the smallest difference between RMS (0.986) and average standard error (ASE) (1.039) and therefore, this model was considered the better model to predict nitrate concentration in groundwater for the study (Fig. 4a). A prediction standard error map was produced for the NO<sub>3</sub> kriging and NO<sub>3</sub>/land cover cokriging interpolation maps (Fig. 4b). The cokriged interpolated surface had higher prediction errors at the extreme eastern/western and central part (around Asheville) of the county including the forested area. These parts of the county had missing well location, and NO<sub>3</sub> concentrations data. The kriged NO<sub>3</sub> map on the other hand had high prediction errors in the same areas as the cokriged maps as well as areas around Candler, Biltmore Forest, Alexander, and Royal Pines.

## 4 Discussion and Conclusion

The level of nitrate concentrations within the whole county ranged from 0.25 to 8.5 mg/L. Even though higher NO<sub>3</sub> concentrations were found in some regions, none of the regions' NO<sub>3</sub> concentrations exceeded the maximum concentration level set by the US EPA (10 mg/L), beyond which is considered to be harmful to human health.

The spatial distribution of NO<sub>3</sub> indicated that areas like Barnardsville, Biltmore Forest, Woodfin, and Black Mountain had very low NO<sub>3</sub>, less than 0.5 mg/L. High concentrations were recorded in Candler, Weaverville, Leicester Fairview, Arden, and some areas in Asheville. The statistical analysis revealed that landcover type in the county was significantly correlated with high NO<sub>3</sub> content, and high NO<sub>3</sub> concentrations were seen in developed urban open space, deciduous forest, and hay/pasture areas. The study did not reveal any statistically significant differences in the

presence of high NO<sub>3</sub> concentration between these landcover types, indicating they all contribute to high NO<sub>3</sub> content. Previous studies correlated high NO<sub>3</sub> content with urban areas where fertilizers were often applied to the lawns, parks, and golf courses (Barringer et al. 1990; Hallberg and Keeney 1993). Hay and pasture lands are known source of high NO<sub>3</sub> derived from animal manure and agricultural runoff (Hallberg and Keeney 1993). In natural undisturbed forest the NO<sub>3</sub> content should be low, but studies have found that, high NO<sub>3</sub> content in forested areas are indicative of anthropogenic disturbance (Hallberg and Keeney 1993; Nolan et al. 1997).

Results indicated that the NO<sub>3</sub> interpolated surface was improved when cokriged with land cover, confirming the results from correlation analysis. Land cover type used in cokriging with the NO<sub>3</sub> point map influenced the level of NO<sub>3</sub> concentrations in parts of the county. The evergreen forested areas, developed intensity (low, medium, high), barren land, and wetlands had very low NO<sub>3</sub> concentrations, whereas hay/pasture, developed open urban space, and deciduous forest areas had high NO<sub>3</sub> concentration.

Future studies can be conducted using this study as the basis to perform more site-specific study in high nitrate areas to monitor the wells located in those areas and detect the cause of the high nitrate content. It is recommended that further research be done especially in deciduous forested areas and developed open space to find out why nitrate content is high in those regions. Additional, this study also serves as a guide for estate planners and developers on choice of site and how vulnerable the area may be to NO<sub>3</sub> contamination.


## References

- Anselin, L., Syabri, I., Kho, Y.: GeoDa: an introduction to spatial data analysis. *Geogr. Anal.* **38**(1), 5–22 (2006)
- Babiker, I.S., Mohamed, M.A., Terao, H., Kato, K., Ohta, K.: Assessment of groundwater contamination by nitrate leaching from intensive vegetable cultivation using geographical information system. *Environ. Int.* **29**(8), 1009–1017 (2004)
- Barringer, T., Dunn, D., Battaglin, W., Vowinkel, E.: Problems and methods involved in relating land use to groundwater quality. *Jawra J. Am. Water Resour. Assoc.* **26**(1), 1–9 (1990)
- Burkholder, J.M., Dickey, D.A., Kinder, C.A., Reed, R.E., Mallin, M. A., McIver, M.R., Deamer, N.: Comprehensive trend analysis of

- nutrients and related variables in a large eutrophic estuary: a decadal study of anthropogenic and climatic influences. *Limnol. Oceanogr.* **51**(1part2), 463–487 (2006)
- Burow, K.R., Nolan, B.T., Rupert, M.G., Dubrovsky, N.M.: Nitrate in groundwater of the United States, 1991–2003. *Environ. Sci. Technol.* **44**(13), 4988–4997 (2010)
- Drever, J.I.: *The Geochemistry of Natural Waters: Surface and Groundwater Environments*, 436 pp (1997)
- George, D., Mallery, P.: *IBM SPSS Statistics 23 step by step: a simple guide and reference*. Routledge (2016)
- Hallberg, G.R., Keeney, D.R.: In: Alley, W.J. (ed.) *Nitrate, Regional Groundwater Quality* (1993)
- Hardin, S.L., Spruill, T.B.: Ionic Composition and Nitrate in Drainage Water from Fields Fertilized with Different Nitrogen Sources, Middle Swamp Watershed, North Carolina, August 2000–August 2001. Scientific Investigations Report. United States Geological Survey, 24 (2004)
- McLay, C.D.A., Dragten, R., Sparling, G., Selvarajah, N.: Predicting groundwater nitrate concentrations in a region of mixed agricultural land use. *Environ. Pollut.* **115**, 191–204 (2001)
- Messier, K.P., Kane, E., Bolich, R., Serre, M.L.: Nitrate variability in groundwater of North Carolina using monitoring and private well data models. *Environ. Sci. Technol.* **48**(18), 10804–10812 (2014)
- NCDHHS: *Well Water and Health; Contaminants by County* (2014). Retrieved from: [http://epi.publichealth.nc.gov/oe/wellwater/by\\_county.html](http://epi.publichealth.nc.gov/oe/wellwater/by_county.html)
- Nolan, B.T., Ruddy, B.C., Hitt, K.J., Helsel, D.R.: Risk of Nitrate in groundwaters of the United States a national perspective. *Environ. Sci. Technol.* **31**(8), 2229–2236 (1997)
- Rahman, A.: A GIS based DRASTIC model for assessing ground water vulnerability in shallow aquifer in Aligarh, India. *Appl. Geogr.* **28**, 32–53 (2008)
- Shamrukh, M., Corapcioglu, M., Hassona, F.: Modeling the effect of chemical fertilizers on ground water quality in the Nile Valley Aquifer, Egypt. *Groundwater* **39**(1), 59–76 (2001)
- Thorburn, P.J., Biggs, J.S., Weier, K.L., Keating, B.A.: Nitrate in groundwaters of intensive agricultural areas in coastal Northeastern Australia. *Agr. Ecosyst. Environ.* **94**(1), 49–58 (2003)
- Townsend, M.A., Young, D.P.: Factors affecting nitrate concentrations in ground water in Stafford County, p. 238. *Bull. Kansas* (1995)
- Trapp, H., Horn, M.A.: *Ground Water Atlas of the United States, Delaware, Maryland, New Jersey, North Carolina, Pennsylvania, Virginia, West Virginia*. US Geol. Surv. Hydrol. Atlas HA (1997)
- USDA NRCS: *Geospatial Data Gateway* (2008). Retrieved from <https://datagateway.nres.usda.gov>
- U.S. Environmental Protection Agency: *Drinking Water Regulations and Health Advisories*. EPA Office of Water, Washington, DC (1995)
- Zhang, W.L., Tian, Z.X., Zhang, N., Li, X.Q.: Nitrate pollution of groundwater in northern China. *Agr. Ecosyst. Environ.* **59**(3), 223–231 (1996)



# Land Change, Soil Degradation Processes, and Landscape Management at the Clarinho River Watershed, Brazil

José Augusto de Lollo , João V. R. Guerrero, Ana C. P. Abe, and Reinaldo Lorandi

## Abstract

Since 70's land changes have been the main driving force inducing environmental degradation in Brazil, particularly in São Paulo State. Considering its very close relationship with landscape evolution, land change pattern and landform classification were analyzed to understand soil degradation in Clarinho watershed (40.89 km<sup>2</sup>) and propose specific management measures for recovering and conservation. Land change analysis was assessed using LCM toolbox. Landform evaluation was based on Brazilian approach for terrain evaluation. Results show that temporary and permanent soil exposures, due to extensive livestock in naturally fragile areas (i.e. more erodible soils in major surface runoff taxes), are the main triggers in soil degradation. Terrain evaluation also indicates highly fragile landforms due to its relief characteristics and morphogenetic processes. Thick soil profiles which are developed from medium grained rocks, in wide convex slopes, describe the main landforms attributes in inducing degradation. Areas subject to land changes are those in which susceptibility to erosion is high and where records of erosion processes were more expressive. Clarinho watershed large areas need to be treated as “zone for conditioned farming use”, with specific management directives and measures.

## Keywords

Erosion • Land use/cover • Watershed

## 1 Introduction

In the southeast region of Brazil, the expansion of farming has been the main trigger of soil degradation, particularly erosion, since the early 1960s. Accelerated erosion processes have resulted in large environmental changes in the natural environmental dynamics (He et al. 2006), resulting in serious urban problems (Gupta and Ahmad 1996) and causing serious food production problems (Pimentel 2006).

The northeastern region of São Paulo State, where the studied area is located, presents the highest indicators of potential natural erosion among those identified in Brazil (Silva et al. 2011). The intensification of environmental studies resulted in new legislation focusing on the reduction of rural and urban erosion. Despite these legislations, the adoption of such measures requires proper technical knowledge on the environment to be effective (Bocco et al. 2011).

In the Clarinho River watershed, such studies have not previously been undertaken, resulting in intense erosion processes. Despite the influences of soils and relief on the onset of erosion processes, human activities also caused erosion processes and their intensification (Lorandi and Lollo 2015).

To evaluate the relationship between land use dynamics and erosion in the Clarinho River watershed, this work, which was financially supported by FAPESP (Project 2013/03699-5) and the CAPES and CNPq scholarships, was carried out.

The characterization of land change in the area was conducted using the Land Change Modeler (LCM) module from Idrisi™ Selva (Clark 2012), and the analysis of erosion susceptibility was developed using ArcGis® 10.2 (Esri 2011).

The LCM module was developed to analyze land change, considering the contributions of each land use class on the conversion of other classes (Eastman 2012). The LCM module has been widely used for watershed analyses (Piroli et al. 2011, 2012) and the prediction of future scenarios (Oñate-Valdivieso and Sendra 2010; Huang and Pathirana 2013).

J. A. de Lollo (✉) · A. C. P. Abe  
São Paulo State University (UNESP), Ilha Solteira, Brazil  
e-mail: lolloja@dec.feis.unesp.br

J. V. R. Guerrero · R. Lorandi  
São Carlos University (UFSCar), São Carlos, Brazil

## 2 Studied Area

The Clarinho River watershed is located in the northeastern region of São Paulo State, Brazil (Fig. 1).

The Clarinho River watershed has an area of 40.89 km<sup>2</sup> with a population of 26,410 inhabitants. Its original vegetation consisted of forests and savannahs, which have been replaced by agricultural activities, mainly sugar cane cultivation, and livestock.

The area is located in the Paraná sedimentary basin, with a peripheral depression morpho-sculpture, which developed in Paleozoic and Mesozoic sedimentary rocks (São Paulo—FFLCH/USP-IPT-FAPESP 1997). The local relief comprises hills with tabular large tops, shallows valleys, and wide interfluves. The prevalent altitude varies from 500 to 650 m, and the steepness varies between 5 and 10% (Guerrero 2014).

The climate of the area is humid tropical with a dry winter (May–September) and intense rainfall in the summer (October–April), with rains concentrated in the months of December, January and February (Mendonça and Danni-Oliveira 2007).

The geological units (São Paulo-IG 1981—Fig. 2) are: sandy alluvial deposits with clay and gravel lenses (Q); the Santa Rita Formation—SrpT (sandstones with clay matrix and gravel layers at the base); the Serra Geral Formation—JKsg (tholeiitic basalts with sandy lenses associated with sills and dikes); the Botucatu Formation—JKb (fine to medium sandstones, conglomeratic base); and the Pirambóia Formation—JKp (very fine to medium sandstones with intercalated siltite and argillite).

## 3 Data Survey and Treatment

The main geotechnical properties of the soil units in the area were assessed using the Brazilian standards NBR 6508 (ABNT 1984a), NBR 7181 (ABNT 1984b), ME 258 (DNER 1994). The basic soil characterization included the determination of grain density, particles size distribution, and Mini-MCV compaction with MCT classification.

Using the terrain evaluation technique, we recognized two land systems in the Clarinho River watershed. In these

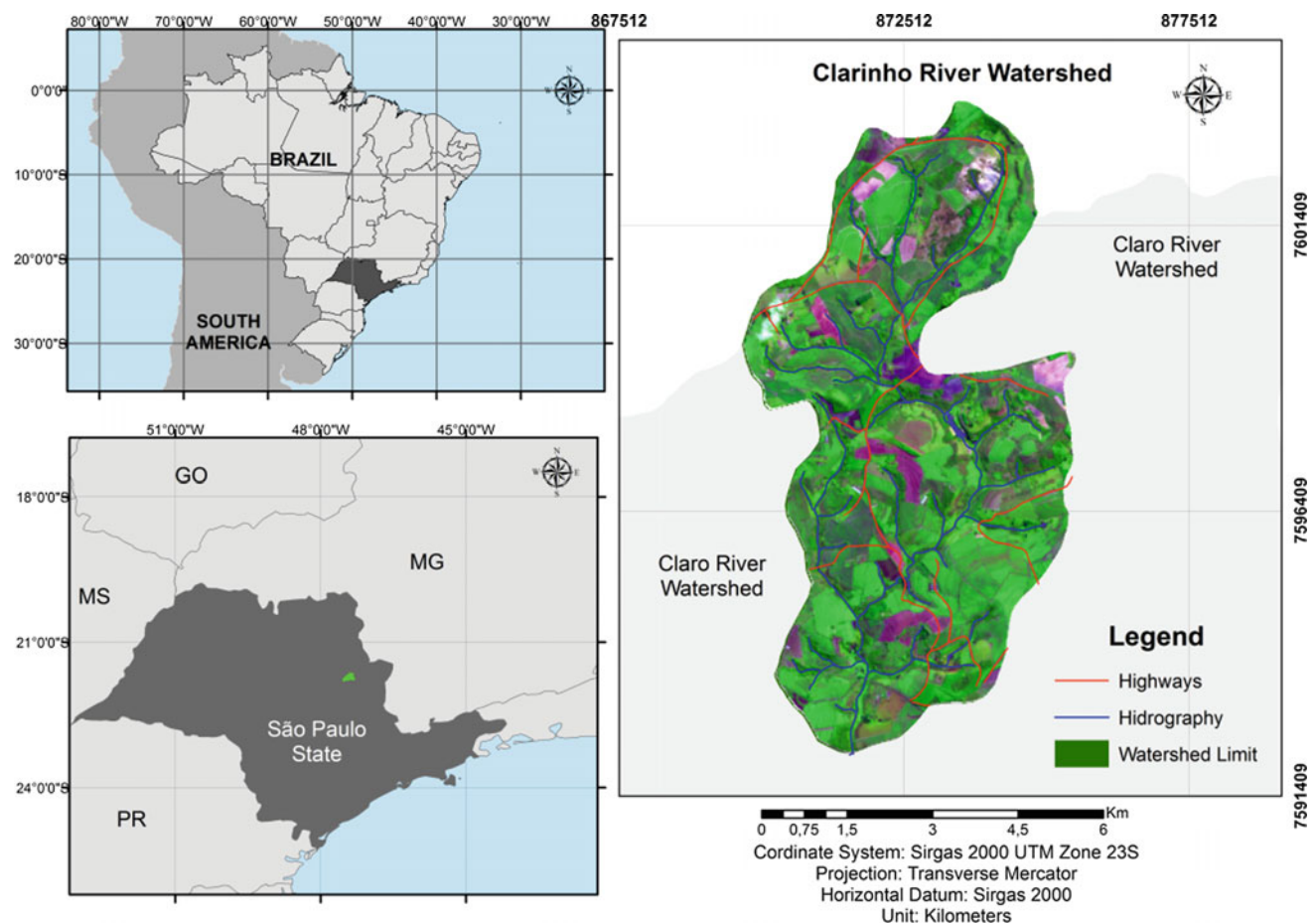
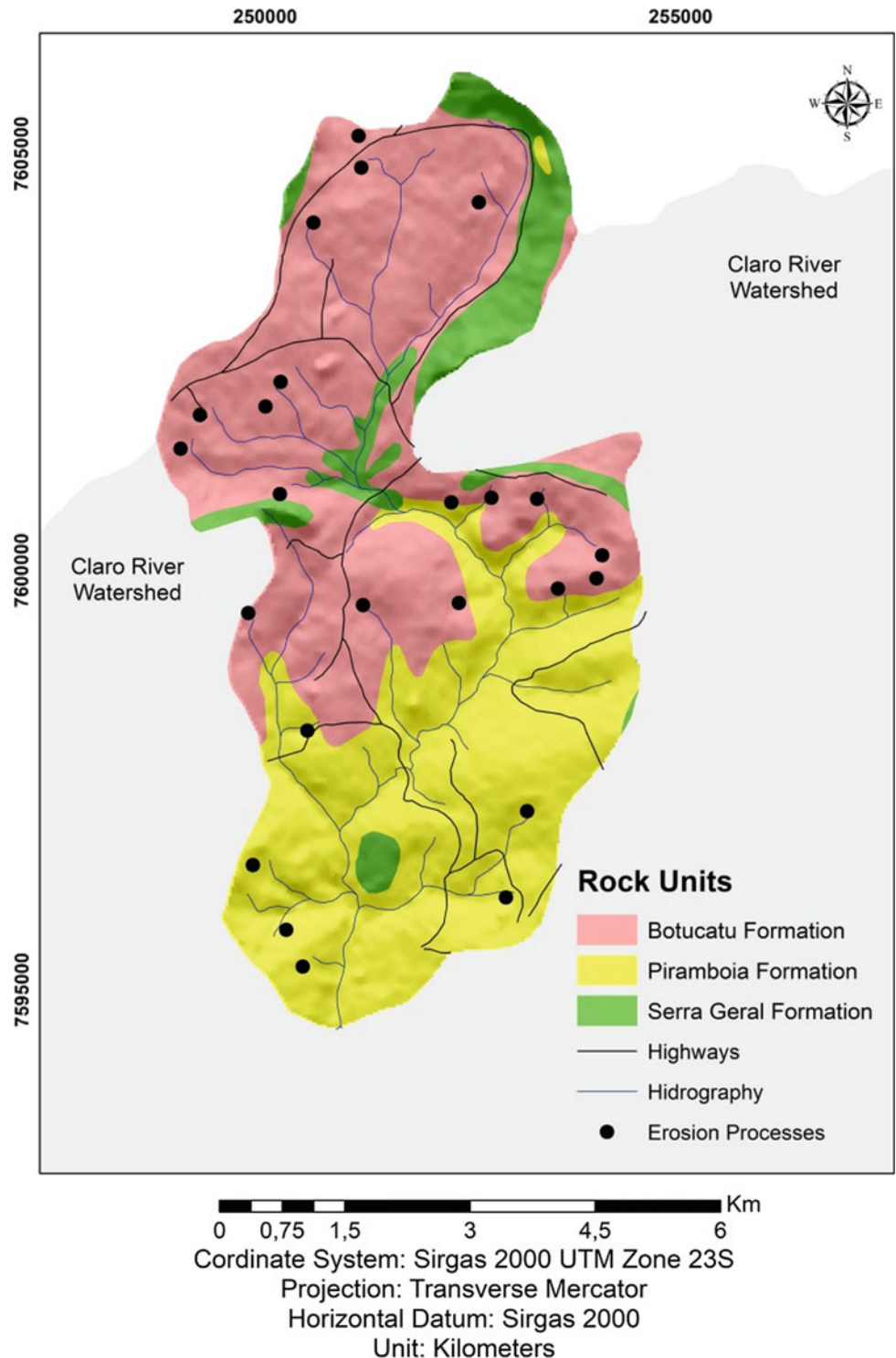


**Fig. 1** Clarinho River watershed location

**Fig. 2** Clarinho River watershed geological map



land systems, five land units were identified, i.e., two in System A and three in System B.

The land use/cover classification was performed with Landsat 5 and 8 images obtained on 03/06/1995 and 17/08/2005 (TM Sensor—Landsat 5) and 09/12/2015 (OLI Sensor—Landsat 8) via a supervised classification technique using the R5G4B3 (Landsat 5) and R6G5B4 (Landsat 8)

compositions and the following adopted classes: forest, pasture, exposed soil, and agriculture.

By using the land use/cover classification results for the years 1995, 2005 and 2015, the LCM module from Idrisi was used to determine the land changes and transitions between classes.

The map of erosion susceptibility was produced according to Lollo and Senna (2012), combining steepness, landforms, soils and land use/land cover. The weight values associated with the susceptibility to soil erosion were 1 for low susceptibility, 2 for intermediate susceptibility, and 3 for high susceptibility. The algebra map was executed in ArcGis® 10.2 (Esri 2011), and the weights are shown in Table 1.

## 4 Results and Discussion

Based on the field surveys, field sampling, and laboratory soil tests (results in Table 2), the soil unit map was produced. The land units identified in the area (described in Table 3) are represented in the land unit chart. The rock unit map, steepness chart, soil map, and land unit chart are shown in Fig. 3.

The map algebra developed according to the principles in Table 1 resulted in the soil erosion susceptibility chart presented in Fig. 4. The chart also presents the erosive processes recorded in the watershed (IPT 2012).

The results show that the natural environmental components resulting in a high susceptibility to soil erosion were sandy thick soil profiles associated with convex slopes, mainly in areas with high steepness values. Despite this, significant part (37.5%) of recorded erosion processes were not

related to an association with these natural conditions, suggesting that other factors (i.e., land use/land cover dynamics) had a relevant influence in the erosion occurring in the area.

The land use/cover classifications for the years 1995, 2005, and 2015 are presented in Fig. 5. The classification considers the land use/cover classes forest, pasture, exposed soil, and agriculture.

The main land changes in 1995–2005 were forest area reductions and increases in pasture class areas. These changes, associated with exposed soil persistence areas, indicate an increase in the soil erosion potential.

During 2005–2015, continuing reduction in forest areas and related pasture areas increases were observed. Pasture increases are also related to exposed soil reduction. Table 4 illustrated these land changes.

Results show that the most significant land changes for 1995–2005 and 2005–2015 were transitions from forest to pasture and, secondarily, transitions from agriculture to exposed soil. During 2005–2015, we also noted the transition of agriculture areas to pasture areas.

When the relationships between high erosion susceptibility areas according to Guerrero (2014), land changes, and erosion process records in the area were considered, it was verified that the expressive areas occupied by pasture and exposed soil coincided with areas with a high susceptibility to erosion and a high concentration of erosion process records.

**Table 1** Classes of attributes and weights for the erosion susceptibility algebra map

Component	Attribute class (weight)		
Steepness	<6% (1)	6–12% (2)	>12% (3)
Landform	Mound, valley (1)	Scarp, concave slope (2)	Convex slope (3)
Soils	Serra Geral (1)	Quaternary (2)	Botucatu, Pirambóia, Sta Rita (3)
Land use/cover	Forest (1)	Pasture, agriculture (2)	Exposed soil (3)

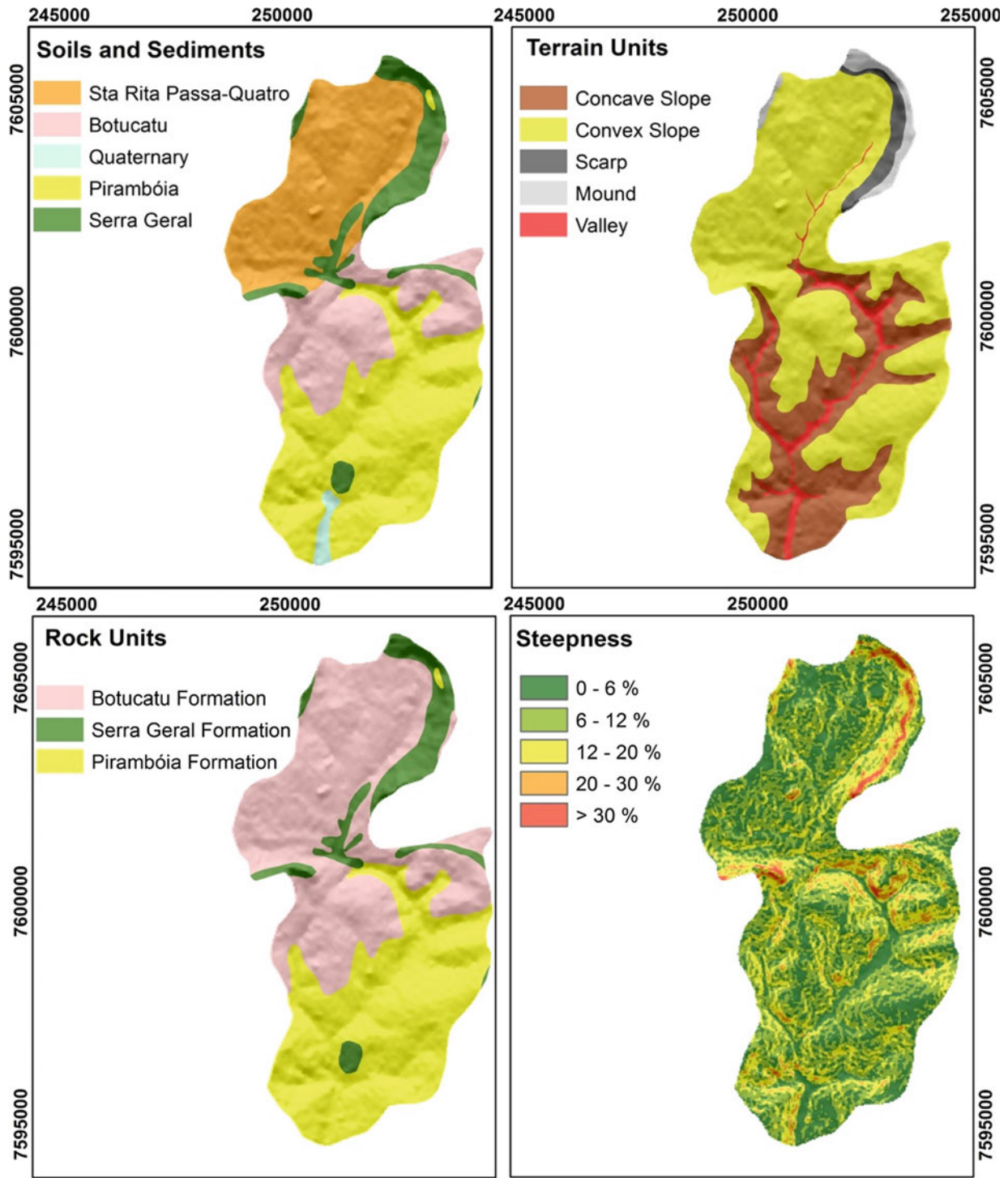
**Table 2** Soil unit geotechnical properties for the Clarinho River watershed

Unit	$Y_g$ (kN/m <sup>3</sup> )	Sand (%)	Silt (%)	Clay (%)	MCT class <sup>a</sup>
Quaternary	26.6	91	4	5	NA
Santa Rita	26.7	70	8	22	NA'
Serra Geral	27.4	23	12	65	LG'
Botucatu	26.5	75	9	16	LA
Pirambóia	26.8	68	11	21	NA'

<sup>a</sup>NA—non lateritic sand; LA—lateritic sand; LG'—lateritic clay; NA'—non lateritic clayey sand

**Table 3** Land units identified in the Clarinho River watershed

Unit	Landform description
A1	Mounds, steepness between 15–30%, very low to low drainage density
A2	Scarps, steepness <30%, high density of aligned drainage channels
B1	Convex slopes, medium drainage density, steepness <10%
B2	Concave slopes, low drainage density, steepness <10%
B3	Valleys, steepness <2%, alluvial deposits



**Cartographic Materials**

Coordinate System: Sirgas 2000 UTM Zone 23S  
 Projection: Transverse Mercator  
 Horizontal Datum: Sirgas 2000  
 Unit: Kilometers

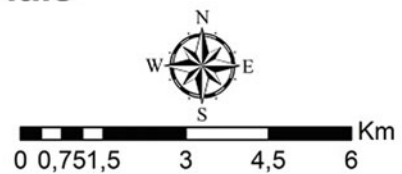


**Fig. 3** Basic maps on Clarinho River watershed

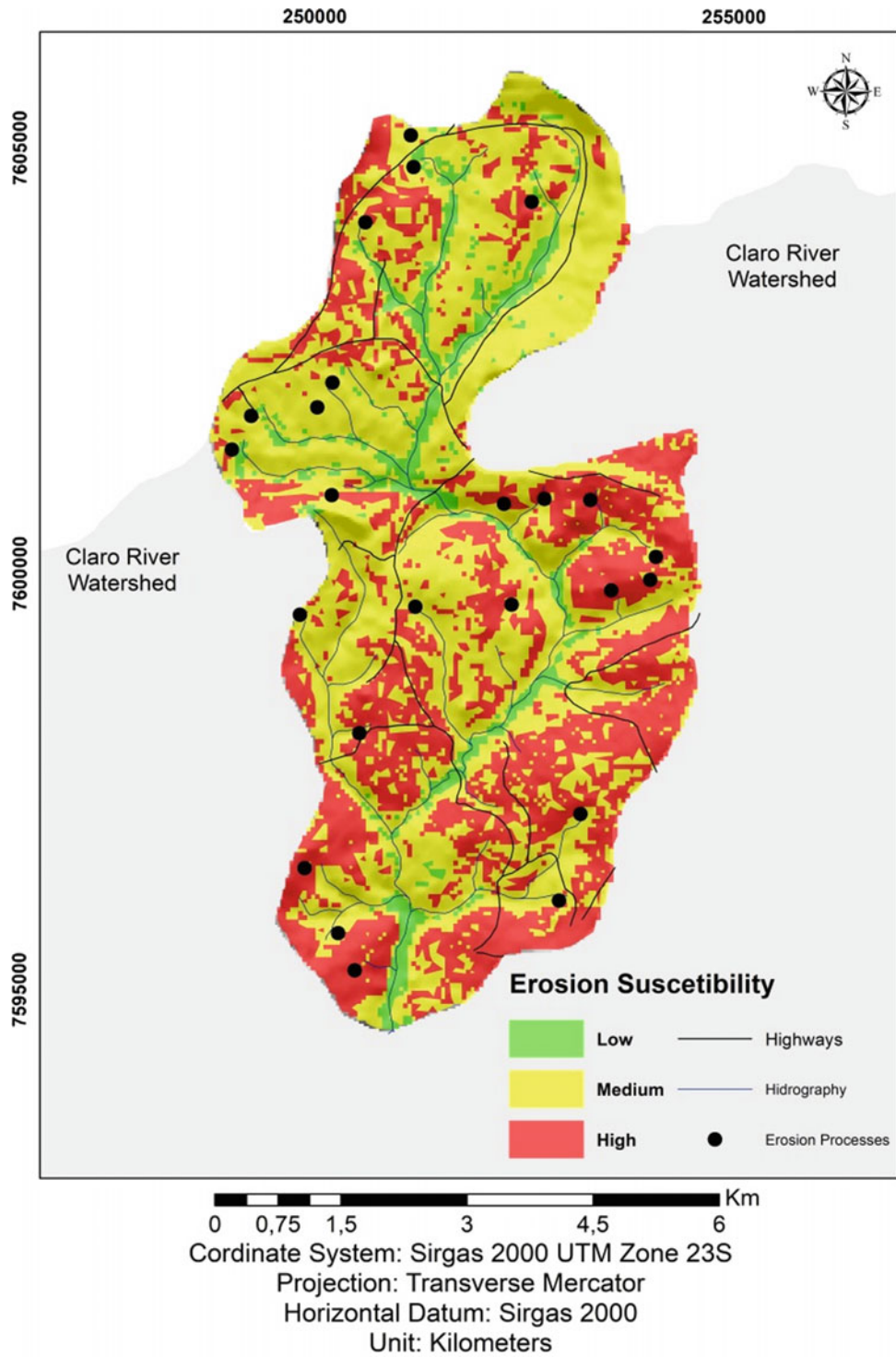


**Fig. 4** Clarinho River watershed soil erosion susceptibility chart

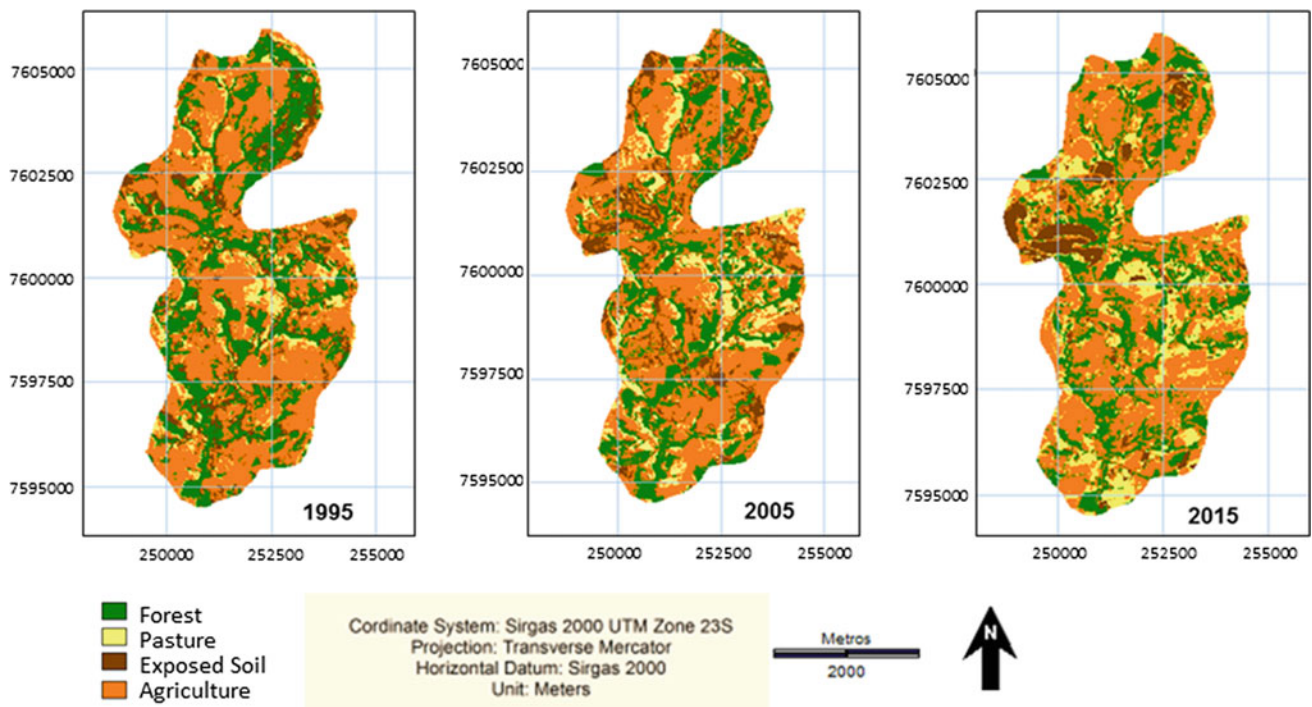


**Fig. 5** Land use/cover classifications of the Clarinho River watershed

**Table 4** Land use/cover classes in 1995, 2005, and 2015

Year/classes	Forest (km <sup>2</sup> )	Pasture (km <sup>2</sup> )	Exposed soil (km <sup>2</sup> )	Agriculture (km <sup>2</sup> )
1995	11.27	3.06	4.60	21.96
2005	10.13	4.36	4.74	21.66
2015	9.71	6.20	3.17	21.81

Regarding the areas that transitioned from forest to agriculture, such effects are less significant, probably due to soil management and conservation practices adopted for sugarcane cultivation in recent years, which have reduced the occurrence of erosive processes.

## 5 Conclusions

The Clarinho River watershed presents natural conditions, especially in terms of soils, that indicate a high susceptibility to erosion processes. However, erosion processes are especially likely to occur in areas where the land use/cover classes are exposed soil and pasture.

The use of the LCM allows us to determine that the major land changes over the past 20 years have been forest removal for agricultural activities and, to a lesser extent, pasture activities. The areas that were more subject to land changes shown several erosion process records, even when its erosion susceptibility were not high.

Thus, special attention should be given to such land changes, accompanied by soil conservation and management practices and other measures to avoid the development of new erosive processes. Forest areas, particularly environmental protection areas, need the proper policing of guidelines related to the restriction of land use, mainly pasture land use.

In agricultural areas, the policies for land use must require proper soil management techniques as a basic condition for cultivation and the expansion of grazing.


## References

- Bocco, G., Mendoza, M.E., Velázquez, A.: Remote sensing and GIS-based regional geomorphological mapping. *Geomorphology* **39**(1) (2001)
- Clark University, Idrisi Selva: Version 17. Worcester, Ma. (2012)
- Eastman, J.R.: Idrisi Selva: Tutorial Version 17. Clark University, Worcester, Ma (2012)
- ESRI: ArcGis 10.2. Environmental Systems Research Institute. Redlands, Ca. (2011)

- Guerrero, J.V.R.: Geo-environmental zoning for Clarinho River Watershed using terrain evaluation, at 1:50.000 Scale. UFSCar, São Carlos. (2014)
- Gupta, A., Ahmad, R.: Urban steeplands in tropics: an environment of accelerated erosion. *Geo. J.* **49**, 143–150 (1996)
- He, X., Zhou, J., Zhang, X., Tang, K.: Soil erosion response to climatic change and human activity during the quaternary of the Loess Plateau. *China. Reg. Environ. Change* **6**, 62–70 (2006)
- Huong, H.T.L., Pathirana, A.: Urbanization and climate change impacts on future urban flooding in Can Tho city, Vietnam. *Hydrol. Earth Syst. Sci.* **17**(1), 379–394 (2013)
- IPT. Registration of erosion and flood points in the State of São Paulo. São Paulo (2012)
- Lollo, J.A., Senna, J.N.: Establishing susceptibility for soil erosion—distinct techniques for distinct decision support phases. In: *Environment Congress Annals*, pp. 178–186. AUGM, Buenos Aires (2012)
- Lorandi, R., Lollo, J.A.: Geo-environmental analytics cartography Claro River Watershed. UFSCar/FAPESP, São Carlos (2015)
- Mendonça, F., Danni-Oliveira, I.M.: *Climatology: basis and climates of Brazil*. Oficina de Texto, São Paulo (2007)
- Oñate-Valdivieso, F., Sendra, J.B.: Application of GIS and remote sensing techniques in generation of land use scenarios for hydrological modeling. *J. Hydrol.* **23**, 256–263 (2010)
- Pimentel, D.: Soil erosion: a food and environmental threat. *Environ. Dev. Sustain.* **8**, 119–137 (2006)
- Pirolí, E.L., Ishikawa, D.T.K., Demarchi, J.C.: Land change analysis in Furnas Stream Watershed, Ourinhos—SP, between 1972 and 2007, and environmental protection areas impacts. In: *Remote Sensing Brazilian Symposium Annals*, pp. 6333–6340. SBSR, Curitiba (2011)
- Pirolí, E.L., Perusi, M.C., Zanata, J.M.: Land changes and soil impacts in Da Veada Stream, Ourinhos—SP. *Revista Geonorte* **1**(4), 855–865 (2012)
- São Paulo. Geological Institute. Geological Map: Santa Rita do Passa-Quatro (SF-23-V-C-V-1). São Paulo (1981)
- São Paulo-FFLCH/USP-IPT-FAPESP. São Paulo State Geomorphological Map. São Paulo (1997)
- Silva, A.M., Alves, C.A., Watanabe, C.H.: Natural potential for erosion in Brazilian territory. *Soil Eros. Stud.* **11**(1), 1–22 (2011)



# Flooding Susceptibility Identification Using the HAND Algorithm Tool Supported by Land Use/Land Cover Data

José Augusto de Lollo , Alice N. Marteli, and Reinaldo Lorandi

## Abstract

In Brazilian urban areas, the increases in human activities and extreme climatic event frequencies have resulted in an increase in floods and flooding. Despite Brazilian laws, risk analyses and management are still rare in Brazilian towns due to poor financial and human resources. Hydrological dynamic surveying coupled with land use information can result in quick and low-cost predictions of flood risks, allowing for the identification of critical areas and the design of intervention proposals. In this paper, this methodology is applied to the Caçula stream watershed using the HAND algorithm combined with land use/cover surveys to identify flood and flooding susceptibility. Imagery classification was developed in IDRISI Selva using OLI sensor bands from the Landsat 8 mission with a supervised classification. The HAND calculations resulted in a DEM for the surface flow analysis, including flooding, based on a normalized 3D model. The adopted method provides an understanding of surface process dynamics and the delineation of critical areas and their hierarchy. The results indicate a strong relationship between flooding susceptibility and land changes in the Caçula watershed.

## Keywords

Natural hazards • Urban planning • Watershed

## 1 Introduction

Areas close to rivers are conducive for human settlement, motivating their habitation. Due to human activities, the hydrological cycle has altered, which has increased runoff

J. A. de Lollo (✉) · A. N. Marteli  
São Paulo State University (UNESP), Ilha Solteira, Brazil  
e-mail: lolloja@dec.feis.unesp.br

R. Lorandi  
São Carlos University (UFSCar), São Carlos, Brazil

and reduced water infiltration and groundwater recharge (Tucci and Orsini 2005).

Floods and flooding expose the fragility of the manmade hydrological system, where small local changes can lead to big changes (Montenegro and Tucci 2005). Several Brazilian cities have experienced a large increase in the number of events, which has resulted in material losses and, above all, human death (Carvalho et al. 2007). According to the National Risk and Disaster Management Center, in Brazil in 2012, 376 natural disasters were recorded, involving 3781 municipalities. In the same year, floods and flooding affected 5,492,618 people (CENAD 2013).

Current challenges for cities related to floods, flooding, erosions and landslides during heavy rainfall periods are mainly consequences of past decisions without proper planning (Silva et al. 2014).

Thus, studies that consider the identification and spatial analysis of geodynamic processes related to land changes have increased by organizations that perform urban planning and environmental management in watersheds and municipalities. Considering this context and the lack of relevant information in small Brazilian municipalities, we verified the response of floods and flooding potential to natural conditions and their relationship with human activities in the area.

## 2 Study Area

Ilha Solteira is located in the extreme northwest of São Paulo (Fig. 1) on the border of Mato Grosso do Sul between meridians 51°00' and 51°30'W and parallels 20°15' and 20°45'S, with an area of 652.45 km<sup>2</sup> (IBGE 2014).

The local terrain is comprised of rounded/slightly rounded hill that are medium to large in size, with gradual slopes and wide valleys. Fine sandy soils are prevalent, and the regional climate is tropical, with rainy summers and dry and mild winters. The original semi-deciduous forest vegetation has been almost completely eliminated by human activities.

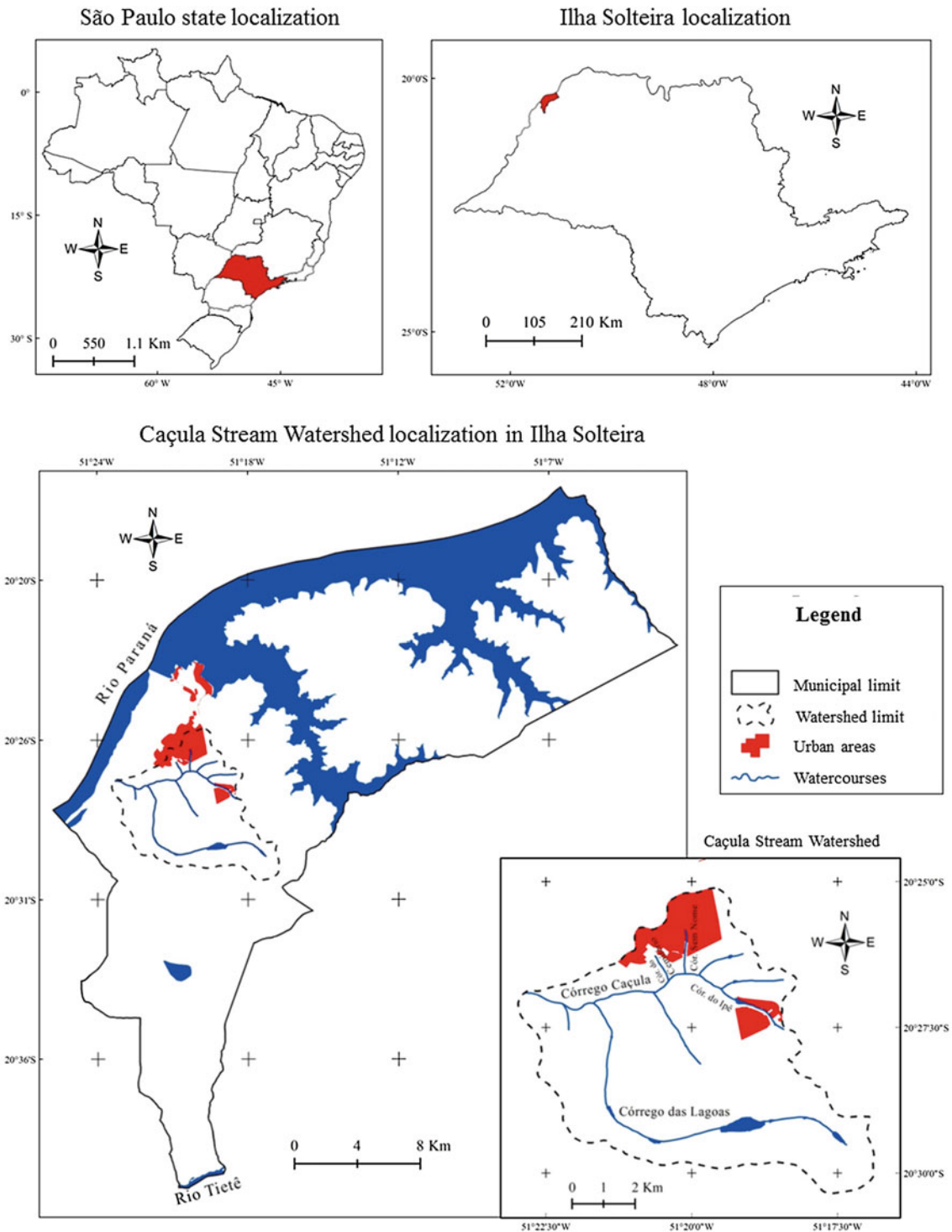


**Fig. 1** Caçula stream watershed localization

Even as a planned city, Ilha Solteira exhibits reoccurring floods and flooding events, most of which occur in the Caçula watershed (Marteli 2015). During intense precipitation events, there are serious impacts on many buildings and the urban infrastructure, and the reactivation of former erosive processes also occurs.

### 3 Data Survey

Data and information surveys were conducted using land use/cover classifications and application of the HAND (Height Above the Nearest Drainage) module. The land

use/cover classification was developed in IDRISI Selva (Eastman E2012) using Landsat 8 imagery, which is available on the USGS website (USGS 2015).

HAND is an algorithm developed by INPE (National Institute for Space Research) (INPE 2013). According to Rennó et al. (2008), it calculates the altitude of each point related to the following drainage outlet using SRTM (Shuttle Radar Topographic Mission) data.

HAND results in a DEM (digital elevation model), which facilitates a hydrological analysis from the normalized topographic data (Nobre et al. 2011) and provides predictions of water levels in soil profiles (Rodrigues et al. 2013). The sequence of procedures used for the HAND calculation and analysis in this paper are summarized in Fig. 2.

For HAND processing, SRTM elevation data with a 1 arc-second (~ 30 m) horizontal resolution were used, with a latitude/longitude projection and datum of WGS84 (USGS 2015). From the SRTM elevation data, a DEM was created using TerraView Hydro software (<http://www.dpi.inpe.br/terraview>).

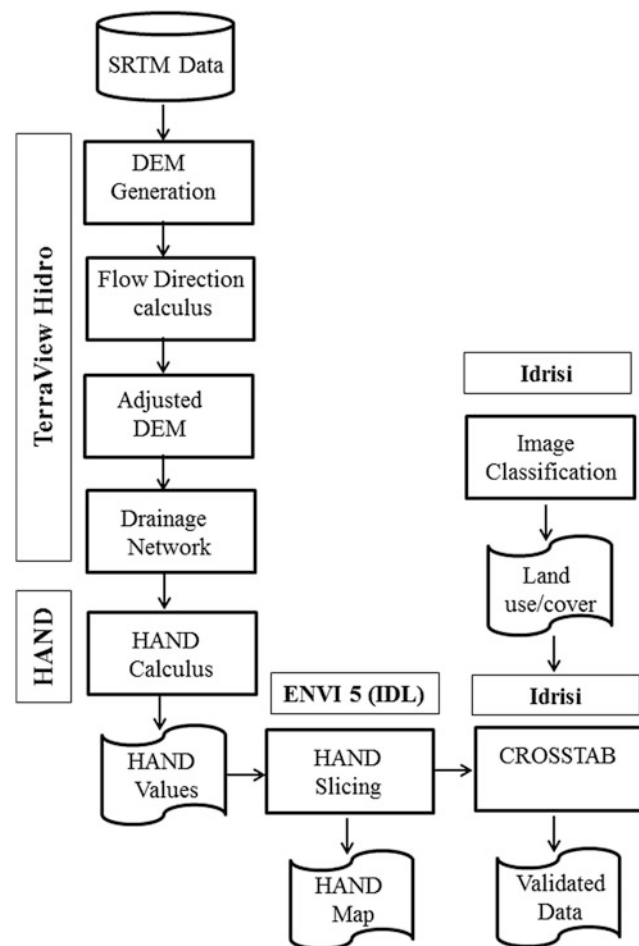


Fig. 2 Procedures used for the HAND calculation and the interpretation of results

From this DEM, TerraView allows us to calculate the flow direction for each point on the grid. The flow direction was defined as the maximum steepness value among eight neighboring points.

Because the flow direction grid can present sinks (i.e., discontinuities), the next step is to provide grid adjustments in order to fill these depressions and summits. From the adjusted grid for flow direction, it is possible to obtain flow accumulation grid values, which provide a drainage network based on the local base level.

After these tests, we observe that a HAND threshold of 2300 calculation interactions provides a better agreement between the HAND drainage network and the local drainage network depicted in the official maps. Therefore, we used this threshold to obtain the drainage network.

From this set of data, HAND calculates the values of relative elevation by considering flow directions and drainage network connections, which results in HAND values.

Therefore, the elevation values are good indicators of flooding susceptibility at each point (Nobre et al. 2011), which can be used to select scenarios for territorial planning in areas prone to flooding (Rodrigues, G.O., Nobre, A.D., Silveira, A.C., Cuartas, L.A.: Effects of SRTM data spatial resolution in terrain description in HAND (height above the nearest drainage)—case study in Manaus/AM. In: Remote sensing brazilian symposium on electronic annals, pp. 5568–5575, INPE, Foz do Iguacu 2013).

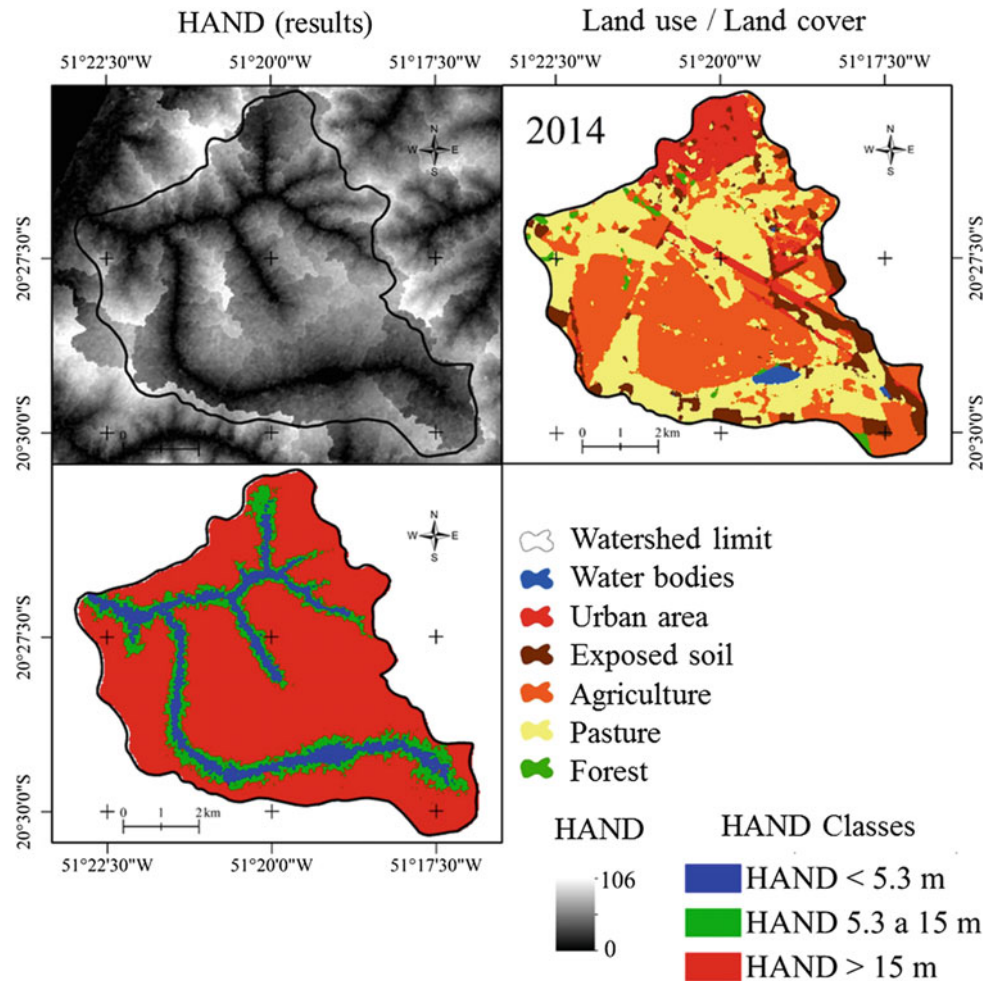
The resulting HAND grid image was so processed with ENVI 5 in IDL (the Interactive Data Language, which is the original language of HAND), where class slicing was performed, and three classes of flooding potential were obtained.

For land use/cover classification, we used the R5G4B3 composition from OLI sensor bands (Landsat 8). Land use was obtained using a supervised classification, which uses typical spectral signature training samples for each land use/cover class. After training, classification was conducted using a maximum likelihood algorithm. Map calculations between HAND and the land use/cover classes were operated in Idrisi Selva.

After the map calculations, we applied a non-parametric test (chi-square) using two independent samples (i.e., groups of pixels) to assess the relationship between land use/cover and HAND classes. This was implemented to test independence, which was calculated from the sum of observed and expected frequencies, according to Eq. (1). Independence was applied at 200 randomly selected points using the standardized CROSSTAB grid.

$$\sum_i \binom{l}{1} \sum_j \binom{c}{1} \frac{(FAObs_{ij} - FAEsp_{ij})^2}{FAEsp_{ij}} \sim \chi^2 \quad (1)$$

**Fig. 3** HAND and land use/land cover classes in the Caçula watershed



#### 4 Results and Discussion

Spatial land use/cover classes in the Caçula watershed and the HAND results are presented in Fig. 3. Low HAND value areas (near zero) represent shallow groundwater levels, with soil profiles that are nearly saturated. Areas with high HAND values are related to deep groundwater levels in well-drained soils (Rennó et al. 2008; Pires and Borma 2013).

In the northern portion of the basin, excessive water-proofing due to urban use was observed. In this area, HAND values were lower than 5.3 m for 3.2% of the urban area. According to Rennó et al. (2008), these results indicate areas with a very low groundwater level. The results also show that 14.8% of the urban area has HAND values varying from 5.3 to 15 m, and 82% of areas have HAND values higher than 15 m.

Using the grid of 200 sample points and the results from Fig. 2, we obtain the class frequencies used for the independence test calculation. From the independence test, the

null hypothesis was rejected with 5% significance (i.e., classes are more favorable to occur in areas where HAND values are higher than 15 m).

This preference (classes occurring in areas where HAND values are higher than 15 m) is expected because it occurs in a much larger area in relation to other classes. Despite this observation, sample frequencies increased when the susceptibility to flooding decreased, which is a result of an increase in HAND value.

The urban area data do not show high HAND potential values (classes less than 5.3 m) once these areas exhibit fewer dimensions than other HAND classes areas. However, for the analysis of data observed in the urban area, sampling points with the potential for flooding and overflow occur (HAND < 5.3 m). This was due to the small size of the area in relation to other areas. However, this area presents high susceptibility due to its urban use.

From the land use/cover and HAND class calculations, we obtain flooding susceptibility according the following classes: Class A—very low floods and flooding potential; Class B—low floods and flooding potential; and Class

**Table 1** HAND classes versus land use/land cover classes in the study area

Land use/land cover	HAND classes		
	<5.3	5.3–15	>15
Water	C	C	B
Urban	C	C	B
Exposed soil	B	A	A
Agriculture	A	A	A
Pasture	C	B	A
Forest	A	A	A

C—high floods and flooding potential. HAND classes were associated with land use/cover classes according to Table 1, which resulted in the potential for floods and flooding in the Caçula stream watershed.

The main contribution of the HAND results was the floods and flooding analysis, where HAND values indicated that only the surface geometry controls surface water flow,

and surface roughness was disregarded due to its irregularity and runoff/infiltration balance caused by surface recovery from land use/cover.

We can observe that land use/cover can heighten flooding processes. In natural vegetation and agricultural areas, the application of proper management techniques reduces this potential because they result in well drained areas. In urban areas with low HAND values, the flooding potential increases depending on the low permeability of the surface and the decrease in surface roughness.

Potential for floods and flooding results are presented in Fig. 4. In this figure, we also present the places with long historical records of floods and flooding over the past twenty years in the Caçula watershed.

We can observe that most of these records are related to areas that are classified as “high potential for floods and flooding” in the watershed. The only two records that do not belong to this class are local, which have serious problems in the urban drainage system due to improper engineering.

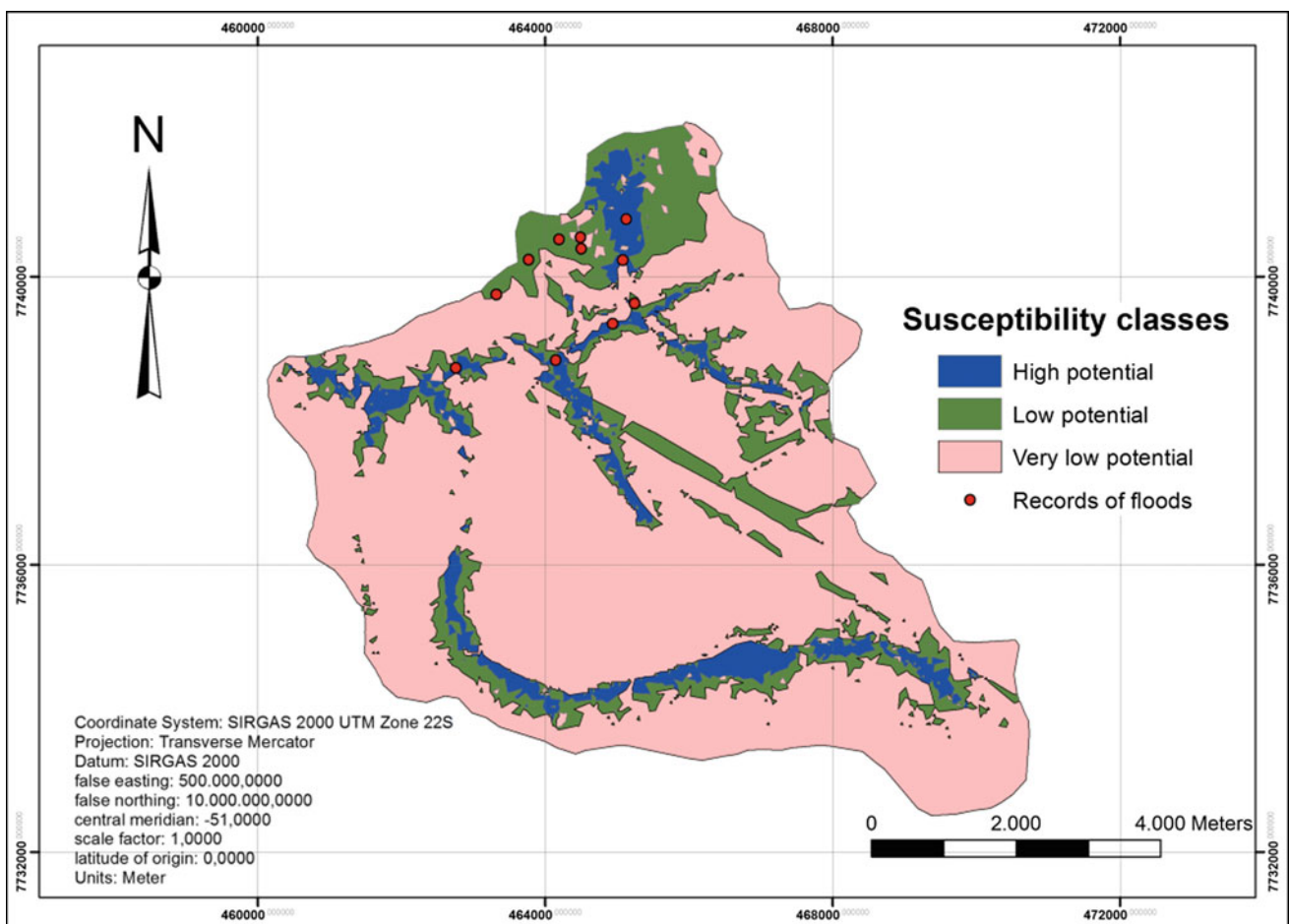


**Fig. 4** Susceptibility chart based on flood and flooding classes

## 5 Conclusions

Low HAND values obtained in the study area coincide with depressed terrain areas in the Caçula stream watershed, indicating that the usage of SRTM data in the HAND algorithm results in an effective characterization of natural conditions in the area and its potential use in studies for physical environment mitigation.

Despite these results, HAND values alone were not sufficient to diagnose potentials for floods and flooding because they do not consider variations in roughness and infiltration conditions. The land use/cover classification provides an additional set of data for floods and flooding potential identification. The existence of persistent floods and flooding records shows that the association of land use/cover data with HAND results allows for the improved and precise analysis of flooding potential areas in the Caçula watershed.

Urban areas where flood records did not coincide with the high potential for floods and flooding require special attention in the review of drainage networks.

The chi-square test proved (with 98% confidence) that the dependence between land use/cover and flooding potential in this area was confirmed by historical flood and flooding records in the area. All the evidence shows that urban expansion was the main trigger for floods and flooding, indicating the need for the protection and recovery of natural vegetation areas.

## References

- Carvalho, C.S., Macedo, E.S., Ogura, A.T. Mapping risks in slopes and river margins. [http://www.cidades.gov.br/images/stories/Arquivos/SNPU/Biblioteca/PrevencaoErradicacao/Livro\\_Mapeamento\\_Enconstas\\_Margens.pdf](http://www.cidades.gov.br/images/stories/Arquivos/SNPU/Biblioteca/PrevencaoErradicacao/Livro_Mapeamento_Enconstas_Margens.pdf). Last accessed 22 Apr 2014
- CENAD—National Centre for Disasters and Risk Management. [http://www.integracao.gov.br/c/document\\_library/get\\_file?uuid=f22cccd-281a-4b72-84b3654002cff1e6&groupId=185960](http://www.integracao.gov.br/c/document_library/get_file?uuid=f22cccd-281a-4b72-84b3654002cff1e6&groupId=185960). Last accessed 28 Aug 2014
- Eastman, J.R.: Idrisi Selva: manual version 17. Clark University, Worcester, MA (2012)
- IBGE—Brazilian Institute of Geography and Statistics. <http://www.cidades.ibge.gov.br/xtras/perfil.php?lang=&codmun=352044>. Last accessed 13 Apr 2013
- INPE—National Institute for Spatial Research. <http://www.dpi.inpe.br/menu/Projetos/terrahidro.php>. Last accessed 01 Apr 2013
- Marteli, A.N.: Geodynamic processes related to land use change: Caçula watershed (Ilha Solteira—SP). UNESP, Ilha Solteira (2015)
- Montenegro, M.H., Tucci, C.E.M.: Environmental sanitation and pluvial water. In: Brasil. Territory management and integrate management of urban water. Cities Ministry, Brasília (2005)
- Nobre, A.D., Cuartas, L.A., Hodnett, M., Rennó, C.D., Rodrigues, G., Silveira, A., Waterloo, A.M., Saleska, S.: Height above the nearest drainage—a hydrologically relevant new terrain model. *J. Hydrol.* **404**(1–2), 13–29 (2011)
- Pires, E.G., Borma, L.S.: Using HAND model in watershed mapping in Cerrado environment. In: Remote sensing brazilian symposium, pp. 5568–5575, INPE, Foz do Iguaçu (2013)
- Rennó, C.D., Nobre, A.D., Cuartas, L., Soares, J., Hodnett, M., Tomasella, J., Waterloo, M.: Hand, a new terrain descriptor using SRTMDEM: mapping terra-me rainforest environments in Amazonia. *Remote Sens. Environ.* **112**(9), 339–358 (2008)
- Rodrigues, G.O., Nobre, A.D., Silveira, A.C., Cuartas, L.A.: Effects of SRTM data spatial resolution in terrain description in HAND (height above the nearest drainage)—case study in Manaus/AM. In: Remote sensing brazilian symposium on electronic annals, pp. 5568–5575, INPE, Foz do Iguaçu (2013)
- Silva; B.R., Pinheiro, H., Lopes, D.D.: Environmental indicators selection for drainage urban system evaluation. In: Benini, S.M., Bruna, G.C. (ed.) Routes for urban sustainability. ANAP, Tupã (2014)
- Tucci, C.E.M., Orsini, L.F.: Urban waters in Brazil: actual scenario and sustainable development. In: Brasil. Environmental Sanitation National Secretary. Cities Ministry, Brasília (2005)
- USGS—United States Geological Survey. <http://earthexplorer.usgs.gov/>. Last accessed 03 Mar 2015

# Soil Mixing for Remediation of Contaminated Sites

Charles M. Wilk

## Abstract

Soil mixing involves mixing an additive into soil to change the physical or chemical properties of a soil. This geotechnical method is called solidification/stabilization (S/S) treatment when applied for remediation of contaminated soil or sediment. S/S is an established technology for contaminated site remediation. The effectiveness of S/S treatment for a broad variety of soil contaminants is demonstrated by the technology's high selection rate for remedies at U.S. Superfund sites. According to U.S. Environmental Protection Agency's 2017 report on Superfund remedies, S/S has been selected for 21% of in situ treatment source control remedies. Most Superfund projects involve contaminated soil. S/S is of increasing interest in in-place or in situ treatment of contaminated soil such as those found at former industrial properties. In situ S/S can prepare "brownfield" sites for redevelopment. S/S treatment protects human health and the environment by immobilizing hazardous constituents within the treated material. Successful treatment is accomplished through physical changes to the soil and often, chemical changes to the hazardous constituents themselves. S/S binding agents are mixed into contaminated soil through a variety of construction techniques including shallow and deep soil mixing. An appreciation of the versatility for the treatment technology can be gained by review of example projects. This paper discusses the principles and application of S/S treatment technology for soil and sediment.

## Keywords

Soil mixing • Solidification/stabilization • Remediation • In situ treatment

## 1 Soil Mixing for Remediation of Contaminated Soil

### 1.1 Soil Mixing as Solidification/Stabilization Treatment

Soil mixing involves mixing an additive into soil to change the physical or chemical properties of a soil. This geotechnical method is often used in soil engineering to improve the bearing capacity and stability or to reduce the hydraulic conductivity of a soil. In environmental engineering, the same soil mixing methods are used to remediate contaminated soil. Use of soil mixing methods to address contaminated soil is termed solidification/stabilization (S/S) treatment.

Solidification/Stabilization (S/S) is a widely used treatment for the management/disposal of a broad range of contaminated media and wastes; particularly those contaminated with substances classified as hazardous in the United States. The treatment involves mixing a binding agent into the contaminated media (e.g. soil, sediment) or waste. Binding agents most commonly used include portland cement and slag cement. Other agents used include cement kiln dust (CKD), fly ash, bentonite clay, activated carbon, phosphate mixtures, and a variety of proprietary agents.

The treatment protects human health and the environment by immobilizing hazardous constituents within the treated material. Immobilization within the treated material prevents migration of the hazardous constituents to human, animal and plant receptors. S/S treatment can be performed on contaminated soil that remains in-place- in situ or on material that has been excavated- ex situ.

The terms *solidification* and *stabilization* sound similar, but they describe different effects that the binding agents create to immobilize hazardous constituents. Solidification refers to changes in the physical properties of a waste. The desired changes usually include an increase of the compressive strength, a decrease of permeability, and

C. M. Wilk (✉)  
SolidStable Remediation Consulting Inc,  
Arlington Heights, IL, USA  
e-mail: solidstable@gmail.com

encapsulation of hazardous constituents. Stabilization refers to chemical changes of the hazardous constituents in a waste. The desired changes include converting the constituents into a less soluble, mobile, or toxic form.

## 1.2 The Case for S/S Treatment of Contaminated Soil

**Established Treatment Technology.** S/S treatment has been used to treat radioactive wastes since the 1950s and hazardous waste since the 1970s (Conner 1990). S/S continues as a cornerstone treatment technology for the management of radioactive waste, hazardous waste, contaminated site remediation and Brownfield redevelopment.

The U.S. Environmental Protection Agency (EPA) considers S/S an established treatment technology. S/S is a key treatment technology for the management of industrial hazardous wastes. These wastes are regulated in the United States under the Resource Conservation and Recovery Act (RCRA). RCRA hazardous wastes are grouped into two classes: RCRA-listed and RCRA-characteristic. RCRA-listed hazardous wastes are wastes produced by industry that are generally known by the EPA to be hazardous. These wastes are “listed” in RCRA regulations and must be treated, stored, and disposed according to RCRA hazardous waste management regulations. RCRA-listed wastes destined for land disposal are required to be treated to reduce hazards posed by the wastes after land disposal. EPA has identified S/S as Best Demonstrated Available Technology (BDAT) for 57 RCRA-listed hazardous wastes

(United States Environmental Protection Agency 1993). RCRA-characteristic wastes are less routinely produced wastes that are found to be hazardous due to a characteristic of the waste. For RCRA-characteristic wastes, S/S can often be used to eliminate the hazardous characteristic. With the hazardous characteristic addressed the treated waste can be disposed at a lower cost or re-used.

S/S treatment is used to treat contaminated media during remediation of contaminated properties. There are many federal and state programs that require or influence voluntary remediation of contaminated property. The best-known and best-documented remediation program in the United States is conducted under the Comprehensive Environmental Response, Compensation, and Liability Act (CERCLA). This remediation program is commonly called the “Superfund” program.

**High Frequency of S/S Treatment Selection for Remediation.** S/S is the second most frequently selected technology for treating the source of environmental contamination at Superfund program remedies. From 1982 to 2014, S/S has been selected for seventeen percent (17%) of Superfund ex situ source treatment remedies (290 of 1705 ex situ remedies). During this same period, S/S has been selected for twenty-one percent (21%) of Superfund in situ source treatment remedies (170 of 806 in situ remedies) (United States Environmental Protection Agency 2017).

**Contaminated Soil Frequently Found at Superfund Sites.** Since the beginning of the Superfund program in 1980, contaminated soil has been the most frequently encountered contaminated media at Superfund sites. Table 1 indicates that eighty-one percent (81%) of Superfund remedies involved contaminated soil.

**Table 1** Media Addressed at Superfund Sites with Remedies FY 1982–2014. *Source* EPA-542-R-17-001 (United States Environmental Protection Agency 2017)

Media	Number of Sites	Percentage of Sites
<b>Source Media</b>	<b>1,293</b>	<b>89%</b>
Soil	1,175	81%
Sediment	435	30%
Solid waste	427	30%
Debris	218	15%
Buildings and structures	159	11%
Sludge	144	10%
Leachate	126	9%
Liquid waste	115	8%
<b>Groundwater</b>	<b>1,218</b>	<b>84%</b>

- Total number of sites with remedies: 1,447.
- Table 2 does not include NAPL, or soil gas and air media addressed by vapor intrusion technologies.



**Effective Treatment on Contaminants in Soil.** There is a great variety of contaminants of concern (COCs) found in soil at Superfund sites. Figure 1 indicates the proportion of different general classes of chemical contaminants found in Superfund site soil.

As shown on the Table 2, S/S treatment has been used to treat all general chemical classes of contaminants typically found at Superfund sites.

**Versatility of S/S Treatment.** The ability to effectively treat a wide variety of contaminants within the same media is a key reason why S/S is so frequently used in remediation. Adding to the versatility of S/S treatment is the fact that contaminated material can be treated in situ or ex situ as previously segregated waste or excavated material. S/S treatment contractors have devised a variety of methods to accomplish the mixing, as demonstrated in the example projects described further below.

**Brownfields.** A more recent development in U.S. remediation programs is the advent of “brownfield” initiatives. Brownfield sites are typically previously used industrial or urban properties that have not been re-used because of environmental contamination and the liabilities that attach to the properties because of the contamination. Recent initiatives in U.S. liability law and funding encourage the remediation and re-use of brownfield sites. S/S is increasingly being used to address contaminated brownfield sites. Developers quickly realized that S/S treatment not only addresses contamination, but can improve the physical properties of soil for subsequent building.

Examples of S/S use at brownfields include remediation of former Manufactured Gas Plant (MGP) sites. EPA estimates there are 5000 former MGP sites in the U.S (United

States Environmental Protection Agency 1999). MGPs produced “town gas”. This flammable gas was used for lighting and cooking before being replaced by natural gas distribution systems. Originally built on the outskirts of a town, most former MGP sites are now located within urban areas due to sprawl and are often prime “brownfield” properties. Town gas was produced by heating coal in the absence of air. Coal tar—comprised of polycyclic aromatic hydrocarbons (PAHs), petroleum hydrocarbons, benzene, cyanide, metals and phenols were residues of this process (United States Environmental Protection Agency 1999). Cement-based In Situ Solidification/Stabilization (ISS) is now a common technology used to address coal tar contaminated soil remaining on former MGP sites (The Interstate Technology and Regulatory Council Solidification/Stabilization Team 2011).

**Re-use of Dredged Material as Engineered Fill by Ex Situ S/S.** Ex situ S/S treatment can be used to create an “engineered fill” from impacted or otherwise unsuitable material. This is common practice in the New York/New Jersey harbor system where dredged sediment is treated with cement and re-used as engineered fill upon land (Loest and Wilk 1998).

### 1.3 Cements Are Common Additives for S/S Treatment and Soil Mixing

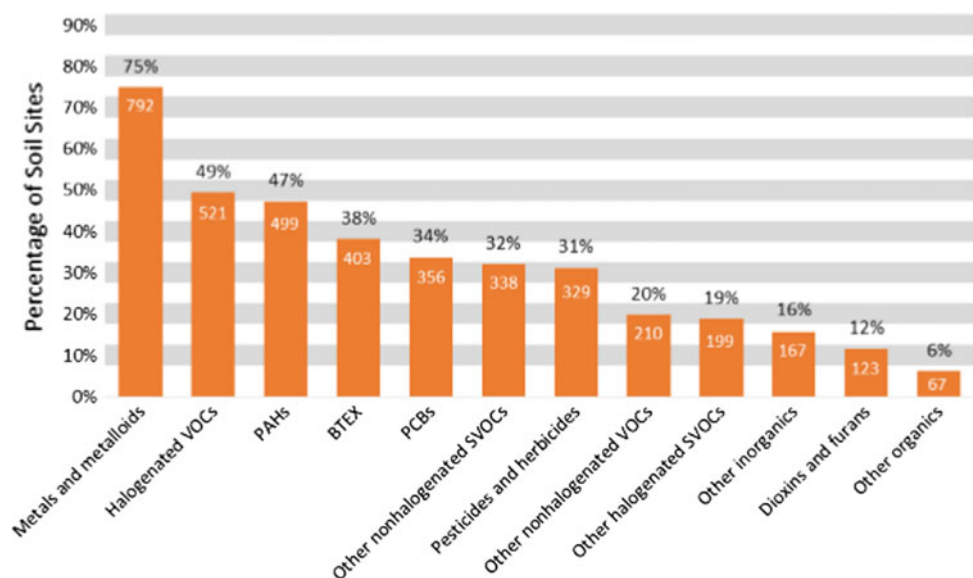
**Portland Cement.** Portland cement is a commonly available, generic material principally used in concrete for construction. This material is also a versatile S/S binding agent with the ability to both solidify and stabilize a wide variety

**Fig. 1** Detailed COCs in soil at superfund sites FY 1982–2014.

Source EPA-542-R-17-001

(United States Environmental Protection Agency 2017).

Abbreviations in this figure include VOCs for volatile organic compounds, PAHs for polycyclic aromatic hydrocarbons, BTEX for benzene, toluene, ethylbenzene and xylene, and SVOCs for semi-volatile organic compounds



- Number of soil sites with a COC and a remedy = 1,056.

**Table 2** Contaminants Treated by Superfund Source Treatment Projects FY 1982–2005. *Source* EPA-542-R-07-012 (United States Environmental Protection Agency 2007)

Technology	Total number of projects <sup>a</sup>	Polycyclic aromatic hydrocarbons (PAHs)	Other nonhalogenated semivolatile organic compounds <sup>b</sup>	Benzene-toluene-xylene (BTEX)	Other nonhalogenated organic compounds <sup>c</sup>	Organic pesticides and herbicides	Other halogenated volatile organic compounds <sup>d</sup>	Halogenated semivolatile organic compounds <sup>e</sup>	Polychlorinated biphenyls	Metals and metalloids
Bioremediation	113	37	51	33	33	24	17	22	2	5
Chemical Treatment	29	1	2	3	4	1	4	12	4	13
Multi-Phase Extraction	46	9	3	11	6	4	8	18	1	1
Electrical Separation	1	0	0	0	0	0	0	1	0	0
Flushing	17	3	5	5	5	1	3	11	0	5
Incineration	147	27	41	33	23	36	34	52	36	6
Mechanical Soil Aeration	7	0	0	3	1	0	1	7	0	0
Neutralization	15	2	0	0	0	0	0	0	0	6
Open Burn/ Open Detonation	4	0	1	0	0	0	0	0	0	0
Physical Separation	21	4	2	1	0	3	0	0	4	5
Phytoremediation	7	1	2	2	2	1	1	4	0	4
Soil Vapor Extraction	255	15	31	107	51	3	33	217	1	0
Soil Washing	6	1	1	0	0	2	0	0	1	2
Solidification/ Stabilization	217	17	18	13	13	16	7	20	35	180
Solvent Extraction	4	2	1	0	1	1	0	2	2	1
Thermal Desorption	71	21	17	24	15	8	12	33	16	0
In Situ Thermal Treatment	14	5	0	2	0	3	3	8	0	0
Vitrification	3	0	0	1	1	0	1	3	2	1
<b>Total Projects</b>	<b>977</b>	<b>145</b>	<b>175</b>	<b>238</b>	<b>155</b>	<b>103</b>	<b>124</b>	<b>410</b>	<b>104</b>	<b>229</b>

of wastes. Portland cement-based mix designs have been applied to a greater variety of wastes than any other S/S binding agent (Conner 1990). Cement is frequently selected for the agent's ability to (a) chemically bind free liquids, (b) reduce the permeability of the waste form, (c) encapsulate waste particles surrounding them with an impermeable coating, (d) chemically fix hazardous constituents by reducing their solubility, and (e) facilitate the reduction of the toxicity of some contaminants. This is accomplished by physical changes to the waste form and, often, chemical changes to the hazardous constituents themselves. Cement-based S/S has been used to treat wastes that have either or both inorganic and organic hazardous constituents. Mix designs often include byproducts or additives in addition to portland cement that may improve effectiveness in treatment of specific hazardous constituents.

**Slag Cement.** Slag cement is increasingly being used in soil mixing. Soil mixing mix designs often include slag cement. Slag cement is almost entirely comprised of the industrial byproduct from manufacture of steel known as ground granulated blast furnace slag (GGBFS). Reuse of GGBFS in soil mixing and S/S can contribute to the “sustainability” rating of a project (Wilk and Tiefenthaler 2017).

## 2 Example Soil Mixing and S/S Treatment Projects

### 2.1 Former Wood Treating Facility, Port Newark, New Jersey

Two types of mixing techniques (Fig. 2) were used to treat soils contaminated by wood preserving operations at a former wood treating facility in Port Newark, New Jersey (Delisio 2002).

Approximately 3.2 ha (8 acres) of soil at the site were contaminated with arsenic, chromium, and PAHs. In situ soil mixing was used to treat 17,000 m<sup>3</sup> (22,000 cu yd) of soil from 0.6 m (2 ft) to 3.7 m (12 ft). This treatment involved (1) pre-excavation of contaminated material, (2) placement of the stockpiled material back into the excavated area in lifts, and (3) portland cement-based S/S treatment of each lift with an excavator-mounted soil mixer. Performance standards set for the treatment of the soil included attaining a minimum of 0.17 MPa (25 psi) unconfined compressive strength (UCS). S/S-treated soils exceeded this requirement.

**Fig. 2** Left photo: excavator mounted soil mixer, Right photo: Pugmill mixing



20,000 m<sup>3</sup> (26,000 cu yd) of contaminated soil were treated ex situ using a pugmill to mix portland cement into contaminated soil. Contaminated soil mixed with the pugmill was placed on top of the in situ treated soils in a 0.6 m (2 ft) layer. This layer was carefully compacted to have the similar structural properties as that of soil-cement. This soil-cement-like layer achieved UCS of greater than 1.7 MPa (250 psi), providing an excellent base for pavement placed over the entire site. The mix design for both mixing techniques called for an addition rate of 8% portland cement by wet weight of the soil. Future use of the site is a paved shipping container storage area.

## 2.2 Former Manufactured Gas Plant Site, Augusta, Georgia

Cement-based solidification/stabilization treatment was completed at a former MGP site in Augusta, Georgia (Wilk 2003). The site is adjacent to a residential area near downtown Augusta. The 0.73 ha (1.8-acre) parcel of land treated by S/S was the former location of the MGP operating facilities and gas holders, which were in use from 1852 to 1955.

Byproducts from the manufacture of town gas impacted soil at this site. The depth of impacted soil ranged from just under the surface to 9 m (30 ft) below ground surface. The impacted soil is considered a source of groundwater contamination for the surrounding area. The groundwater table at the site was approximately 3 m (10 ft) below ground

level. The layer of impacted soil above the groundwater table was excavated and transported off site for disposal at an industrial landfill. Approximately 44,000 metric tons (48,000 tons) of site soil was excavated and disposed.

Cleanup plans for soil within the groundwater saturated zone included S/S. As an established treatment technology protective of human health and the environment, S/S treatment was approved for the Augusta site by the Georgia Environmental Protection Division. S/S had already been successfully used in the cleanup at other former MGP sites in Georgia. At the Augusta site, S/S was selected for the shallow groundwater saturated soil to enable remediation to be completed in a shorter time and to minimize heavy truck traffic, with its risks and inconvenience, through the community.

After impacted surface soil was removed for off-site disposal, In Situ S/S treatment began. The shallow groundwater saturated zone was located approximately 3–9 m (10–30 ft) below the original ground surface. A soil mixing auger was used to inject and mix portland cement into the soil. The 3 m (10 ft) diameter auger was advanced through the soil. The auger had a hollow stem with auger flights equipped with nozzles. Cement-based grout was injected into the soil. The depth of auger mixing continued through the groundwater saturated zone and a few feet into the soft fractured rock zone beneath. An overlapping pattern of mixing “columns” was used to insure complete mixing and treatment of the area (Fig. 3).

**Fig. 3** Right photo: Crane-mounted auger ISS, Left photo: Note change in grade for ISS beginning at water table



**Fig. 4** Right photo: Mixing cement into barge of sediment, Left photo: Port-side treatment



Within the treated area, the tar-like source material in the impacted soil was solidified in place. S/S changed the physical properties of the treated soil, creating a mass impervious to infiltrating precipitation and groundwater while further inhibiting leaching and transport of source material.

Goals for S/S-treated soil at the site included: (a) UCS of at least 0.34 MPa (50 psi), (b) reduction of hydraulic conductivity by 2–4 orders of magnitude compared to untreated soil surrounding the site, and (c) durability of the treated mass based on wet-dry cycling and compressive strength tests.

### 2.3 Re-use of New York Harbor Sediments

Federal regulations restrict the ocean disposal of sediment dredged from the harbors of New York and Newark, NJ. The Port Authority of New York and New Jersey is faced with a critical situation: find land-based disposal/uses for tens of millions of cubic meters of sediment or lose its standing as a primary commercial port for ocean-going ships. One of the technologies routinely employed to manage the sediment is portland cement-based S/S treatment (Loest and Wilk 1998). Millions of cubic meters of the sediment have undergone cement-based S/S treatment. This treatment immobilizes heavy metals, dioxins, PCBs, and other organic contaminants in the sediment.

The treatment changes the sediment from an environmental liability into a valuable structural fill. Dredged sediment was transported by barge to a pier. At the pier, cement was mixed into the sediment while it remained in the barge. The mixing method used an excavator-mounted soil mixing head. The treated material was removed from the barge and used as structural fill (Fig. 4). This structural fill has already been used at two properties. The first property is an old municipal landfill in Port Newark, NJ. The treated sediment was used as structural fill to cover about 8 ha (20 acres) of the landfill. Covering the landfill with competent structural fill allowed redevelopment of the landfill property into a shopping mall.

The second property called the Seaboard site was the location of a former coal gasification facility and later a

wood preservation facility. This 65 ha (160-acre) property has been designated for brownfield redevelopment. More than 1.1 million m<sup>3</sup> (1.5 million cu yd) of treated sediment already covers this site.

Sediment dredged from New York and Newark harbors was processed through a large-scale stationary pugmill in Bayonne, NJ. Approximately 2,300,000 m<sup>3</sup> (3,000,000 cu yd) were treated and re-used as structural fill to create a golf course. This S/S treatment used portland cement as the binding agent added at a rate of 8% per wet weight of the dredged sediment. Additional properties owned by the land developer hold capacity for another 2,300,000 m<sup>3</sup> (3,000,000 cu yd) of S/S treated sediment when the dredged material becomes available. Due to the ban on ocean disposal of some New York and Newark harbor dredge material, cement-based treatment of the material to produce an engineered fill continues to be considered for other properties near the harbor area.

## 3 Conclusion

Soil mixing methods are used to treat contaminated soil and sediment in a treatment technology called Solidification/Stabilization. S/S treatment protects human health and the environment by safely immobilizing contaminants within the treated material.

Superfund program sites comprise some of our nation's worst contaminated soil sites. The latest data from EPA indicate that S/S has been selected for a high proportion of in situ and ex situ treatment remedies within the Superfund program. S/S has been demonstrated to effectively treat a broad variety of contaminants of concern found in soils. Adding to the popularity of the treatment are the common availability of generic binding agents (cements) used in the treatment and the variety of mixing methods devised by remediation contractors. An appreciation of the versatility for the treatment technology can be gained by review of example projects. S/S is expected to continue to be an indispensable tool in waste management, remediation, and redevelopment.

## References

- Conner J.R.: Chemical Fixation and Solidification of Hazardous Wastes, Van Nostrand Reinhold (1990)
- Loest, K., Wilk, C.M.: Brownfield Reuse of Dredged New York Harbor Sediment by Cement-based Solidification/Stabilization, Presented at the Air & Waste Management Association's 91st Annual Meeting & Exhibition, San Diego, California, 14–18 June 1998
- The Interstate Technology & Regulatory Council Solidification/Stabilization Team.: Development of Performance Specifications for Solidification/Stabilization, ITRC S/S-1 (2011)
- United States Environmental Protection Agency.: A Resource for MGP Site Characterization and Remediation, EPA-542-R-99-005 (1999)
- United States Environmental Protection Agency.: Superfund Remedy Report 12th Edition, EPA-542-R-07-012 (2007)
- United States Environmental Protection Agency.: Superfund Remedy Report 15th Edition, EPA-542-R-17-01 (2017)
- United States Environmental Protection Agency.: Technical Resource Document Solidification/Stabilization and Its Application to Waste Materials, EPA-530-R-93-012 (1993)
- Wilk C.M., Delisio, R.: Solidification/Stabilization Treatment of Arsenic- and Creosote-Impacted Soil at a Former Wood-Treating Site SR997, Portland Cement Association, Skokie, Illinois (2002)
- Wilk C.M., Tiefenthaler, L.: Sustainability: A Role For Blended Cements and Industrial Byproducts in Soil Mixing, Grouting, and Slurry Walls Proceedings of Deep Foundations Institute 42<sup>nd</sup> Annual Conference on Deep Foundations, New Orleans, Louisiana, 23–28 Oct 2017
- Wilk C.M.: Augusta Manufactured Gas Plant Cleanup Using Cement-based Solidification/Stabilization, SR998, Portland Cement, Skokie, Illinois (2003)

# Harry Ferguson's Theory of Valley Stress Release in Flat-Lying Sedimentary Rocks

James V. Hamel

## Abstract

Harry Ferguson developed his theory of valley stress release in flat-lying sedimentary rocks by observing rock characteristics, behavior, and discontinuities in foundation excavations for navigation locks and dams and flood control dams in the Upper Ohio River Basin in the late 1950s and 1960s. He first presented his theory at the AEG Annual Meeting in 1966, then published it in the AEG Bulletin in 1967. Over the past five decades, this theory has provided a unifying framework for world-wide geologic observations and geotechnical interpretations in flat-lying sedimentary rocks. It is appropriate here to review this theory for an international audience and a new generation of engineering geologists. Essential elements of the theory are:

1. Flat-lying sedimentary rocks near the earth's surface typically have horizontal stresses greater than vertical stresses corresponding to existing overburden.
2. River (or stream) erosion removes horizontal support from valley walls and vertical support from valley floors.
3. Valley walls deform inward and valley floors deform upward in response to this loss of support.
4. These deformations relieve stresses in rocks of the valley walls and floors.
5. Deformations and stress release produce characteristic patterns and types of fractures and other discontinuities in rocks of valley walls and floors.

This theory of valley stress release has both geologic and engineering implications. Geologic implications include a mechanism for on-going valley development independent of tectonic processes; groundwater flow through stress release fractures with associated processes of weathering and alteration plus solution in soluble rocks; mass-wasting processes,

e.g., rock slides, rock falls, rock block creep, colluvium development, on valley walls. Engineering implications include layout and interpretation of subsurface exploration programs; foundation depths and treatments; slope and foundation stability; rock excavation and support, both surface and underground; excavation dewatering; dam foundation and abutment grouting.

## Keywords

Valley formation • Flat-lying rocks • Stress release

## 1 Introduction

In 1990, Harry F. Ferguson (Fig. 1) was posthumously awarded Honorary Membership in the Association of Engineering Geologists (AEG) at its 33rd Annual Meeting in Pittsburgh, Pennsylvania. Harry's most significant contribution to Engineering Geology was his theory of valley stress release in flat-lying sedimentary rocks. This theory was developed in the late 1950s and 1960s, primarily from field observations in the Allegheny Plateau of the northeastern United States.

Over the years, Harry's theory has provided a unifying framework for worldwide geologic observations and geotechnical interpretations in flat-lying sedimentary rocks (e.g., Imrie 1991) and it has also been extended to extrusive igneous rocks (Cabrera 1986).

I was fortunate to have met Harry in 1968 and worked closely with him from 1974 until his death in 1989. Over this period, Harry explained his valley stress release theory in detail and illustrated it with numerous field examples.

The purpose of this present paper is to review Harry's theory for an international audience and a new generation of engineering geologists. First, historical development of the theory is summarized. Next, essential elements of the theory are outlined. Finally, geologic and engineering implications of the theory are presented.

J. V. Hamel (✉)  
Hamel Geotechnical Consultants, 1992 Butler Dr., Monroeville,  
PA 15146, USA  
e-mail: jvhamel3918@gmail.com

**Fig. 1** Harry Ferguson at valley stress relief joints in Sandstone near Pittsburgh, Pennsylvania—March 15, 1981 (photo by James Hamel)



## 2 Historical Development of Valley Stress Release Theory

After several years of experience in groundwater geology and military geology, Harry joined the Pittsburgh District, U. S. Army Corps of Engineers, in 1956 and transitioned to engineering geology (Hamel 1991). For the next decade, he assisted Dr. Shailer S. Philbrick, Honorary Member, AEG, on geological and geotechnical aspects of all military and civil works projects in the Pittsburgh District which includes the Upper Ohio River Basin. This area is underlain by flat-lying sedimentary rocks of Middle Devonian to Permian age. The northern part of the area was glaciated during Pleistocene time.

The Pittsburgh District was heavily involved with investigation, design, and construction of navigation locks and dams and flood control dams during the 1950s and 1960s. Observations in foundation and abutment excavations for these structures led to the valley stress release theory.

At the 1959 Annual Meeting of the Geological Society of America in Pittsburgh, Harry presented a paper (co-authored by Dr. Philbrick) on faults in bedrock foundations of 11 of 18 flood control and navigation structures designed or constructed by the Pittsburgh District from 1934 to 1959 (Ferguson and Philbrick 1959). All these faults were found in river valleys and most were low angle thrusts with a displacement of 0.6 m (2 ft) or less. The faults had soft gouge or breccia zones up to 0.5 m (1.5 ft) thick. There was no general orientation of fault strikes and no apparent relationship to regional geologic structures.

Additional observations in lock and dam foundation excavations from 1959 to 1966 produced the valley stress release theory. Harry developed this theory in the classical manner of observational engineering geology. He observed rock features in foundation and abutment excavations (Figs. 2 and 3). He correlated these observations with boring data and stratigraphy on carefully plotted cross-sections. Then he interpreted this information within the context of valley formation, including erosion, stress release, and rock response as a function of strength and deformability of individual strata or suites of rock (Fig. 4).

Harry first presented his theory at the 9th Annual Meeting of AEG at Anaheim, California, in 1966. He then published a short paper in the AEG Bulletin (Ferguson 1967).

After further work, Harry presented a more detailed paper at the American Society of Civil Engineers National Meeting on Water Resources Engineering at Los Angeles, California, in 1974. This paper was available as a meeting preprint but it was never published (Ferguson 1974).

In the early 1970's, Harry began teaching me about valley stress release. We reviewed relevant literature and updated and summarized his valley stress release concepts in a 1981 paper (Ferguson and Hamel 1981). I later extended some of the valley wall stress release concepts from that paper to develop a failure mechanism for Pleistocene rock slides (Hamel 1998).

The most significant recent development relative to Harry's theory has been the work of Cole (2008). He reviewed literature, field observations, and previous analytical studies, then performed numerical analyses of stress release in layered rocks of valley walls and floors.



**Fig. 2** Thrust Fault in Dam Foundation Excavation, early 1960s (photo by Harry Ferguson)

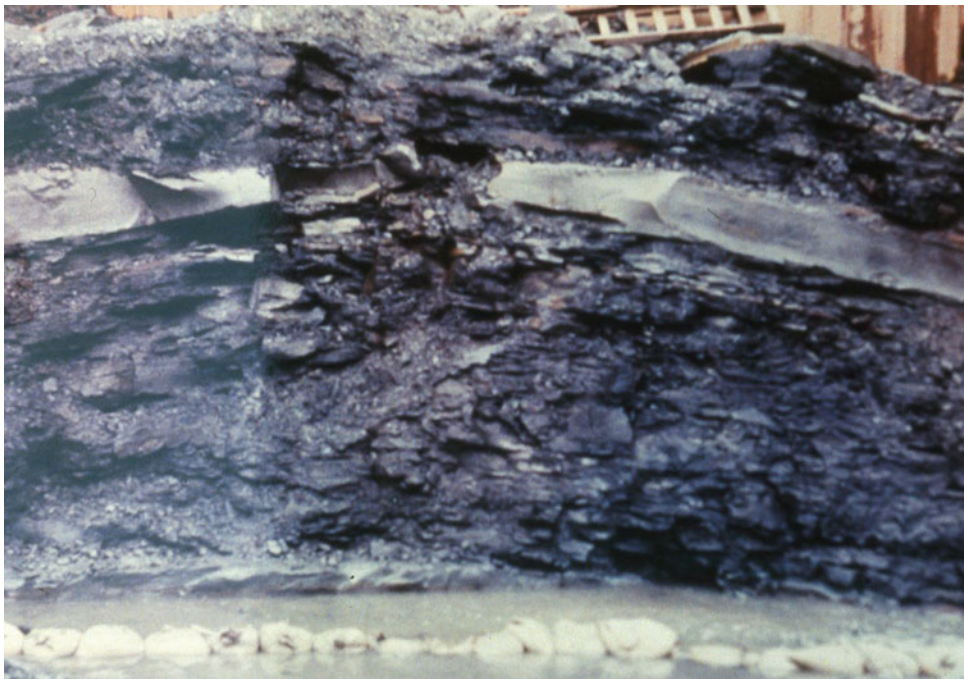


**Fig. 3** Arched Sandstone over broken silt shale in Shenango Dam Foundation Excavation, early 1960s (after Ferguson 1967, used with permission)



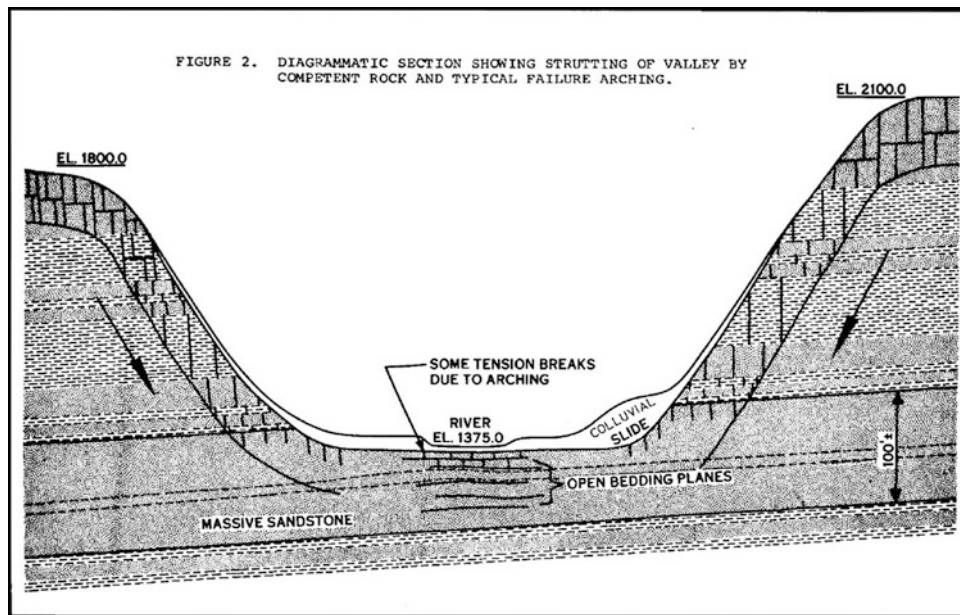


Fig. 4 Valley stress release cross-section (after Ferguson 1967, used with permission)

### 3 Essential Elements of Valley Stress Release Theory

#### 3.1 General

Numerous rock mechanics investigations over the past several decades have shown that flat-lying sedimentary rocks near the earth's surface typically have horizontal stresses greater than vertical stresses corresponding to existing overburden. These high horizontal stresses, relative to vertical stresses, result from previous overburden (soil, rock, glacial ice) subsequently removed by erosion (or melting).

River and stream erosion removes lateral support from valley walls and vertical support from valley floors. Valley walls deform inward and valley floors deform upward in response to this support removal. These deformations relieve stresses in rocks of the valley walls and floors.

Details of this deformational response depend on many factors including stratigraphic sequences and the strength and deformability of individual rock strata. Deformation can continue over a considerable period of geologic time as rivers and streams erode deeper and wider valleys and stresses are relieved further into valley walls and deeper into valley floors. Stress release may continue long after valley erosion in rock has ceased due to time dependent effects (Nichols 1980).

The erosional history of a valley is important here. It is expected that stress release will occur relatively rapidly when rivers and streams are actively eroding valleys in rock as occurred in many areas during Pleistocene time with

heavy flows from glacial meltwater and periglacial precipitation. High water pressures in rock pores and fractures resulting from Pleistocene hydraulic activity (meltwater flows, ponding events, heavy precipitation), along with periglacial processes, may have enhanced stress release effects (Ferguson 1974; Patton and Hendron 1974; Hamel 1998; Hutchinson 1991).

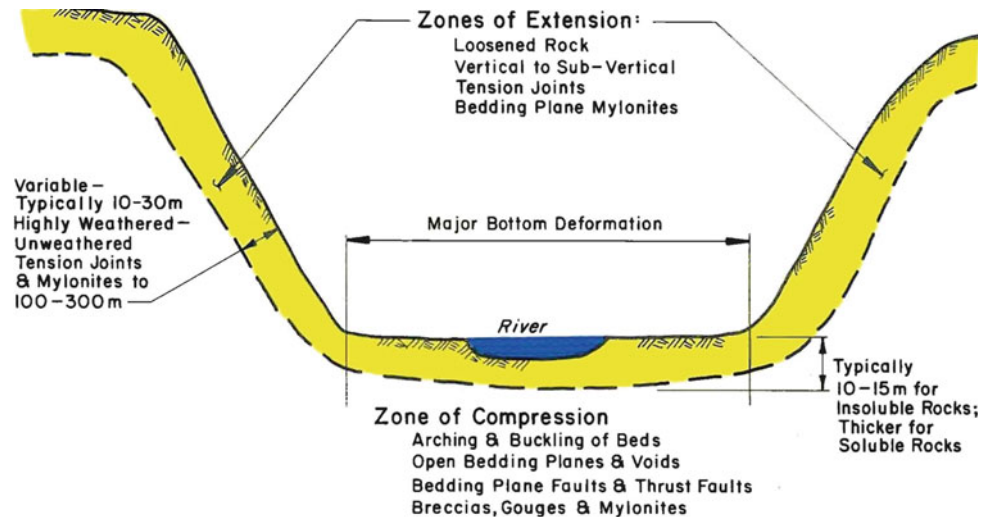
Stress release and associated deformations produce characteristic types and patterns of fractures and other discontinuities in rocks of the valley walls and floors. The valley walls are zones of extension and the valley floors are zones of compression (Fig. 5).

Fracture patterns typically consist of compression fractures, thrust faults, and bedding plane faults in valley floors along with extension fractures and bedding plane shear zones in valley walls. Thrust faults and bedding plane faults in valley floors and bedding plane shear zones in valley walls tend to develop along contacts between beds of different strength and stiffness. Numerical modeling of these fracture patterns has been done by Cole (2008).

Stress release fractures in valley walls and floors have been observed in vertical and inclined borings, excavations, tunnels, and surface and underground mines. The patterns and characteristics of these fractures are best observed in large excavations (Figs. 2 and 3).

Cambering and valley bulging of the type reported in England and elsewhere (e.g., Horswill and Horton 1976) and valley rebound of the type reported in weak argillaceous rocks of midwestern North America and elsewhere (e.g., Matheson and Thomson 1973) can be considered special cases of valley stress release.

**Fig. 5** Schematic valley cross-section (after Ferguson and Hamel 1981, ©1981 Taylor and Francis Group, London UK; used with permission)



### 3.2 Valley Wall Features

The main fractures are generally parallel or sub-parallel to the valley wall, vertical to sub-vertical, and limited vertically to individual rock strata. Ferguson (1974) stated that each rock type develops its own pattern and frequency of main fractures depending on:

1. Thickness of bed
2. Competency (i.e., strength and stiffness) of bed
3. Competency of adjacent beds
4. Position in valley wall.

A second set of vertical to sub-vertical fractures perpendicular or sub-perpendicular to the main fractures (Fig. 1) results from breakage of rock into blocks along the valley wall (Ferguson 1974). Fractures of both sets are most closely spaced and open at and near the valley wall. Their apertures and frequencies both decrease with distance from the valley wall. Fractures in a given bed often terminate at the base of the bed in a shear zone or mylonite seam resulting from outward movement above the bedding contact. Where a tributary valley intersects a main valley, fracture patterns on the walls of both valleys may reflect a tangential release of stress from the valleys (Ferguson 1967).

Figure 6 is a schematic of valley wall fracture systems in typical interbedded strong and weak rocks (e.g., Coal Measure rocks). Vertical to sub-vertical tension joints form in strong, brittle rocks, e.g., sandstone, and rocks of intermediate strength and stiffness, e.g., shale. Non-linear, sometimes curved, shear joints form in weak, deformable rocks, e.g., claystone. Shear zones with gouge or mylonite seams, along which shear strengths have been reduced to residual levels in the direction toward the valley, form along

weak bedding contacts, particularly those in argillaceous rocks. For all rocks, stress release effects diminish with distance into the valley wall.

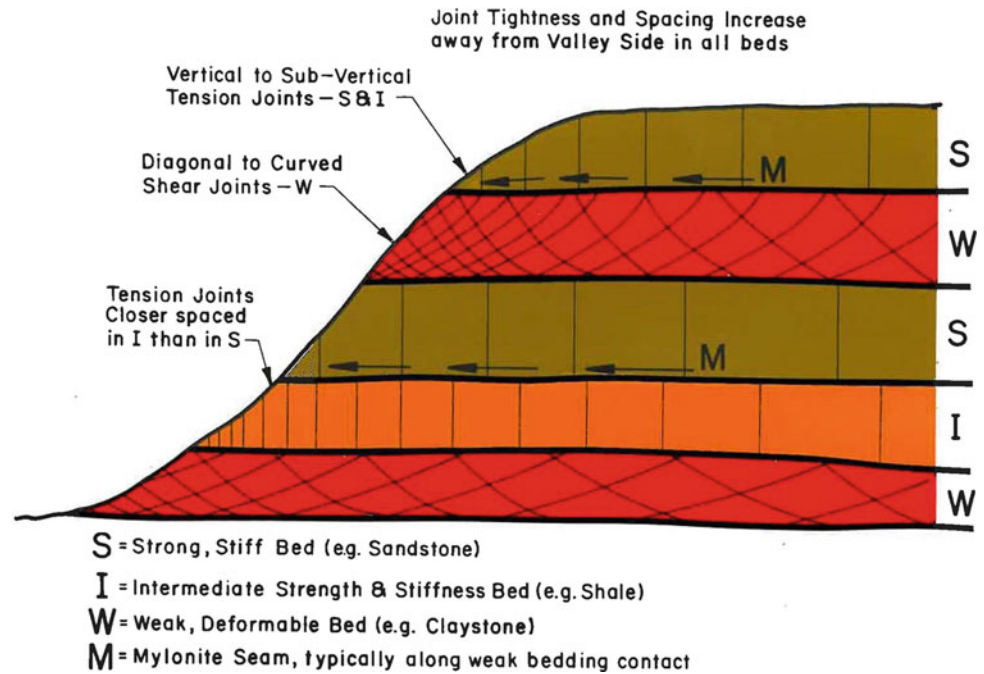
### 3.3 Valley Floor Features

The most common valley floor features in all rock types are thrust faults and bedding plane faults with breccias, gouges, and mylonites (Fig. 2). Arched and buckled beds with open bedding planes and voids occur where the valley floor has thick beds of strong, stiff rock, e.g., sandstone. Crushed and broken zones or wedges sometimes occur near the center of a valley (Fig. 3).

Ferguson and Hamel (1981) stated that the depth of valley floor rock defects of engineering significance in insoluble flat-lying sedimentary rocks is on the order of 10–15 m (30–50 ft), regardless of valley geometry (Fig. 5). This was based on foundation treatment considerations, mainly for dams. Observations indicate that valley bottom stress release features in insoluble sedimentary rocks diminish sharply below about 10–15 m beneath the bedrock surface. At most sites, there are no stress release fractures below this nominal depth, or where present, fractures are tight and have essentially no influence on foundation behavior (Discussion, Ferguson and Hamel 1981).

Stress release fracturing extends to much greater depths under valleys as indicated in the Discussion of Ferguson and Hamel (1981). Borings showed thin, tight, and apparently discontinuous bedding plane shear zones to depths of 27–30 m (88–100 ft) below the bedrock surface in shales and siltstones at Alum Run Dam in Ohio. These features were too deep, tight, and thin to influence dam foundation behavior. In this Discussion, they also mentioned a groundwater investigation that found apparent voids or extensively broken zones

**Fig. 6** Schematic valley wall cross-section (after Ferguson and Hamel 1981 © 1981 Taylor and Francis Group, London, UK; used with permission)



at depths of 14–34 m (46–112 ft) below the bedrock surface in a small valley near Pittsburgh.

Molinda et al. (1992) found bedding plane faults and low angle thrust faults to depths of 90 m (300 ft) in underground coal mines beneath valleys in western Pennsylvania. These and other compressional features in mine roof rocks were attributed to valley stress release.

## 4 Implications of Valley Stress Release Theory

### 4.1 Geologic

Valley stress release is a geologic process that significantly influences other geologic processes. Stress release fracturing breaks down rocks of the valley walls and floor, enhancing their erodibility. Thus, valley stress release provides a mechanism for on-going valley development independent of tectonic processes and fault control.

Groundwater flow through stress release fractures is important in developing groundwater resources (e.g., Wyrick and Borchers 1981). Groundwater flow through stress release fractures also enhances processes of weathering and alteration in all rocks as well as solution in soluble rocks (e.g., Sasowsky and White 1994). Weathering and alteration, along with water pressures in stress relief fractures, contribute to processes of mass-wasting, e.g., rock slides, rock falls, rock block creep, and colluvium development, on valley walls (Patton and Hendron 1974, Ferguson and Hamel 1981, Hamel 1998).

### 4.2 Engineering

Engineering implications result mainly from the presence and characteristics of rock discontinuities resulting from valley stress release. Bedding plane features (faults, gouge and mylonite seams) have strengths reduced to residual levels in the direction of stress release movement, i.e., perpendicular or sub-perpendicular to valley walls. In other directions, strengths will have been reduced from that of intact rock, but not to residual levels. Thus, stability will be more critical for rock masses and structures parallel to valley walls than for rock masses and structures with other orientations, e.g., dams across valleys.

Other engineering implications include layout and interpretation of subsurface exploration programs; foundation depths and treatments for various structures; slope and foundation stability; rock excavation and support, both at the ground surface and underground (tunneling, mining); installation of field instrumentation and interpretation of data therefrom; and groundwater issues, e.g., excavation dewatering, dam foundation and abutment grouting and other seepage cutoffs, pollution or contaminant migration, and development of groundwater resources.

## References

- Cabrera, J.G.: Buckling and shearing of basalt flows beneath deep valleys. In: Proceedings Fifth International Conference International Association of Engineering Geology, Buenos Aires, vol. 2, pp. 589–594. Balkema, Rotterdam (1986)

- Cole, T.M.: The role of horizontal stress in the formation of valley stress release features in flat-lying sedimentary rocks. Ph.D. Dissertation, University of Illinois, 323p (2008)
- Ferguson, H.F.: Valley stress release in the Allegheny Plateau. *Bull. Assoc. Engr. Geol.* **4**(1), 63–71 (1967)
- Ferguson, H.F.: Geologic observations and geotechnical effects of valley stress relief in the Allegheny Plateau. Preprint, American Society of Civil Engineers National Meeting on Water Resources Engineering, Los Angeles, California, 31p (1974)
- Ferguson, H.F., Hamel, J.V.: Valley stress relief in flat-lying sedimentary rocks. In: Akai, K., Hayashi, M., Nishimatsu, Y. (eds.) *Weak Rock: Proceedings International Symposium on Weak Rock Tokyo*, vol. 2, pp. 1235–1240, Discussion, vol. 3, pp. 1428–1429. Balkema, Rotterdam (1981)
- Ferguson, H.F., Philbrick, S.S.: Faulting in engineering structures located in the Allegheny Plateau. Abstract, *Bull. Geol. Soc. Amer.* **70**(12) Pt. 2, 1601–1602 (1959)
- Hamel, J.V.: Harry F. Ferguson (1921–1989), Honorary Member Association of Engineering Geologists. *Bull. Assoc. Engr. Geol.* **28**(1), 1–4 (1991)
- Hamel, J.V.: Mechanism of Pleistocene rock slides near Pittsburgh, Pennsylvania. *Int. J. Rock Mech. Min. Sci.* **35**(4–5) (paper no. 032), 16p. Elsevier, Amsterdam (1998)
- Horswill, P., Horton, A.: Cambering and valley bulging in the Gwash valley at Empingham, Rutland. *Phil. Trans. R. Soc. Lond. A* **283**, 427–462 (1976)
- Hutchinson, J.N.: Periglacial and slope processes. In: Forster, A., Culshaw, M.G., Cripps, J.C., Little, J.A., Moon, C.F. (eds.) *Quaternary Engineering Geology*, *Geol. Soc. Eng. Geol. Spec. Pub. No. 7*, 283–331 (1991)
- Imrie, A.S.: Stress-induced response from both natural and construction-related processes in the deepening of the Peace River Valley, B.C. *Can. Geo. J.* **28**(3), 719–728 (1991)
- Matheson, D.S., Thomson, S.: Geologic implications of valley rebound. *Can. J. Earth Sci.* **10**, 961–978 (1973)
- Molinda, G.M., Heasley, K.A., Oyler, D.C., Jones, J.R.: Effects of horizontal stress related to stream valleys on the stability of coal mine openings. U. S. Bureau of Mines Report of Investigations 9413, 26p (1992)
- Nichols, T.C.: Rebound, its nature and effect on engineering works. *Q. J. Eng. Geol. Lond.* **13**, 133–152 (1980)
- Patton, F.D., Hendron, A.J.: General report on mass movements. In: *Proceedings Second International Conference International Association of Engineering Geology*, Sao Paulo, vol. 1, pp. V-GR. 1–14 (1974)
- Sasowsky, I.D., White, W.B.: The role of stress relief fracturing in the development of cavernous porosity in carbonate rocks. *Water Resour. Res.* **30**(12), 3523–3530 (1994)
- Wyrick, G.G., Borchers, J.W.: Hydrologic effects of stress-relief fracturing in an Appalachian valley. U. S. Geol. Surv. Water-Supply Paper 2177, 51p (1981)

# The Characterization of Tropical Peats for Potentially Toxic Metals Adsorption Purposes in an Abandoned Mine Area

Isabela Monici Raimondi<sup>✉</sup>, Jacqueline Zanin Lima<sup>✉</sup>,  
and Valéria Guimarães Silvestre Rodrigues<sup>✉</sup>

## Abstract

Peat has been used as an alternative, low-cost and efficient material capable of retaining metals. Most studies of adsorption have tended to focus on the characterization and adsorption mechanisms of temperate peats rather than tropical ones, therefore there is insufficient data about their characteristics and subsequent use in contaminated areas. The purpose of this study is to assess the chemical characteristics of tropical peats from the Mogi-Guaçu river Basin (Brazil), to evaluate their ability to capture potentially toxic metals in a contaminated mine area in Brazil. The peats were classified as H5–H6 on the Von Post scale of humification and had 48% ash content. The  $\text{pH}_{\text{H}_2\text{O}}$ ,  $\Delta\text{pH}$  and the point of zero salt effect (PZSE) for peat 1 was 5.1,  $-1.0$  and  $3.6$ , while for peat 2, the values were  $5.9$ ,  $-2.4$  and  $3.1$ , respectively. These data showed materials with low acidity characteristic and a predominance of negative charges, which allows great cation retention. The cation exchange capacity (CEC) was considered high ( $91.0$  and  $116.0 \text{ cmol}_c \text{ kg}^{-1}$ ), especially when considering the organic matter content ( $520.43$  and  $510.06 \text{ g kg}^{-1}$ ). The removal of lead (Pb II) ions from the aqueous solution, investigated under different experimental conditions, revealed a satisfactory efficiency of  $1/50$ , peat/solution ratio. Metals were removed in the descending order  $\text{Pb} > \text{Zn} > \text{Cd}$ , and both peats showed similar efficiency of lead sorption in high concentrations. The results show that the tropical peats have good characteristics to be used as alternative adsorbent materials in abandoned and contaminated mining areas.

## Keywords

Low cost material • Lead • Cadmium • Zinc  
Adsorption

## 1 Introduction

Peat has become important as an organic low cost and efficient material for ion metallic adsorption (Gisi et al. 2016). Peatlands are soils formed by the humification of plant residues in acidic, moist and environments with low oxygen such as wetlands, river floodplains, coastal plains and lacustrine regions (Oliveira et al. 2014; Rezanezhad et al. 2016). Tropical peats are defined as organic soils between latitudes of  $35^\circ\text{N}$  and  $35^\circ\text{S}$ , including the whole of Brazil and Uruguay where there are large areas of peatlands (Andriessse 1988). The composition and texture of tropical peats differ from humid temperate peat deposits (Yonebayashi et al. 1992). In tropical areas, trees are more prevalent in peatland composition than in temperate regions, which are mainly composed by sphagnum moss (Andriessse 1988). The differences in characteristics may also affect adsorption efficiency. Peat is a material with a large surface area ( $>200 \text{ m}^2 \text{ g}^{-1}$ ), high porosity and functional groups responsible for the polar character of this material. These characteristics make peat an efficient agent in the adsorption process (Tripathi and Ranjan 2015).

Adsorption has emerged as an alternative over other processes due to its effectiveness, safety, flexibility and economical treatment (Tripathi and Ranjan 2015). It is an efficient technique often used for soil, groundwater and wastewater treatment (Kocasoy and Guvener 2009). Adsorption is a process that is adaptable for both treatment techniques and containment of pollutants, meaning the adsorbents could be used not only as impermeable barriers (sealing soil) but also for permeable reactive barriers (treatment), controlling the amount of contaminants transported in a porous medium (Zuquette et al. 2008).

I. M. Raimondi (✉) · J. Z. Lima · V. G. S. Rodrigues  
São Carlos School of Engineering, University of Sao Paulo,  
São Carlos, SP, Brazil  
e-mail: isabela.monici@gmail.com

V. G. S. Rodrigues  
e-mail: valguima@usp.br

Numerous studies have attempted to explain the mechanisms of adsorption, controlled by the properties of temperate peats (Kalmykova et al. 2008). However, there is limited information available on the adsorption and desorption of metals of tropical peats, especially their chemical and physical characterizations for metal retention (Oliveira et al. 2014). Tropical peats are rarely used in the treatment of contaminated mining areas due to a lack of knowledge about the material. This paper will investigate the chemical characteristics of two tropical peats from the Mogi-Guaçu river Basin (Brazil), including their adsorption pre-test efficiency, in order to assess peats' ability to be used as future alternative adsorbent material in an abandoned and contaminated mining area in southeastern Brazil (soil and water with high metal concentrations).

## 2 Materials and Methods

Peat 1 was collected in the Mogi-Guaçu river Basin, in city of Cravinhos (the state of São Paulo), Brazil. The area is a commercial peat extraction zone. Peat 2 was also extracted from the Mogi-Guaçu river Basin, but at Km 40 of the SP-255 road in Luis Antonio city, Brazil. Both peats were from a warm tropical climate region, characterized by a dry fall/winter and a rainy summer/spring. As a commercial product, Peat 1 was originally air-dried and homogenized, while peat 2 was air-dried, homogenized in a porcelain mortar and sieved through a 2 mm mesh sieve, after extraction. Both were stored at room temperature prior to analysis. Analysis of the pH in water, the pH in KCl, the degree of decomposition, the cation exchange capacity (CEC), the point of zero salt effect (PZSE), ash and organic matter content were carried out for peat characterization, besides adsorption pre-tests.

### 2.1 $\text{pH}_{\text{H}_2\text{O}}$ , $\text{pH}_{\text{KCl}}$ and $\Delta\text{pH}$

The pH of the peats was potentiometrically measured in the supernatant suspension of a 1/2.5 peat(g)/liquid(mL) ratio according to Brazilian Public Agricultural Research Corporation (2011), in triplicate and using a digital pH meter (Digimed DH 21). The liquid was either distilled water ( $\text{pH}_{\text{H}_2\text{O}}$ ) or a 1 M KCl solution ( $\text{pH}_{\text{KCl}}$ ). The  $\Delta\text{pH}$  index was used to estimate the sign of the net charge and it was calculated from the difference between  $\text{pH}_{\text{KCl}}$  and  $\text{pH}_{\text{H}_2\text{O}}$  values (Mekaru and Uehara 1972).

### 2.2 Ash Content, Organic Matter and Degree of Decomposition

The ash and organic matter content was determined through ignition in a muffle furnace at 550 °C. The degree of

decomposition was determined using the Von Post Scale (Grover and Baldock 2013), which provides a qualitative classification system of humification ranging from H1 (insignificant or very slightly decomposed peat) to H10 (highly humified).

### 2.3 Determining of Point of Zero Salt Effect (PZSE)

The peats' points of zero salt effect were determined using potentiometric titration (Sposito 1984). For each peat, 24 samples of 4 g each were divided into two groups of 12 samples, which distributed in Erlenmeyers containing: 20 mL of KCl 0.1 M, KCl 0.01 M and KCl 0.001 M. Samples from each of these salt concentration groups received 0.002, 0.004, 0.008 and 0.016 M of HCl (a total of 12 acid solutions) and 0.002, 0.004, 0.008 and 0.016 M of NaOH (12 basic solutions). For peat 1, two more concentrations were added to the salt concentration: 0.0032 and 0.064 of HCl (a total of 18 acid solutions) and 0.0032 and 0.064 of NaOH (18 basic solutions). The samples were agitated every 30 min for 24 h. The titration curves were obtained by plotting the pH values determined at the four points of each electrolyte concentration (KCl) as a function of adsorption of  $\text{OH}^-$  or  $\text{H}^+$ , according to the amounts of acid/base (HCl/NaOH) added. The common point of intersection of the three curves was defined as the pH value equivalent to the PZSE.

### 2.4 The Cation Exchange Capacity (CEC)

The CEC in peats were based on the occupation of the exchange sites with hydrogen- ions from a diluted solution of hydrochloric acid, the elimination of excess acid, the displacement of adsorbed hydrogen ions with calcium acetate solution and then the titration of the acetic acid formed with NaOH. The procedure was in accordance with the Brazilian Ministry of Agriculture, Livestock, and Supply (2013) and it is recommended for organic materials.

### 2.5 Adsorption Test

The BET analysis test at room temperature was used in adsorption tests. First, as a preliminary step for adsorption, peat 1 was tested in order to verify the favorable condition of peat/solution ratio for the BET equilibrium test (Roy et al. 1992). Five different ratios were tested: 1/5, 1/10, 1/50, 1/80, 1/100. For this first situation, Pb was used at 100 mg L<sup>-1</sup> because it is a concentration above the highest value of Pb leaching (77 mg L<sup>-1</sup> according to Raimondi

(Raimondi 2014) from mine waste) in the region intended for use of the peats as adsorbent materials. Secondly, an adsorption test was carried out for Pb, Zn and Cd at  $150 \text{ mg L}^{-1}$  using the favorable ratio from step 1 for both peats. The metal contents (Pb, Zn and Cd) were determined using atomic absorption in PerkinElmer PinAAcle 900F equipment.

### 3 Results and Discussion

Analytical data for the peat samples are given in Table 1. According to the Von Post scale of humification degree, the samples of both peats were between two categories: moderately and moderately highly decomposed peats (H5 and H6). It's important to emphasize the large amount of recognizable plant structure (fibres) resistant to decomposition present in both peats, an unusual characteristic for moderately decomposed temperate peats. However, the fibrous feature is commonly found in tropical peat soils (Andriess 1988). Brazilian peats from the Southeast region (including São Paulo state) can be classified as fibric, being composed by fibers and filaments immersed in a gelatinous and dark color matrix (Kiehl 1985), in accordance with the results obtained for Mogi-Guaçu peats. The high fiber content may interfere in adsorption efficiency.

Regarding the organic matter and ash content (Table 1), there were no significant differences between both peats. For organic matter, Peat 1 showed an average of  $520.43 \pm 2.08 \text{ g kg}^{-1}$  as well as peat 2, which was  $510.06 \pm 8.26 \text{ g kg}^{-1}$ . For ash content peat 1 and peat 2 were  $47.9 \pm 0.21\%$  and  $48.9 \pm 0.82\%$ , respectively. In terms of ash content, samples had comparatively higher amounts than the average values found in other studies (Kiehl 1985; Huat et al. 2011). And consequently, lower levels of organic matter (Kiehl 1985; Huat et al. 2011), probably due to the degree of degradation of the peat. For (Huat et al. 2011), peats usually have at least 65% organic matter or less than 35% mineral content. However, in the state of São Paulo (Brazil) high levels of ash is an ordinary characteristic for peats formed near rivers to have, as a consequence of periodic flooding (Cabral Junior et al. 2001). For (Wust et al. 2003) attempted to classify tropical peats in Malaysia based

on ash content to divide the peats into a new system. For the authors, most peat classification schemes are developed in boreal and humid temperate regions, therefore they fail to adequately characterize tropical deposits. Both peats analyzed from the Mogi-Guaçu basin were better adjusted to this new classification system, being classified as very high ash content peats (40–55%).

The cation exchangeable capacity (CEC) was considered favorable for future use of the materials in the adsorption of potentially toxic metals ions (peat 1:  $91.0 \text{ cmol}_c \text{ kg}^{-1}$  and peat 2:  $116.0 \text{ cmol}_c \text{ kg}^{-1}$ —Table 1), despite the organic matter content. To compare results, peats from others Brazilian states (Santa Catarina and Rio de Janeiro) had CECs of 140 and  $67 \text{ cmol}_c \text{ kg}^{-1}$  for their respective organic matter contents: 75 and 32.5% (Petroni et al. 2004; Crescêncio Junior 2008). The organic matter present in soils and peats contributes significantly to the cation exchangeable capacity values (Sparks 1995; Alleoni et al. 2009) and the main exchangeable sites are the functional acid groups (humic acids) (Huat et al. 2011). So, the CEC found indicates both materials are favorable for adsorption of metal in mine contaminated areas.

As the pH of peat increases with increasing humification, CEC is also pH-dependent and generally raises with an increase in the degree of decomposition (Delicato 1996). At pH 7.0, less decomposed peats have CEC values around  $100 \text{ cmol}_c \text{ kg}^{-1}$ . On the other hand, highly decomposed peats have CEC values around  $200 \text{ cmol}_c \text{ kg}^{-1}$  (Andriess 1988).

Peats can be classified into four broad categories based on pH (American Society for Testing and Materials 2013) (Table 2).

Peats usually have low pH, caused by reactions to acid decomposition (Kiehl 1985). Both peats can be classified as slightly acidic according to ASTM D4427—13 (Table 2), with pH values of 5.1 for peat 1 (from Cravinhos city) and 5.9 for peat 2 (from Luis Antônio city) (Table 1). For (Dick et al. 2009) at 4 and 5 pH values, over 90% of the carboxylic functional groups of organic matter (COOH of pKa-3) are already dissociated. And the carboxylic groups are the major contributors to CEC under natural conditions, since phenolic hydroxyl groups dissociate at higher pH (pH 8 to 9), limiting their contribution to CEC.

**Table 1** Peats from Mogi-Guaçu river basin characteristics

Parameter	Peat 1	Peat 2
Organic matter	$520.43 \pm 2.08 \text{ g kg}^{-1}$	$510.06 \pm 8.26 \text{ g kg}^{-1}$
Ash content	$47.9 \pm 0.21\%$	$48.9 \pm 0.82\%$
Degree of humification	H5–H6	H5–H6
$\text{pH}_{\text{H}_2\text{O}}$	$5.1 \pm 0.1$	$5.9 \pm 0.1$
$\text{pH}_{\text{KCl}}$	$4.1 \pm 0.0$	$3.5 \pm 0.1$
$\Delta\text{pH}$	$-1.0 \pm 0.1$	$-2.4 \pm 0.1$
CTC	$91.0 \text{ cmol}_c \text{ kg}^{-1}$	$116.0 \text{ cmol}_c \text{ kg}^{-1}$

**Table 2** Peats' classification based on pH values

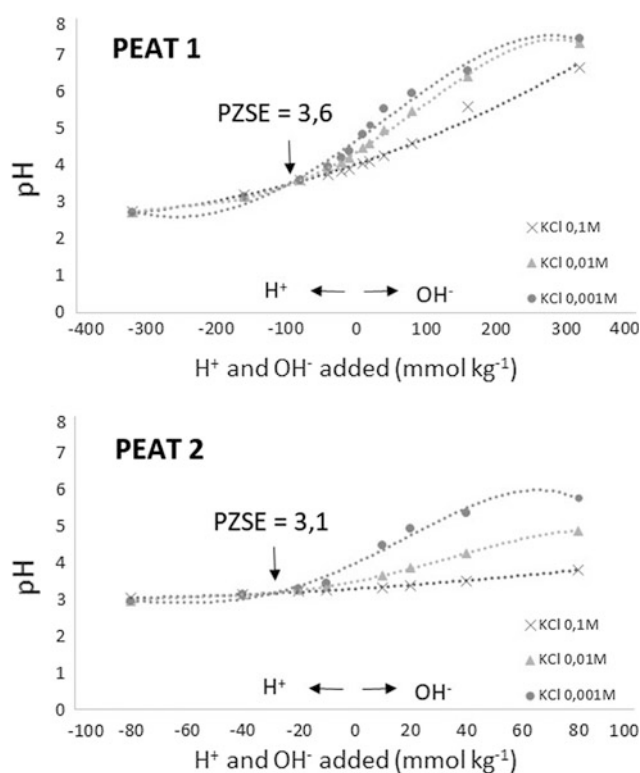
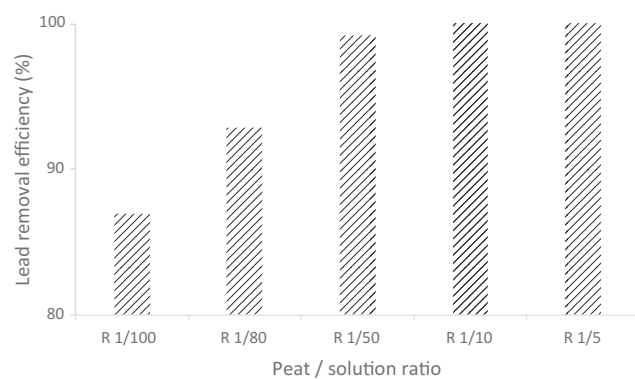
Categories	pH
Highly acidic	pH < 4.5
Moderately acidic	4.5 < pH < 5.5
Slightly acidic	5.5 < pH < 7.6
Basic	pH ≥ 7.0

As shown in Table 1, in relation to the pH in water, the pH of peat suspension is lower when adding an electrolyte to it like KCl ( $pH_{KCl}$  for peat 1 is  $4.1 \pm 0.0$  and for peat 2 is  $3.5 \pm 0.1$ ). These results are important for providing information about whether peats' colloids possess net negative or net positive charges (Mekaru and Uehara 1972). The  $\Delta pH$ , calculated by the difference between  $pH_{KCl}$  and  $pH_{H_2O}$ , is an efficient index used for estimating the signal and the magnitude of the net surface charge of tropical soils (Alves and Lavorenti 2005).

The  $\Delta pH$  determined are  $-1.0 \pm 0.1$  for peat 1 and  $-2.4 \pm 0.1$  for peat 2 (Table 1). These results ( $\Delta pH < 0$ ) indicate the predominance of negative charges, demonstrating the peat's ability to retain more cations than anions—a favorable feature for ion metallic adsorption.

With respect to the point of zero salt effect (PZSE), Fig. 1 shows the titration curves for the two peats. The PZSE for peat 1 and for peat 2 were 3.6 and 3.1, respectively. PZSE is one distinct point of zero charge (Sposito 1984), meaning it is the pH value in which the ionic concentration of the solution does not influence the magnitude of the variable surface charges (Alves and Lavorenti 2005). The pH values in water for peats ( $5.1 \pm 0.1$  and  $5.9 \pm 0.1$ ) were greater than the value of PZSE. These results indicated that the net surface charge of the materials is negative, therefore they have the ability to retain cations from the environment. The results were consistent with the  $\Delta pH$  values of Table 1 ( $-1.0 \pm 0.1$  and  $-2.4 \pm 0.1$ ). PZSE values generally present a positive correlation with  $\Delta pH$ , since as  $\Delta pH$  approaches zero or becomes more positive, there is a corresponding increase in PZSE (Silva et al. 1996). Humic substances of organic soil matter are a major factor in pH-dependent charges in soils (Sparks 1995) and the functional groups existing could gain or lose protons, being the cause of the variation in the superficial liquid charge. At values above 3.6 for peat 1 and 3.1 for peat 2 ( $pH_{H_2O} > PZSE$ ), the hydroxyl groups of the phenolic and carboxylic groups on the surface of the peat undergo deprotonation, becoming negatively charged. For the values below 3.6 and 3.1 ( $pH_{H_2O} < PZSE$ ), the inverse occurs. A low PZSE value for any soil (or for peat) indicates that the material has a negative charge over a wide pH range and consequently a wide pH action to adsorb cations (Sparks 1995).

Regarding the favorable condition of peat/solution ratio for the BET equilibrium test, Fig. 2 provides the results from

**Fig. 1** Potentiometric titration curves (PZSE) of the peats from the Mogi-Guaçu river basin (Brazil)**Fig. 2** Comparative analysis of the percentage of removal of Pb as a function of the peat/solution ratio

the preliminary adsorption test. From the data, it's possible to observe the increase in the percentage of Pb removal up until the ratio 1/50, which is close to the maximum removal



**Table 3** Adsorption efficiency for peats from the Mogi-Guaçu river (Brazil), at an initial concentration of 150 mg L<sup>-1</sup> and a peat solution ratio of 1/50

Elements	Adsorption efficiency	
	Peat 1 (%)	Peat 2 (%)
Pb	93.2	93.6
Zn	48.2	39.8
Cd	37.8	23.6

(being that 99% of removal is at ratio 1/50). For the following ratios (1/10 and 1/5), the efficiency reaches 100%. Thus, the 1/50 ratio was considered satisfactory and feasible for subsequent adsorption tests (Table 3).

For the adsorption of Pb, Zn and Cd at initial concentration of 150 mg L<sup>-1</sup>, the ratio of 1/50 was used. During the test there was no significant variation of pH or electrical conductivity in any of the samples. Lead ion removal from solutions was high for both peats (peat 1: 93.2%, peat 2: 93.6%—Table 3). While the removal of zinc and cadmium were lower (peat 1: Zn-48.2% and Cd-37.8%; peat 2: Zn-39.8% and Cd-23.6%). Peat 1 showed to be more adsorbent for Zn and Cd. Metal ions were removed in a descending order, Pb > Zn > Cd, for both peats, showing the affinity of the sorbent surface for lead. For (Kalmykova et al. 2008), the preference for Pb<sup>2+</sup> could be explained through the binding of specific chelating groups in peats. In their studies, (Kalmykova et al. 2008) showed the metal ions were removed in the following order: Pb > Cd > Zn.

## 4 Conclusions

Both peats from the Mogi-Guaçu River Basin in São Paulo State (Brazil) have organic matter content considered relatively low, compared with the average content in other studies about peats. Still, other results like the CEC, the natural condition of pH (pH<sub>H<sub>2</sub>O</sub>), the ΔpH and the point of zero salt effect showed a predominance of negative charges in the material and characteristics favorable for potentially toxic metal ion adsorption.

The peats were classified as moderately and moderately highly decomposed peats (H5 and H6), according the Von Post scale of humification, but with high levels of fiber. They also had a high ash content. Those characteristics are considered typical for tropical peats, especially for peats from São Paulo state. However, they are characteristics that may influence the adsorption efficiency.

Adsorption pre-tests demonstrated that the maximum efficiency of lead adsorption is reached (or very close to maximum) at a ratio of 1/50 (peat/solution). The metals were removed in the descending order of Pb > Zn > Cd, showing the affinity of both materials for lead. Pb was 93% removed from the solution at an initial concentration of 150 mg L<sup>-1</sup> and a ratio of 1/50.

The results of this study indicated that both peats are promising materials to be used in adsorption techniques for contaminated mining areas. However, only effective adsorption tests can prove this efficiency and reveal their potential for future use as protective barriers against contamination.

**Acknowledgements** The authors are grateful for the National Council for Scientific and Technological Development (CNPq) for financial support (305096/2015-0) and for their PhD fellowship (54134/2016-3). The authors also thank the São Paulo Research foundation (FAPESP) for a research fellowship (2014/07180-7) and for a scholarship (2015/02529-4).

## References

- Alleoni, L.R., Mello, J.M.V., Rocha, W.S.D.: Electrochemistry, adsorption and ion exchange in soil. In: Mello, J.W., Alleoni, L. R. (eds.) *Chemistry and Mineralogy of Soil*, chap. XII, vol. 2, pp. 69–130. Brazilian Society of Soil Science, Viçosa (2009)
- Alves, M.E., Lavorenti, A.: Point of zero salt effect relationships with clay mineralogy of representative soils of the São Paulo State Brazil. *Pedosphere* **5**(15), 545–553 (2005)
- American Society for Testing and Materials—ASTM. D4427: Standard classification of peat samples by laboratory testing (2013)
- Andriessse, J.P.: *Nature and Management of Tropical Peat Soils*, vol. 59. FAO Bulletin—Food and Agriculture Organization of the United Nations, Rome (1988)
- Brazilian Ministry of Agriculture, Livestock, and Supply: MAPA: *Manual of Official Analytical Methods for Fertilizers and Correctives*, 1st edn. MAPA, Brasília (2013). in Portuguese
- Brazilian Public Agricultural Research Corporation: EMBRAPA: *Manual of Methods of Soil Analysis*, 2nd edn. EMBRAPA, Rio de Janeiro (2011). in Portuguese
- Cabral Junior, M., Motta, J.F.M., Mello, I.S.C., Tanno, L.C., Sintoni, A., Salvador, E.D., Chierigatti, L.A.: Mineral resources of the fenerozoic in São Paulo State. *Geociências* **20**(1), 105–159 (2001). (in Portuguese)
- Crescêncio Junior, F.: Study in laboratory for peats as a reactive barrier in aquifers remediation. PhD thesis at Universidade Federal do Rio de Janeiro. Rio de Janeiro (2008) (in Portuguese)
- Delicato, D.M.S.: Physical-chemical properties and sorption characteristics of peat. PhD thesis Dublin City University, Dublin (1996)
- Dick, D.P., Novotny, E.H., Dieckow, J., Bayer, C.: Chemistry of soil organic matter. In: Mello, J.W., Alleoni, L.R. (eds.) *Chemistry and Mineralogy of Soil*, chap. XII, vol. 2, pp. 69–130. Brazilian Society of Soil Science, Viçosa (2009)
- Gisi, S.D., Lofrano, G., Grassi, M., Notarnicola, M.: Characteristics and adsorption capacities of low-cost sorbents for wastewater treatment: a review. *Sustain. Mater. Technol.* **9**, 10–40 (2016)
- Grover, S.P.P., Baldock, J.A.: The link between peat hydrology and decomposition: Beyond von Post. *J. Hydrol.* **479**, 130–138 (2013)

- Huat, B.B.K., Kazemian, S., Prasad, A., Barghchi, M.: State of an art review of peat: general perspective. *Int. J. Phys. Sci.* **6**(8), 1988–1996 (2011)
- Kalmykova, Y., Strömvall, A.N., Steenari, B.M.: Adsorption of Cd, Cu, Ni, Pb and Zn on Sphagnum peat from solutions with low metal concentrations. *J. Hazard. Mater.* **152**(2), 885–891 (2008)
- Kiehl, E.J.: *Organic Fertilizers*. Ceres Agronomic Publisher, Piracicaba (1985). (in Portuguese)
- Kocasoy, G., Guvener, Z.: Efficiency of compost in the removal of heavy metals from the industrial wastewater. *Environ. Geol.* **57**, 291–296 (2009)
- Mekaru, T., Uehara, G.: Anion adsorption in ferruginous tropical soils. *Soil Sci. Soc. Am. Proc.* **36**(2), 296–300 (1972)
- Oliveira, L.K., Melo, C.A., Goveia, D., Lobo, F.A., Armienta Hernández, M.A., Fraceto, L.F., Rosa, A.H.: Adsorption/desorption of arsenic by tropical peat: influence of organic matter, iron and aluminium. *Environ. Technol.* **36**(1–4), 149–159 (2014)
- Petroni, S.L.G., Pires, M.A.F., Munita, C.S.: Use of radiotracer in adsorption studies of copper on peat. *J. Radioanal. Nucl. Chem.* **259**(2), 239–243 (2004)
- Raimondi, I.M.: Geological and geotechnical characterization of mining tailings—Adrianópolis (PR). Master thesis at São Paulo University, São Carlos (2014) (in Portuguese)
- Rezanezhad, F., Price, J.S., Quinton, W.L., Lennartz, B., Milojevic, T., Van Cappellen, P.: Structure of peat soils and implications for water storage, flow and solute transport: a review update for geochemists. *Chem. Geol.* **429**, 75–84 (2016)
- Roy, W.R., Krapac, I.G., Chou, S.F.J., Griffin, R.A.: Batch Type Procedures for Estimating Soil Adsorption of Chemicals. Technical resource document. EPA/530-SW-87-006-F, Cincinnati, EUA (1992)
- Silva, M.L.N., Curi, N., Marques, J.J.G.S.M., Guilherme, L.R.G., Lima, J.M.: Point of zero salt effect and its relations with mineralogical and chemical properties of Brazilian latosols. *Pesquisa agropecuária brasileira* **31**(9), 663–671 (1996). (in Portuguese)
- Sparks, D.L.: *Environmental Soil Chemistry*. Academic Press, San Diego, California (1995)
- Sposito, G.: *The Surface Chemistry of Soils*. Oxford University Press, New York (1984)
- Tripathi, A., Ranjan, M.R.: Heavy metal removal from wastewater using low cost adsorbents. *Bioremediat. Biodegradation* **6**(6), 1–5 (2015)
- Wust, R.A.J., Bustin, R.M., Lavkulich, L.M.: New classification systems for tropical organic-rich deposits based on studies of the Tasek Bera Basin, Malaysia. *Catena* **53**, 133–163 (2003)
- Yonebayashi, K., Okazaki, M., Pechayapisit, J.: Woody fragments in tropical peat soils. In: Kyuma, K., Vijarnsorn, P., Zakaria, A. (eds.) *Coastal Lowland Ecosystems in Southern Thailand and Malaysia*. Showado-Printing, Kyoto (1992)
- Zuquette, L.Z., Silva Júnior, E.M., Garcia, A.: Sorption aspects for the unconsolidated materials of the region of São Carlos (SP), Brazil (In Portuguese). *Revista Escola de Minas* **61**(2), 219–230 (2008)

# Carolina Piedmont Groundwater System— Existence of the Transition Zone Between Regolith and Bedrock

Malcolm F. Schaeffer

## Abstract

The groundwater system in the Carolina Piedmont Province is comprised of two interconnected layers: regolith (residuum/saprolite and weathered rock) overlying fractured crystalline bedrock. The presence of a transition zone (TZ) at the base of the regolith has been interpreted in many areas of the Piedmont and is theorized to be the most permeable part of the system. Most information supporting the existence of the TZ is qualitative and based on observations made during drilling operations. A database of 1410 horizontal conductivity measurements in boreholes at 12 locations in the Piedmont is utilized to quantitatively assess the existence of the TZ. Hydraulic conductivity measurements are grouped into four hydrostratigraphic units based on Standard Penetration Testing (N-Values) and Rock Core Recovery (REC)/Rock Quality Designation (RQD): (1) M1—Soil/Saprolite;  $N < 50$ , (2) M2—Saprolite/Weathered Rock;  $N \geq 50$  or  $REC < 50\%$ , (3) WF—Partially Weathered/Fractured Rock—TZ;  $REC \geq 50\%$  and  $RQD < 50\%$ , and (4) D/BR—Sound Rock;  $REC \geq 85\%$  and  $RQD \geq 50\%$ . The 12 locations are grouped into two conceptual models for Piedmont bedrock: layered/foliated bedrock and massive/plutonic bedrock. The following hypothesis was formulated corresponding to the definition of the TZ in the literature: the hydraulic conductivity of the TZ is greater than the hydraulic conductivity of both the overlying regolith and underlying bedrock. The hypothesis was statistically tested on the two conceptual models utilizing a 2-Sample T-Test on the log values of the hydraulic conductivity measurements. Results indicate a TZ of higher hydraulic conductivity exists between regolith and bedrock in both conceptual models.

## Keywords

Piedmont province • Transition zone • Hydraulic conductivity

## 1 Introduction

A database of in situ horizontal hydraulic conductivity ( $k_h$ ) measurements in soil and bedrock (open borehole falling head and constant head, slug, and pressure [packer] tests in boreholes) has been compiled over the years by the author. It comprises 1410 measurements (including 1239 measurements from studies in which the author has been directly involved) collected at 12 locations in the Carolina Piedmont Province (Piedmont; Fig. 1). The database is used to quantitatively assess the existence of a transition zone between the regolith and crystalline bedrock for two conceptual bedrock groundwater models of the Piedmont.

## 2 Piedmont Groundwater System

The groundwater system in the Piedmont comprises two interconnected layers, or mediums: Layer 1—regolith consisting of residuum/saprolite and weathered rock overlying Layer 2—fractured crystalline bedrock (Fig. 2) (Heath 1980; Harned and Daniel 1992). In Layer 1, a thoroughly weathered and structureless material termed residuum (soil) occurs near the ground surface with the degree of weathering decreasing with depth. The residuum grades into a coarser-grained material (saprolite), which retains the structure of the parent bedrock. Partially weathered/fractured bedrock occurs beneath the saprolite and grades with depth into sound bedrock. Because the mantle of residual soil, saprolite, and weathered rock that forms Layer 1 is a product of near-surface weathering, its lateral extent is largely unconstrained by geologic contacts present in the underlying parent bedrock (LeGrand 1988). It thus forms a hydrogeologic unit that

M. F. Schaeffer (✉)

HDR Engineering, Inc. of the Carolinas, 440 South Church Street,  
Suite 900, Charlotte, NC 28202-2075, USA  
e-mail: malcolm.schaeffer@hdrinc.com

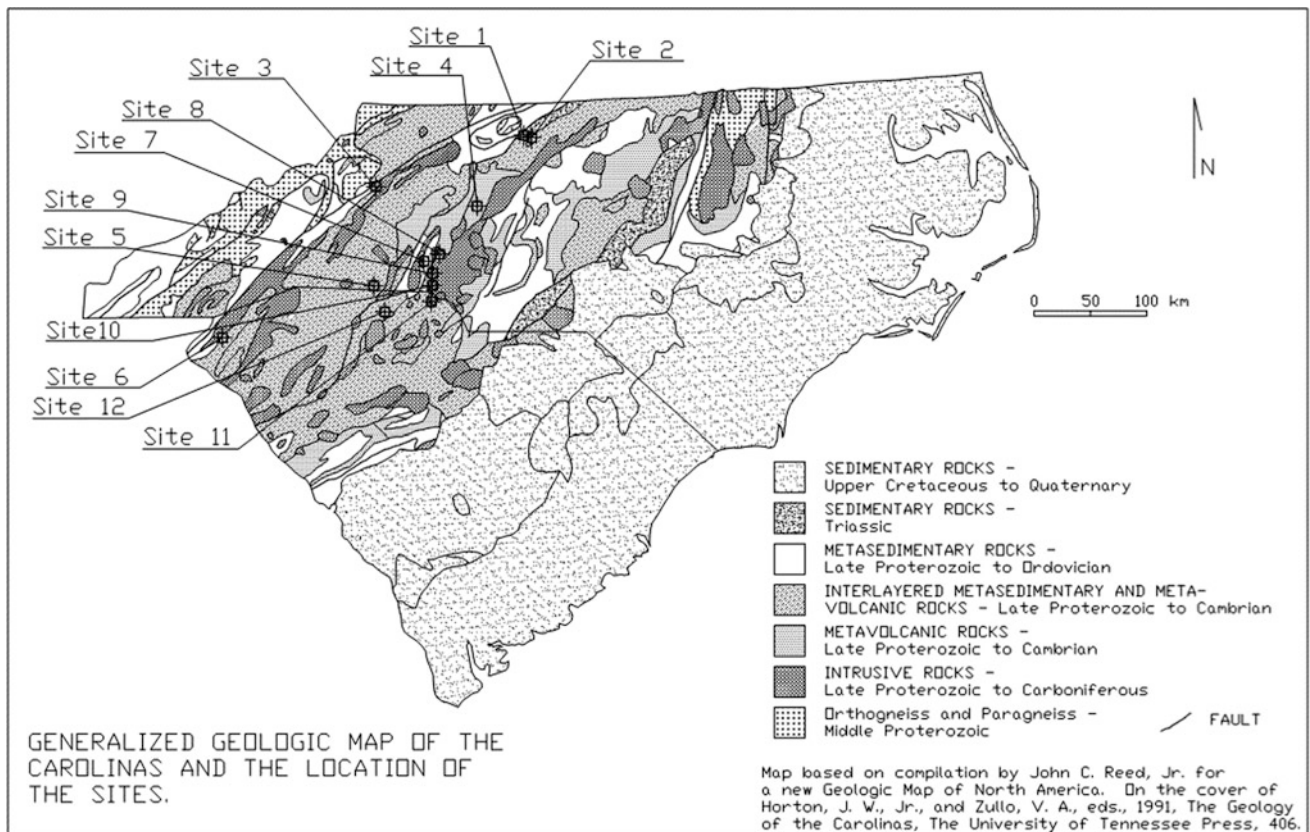


**Fig. 1** Generalized geologic map of the Carolinas showing the location of the 12 sites from which in situ horizontal hydraulic conductivity ( $k_h$ ) measurements were collected (Reed 1991)

commonly includes variably weathered remnants of various types of rock and provides an intergranular medium through which the recharge and discharge of water into and from the underlying fractured rock occurs (LeGrand 1988). Layer 2 consists of fractured, nonporous crystalline bedrock in which groundwater occurs along planes of secondary porosity (fractures). The fractures control both the hydraulic conductivity and storage capacity of the rock mass (Heath 1980; Singhal and Gupta 2010). A transition zone (TZ) at the base of the regolith has been interpreted to be present in many areas of the Piedmont. The zone consists of partially weathered bedrock and lesser amounts of saprolite that grades downward into competent bedrock and has been described as “being the most permeable part of the system, even slightly more permeable than the soil zone” (Harned and Daniel 1992). The TZ may serve as a conduit for rapid groundwater flow and has the potential for enhanced migration of contaminated groundwater (Harned and Daniel 1992).

Most information supporting the existence of the TZ in the Piedmont is qualitative and based on observations made during drilling of boreholes and water wells (Harned and Daniel 1992; Daniel and Sharpless 1983; Daniel 1989). Some quantitative data are available for the existence of the

TZ at locations in the Piedmont of Georgia (Stewart 1962, 1964), Maryland (Nutter and Otton 1969), and North Carolina (Daniel and Sharpless 1983; Daniel 1996), but in general, very little substantial quantitative data are available for the Piedmont region that support the presence of a TZ.

Characteristics of a TZ may vary due to different rock types and associated rock structure (Harned and Daniel 1992). Harned and Daniel (1992) proposed two conceptual models for Piedmont bedrock: (A) foliated/layered bedrock and (B) massive/plutonic bedrock (Fig. 3). Strongly foliated/layered crystalline rocks (metasedimentary and metavolcanic) are thought to have a well-developed, distinct TZ due to enhanced water infiltration and weathering along intersecting foliation planes and joints, resulting in the generation of numerous rock fragments (Harned and Daniel 1992). More massive rocks, such as plutonic and metaplutonic bodies, are thought to develop an indistinct TZ as foliation planes and compositional layering are typically absent or far less pervasively developed than in foliated/layered bedrock (Harned and Daniel 1992). As a result, plutonic and metaplutonic bodies tend to weather along relatively widely spaced fractures (Harned and Daniel 1992).

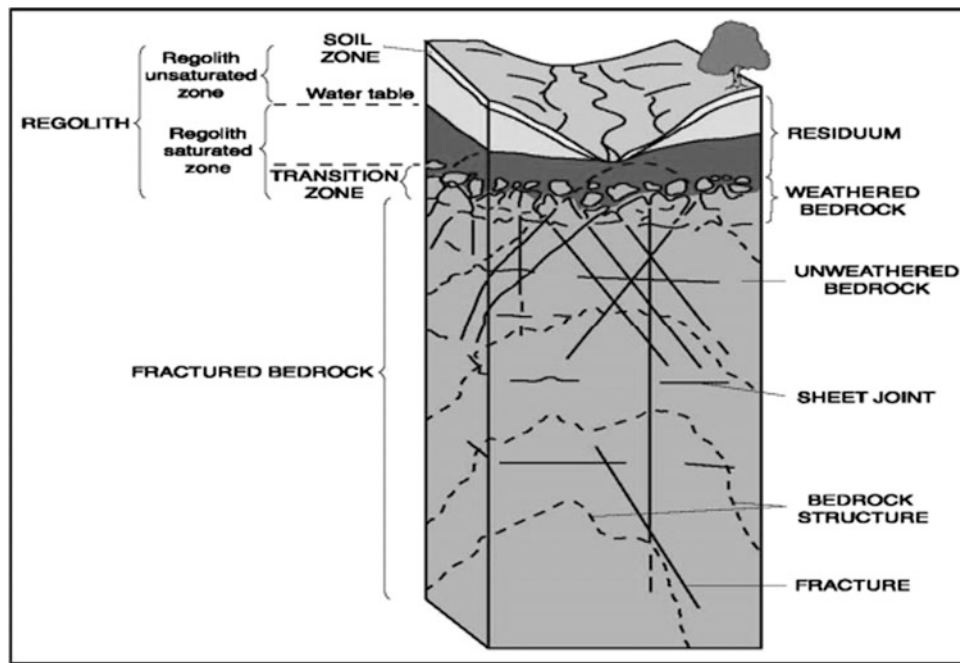


**Fig. 2** Groundwater system in the Carolina Piedmont Province (Harned and Daniel 1992)

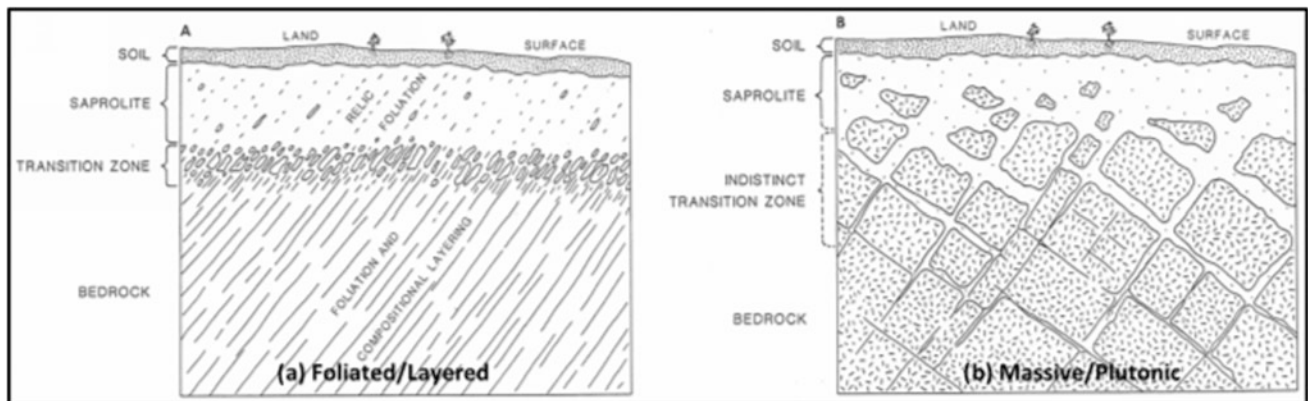


**Fig. 3** Conceptual models for Piedmont crystalline bedrock (Harned and Daniel 1992)

In this study, the two-layer Piedmont groundwater system is further divided into four hydrostratigraphic units based on Standard Penetration Testing (SPT; N-Values) and Rock Core Recovery (REC)/Rock Quality Designation (RQD) for the analysis of the hydraulic conductivity data: (1) M1–Soil/Saprolite,  $N < 50$ ; (2) M2–Saprolite/Weathered Rock,  $N \geq 50$  or  $REC < 50\%$ ; (3) WF/TZ–Partially Weathered/Fractured Rock,  $REC \geq 50\%$  and  $RQD < 50\%$ ; and (4) D/BR–Sound Rock (bedrock),  $REC \geq 85\%$  and  $RQD \geq 50\%$ . The M1 and M2 units correspond to Layer 1, the D/BR unit corresponds to Layer 2, and the WF/TZ unit corresponds to the TZ of the groundwater system.

### 3 Geology of the Sites

Sites 1 through 6 are foliated/layered sites (Conceptual Model A). Site 1 is in the Dan River Basin within the Milton terrane and is underlain by conglomerate, sandstone, siltstone, mudstone, and shale with little to no primary porosity (Heath 1992; Thayer and Robbins 1992). Site 2 is in the Milton terrane and is underlain by a complexly folded and faulted sequence of interlayered mica schist, schistose mica gneiss, augen gneiss, flaser gneiss, quartzo-feldspathic gneiss, and biotite gneiss, with minor hornblende schist

and gneiss. Site 3 is in the Tugaloo terrane of the Inner Piedmont zone and is underlain by interlayered biotite gneiss, augen biotite gneiss, mica schist, and garnet mica schist with minor amphibolite. Site 4 is in the Charlotte terrane of the Carolina superterrane and is underlain by a felsic to mafic metavolcanic sequence of tuffs and flows metamorphosed to amphibolite grade. Site 5 is located in the Cat Square terrane within the Inner Piedmont zone and consists of interlayered mica gneiss, mica schist, and sillimanite-mica schist, with minor quartzite and biotite gneiss. Site 6 is located in the Tugaloo terrane of the Inner Piedmont and is underlain by interlayered, strongly foliated and layered granitic gneiss and biotite-hornblende gneiss and schist with granitic gneiss being dominant.

Sites 7 through 12 are massive/plutonic sites (Conceptual Model B). Site 7 is located primarily in the Charlotte terrane with a portion underlain by the Kings Mountain terrane within the Carolina superterrane. It is underlain by an igneous and metaigneous complex consisting of meta-quartz diorite and metavolcanic rocks of granodioritic composition intruded by biotite granite. Site 8 is in the Charlotte terrane of the Carolina superterrane and is underlain by granite and quartz diorite. Sites 9, 10, and 11 are located in the Charlotte terrane of the Carolina superterrane and are underlain by a metaigneous complex consisting of meta-quartz diorite and meta-diorite intruded by meta-diabase dikes. Site 12 is located in the Kings Mountain terrane of the Carolina superterrane and is underlain by meta-granodiorite intruded by meta-quartz diorite and meta-diabase dikes.

#### 4 Hydraulic Conductivity Data

A database of 1410 horizontal hydraulic conductivity ( $k_h$ ) measurements in boreholes at the 12 locations in the Piedmont has been compiled from results of in situ borehole tests (both falling and constant head tests in soil/saprolite/ weathered rock), slug tests in piezometers and groundwater

monitoring wells (in soil/saprolite/ weathered rock/bedrock) and pressure (packer) testing (in bedrock). The hydraulic conductivity measurements at each site are grouped into the four hydrostratigraphic units defined by SPT testing and rock core REC/RQD. The 12 locations were classified into the two conceptual models based on variation of TZ characteristics due to rock type/structure: the foliated/layered bedrock model (Conceptual Model A—Sites 1 to 6; Fig. 1) and the massive/plutonic bedrock model (Conceptual Model B—Sites 7 to 12; Fig. 1). A total of 1339 measurements were used in the statistical analysis; 71 measurements were eliminated from the analysis because they crossed the defined hydrostratigraphic units.

The hydraulic conductivity measurements in each hydrostratigraphic unit have a log normal distribution (Schaeffer 2009; Schaeffer and Townsend 2016). Table 1 summarizes hydraulic conductivity values for the two conceptual models based on the geometric mean and geometric standard deviation of the data ( $k_h(m) = 10^{(u)}$  and  $k_h(m \pm 1 SD) = 10^{(u \pm 1SD)}$  where  $u$  is the mean of the normal distribution of the log ( $k$ ) values and SD is the standard deviation of the log values for the various hydrostratigraphic units). Figure 4 presents the data in graphical form.

#### 5 Statistical Analysis

To investigate the existence of the TZ in the Piedmont, the following hypothesis was formulated based on the definition of the TZ postulated in the literature: the hydraulic conductivity of the TZ is greater than the hydraulic conductivity of both the directly overlying regolith (saprolite/ weathered rock, M2) and underlying bedrock (D/BR). The hypothesis was tested two ways: (1) the mean values of the hydrostratigraphic unit grouped data were compared to verify the mean  $k_h$  of the WF/TZ is greater than both the mean  $k_h$  of the overlying M2 unit and the mean  $k_h$  of the underlying D/BR unit; and (2) the mean values of the grouped

**Table 1** Statistical summary of horizontal hydraulic conductivity ( $k_h$ ) data for the two conceptual models of the Carolina Piedmont Province

Conceptual model	Hydrostratigraphic unit	Count (N)	GeoMean (cm/sec)	+1 standard deviation (cm/sec)	-1 standard deviation (cm/sec)	Median (cm/sec)
Foliated/Layered model (A)	M1	137	1.9E-04	1.5E-03	2.4E-05	2.2E-04
	M2	62	9.9E-05	7.5E-04	1.3E-05	1.0E-04
	WF/TZ	168	4.8E-04	3.0E-03	7.9E-05	6.7E-04
	D/BR	337	7.9E-05	8.5E-04	7.3E-06	8.6E-05
Massive/Plutonic model (B)	M1	161	2.4E-04	2.0E-03	2.8E-05	3.1E-04
	M2	79	1.1E-04	1.0E-03	1.2E-05	1.3E-04
	WF/TZ	115	2.2E-04	1.6E-03	2.9E-05	2.4E-04
	D/BR	280	4.2E-05	4.8E-04	3.6E-06	4.6E-05

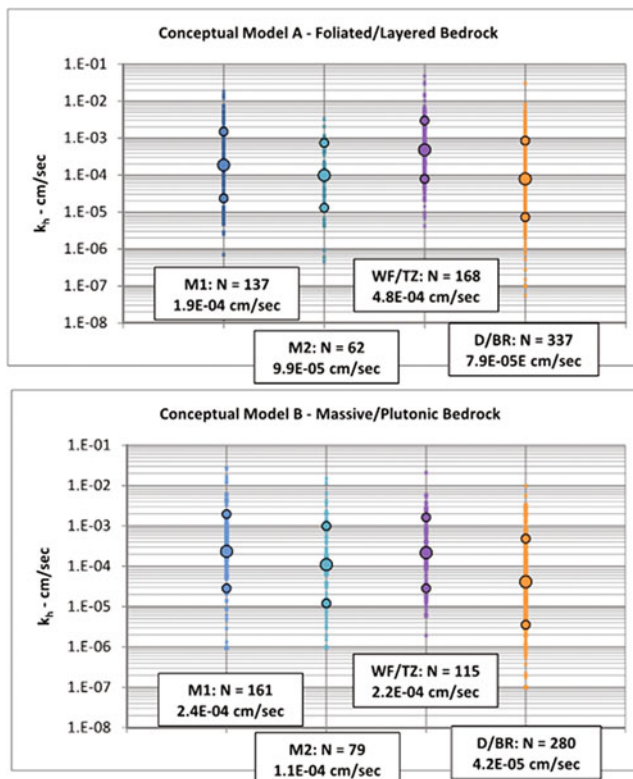


**Fig. 4** Graphs of horizontal hydraulic conductivity ( $k_h$ ) to the hydrostratigraphic units for the two conceptual groundwater bedrock models. Large circles represent the mean; smaller circles represent the mean plus and minus one standard deviation. The boxes show the hydrostratigraphic unit, the number of measurements, N, for each unit, and the mean horizontal conductivity,  $k_h$ , of the unit

hydrostratigraphic unit data for the two conceptual models were statistically compared to determine if the mean values are statistically different. The 2-Sample T-Test was used to compare the population mean values of the hydrostratigraphic units at the 0.05 significance level for the two conceptual models.

The assumptions for the test are: (1) both sampled populations have relative frequency distributions that are approximately normal, (2) the population variances are equal for small samples ( $N < 30$ ), and (3) the samples are random and independently selected from the population. The T-Test is also appropriate for large samples ( $N \geq 30$ ) with normally distributed populations and unknown population variances (McClave and Sincich 1997). The M1, M2, and WF/TZ units sample data are random. The D/BR unit sample data are not entirely random. They are skewed toward higher hydraulic conductivity values, as packer tests were generally performed in boreholes where the rock core included natural fractures and slug tests were performed in piezometers or monitoring wells with screens set across fractured rock zones. The hydraulic conductivity values of the defined hydrostratigraphic units have a log normal distribution; the logs of the values have a normal distribution (Fig. 4)

(Schaeffer 2009; Schaeffer and Townsend 2016). The 2-Sample T-Tests (two-tailed tests at the 0.05 significance level) are made on the  $\log(k_h)$  values of the data.

As shown in Table 1 and Fig. 4, the mean hydraulic conductivity value of the WF/TZ unit is greater than the mean values of the overlying M2 unit and underlying D/BR unit for both conceptual models consistent with the hypothesis put forth for the TZ. Results of the 2-Sample T-Tests between the hydrostratigraphic units for the two conceptual models are shown in Table 2. The means of the overlying M2 unit and the underlying D/BR unit are not equal to and are less the means of the WF/TZ unit for both conceptual models indicating a TZ of higher horizontal conductivity is present between regolith and bedrock when considering the two conceptual bedrock models of the Piedmont groundwater system.

## 6 Discussion

Many researchers over the years have indicated that identification of the TZ can be subjective, requiring careful observations of rock core. As a result, accurately describing and delineating the boundaries of the TZ can be difficult. Common descriptions of the TZ in the literature include:

- “partially weathered bedrock and lesser amounts of saprolite with particles ranging in size from clays to large boulders of unweathered bedrock” (Daniel and Harned 1998; Cunningham and Daniel 2001);
- “partially weathered, highly fractured rock that has dominant anisotropy from fractures and retains some primary porosity” (Chapman et al. 2001);
- “partially weathered bedrock and numerous, open, low-angle fractures” (Chapman et al. 2001);
- “bedrock that is weathered and altered, but not to the degree needed to create sand- and gravel-size particles and/or substantial clay minerals” (Daniel 1990);
- “slightly weathered rock with some subhorizontal fractures” (McSwain et al. 2005); and
- “numerous open fractures in partially weathered to competent rock” (Pippen et al. 2008).

The TZ at the study sites can be described by one or more of the preceding descriptions. A motivating factor in using a strict definition based on SPT N-Values and rock core REC/RQD values for the hydrostratigraphic units and the TZ in particular was to provide an objective approach for defining the TZ as an alternative to reliance on a subjective, descriptive approach.

Based on the results of statistical testing of the combined data, it is possible to define and delineate the TZ in the Piedmont in the context of both the foliated/layered and

**Table 2** Results of 2-Sample T-Tests for the hydrostratigraphic units for the two conceptual models of the Piedmont groundwater system comparing the mean horizontal hydraulic conductivities ( $k_h$ ). A = Accept the null hypothesis, the mean values are equal; R = Reject the null hypothesis, the mean values are not equal

<i>Concept A—foliated/layered: 2-sample T-tests</i>				
	M1	M2	WF/TZ	D/BR
M1		R	R	R
M2			R	A
WF/TZ				R
<i>Concept B—massive/plutonic: 2-sample T-tests</i>				
	M1	M2	WF/TZ	D/BR
M1		R	A	R
M2			R	R
WF/TZ				R

massive/plutonic conceptual models. The mean hydraulic conductivity of the TZ is greater than that of the overlying M2 and underlying D/BR units at all six foliated/layered sites (Schaeffer and Townsend 2016), consistent with Harned and Daniel (1992) hypothesis that these sites would have a well-developed TZ. Such consistency was not uniformly observed at the massive/plutonic sites (Schaeffer 2009; Schaeffer and Townsend 2016). Two sites (Sites 9 and 11), underlain by a metaigneous complex consisting of meta-quartz diorite and meta-diorite intruded by meta-diorite dikes, do not have a TZ as defined by SPT N-values and REC/RQD values and associated hydraulic conductivity values (Schaeffer 2009; Schaeffer and Townsend 2016). There is instead a decrease in hydraulic conductivity with depth in the four hydrostratigraphic units, with no enhanced hydraulic conductivity suggestive of a TZ at the interface between regolith and bedrock. Both sites have very thick soil/saprolite zones (15 to 85 m thick) (Schaeffer and Townsend 2016). Site 10, however, underlain by the same metaigneous complex and characterized by similar soil/saprolite thicknesses does have a TZ based on the methodology described herein (Schaeffer and Townsend 2016). Harned and Daniel (1992) indicated that massive/plutonic bedrock sequences sometimes have a non-distinct TZ and the hydraulic conductivity measurements at these three sites support this conclusion. A distinct TZ may be absent in some Piedmont massive/plutonic rock sequences, but is expected in Piedmont foliated/layered sequences.

3-D models of the sites utilizing the hydrostratigraphic units as defined in this study show, within the limits of the modeling methodology, the highly variable geometry and complexity of the TZ (Schaeffer 2011, 2014). The TZ is not a continuous layer between regolith and bedrock; the thickness is variable within short distances and can be locally absent. The thinning, thickening, or absence of the TZ is directly related to the characteristics of the underlying bedrock (Schaeffer 2011, 2014).

## 7 Conclusions

The methodology described herein is recommended as a reliable, objective means of defining the TZ (and the other hydrostratigraphic units) as part of groundwater studies in the Piedmont where SPT testing and rock core REC/RQD values are available. It is supported by the statistical analysis showing higher hydraulic conductivity values in the TZ than in the overlying regolith and underlying bedrock when considering the two conceptual groundwater bedrock models, in particular for the foliated/layered model and in general for the massive/plutonic model, for Piedmont crystalline bedrock.

**Acknowledgements** The data presented in this paper represents the work of a large group of geologists, engineers, and field technicians involved in field data collection as well as data reduction and analysis in the office. Their considerable contribution is acknowledged. Sarah Townsend reviewed several drafts of the abstract submitted for the meeting and greatly improved it. The paper has benefited from and been improved by reviews by Dave Campbell, Tracy Campbell, Carey Fraser, Steve Godfrey, Sarah Townsend, Ryan Tinsley, Richard Walther, and two anonymous reviewers for the proceedings volume. The author is responsible for all errors that may remain.

## References

- Chapman, M.J., Bolich, R.E., Huffman, B.A.: Hydrogeologic setting, ground-water flow, and ground-water quality at the Lake Wheeler Road Research Station, 2001–2003, North Carolina Piedmont and Mountains Resource Evaluation Program. U. S Geological Survey Scientific Investigations Report 2005-5166 (2005)
- Cunningham, W.L., Daniel, C.C.III: Investigation of ground-water availability and quality in Orange County, North Carolina. U. S. Geological Survey Water-Resources Investigations Report 00-4286 (2001)
- Daniel, C.C., III: Statistical analysis relating well yield to construction practices and siting of wells in the Piedmont and Blue Ridge Provinces of North Carolina. U. S. Geological Survey Water-Supply Paper 2341-A (1989)



- Daniel, C.C., III: Evaluation of site-selection criteria, well design, monitoring techniques, and cost analysis for a ground-water supply in Piedmont Crystalline Rocks, North Carolina. U. S. Geological Survey Water-Supply Paper 2341, Chapter B (1990)
- Daniel, C.C., III: Ground-water recharge to the regolith-fractured rock crystalline rock aquifer system, Orange County, North Carolina. U. S. Geological Survey, Water-Resources Investigations Report 96-4220 (1996)
- Daniel, C.C., III, Harned, D.A.: Ground-water recharge and storage in the regolith-fractured crystalline rock aquifer system, Guilford County, North Carolina. U. S. Geological Survey Water-Resources Investigations Report 97-4140 (1998)
- Daniel, C.C., III, Sharpless, N.B.: Ground-water supply potential and procedures for well-site selection in the Upper Cape Fear River Basin. North Carolina Department of Natural Resources and Community Development, North Carolina (1983)
- Harned, D.A., Daniel, C.C., III: The transition zone between bedrock and regolith: Conduit for contamination? In: Daniel, C.C., III, White, R.K., Stone, P.A. (eds.) Proceedings of a Conference on Ground Water in the Piedmont of the Eastern United States, pp. 336–348. Clemson University, Clemson, South Carolina (1992)
- Heath, R.C.: Basic elements of ground-water hydrology with references to conditions in North Carolina. U. S. Geological Survey Water-Resources Open-File Report 80-44 (1980)
- LeGrand, H.E.: Region 21, Piedmont and Blue Ridge. In: Black, W., Rosenhein, J.S., Seaber, P.R. (eds.) Hydrogeology. Geological Society of America, The Geology of North America, vol. 2, pp. 201–208. Boulder, Colorado (1988)
- McClave, J.T., Sincich, T.: A First Course in Statistics, 6th edn. Prentice Hall, Upper Saddle River, New Jersey (1997)
- McSwain, K.B., Bolich, R.E., Chapman, M.J., Huffman, B.A.: Water-resources data and hydrogeologic setting at the Raleigh Hydrogeologic Research Station, Wake County, North Carolina, 2005–2007. U. S. Geological Survey Open-File Report 2008-1377 (2008)
- Nutter, L.J., Otton, E.G.: Ground-water occurrence in the Maryland Piedmont: Maryland Geological Survey Report of Investigations, No. 10 (1969)
- Pippen, C.G., Chapman, M.J., Huffman, B.A., Heller, M.J., Schelgel, M.E.: Hydrogeologic setting, ground-water flow, and ground-water quality at the Langtree Peninsula Research Station, Iredell County, North Carolina. U. S. Geological Survey Scientific Investigations Report 2008-5255 (2008)
- Reed Jr., J.C.: Geologic map of North America. In: Horton Jr., J.W., Zullo, V.A. (eds.) The Geology of the Carolinas. University of Tennessee Press, Knoxville, Cover (1991)
- Schaeffer, M.F.: Hydraulic conductivity of the Carolina Piedmont soil and bedrock: Is a transition zone present between the regolith and bedrock? In: 17th Annual David S. Snipes/Clemson Hydrogeology Symposium, pp. 32–36. Clemson, South Carolina (2009)
- Schaeffer, M.F.: Carolina Piedmont groundwater system: what does the transition zone look like? In: 19th Annual David S. Snipes/Clemson Hydrogeology Symposium, pp. 43–44. Clemson, South Carolina (2011)
- Schaeffer, M.F.: Piedmont groundwater system, Part 2—The transition zone between regolith and bedrock: Characteristics. *Geol. Soc. Am. Abs. Program* **46**(3), 27 (2014)
- Schaeffer, M.F., Townsend, S.K.: The transition zone between regolith and bedrock in the Piedmont groundwater system: further confirmation. In: 24th Annual David S. Snipes/Clemson Hydrogeology Symposium, pp. 29–33. Clemson, South Carolina (2016)
- Singhal, B.B.S., Gupta, R.P.: Applied Hydrogeology of Fractured Rocks, 2nd edn. Springer, Dordrecht (2010)
- Stewart, J.W.: Water-yielding potential of weathered crystalline rocks at the Georgia Nuclear Laboratory. U. S. Geological Survey Professional Paper 450-B, pp. 106–107 (1962)
- Stewart, J.W.: Infiltration and permeability of weathered crystalline rocks, Georgia Nuclear Laboratory. U. S. Geological Survey Bulletin 1113-D (1964)
- Thayer, P.A., Robbins, E.L.: Sedimentology of Triassic Dan River Group, North Carolina and Virginia. In: Dennison, J.M., Stewart, K. G. (eds.) Geologic Field Guides to North Carolina and Vicinity. Southeastern Section, Geological Society of America Field Trip Guides, Geologic Guidebook No. 1, pp. 189–200, Department of Geology, University of North Carolina, Chapel Hill, North Carolina (1992)



# The Consequences of Pyrite Degradation During Construction—UK Perspective

M. A. Czerewko and J. C. Cripps

## Abstract

Whilst it is recognised that aggressive ground conditions are associated with a wide range of factors encompassing physical, chemical and biological processes, a high proportion of such problems relate to the presence of sulfate ions in groundwater. Such conditions, which are implicated in the degenerative attack on ground-placed engineering materials and sometimes to volume changes, arise due either to the dissolution of primary sulfate minerals or, more commonly, to the oxidation of sulfide minerals, where in the latter case the groundwater may also become acidic. Notwithstanding that pyrite-bearing strata are distributed widely across the UK and are frequently encountered in foundation works and during the construction and improvement of the arterial highway infrastructure, consideration of the possible adverse implications of pyrite for construction and highway works tends to be overlooked. Furthermore, adverse impacts can develop rapidly during construction in periods of adverse weather, whereas under favourable conditions they would not be suspected. Equipping the design team with the necessary information to identify and address the problems should enable an optimum construction sequence and on-going management during the design life of the structure to be used. British, European and other standards promote good practice in carrying out ground investigations, but often potential problems are not adequately anticipated and catered for. The paper discusses reasons for this and provides guidance on avoiding problems, without the need to preclude the inclusion of the sulfur bearing materials from projects.

## Keywords

Pyrite • Mudrocks • Gypsum

## 1 Introduction

Sulfur is one of the most abundant elements in the earth's crust and occurs as a solid, liquid and gas. It is highly mobile and can change form and properties rapidly in response to changes in the environment, such as those brought about by and in the course of ground engineering works. In geological and construction materials sulfur commonly occurs as sulfates in solution or as crystals of selenite/gypsum:  $\text{Ca}_2\text{SO}_4 \cdot 2\text{H}_2\text{O}$  and in a reduced form (pyrite:  $\text{FeS}_2$ ) and other sulfides (pyrrhotite ( $\text{FeS}$ ) and marcasite  $\text{FeS}_2$ ). It may also occur in organic compounds and waste products from industrial and mining operations. Hence deposits containing sulfur compounds are widely distributed and are frequently encountered in civil and environmental engineering projects (Czerewko et al. 2016). Not all forms of sulfur are troublesome for construction, although this depends upon the environmental conditions. For example barytes, celestine, and organic sulfur are relatively stable in weathering environments, and do not normally contribute to the sulfur present in groundwater. This paper discussed examples from the UK, but cases of structural damage caused by expansion of pyritic mudstone have also been documented on a number of occasions from areas of USA (Hoover and Lehman 2009) and Canada (Quigley and Vogin 1970).

BRE (1991) have provided guidance for routine UK assessment of potential ground aggressivity based upon water and acid soluble sulfate content and acidity of soil and groundwater samples, this worked well for many decades with few instances of sulfate attack on buried concrete reported. However following investigation of sulfate attack and disruptive ground heave cases, Hawkins and Pinches (1987) noted that the possible consequences of pyrite were not being considered. As a result of this, problems of the

M. A. Czerewko (✉)  
AECOM, Chesterfield, S41 7SL, UK  
e-mail: mourice.czerewko@aecom.com

J. C. Cripps  
Department of Civil and Structural Engineering,  
University of Sheffield, Sheffield, S1 3JD, UK

types listed below due to the presence of pyrite, were not being identified:

- Rapid degradation of mudrock fill, reduced permeability of limestone drainage layers and fatal production of carbon dioxide (Pye and Miller 1990);
- Heave damage to structural foundations and highway subgrades (Hawkins and Pinches 1987; Wilson 1987; Czerewko 2015);
- Rapid deterioration and degradation of natural ground material and slope failure (Vear and Curtis 1981; Steward and Cripps 1983; Czerewko et al. 2011);
- Heave problems associated with ground stabilisation for highway construction, (Snedker 1990);
- Heave in ground stabilised for foundation construction (Longworth 2004);
- Chemically aggressive conditions during tunneling and construction (Bracegirdle et al. 1996; Dunster 2001);
- Corrosion of buried steel structures (Reid et al. 2001, 2005);
- Thauasite form of concrete attack (Floyd 2003; Thauasite Expert Group 1999).

In these problems chemically aggressive soluble sulfates and acidity resulted from the oxidation of the pyrite present in the ground material or fill. Prior to 2001 appropriate guidance was not available: merely determining the total sulfate content of a soil or fill would be insufficient. But revision to recommendations for assessing structural backfills (Reid et al. 2001, 2005) and the design of concrete in aggressive ground (BRE 2001) were produced that involve not only the determination of sulfate content of material but also potential sulfate content, derived from the sulfide present.

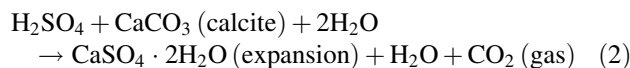
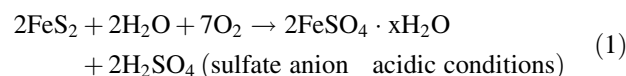
Although macroscopic crystalline pyrite ( $\text{FeS}_2$ ) is easily identified from its appearance as gold coloured cubic crystals or nodular aggregates (Fig. 1), it commonly occurs in unweathered, dark coloured, organic rich over-consolidated clays, mudrocks and argillaceous limestones as scattered microscopic crystals and clusters of microcrystals <1 to 10 microns in size, known as framboids (Fig. 2). Due to small size and black colour the latter are not visible to the naked eye. UK deposits containing pyrite in this form occur in formations from and including the Carboniferous to the Recent, such that as Fig. 3 shows they are very widely distributed. On account of a high specific surface area and lower density (Pugh et al. 1981) which can increase oxidation rate 10 fold, framboidal and microscopic forms of pyrite are susceptible to rapid breakdown when exposed to atmospheric conditions, such that problems during construction are very likely to occur.

Revised protocols for evaluating potential ground aggressiveness (Reid et al. 2001, 2005; BRE 2001) advocate a staged approach for the appraisal of ground aggressiveness based on an initial review of the geological setting, followed by a planned investigation programme and detailed ground assessment. This requires an awareness of potentially aggressive material and importance of a focused chemical testing. Besides crystal form the rate and severity of the consequences of pyrite oxidation depend on the permeability and chemistry of the host deposits as well as the ground-water conditions. It also requires that the consequences of the construction activity and weather related issues in the construction period and beyond, need to be fully addressed to provide an adequate basis for the design of appropriate preventative and mitigation measures.

## 2 Development of Pyrite Oxidation

Pyrite is unstable in the presence of both air and water during surface or-near surface weathering conditions, as shown in Eq. 1. The sulfuric acid thus liberated is aggressive to buried steel and concrete and can raise sulfate to harmful levels. Reactions with other minerals such as calcite in Eq. 2, give rise to selenite/gypsum, and this involves expansion. The oxidation process can be greatly accelerated by the presence of bacteria, such as *Acidithiobacillus sp* that rely on electron transfer between  $\text{Fe}_2^+$ / $\text{Fe}_3^+$  for their metabolic process (Sasaki et al. 1998). These microbes thrive in acidic, warmed conditions generated by pyrite oxidation, which is exothermic. Observations by Bromley and Pettifer (1997) document abiotic pyrite oxidation in concrete blocks containing pyritic aggregate where pH of pore fluids in the concrete were around pH >12. This reaction mechanism can also occur when pyrite bearing ground is treated using lime and cement.

The end product of pyrite oxidation processes is hydrous iron oxide/hydroxide yellow brown to orange brown amorphous precipitate known as ochre, typically evident as yellow-brown staining to surfaces. In the absence of calcite to buffer the acid, reactions with potassium feldspar and clay minerals result in jarosite-alunite.



More detailed reviews of the various pathways possible and reaction stages are found in Lowson (1982), Hawkins and Pinches (1987), and Reid et al (2001, 2005).

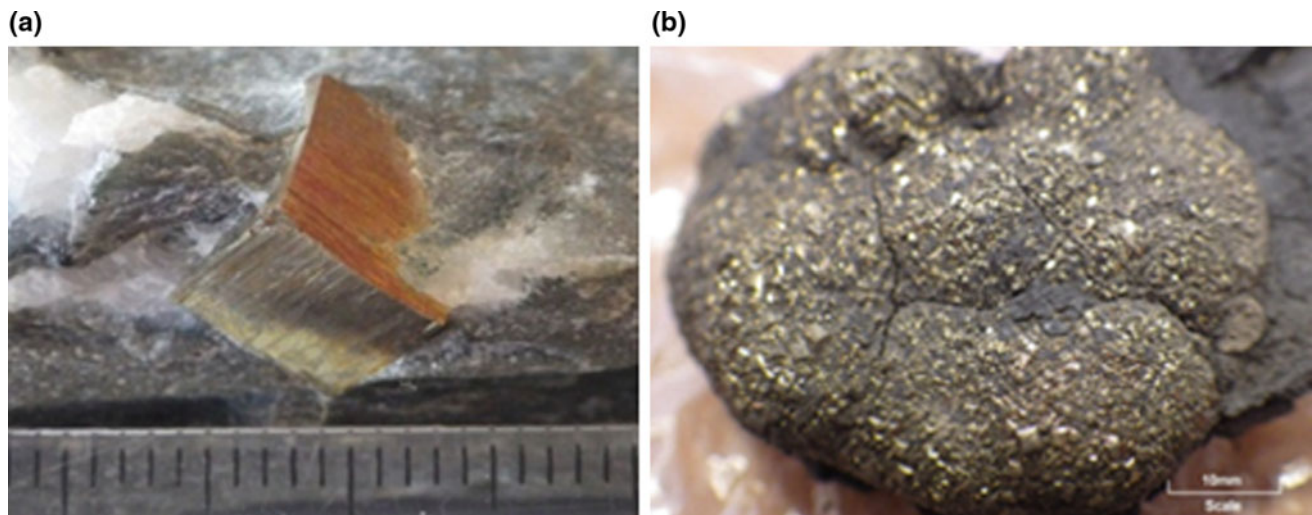
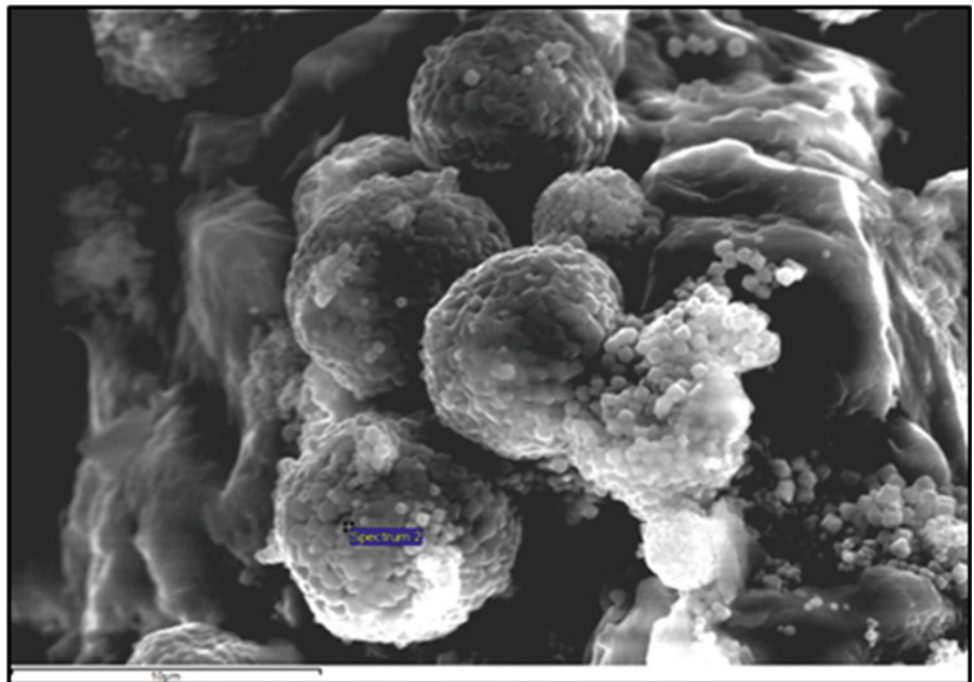


**Fig. 1** a Visible striated pyrite cube in Cambrian slate; b Crystalline pyrite nodule in Carboniferous strata

**Fig. 2** Pyrite framboids in fresh London Clay (Eocene)



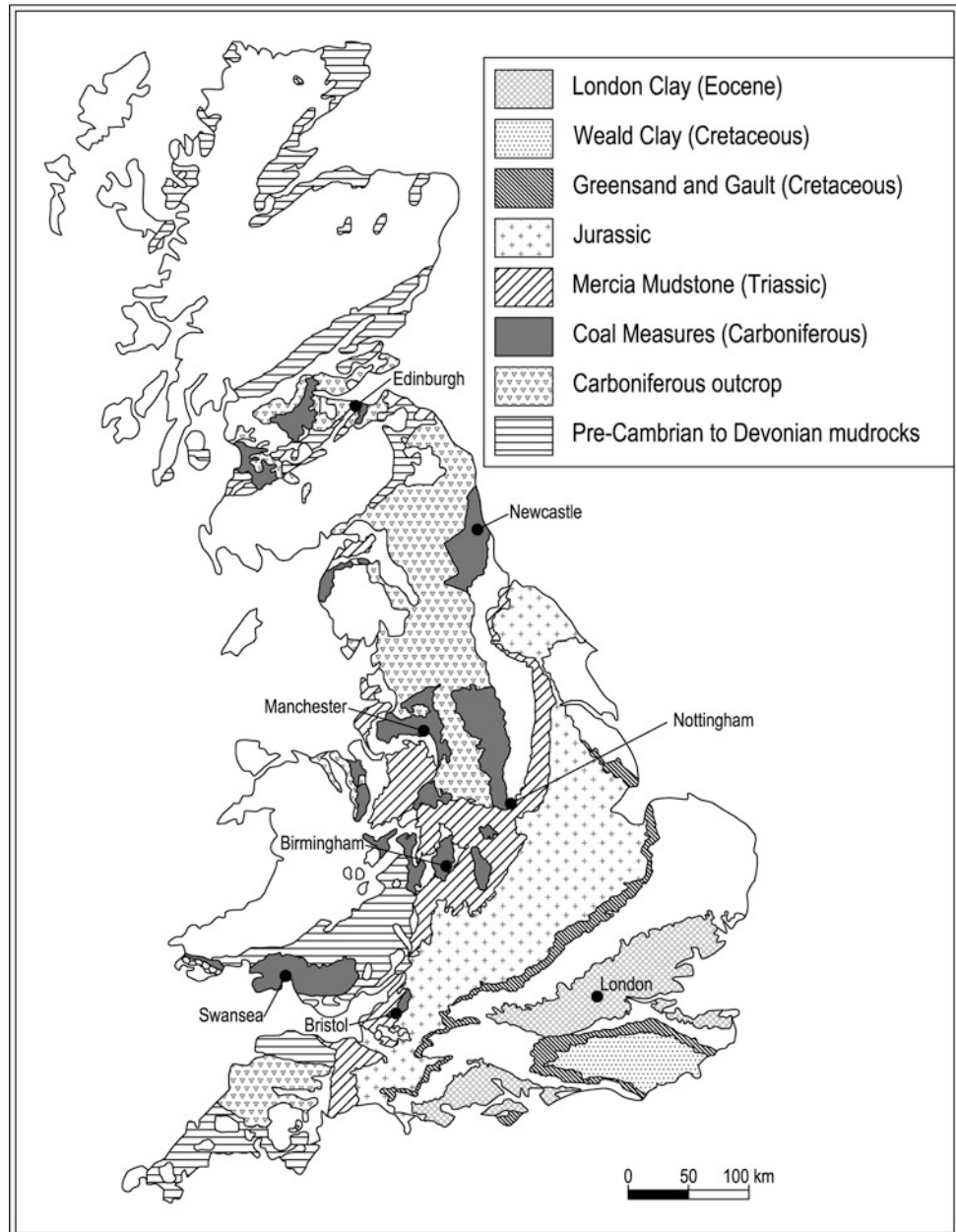
### 3 Implications for Highways and Construction

The oxidation of pyrite following exposure of pyrite bearing deposits during earthworks and construction activities has been observed to progress rapidly on a timescale significant to construction, and the process produces conditions that are chemically aggressive to engineering material particularly buried steel and concrete (Reid et al. 2001, 2005; BRE 2001). In some cases lowering of the water table associated with construction or mining activities has been responsible

for exposing pyrite-bearing lithologies to oxidation (Hawkins and Higgins 1997). The rapid weathering process also causes adverse changes in the geotechnical properties of mudrock (Anderson and Cripps 1993) or ground heave due to precipitation of sulfate minerals (Wilson 1987; Cripps and Edwards 1997), particularly if a calcareous component is present.

The replacement of pyrite and calcite by gypsum in Eq. 2 is significantly expansive, because the reaction products occupy a larger volume than the original calcite and pyrite as simple replacement entails a volume increase of 103% (Taylor 1984). The precipitation of gypsum can exert

**Fig. 3** Distribution of pyrite bearing sedimentary strata in UK



pressures of up to 100–500 kPa in confined conditions leading to significant ground stresses with development of differential ground heave (Taylor 1984). Gypsum has low solubility (Deer et al. 1992), a significant factor for ground heave. While calcium and sulfate ions are carried in solution they are mobile and may travel some distance before precipitation occurs. But once gypsum is formed, it is not readily re-dissolved or removed by groundwater, unless acidic (Hawkins and Pinches 1987). The products tend to be precipitated as discrete crystals at fabric and structural interfaces such as joints in rock masses (Fig. 4), or at construction boundaries and in fill (Fig. 5) or at the embankment and subgrade interface (Fig. 6). Volume increases at the

precipitation site can far exceed that caused by pyrite in the immediate vicinity (Cripps et al. 1993) and the growth of selenite crystals by nucleation involves the enlargement of discrete crystals. In indurated rocks this causes widening of cracks and fissures and where sub-horizontal fissility is present it causes vertical heave (Hawkins and Pinches 1987), whereas in clays and compaction mudrocks randomly distributed gypsum crystals produce more uniform heave (Fig. 7).

The amount of ground movement can be catastrophic to lightly loaded structures such as residential developments with documented cases from Japan (Yamanaka et al. 2002), Canada (Quigley and Vogan 1970), USA (Dougherty and

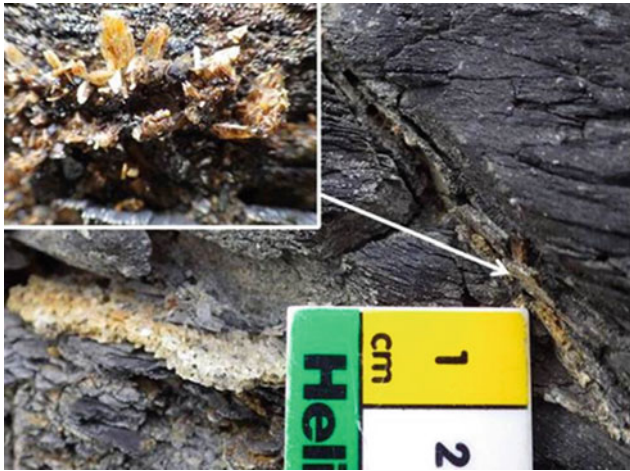


**Fig. 4** Selenite growth within joints in Bowland Shale as consequence of pyrite oxidation



**Fig. 6** Rapid deterioration due to pyrite oxidation of highway formation surface showing desiccation and selenite

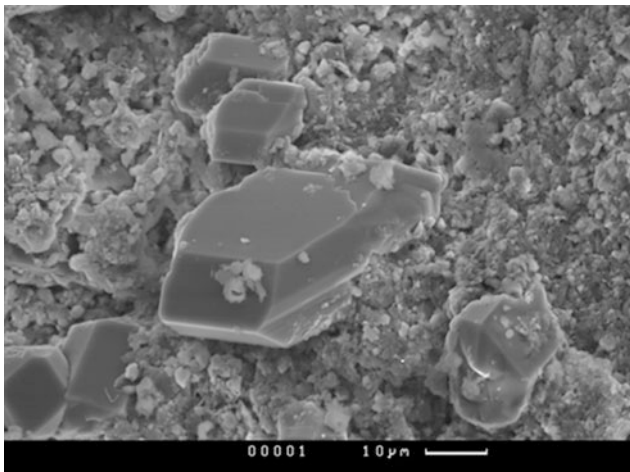


**Fig. 5** Selenite growth on cementitious blockwork at the interface between pyritic fill producing ground heave



**Fig. 7** Development of randomly orientated selenite crystals within a weak soil-like mass of Lower Lias Clay

Barsotti 1972) & Ireland (Matheson and Jones 2015). Many cases of lightly loaded highway construction in the UK have also experienced problems (Czerewko and Cross 2015). Ground disturbance and alkali conditions are both inherent in soil stabilisation, with pyrite oxidation causing sulfate attack with the formation of expansive materials such as ettringite and thaumasite (Higgins et al. 2002).

#### 4 Ground Investigation and Assessment of Conditions

Due to a lack of appreciation of the potential consequences of pyritic oxidation processes, the need for long-term mitigation measures within the construction design may be missed. Furthermore, early stage signs of reactions may not

be recognised, thus hindering early intervention (Fig. 8). Therefore these issues need to be clearly addressed at preliminary design stages before construction commences.

It is necessary to consider the type and distribution of all sulfides and sulfates in ground and fill. However it is also worth remembering that sulfides pose no threat to construction if oxygen and mobile water are absent, for example where strata are not disturbed, such as in some pile construction (BRE 2001). Generally a well-formulated ground investigation that documents the variation in ground conditions and distribution of potentially deleterious materials over and beyond the intended zone of construction is required to avoid problems. British Standards (BSI 2015), Eurocodes (BSI 2007), other international standards, and best practice technical documents (BRE 2001) offer invaluable guidance on sampling and investigation for determination of ground

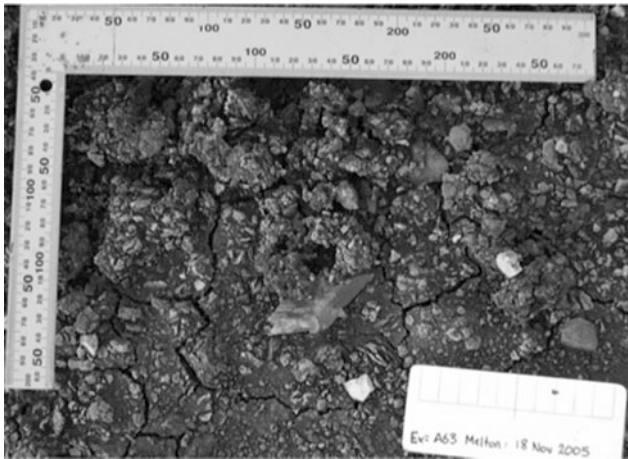


**Fig. 8** Reaction at pavement formation level with heave & rapid growth of selenite in Jurassic Ancholme Clay

aggressiveness. The investigation should adopt a staged approach with initial desk study and review of available geological and ground reference data (BRE 2001); preliminary ground investigation to substantiate desk study assumptions; and detailed investigation to provide the detailed distribution of ground material necessary for detailed design and appropriate mitigation.

In the development of highway infrastructure, the potential for deterioration of materials is often overlooked, ignoring the consequences of rapid weathering of materials. Durability testing of material is needed with analysis for sulfate content of the water used and samples observed for precipitated minerals following drying (Fig. 9). Simple weathering exposure observations may also help elucidate the likely behaviour of materials, as seen in Figs. 10a–c (Czerewko et al. 2011). The designer must anticipate the



**Fig. 9** Oxidation of pyrite forming selenite observed in sample on right during stages of Slake Durability Testing

likely engineering behavior of the material at different stages of construction and take the possibility of adverse weather conditions into account.

Characteristic factors indicative of the possible presence of pyrite include:

- Dark coloured (grey or dark grey), organic rich mudrock, calcareous mudrock or clay.
- Presence of finely disseminated gold and dark green-grey to bronze-grey coloured crystals often along partings or discrete lenses.
- Orange-brown and brown staining or precipitates at exposed surfaces or associated with seepages (Fig. 11).
- Sulfurous odour when the rock is hit or scratched.
- Presence on surfaces of clear or white-grey crystals which it is possible to scratch with a finger nail or of a white surface coating when the material is dried.

Pyrite is often associated with organic carbon where <0.5% can impart a grey colour in mudstones, siltstones and sandstones. The weathering related change of these grey deposits to shades of brown is often accompanied by precipitation of granular saccharoidal selenite crystals in calcite rich materials, often mistaken for sand (Fig. 12).

Comprehensive assessment and identification of potentially aggressive and deleterious ground conditions may be carried out by a combination of techniques as demonstrated in Fig. 13, including:

- Inspection of the in situ ground conditions;
- Inspection of sample material recovered from boreholes;
- Selective chemical testing to determine sulfur and calcite presence.

Due to the difficulties posed by the visual identification of pyrite, dark coloured mudrocks, clays and limestone need to be tested for the presence of pyrite. Current guidance (Reid et al. 2001, 2005; BRE 2001) recommends that oxidisable-sulfur (total sulfur minus acid soluble sulfur, assumed as pyritic) >0.1%, then it is likely that pyrite is present. The distribution of sulfur compounds in soils and rocks can be highly variable so testing must be sufficient to ensure that sulfur-bearing horizons are not missed and a suitable value for design is selected. Material selected for laboratory trials and testing should focus on the construction zone but also evaluate other strata that may also be affected by construction activities. Although sulfate minerals can be present, sulfide minerals may predominate at greater depths where oxidation has not occurred. It is recommended that at least five samples should be tested from each location (Reid et al. 2001, 2005; BRE 2001), with the mean of the highest two values used for comparison with the limiting values. It is

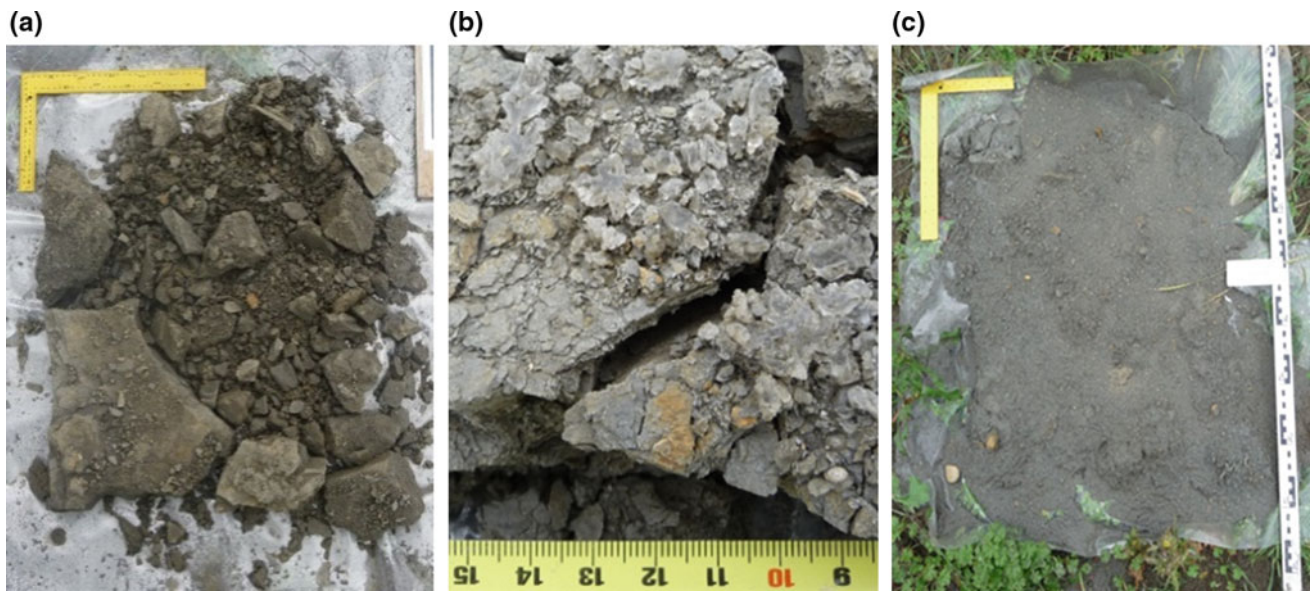


**Fig. 10** Blue Lias Mudstone; **a** 1 day after excavation: intact blocks and fragments. **b** Sample 10a after 19 days exposure: evident selenite development. **c** Sample 10a after 41 days exposure: fine soil mass



**Fig. 11** Colour changes clearly evident in a weathering profile affected by pyrite oxidation seen in Oxford Clay



**Fig. 12** Saccharoidal selenite with hydrous iron oxide surface staining in weathered Lower Lias Clay

also necessary to consider the weather conditions at the time of sampling and the impact of adverse weather conditions during the construction period, as well as longer-term climatic changes that may affect the on-going environmental conditions.

Various chemical test methods for pyrite bearing materials are reviewed by Reid et al. (2017): the total sulfur content of samples is a useful screening test. When framboidal pyrite is suspected, then the amount of sulfide-sulfur (referred to as Oxidisable Sulfide—‘OS’ in (Reid et al. 2001,



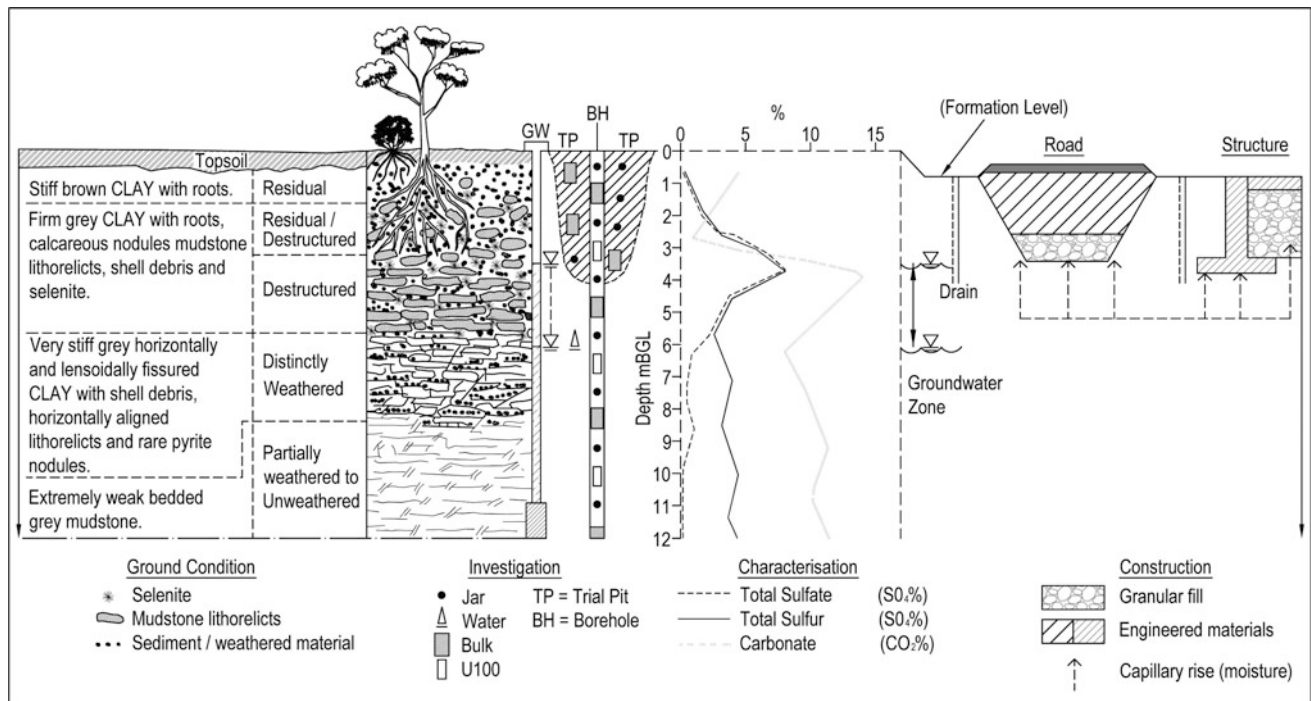


**Fig. 13** Schematic representation of assessment of ground aggressiveness and weathering

2005; BRE 2001), is a good indicator of the potential for oxidation reactions.

## 5 Conclusions

The assessment of ground aggressivity and aggregate suitability in ground engineering forms part of the geotechnical design process for construction and includes verification of aggregates. At an early stage assessment is carried out to evaluate conditions and determine potential implications for mitigation during the design process. Although the mechanism of pyrite oxidation, which is one of the main cases of ground aggressivity has been discussed, the implications to construction and the success of the earthworks tend to be controlled by site specific conditions largely related to the type and properties of material present and the site environment. The site investigation may confirm the presence of significant quantities of pyrite, gypsum and calcite but these values alone do not facilitate assessments of the reaction rate and significance to construction.

The susceptibility of the materials to rapid deterioration and the oxidation of pyrite must be ascertained. Discolouration, softening and presence of selenite are all indicators of pyrite oxidation processes. Simple procedures such as block weathering, compaction tests, slake durability with determination of water soluble sulfate of extracts, may further inform

the design process. Determination and evaluation in terms of the engineering operations, of the type and distribution of sulfur compounds in the ground and geological construction materials are of fundamental importance.

## References

- Anderson, W.F., Cripps, J.C.: The effects of acid leaching on the shear strength of Namurian shale. In *Engineering Geology of Weak Rocks*, Geol. Soc. Eng. Geol. Special Publication No. 8, Balkema, Rotterdam, 1993, pp. 159–168
- Bracegirdle, A., Jefferis, S.A., Tedd, P., Crammond, N.J., Chudleigh, I., Burgess, N.: The investigation of acid generation within the Woolwich and Reading Beds at Old Street and its effect on tunnel linings. In: Mair, R.J., Taylor, R.N. (eds.) *Geotechnical Aspects of Underground Construction in Soft Ground*. Balkema, Rotterdam (1996)
- BRE.: *Concrete in sulphate-bearing soils and water*. Digest No 363, 1991. BRE-IHS, Building Research Establishment, Bracknell, UK
- BRE.: *Concrete in Aggressive Ground. Part 1: Assessing the aggressive chemical environment*. SD 1, 1st edn, 2001; 3rd edn. BRE-IHS, Building Research Establishment, Bracknell (2005)
- Bromley A., Pettifer K.: *Sulfide-related degradation of concrete in Southwest England (The mundic problem)*. Building Research Establishment, Watford, 1997, BRE Lab Report 325
- BSI 2007. BS EN 1997-2:2007. Eurocode 7—Geotechnical design—Part 2: Ground Investigation and testing. British Standards Institution, London
- BSI 2015. BS 5930:2015. Code of practice for ground investigations. British Standards Institution, London

- Cripps, J.C., Edwards, R.L.: Some geotechnical problems associated with pyrite bearing rocks. In Hawkins, A.B. (ed.) Proceedings of International Conference on the Implications of Ground Chemistry/Microbiology for Construction, 77–87, Balkema, Rotterdam (1997)
- Cripps, J.C., Hawkins, A.B., Reid, J.M.: Engineering problems with pyritic mudrocks. *Geoscientist* **3**(2), 16–19 (1993)
- Czerewko, M.A., Cross S.A.: The benefits of a granular interface over pyritic subgrade. *Proc. Inst. Civ. Eng.—Geotech. Res.* **2**, 97–122 (2015)
- Czerewko, M.A., Cross, S.A., Dumelow, P.G., Saadvandi, A.: Assessment of pyritic Lower Lias mudrocks for earthworks. *Proc. Inst. Civ. Eng.—Geotech. Eng.* **164**, 59–77 (2011)
- Czerewko, M.A., Longworth, I., Reid, J.M., Cripps, J.C.: Standardised terminology and test methods for sulfur mineral phases for the assessment of construction materials and aggressive ground. *QJEGH, London* **49**, 245–265 (2016)
- Deer W.A., Howie R.A., Zussman J.: *An Introduction to the Rock-Forming Minerals*, 2nd edn. Wiley (1992)
- Dougherty, M.T., Barsotti, N.J.: Structural damage and potentially expansive sulfide minerals. *Bull. Assoc. of Eng. Geol.* **9**(2), 105–125 (1972)
- Dunster, A.: Avoiding deterioration of cement-based building materials and components. Lesson from case studies: 4. BRE, Watford, 2001, BRE Report BR441
- Floyd M., Czerewko M.A., Cripps, J.C., Spears D.A.: Pyrite oxidation in Lower Lias Clay at concrete highway structures affected by thaumasite, Gloucestershire, UK. *Cem. & Concr. Comp.* **25**, 1015–1024 (2003)
- Hawkins, A.B., Pinches, G.M.: Cause and significance of heave at Llandough Hospital, Cardiff—a case history of ground floor heave due to gypsum growth. *QJEG, London* **25**, 17–30 (1987)
- Hawkins, A.B., Higgins, M.D.: The generation of sulphates in the proximity of cast in situ piles. In Hawkins, A.B. (ed.) *Ground Chemistry: Implications for Construction*. Balkema, Netherlands (1997)
- Higgins, D.D., Thomas, B., Kinuthia J.: Pyrite oxidation, expansion of stabilised clay and the effect of GGBS. In: Zorob, S.E., Collop, A., Brown, S.F. (eds.) *Performance of Bituminous and Hydraulic Materials in Pavements*, pp. 161–167. CRC Press, Nottingham (2002)
- Hoover, S.E., Lehman, D.: The expansive effects of concentrated pyritic zones within Devonian Marcellus Shale Formation of North America. *QJEGH, London* **42**, 157–164 (2009)
- Longworth, T.I.: Assessment of sulfate-bearing ground for soil stabilisation for built development. *Ground Engineering*, 56–59 (2004)
- Lowson, R.T.: Aqueous oxidation of pyrite by molecular oxygen. *Chem. Rev.* **82**(5), 461–497 (1982)
- Matheson, G.D., Jones, G.L.I.: The habit and form of gypsum crystals in Irish mudstone aggregate affected by pyrite-induced swelling. *QJEGH, London* **48**, 167–174 (2015)
- Pugh, C.E., Hossener, L.E., Dixon, J.B.: Pyrite and marcasite surface area as influenced by morphology and particle diameter. *Soil Sci. Soc. of Am. J.* **45**(5), 979–982 (1981)
- Pye, E.K., Miller, J.A.: Chemical and biochemical weathering of pyritic mudrocks in a shale embankment. *QJEG, London* **23**, 365–381 (1990)
- Quigley, R.M., Vogan, R.W.: Black shale heaving at Ottawa, Canada. *Can. Geot. J.* **7**, 106–115 (1970)
- Reid J.M., Czerewko M.A., Cripps, J.C.: Sulfate specification for structural backfills. TRL Report 447, 2001 & 2005, TRL Limited, Crowthorne
- Reid, J.M., Czerewko, M.A., Longworth, I., Cripps, J.C.: Sulfur compounds in soils and rocks—avoiding pitfalls in terminology, test procedures and ground assessment. *Ground Eng.*, 30–36 (2017)
- Sasaki, M., Tsunekawa, M., Ohtsuka, T., Konno, H.: The role of sulfur-oxidising bacteria *Thiobacillus thio-oxidans* in pyrite weathering. *Colloids Surf. A: Physicochem. and Eng. Aspects* **133**, 269–278 (1998)
- Snedker, E.A., Temporal J.: M40 Motorway Banbury IV Contract—lime stabilisation. *Highways and Transportation*, 7–8 (1990)
- Steward, H.E., Cripps, J.C.: Some engineering implications of chemical weathering of pyritic shale. *QJEG, London* **16**(4), 281–289 (1983)
- Taylor R.K., Cripps J.C.: Mineralogical controls on volume change. In: Attewell, P.B., Taylor, R.K. (eds.) *Ground Movements and their Effects on Structures*, pp. 268–302. Surrey Uni Press, UK (1984)
- Thaumasite Expert Group.: The thaumasite form of sulfate attack: Risks, diagnosis, remedial works and guidance on new construction. DETR, London (1999)
- Vear, A., Curtis, C.: A quantitative evaluation of pyrite weathering. *Earth Surf. Proc. Land.* **6**, 191–198 (1981)
- Wilson, E.J.: Pyritic shale heave in the Lower Lias at Barry, Glamorgan. *QJEG, London* **20**, 251–253 (1987)
- Yamanaka, T., Miyasaka, H., Aso, I., Tanigawa, M., Shoji, K.: 2002 Involvement of sulfur- and iron-transforming bacteria in heaving of house foundations. *Microbiol. J.* **19**, 519–528 (2002)

# Measuring Fault Displacements Caused by Salt Tectonics Using Marine Geophysical Data

J. Yeakley, Abdul Shakoor, and W. Johnson

## Abstract

Previously obtained marine geophysical data for proposed Galsi pipeline route from Algeria to Sardinia were used for analysis of buried salt distribution and calculation of associated fault displacements. Crossing convergent African/Nubian–European plate boundary, the southern section of the proposed route also traverses continental shelves and slopes of Algeria and Sardinia, as well as the Algerian abyssal plain of the Western Mediterranean. Deeply buried Messinian-age salt is present throughout this study area. Uncompressible due to the crystal structure, salt is less dense and therefore more buoyant than clastic overburden sediment, having a tendency to flow and form diapiric structures. We conducted analyzes to determine distribution and influence of salt tectonics (halokinesis) on seafloor morphology, focusing on fault displacements above diapiric structures, comparing displacement rates near compressive plate boundary with those within passive margin environments. Seismic reflection sub-bottom profile interpretations, along with age-dated cores, were used to calculate sedimentation rates that led to quantification of rates of movement along faults caused by salt tectonics. Measured and plotted offsets from different resolution seismic profiles were correlated with predicted sediment age at depth of offset. Results show the average estimated rates of salt movement to be 1–2 cm per thousand years, over the top of salt diapirs in the Abyssal Plain, as opposed to 3–5 cm per thousand years near the active convergent plate boundary

in the south and near the Sardinian slope to the north where increased stress on salt may be due to the confinement of Sardinian bedrock.

## Keywords

Geophysics • Tectonics • Halokinesis

## 1 Introduction

### 1.1 Background and Area of Interest

Marine surveys undertaken for the southern portion of the proposed Galsi pipeline, proposed to pass between the northeastern coast of Algeria (Kouidet Draouche) and the southwestern tip of Sardinia (Porto Botte), are utilized in analysis of faulting related to the distribution of subsurface Messinian [late Miocene, about 5.4 million years ago (ma)] age salt (Fig. 1). Physiographically, the southern pipeline route crosses the continental shelves and slopes of Algeria and Sardinia, as well as the abyssal plain of the Western Mediterranean. Geologically, the route crosses the convergent African/Nubian–European plate boundary (dashed line in Fig. 1) along the edge of the Algerian continental shelf (Kherroubi et al. 2009; Meghraoui and Pondrelli 2012). In connection with this, there have been active thrust systems identified offshore Annaba, located in the northeastern corner of Algeria, striking ENE–WSW to E–W nearly perpendicular to the present-day maximum stress direction and possibly absorbing much of the African–European plate motion (Deverchère et al. 2007).

Much of the route crosses areas where Messinian-age evaporite deposits, lower carbonates and evaporitic sediments, the mobile halite and anhydrite, as well as upper marls and gypsum (Sage et al. 2005), were emplaced during the Messinian Salinity Crisis (MSC), but their detailed distribution has not been previously mapped in this area. The

J. Yeakley (✉)

Gannett Fleming, EA, P. C., Akron, OH, USA  
e-mail: jyeakley@GFnet.com

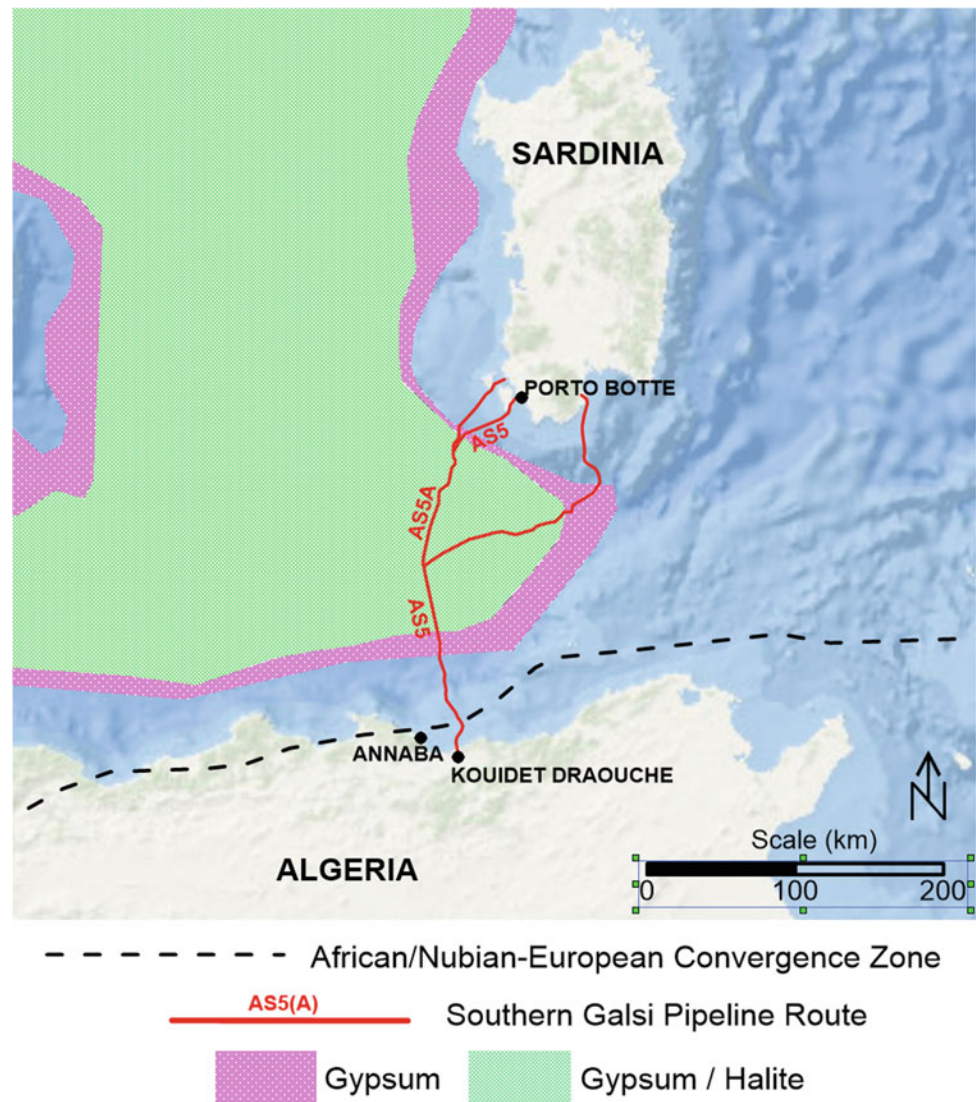
A. Shakoor

Kent State University, Kent, OH, USA  
e-mail: ashakoor@kent.edu

W. Johnson

Rhea Engineers and Consultants, Valencia, PA, USA  
e-mail: bill.johnson@rhea.us

**Fig. 1** Map showing extent of Messinian salt distribution as published by (Bertoni and Cartwright 2015)



data provide information for determining the amount, timing and style of faulting with respect to salt tectonics.

## 1.2 Geological History of Area

About 22–21 ma, a block of continental crust, presently known as Sardinia, rotated away from France and reached its current location about 16–15 ma (Rosenbaum et al. 2005). The Sardinia Channel, connecting the Algero-Provençal basin and SW Tyrrhenian abyssal plain southeast of Sardinia, is a result of a compressional event with crustal thickening followed by extension and thinning out (Masclé et al. 2001). The reason this is significant is that this area would normally be part of the abyssal plain region if not for this crustal block and therefore has minimal sources of terrigenous sedimentation to collect along the slope (Johnson 2011).

The MSC affected the entire Mediterranean over a relatively short period of time (5.96–5.33 ma) when the Mediterranean-Atlantic connection progressively closed (García-Castellanos and Villasenor 2011). This lack of connectivity between the Atlantic and the Mediterranean at the time of the MSC is thought to have resulted from tectonic uplift of the Gibraltar arc seaway, as well as global sea-level changes, both of which controlled and still control the inflow of water to the Mediterranean (García-Castellanos and Villasenor 2011). Sea level in the Mediterranean dropped by as much as 1.5 km and was associated with sub-aerial erosion along the margins. Evaporite deposition (anhydrite, halite and potash) of as much as 2 km occurred in the deep basin, whereas carbonates were deposited in shallower regions (Pawlewicz 2004). The thickness of mobile Messinian salt in the Algerian basin is estimated to be close to 1 km (Dal Cin et al. 2016; Mauffret 2007). Overlying the evaporites is a

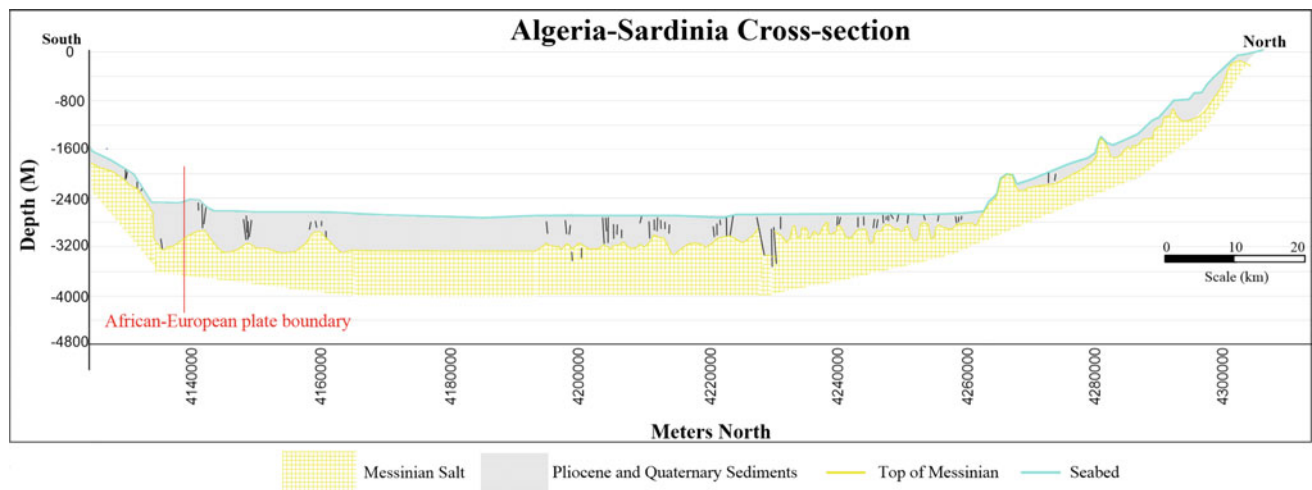


**Fig. 2** S-N geologic cross-section along pipeline route generated from Ultra High Resolution (UHR) seismic lines with focus on Messinian salt

Pliocene and Quaternary clastic sequence (Fig. 2). Post MSC (Pliocene and Pleistocene), low sedimentation rates occurred during the Pliocene due to the rapid eustatic rise in sea level and flooding of the Mediterranean (Cita et al. 1978). Studies on the Gulf of Lions in the western Mediterranean noted the Zanclean transgression, or the infilling of the Mediterranean around 5.33 ma, happening in two different stages (Bache et al. 2009). Primarily, the sea level slowly rose, smoothing margins by wave abrasion and then later rising faster, preserving features of the MSC (Garcia-Castellanos and Villasenor 2011). Quaternary accumulation increased and has since reached rates similar to those before the MSC (Cita et al. 1978). Late Quaternary fluctuations in sedimentation have also been affected by sea level changes related to glacial and interglacial cycles and sediment load fluctuations, as well as climatically-driven continental loads. Subsidence of the basin continues today and is believed to result from cooling of the oceanic lithosphere and sediment loading (Pawlewicz 2004).

The distribution of thick salt generally corresponds to the location of the abyssal plain and is limited near the base of the slope (Mauffret 2007), but the study of the continental slope south of Sardinia (Johnson 2011), along with this study, show that this salt is found at much shallower depths than the abyssal plain. The cross-section generated from this study (Fig. 2) depicts the presence of Messinian salt throughout the entire study area, where data was available. The central Mediterranean is an area where the distribution of salt has not been sufficiently studied and the stresses that have caused diapiric structures to form are not well defined or understood.

Diapiric salt structures, observed in one example of many in Fig. 3 with top of Messinian salt depicted by yellow line, are commonly associated with passive margins, which display thick layers of evaporites, dominated by halite,

deposited during and/or immediately after continental rifting (Fort and Brun 2011). This example is chosen because it best depicts the diapiric structures in the area and how they relate to fault displacements. Such salt basins lack stability, as salt is very weak and able to flow under very low differential stresses, even at surface temperature conditions (Fort and Brun 2011). Halokinesis or movement of salt is due to density inversion, differential loading and slope at the base of the salt layer, which are all typically present in passive-margin basin environments (Van Der Pluijm and Marshak 2004). In these passive environments, where no regional tectonic effects are recorded, the observed deformations are usually gravity driven. However, the situation along the Galsi pipeline route is not as straightforward. The Algerian margin corresponds to the plate boundary between the European and African plates with the Algerian basin to the north and an Alpine-type belt called Maghrebides to the south that formed from the subduction and closure of the Tethyan ocean beneath the European plate during the Miocene (Leprêtre et al. 2013). Along the Algerian margin there is an uplifted area with squeezed salt walls and anticlines associated with African/European plate interaction as have been identified by recent studies (Kherroubi et al. 2009; Domzig et al. 2010). The nature of salt tectonics within the abyssal plain and the Sardinian continental slope is essentially unknown and is analyzed in this study.

## 2 Methods

### 2.1 Data Analysis

High-resolution autonomous underwater vehicle (AUV) based Chirp profiles were used in this study to

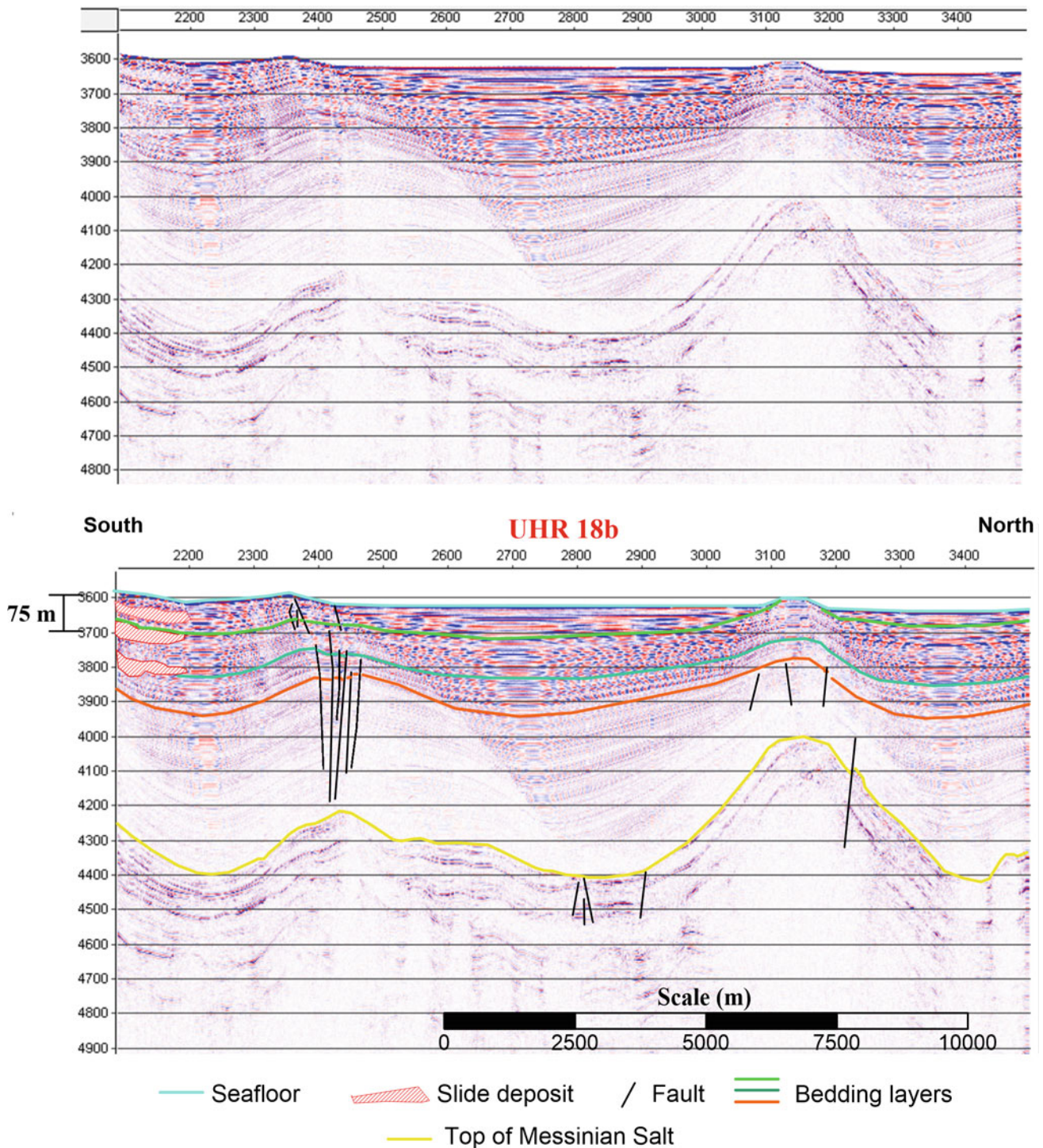


**Fig. 3** Example of plain and annotated UHR seismic profile showing deeper faults over salt diapirs

analyze shallow structures close to the seafloor (example in Fig. 4). Chirp sub bottom profiles are named after the “Chirping” technique, which refers to varying the amplitude and frequency of an emitted pulse in a fixed pattern ( $3 \times 4$  array transducers operating in a range of frequencies between 2 kHz and 7 kHz), in an attempt to reduce error

once the received and emitted signals are cross-correlated (McGee 1995). Interpretations in this study are examples of how structures, such as faulting at the seafloor surface, can be analyzed as a result of salt movement and correlated with the deeper UHR profiles to evaluate how the deeper salt is affecting the seafloor and at what rate this deformation is

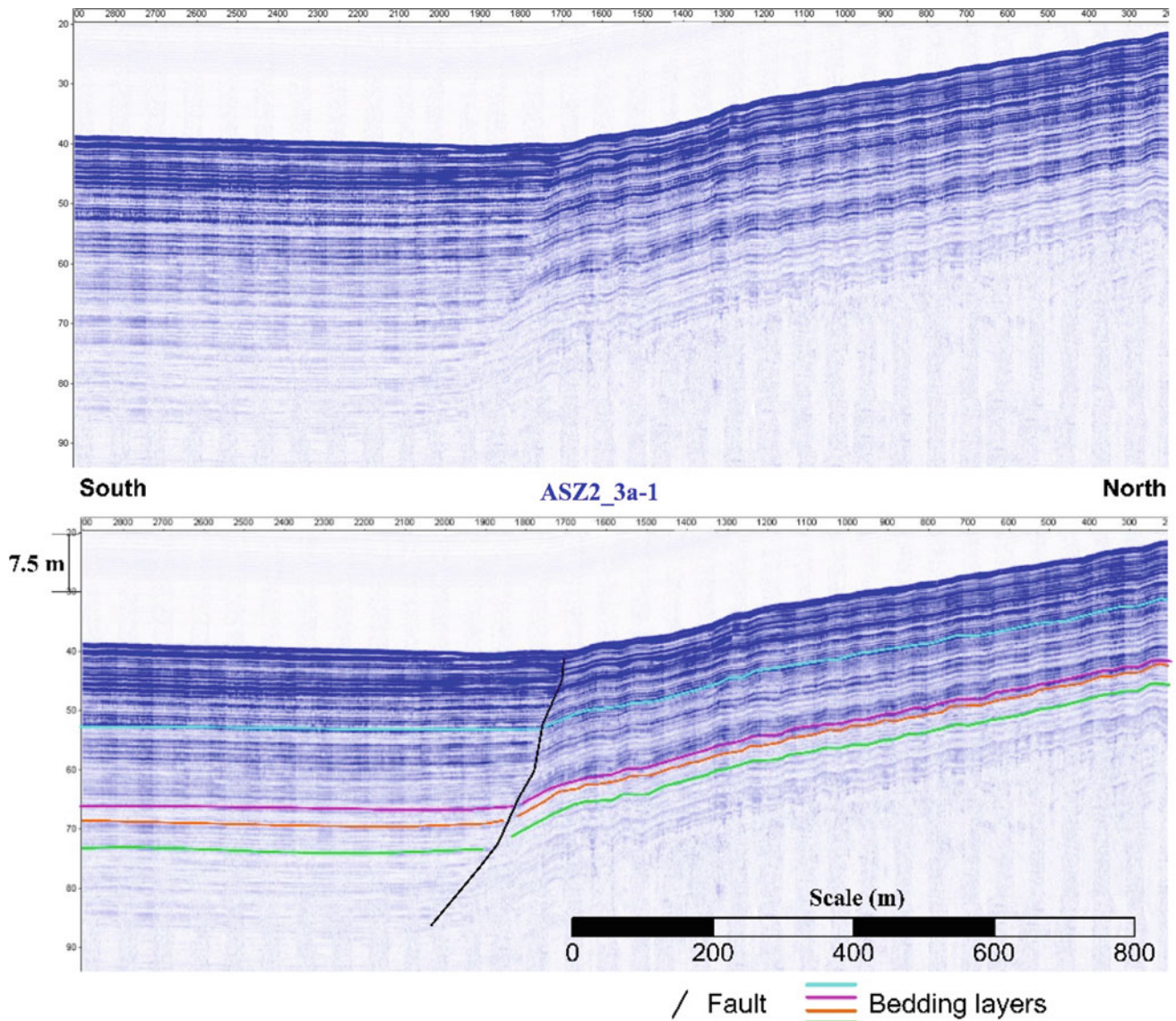


**Fig. 4** Example of plain and annotated chirp seismic profile showing a fault near the surface over top of a salt diapir

occurring (example in Fig. 3). Different resolution profiles are combined in order to analyze the generation of such structures and seafloor deformation due to salt movement.

Quantitative analysis of sediment deposition rates and sedimentary structure based on the interpretation of the seismic reflection profiles (sub-bottom profiles), together with the results of age-dating studies undertaken from core samples, form the basis for determining rates of fault displacements. Deep-rooted faults are identified from the UHR seismic profiles and their seafloor expressions evaluated from the shallower Chirp seismic profiles. Using carbon-14 dated core samples to calculate local sedimentation rates, the age at different depths along the Chirp seismic profiles are estimated. The displacements of different marker layers along the fault are measured based on calculated depths and

age is used to evaluate how much movement has occurred over specific time intervals.

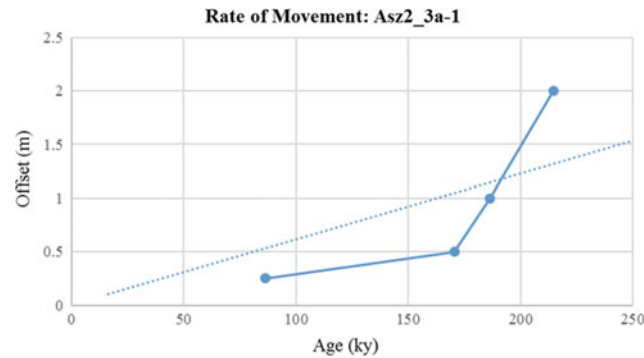
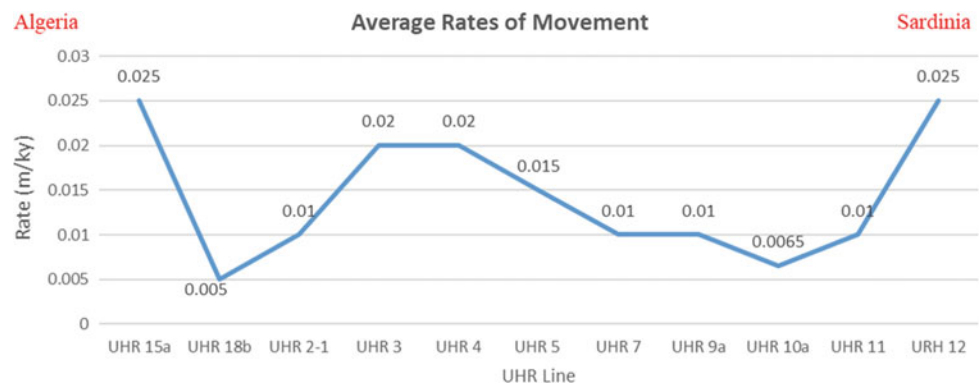
### 3 Discussion

#### 3.1 Results

The diapiric structures associated with Messinian evaporites affect the continental slope along the southern Sardinian margin, as previously documented (Johnson 2011). This study identifies several erosion channels and slope deposits that could have originated largely from movement of underlying salt identified within the continental slope south of Sardinia (the Cagliari slope). Moreover, the upper part of

**Table 1** Age date associated with different offsets along fault from Fig. 4

Offset (m)	Depth (m)	Est. age (ky)	Est. rate (m/ky)
0.25	9.5	86	0.003
0.5	18.8	170	0.003
1	20.5	186	0.005
2	23.6	215	0.009

**Fig. 5** Rate of movement (with dashed trendline) calculated along fault in chirp profile ASz2\_3a-1, correlating with UHR profile 18b**Fig. 6** Overall average rates of displacement along faults from Algeria to Sardinia based on data and estimated sedimentation rates

this slope is strongly affected by salt-related fault movements. Previous studies (Johnson 2011) focused on the precise pipeline route, but the available data encompass a much greater area giving rise for this study to analyze the data in greater detail.

Given the example from Fig. 4, offset at each depth is recorded in Table 1 and graphed in Fig. 5 to determine rate of movement. Based on calculated sedimentation rate from nearest corehole of 0.11 m/ky, the rate of movement along this fault is determined to average about 0.005 m/ky.

An observation made in other parts of the world is that when salt diapirs in sedimentary basins vertically rise through overburden sediments, complex fault systems, such as polygonal fault patterns, can develop (Carruthers and Thomas 2012). This type of fault pattern has not been documented in the Mediterranean, but diapiric structures (salt domes) are clearly identified on the Ultra High Resolution

(UHR) profiles (example in Fig. 3) obtained along the pipeline route. Faulting is present throughout the entire dataset from Algeria to Sardinia and is mapped and analyzed within all Chirp seismic profiles with the exception of those where failure events predominate on the Cagliari slope off southern Sardinia. Overall average rates of movement along such faults are documented in Fig. 6.

## 4 Conclusion

The rates of displacement are similarly low with an average of 0.01–0.02 m/ky, with a higher rate of 0.03 m/ky near the Cagliari or Sardinian slope, as well as the convergent plate boundary in the south. Faulting over such structures sometimes occurs in a polygonal pattern because of the presence of domes and the way the pressure is dispersed. Due to less



overburden sediment on the Cagliari slope, this area is more sensitive to seafloor deformation with regard to salt tectonics, allowing increased rates of fault displacement and slope failures to be more predominant. Further analysis in this area with 3D seismic data is needed to further investigate the true extent of seafloor deformation with regards to diapiric structures and to see the dimension of the polygonal fault systems present.

**Acknowledgements** All of the support of my advisor Dr. Abdul Shakoor is greatly appreciated as well as the expertise on this subject matter provided to me by my committee member William Johnson, formerly with D'Appolonia Engineers. I would like to especially thank James Nichols for providing me with this data.

## References

- Bache, F., Olivet, J.L., Gorini, C., Rabineau, M., Baztan, J., Aslanian, D., Suc, J.P.: Messinian erosional and salinity crises: view from the Provence Basin (Gulf of Lions, Western Mediterranean). *Earth Planet. Sci. Lett.* **286**(1), 139–157 (2009)
- Bertoni, C., Cartwright, J.: Messinian evaporites and fluid flow. *Mar. and Petrol. Geol.* **66**(Part 1), 165–176 (2015)
- Carruthers, T.: Interaction of polygonal fault systems with salt diapirs. Unpublished PhD Thesis, Cardiff University (2012)
- Cita, M.B., Ryan, W.B.F., Kidd, R.B.: Sedimentation rates in Neogene Deep-sea sediments from the Mediterranean and geodynamic implications of their changes. In: Initial Reports of the Deep Sea Drilling Project, pp. 991–1002 (1978)
- Dal Cin, M., Del Ben, A., Mocnik, A., Accaino, F., Geletti, R., Wardell, N., Zgur, F., Camerlenghi, A.: Seismic imaging of Late Miocene (Messinian) evaporites from Western Mediterranean back-arc basins. *Petrol. Geosci.* (2016). <https://doi.org/10.1144/petgeo2015-096>
- Deverchère, J., Yelles, K., Domzig, A., Mercier De Lépinay, B., Cattaneo, A., Gullier, V., Kherroubi, A.: Overall Tectonic Pattern of the Algerian margin: evidence for active folding and thrusting from the 2003 and 2005 MARADJA Cruises, *Rapp. Comm. Int. Mer Médit.*, 38 (2007)
- Domzig, A., Deverchère, J., Strzeczynski, P., Yelles, K., Babonneau, N., Cattaneo, A., Mercier de Lépinay, B., Graindorge, D., Bracene, R., Kerroubi, A., Gaullier, V.: The Algerian margin: a case study of interaction between Plio-Quaternary sedimentation and tectonics, search and discovery article adapted from oral presentation at AAPG Convention, Denver, CO, 7–10 June 2009 (2010)
- Fort, X., Brun, J.P.: Salt tectonics at passive margins: Geology versus models. *Mar. Pet. Geol.* **28**, 1123–1145 (2011)
- García-Castellanos, D., Villasenor, A.: Messinian salinity crisis regulated competing tectonics erosion Gibraltar arc. *Nature* **480**, 359–363 (2011)
- Johnson, W.J., et al. Geohazard interpretation of the Cagliari slope (Southern Sardinia, Italy). *Geo-Risk 2011- Risk assessment and management*, pp. 820–828 (2011) [https://doi.org/10.1061/41183\(418\)86](https://doi.org/10.1061/41183(418)86)
- Kherroubi, A., Déverchère, J., Yelles, A., Mercier de Lépinay, B., Domzig, A., Cattaneo, A., Bracène, R., Gaullier, V., Graindorge, D.: Recent and active deformation pattern off the easternmost Algerian margin, Western Mediterranean Sea: new evidence for contractional tectonic reactivation. *Mar. Geol.* **261**, 17–32 (2009)
- Leprêtre, A., Klingerhoefer, F., Graindorge, D., Schnurle, P., Beslier, M.O., Yelles, K., Déverchère, J., Bracene, R.: Multiphased tectonic evolution of the Central Algerian margin from combined wide-angle and reflection seismic data off Tipaza, Algeria. *J. Geophys. Res. Solid Earth* **118**, 3899–3916 (2013)
- Masclé, G.H., Tricart, P., Torelli, L., Bouillin, J., Rolfo, F., Lapierre, H., Monié, P., Depardon, S., Masclé, J., Peis, D.: Evolution of the Sardinia Channel (Western Mediterranean): new constraints from a diving survey on Cornacya seamount off SE Sardinia. *Mar. Geol.* **179**, 179–202 (2001)
- Mauffret, Alain: The Northwestern (Maghreb) boundary of the Nubia (Africa) Plate. *Technophysics* **429**, 21–44 (2007)
- McGee, T.M.: High-resolution marine reflection profiling engineering environmental purposes. Part A: Acquiring analogue seismic signals. *J. Appl. Geophys.* **33**, 271–285 (1995)
- Meghraoui, M., Pondrelli, S.: Active faulting and transpression tectonics along the plate boundary in North Africa. *Ann. Geophys.* **55** (5) (2012). <https://doi.org/10.4401/ag-4970>
- Pawlewicz, M.: The Pre-Messinian total petroleum system of the Provence Basin, Western Mediterranean Sea. *USGS Bulletin 2204-A* Retrieved from: <http://pubs.usgs.gov/bul/b2204-a/b2204-a.html>. Accessed 10 Aug 2014
- Rosenbaum, G., Regenauer-Lieb, K., Weinberg, R.: Continental extension: from core complexes to rigid block faulting. *Geology* **33**, 609–612 (2005)
- Sage, F., Gronefeld, G.V., Déverchère, J., Gaullier, V., Maillard, A., Gorini, C.: Seismic evidence for Messinian detrital deposits at the western Sardinia margin, Northwest Mediterranean. *Mar. Pet. Geol.* **22**, 757–773 (2005)
- Van Der Pluijm, B.A., Marshak, S.: *Earth Structure: An Introduction to Structural Geology and Tectonics*, 2nd edn, pp. 26–30 (2004)

# Environmental and Geological Characters and Stability Problems in the Historic Centre of Matera (South Italy)

Vincenzo Simeone, Angelo Doglioni, Rosa Maria Lacertosa, and Francesco Sdao

## Abstract

The paper briefly illustrates the main environmental and geological characteristics of the ancient historic centre of Matera, where the rupestrian settlements called “Sassi” are located. It illustrates how these characteristics conditioned the development and safeguarding of the old town. The main purpose of the paper is to present how Matera is an extraordinary example of geological and geo-mechanical features conditioning the human settlement development and their stability and safeguard.

## Keywords

Matera • Rupestrian settlement, stability of ancient town • Sandstone stability

## 1 Environmental and Geological Characteristics

The rupestrian settlements of the ancient historic center of Matera (Fig. 1) are prodigious examples of the use of a natural environment for the development of the town. The urban organization of and the human settlement are closely related to the natural and geological environment that condition the structural and architectural choices (Grassi et al. 2004, 2007). The development of the settlement is strongly conditioned by the geomorphological features of the site.

V. Simeone (✉) · A. Doglioni  
Department of Civil, Environmental and Construction Engineering and Chemistry, Technical University of Bari, via E. Orabona 4, 70125 Bari, Italy  
e-mail: vincenzo.simeone@poliba.it

R. M. Lacertosa  
Freelance Consulting Engineer, Contrada Giardinelle 2c, 75100 Matera, Italy

F. Sdao  
School of Engineering, Basilicata University of Bari, 85100 Potenza, Italy

It develops on the right-hand side of a deep narrow valley called Gravina (Figs. 1 and 2).

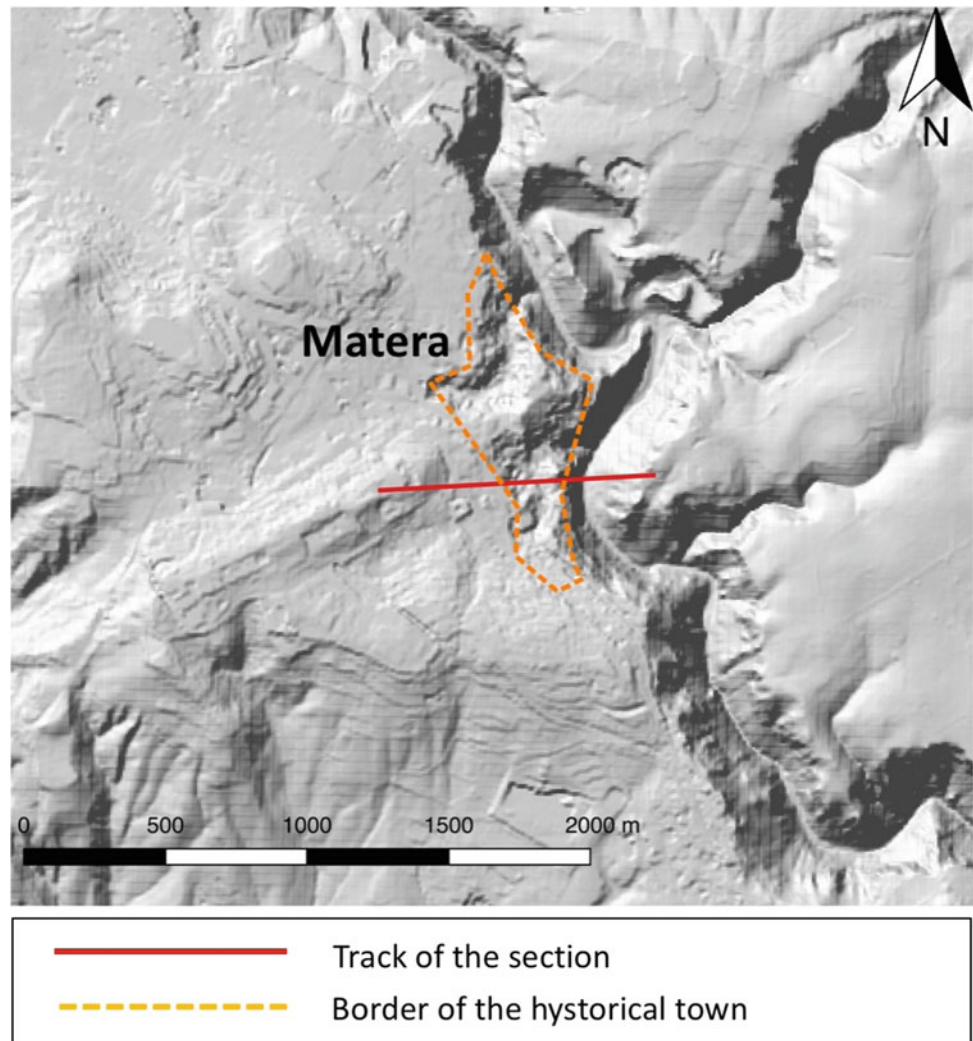
The geology of the area is characterized by substratum of Cretaceous limestone covered by a sequence of Pleistocene transgressive and regressive deposits (Fig. 3) (Baldassarre 1990; Radina 1973).

The base of the transgressive deposit is a weak calcareous sandstone rock called “calcareonite” easy to be carved and used as building material (Cotecchia and Grassi 1975; Cherubini et al. 1996; Lionetti and Simeone 2015). It outcrops on the upper part of the flank of the valley (Fig. 4), characterized by manifold morphological terraces where the historical town develops. The other deposits outcrops on the neighbour hill, where the XX century the modern town developed. The “Calcareonite” terraces were quarried to build the historic town modifying and regulating their shapes by human activities. In addition, these activities allowed to repair rock collapses due both to the natural evolution of these terraces and to human rearrangements (Cotecchia and Grassi 1975; Cherubini et al. 1996; Lionetti and Simeone 2015). On the vertical front of the terraces, deep grottoes were dug slightly inclined (Fig. 5); these were used as rupestrian homes until the middle of the XX century (Cotecchia and Grassi 1975). This was possible also because the sandstone is not permeable and is self-supporting and poorly deformable. Therefore, the rock masses were completely exploited according both to the horizontal and vertical directions.

This weak sandstone is also potentially easy-to-be modelled. This allowed to provide the buildings also with aesthetically pleasing decorations. Moreover, since a certain age, a more defined artistic and decorative character was given to the interior elements of the settlement (Fig. 6), which could be comparable to that of outside.

It is common opinion that rupestrian settlements developed in southern Italy during the early Middle Ages, just after the fall of the Roman Empire. However, Matera shows rupestrian settlements with evidences of presences since the Neolithic age (Lionetti and Pelosi 2009). Since that time onward, the capacity at digging rock on rock, using

**Fig. 1** Location of historical town of Matera on the border of Gravina valley



limestone to dig sandstone developed. There are sites where heritages of settlements dating to the Bronze and Iron ages exists (Lionetti and Pelosi 2009; Padula et al. 1995). In fact, in the areas in front of these settlements, fragments of pottery of bronze and iron ages were found, as well as of ancient Greek, Roman and Middle Age periods (Lionetti and Pelosi 2009).

These give an idea of the continuity of presence, both in the countryside and in the town, where there are elements of coexistence of different periods.

## 2 Safety and Stability Problems

Rupestrian settlements have suffered during all their history of precarious stability conditions. These pertain to the intrinsic fragility, due to constructive techniques and to the irregular distribution of voids and solids rock in sandstone related to quarrying (Grassi et al. 2004; Lionetti and

Simeone 2015). “Calcarenite” rock masses are characterized by severe differences due to variation of the deposition environment, with sudden variations in facies, porosity and diagenesis degree. (Lionetti and Simeone 2015). This affects the degree of imbibition, thus there are areas that are vulnerable to erosion and water-related degradation (Fig. 7) (Sdao et al. 2013; Pascale et al. 2013).

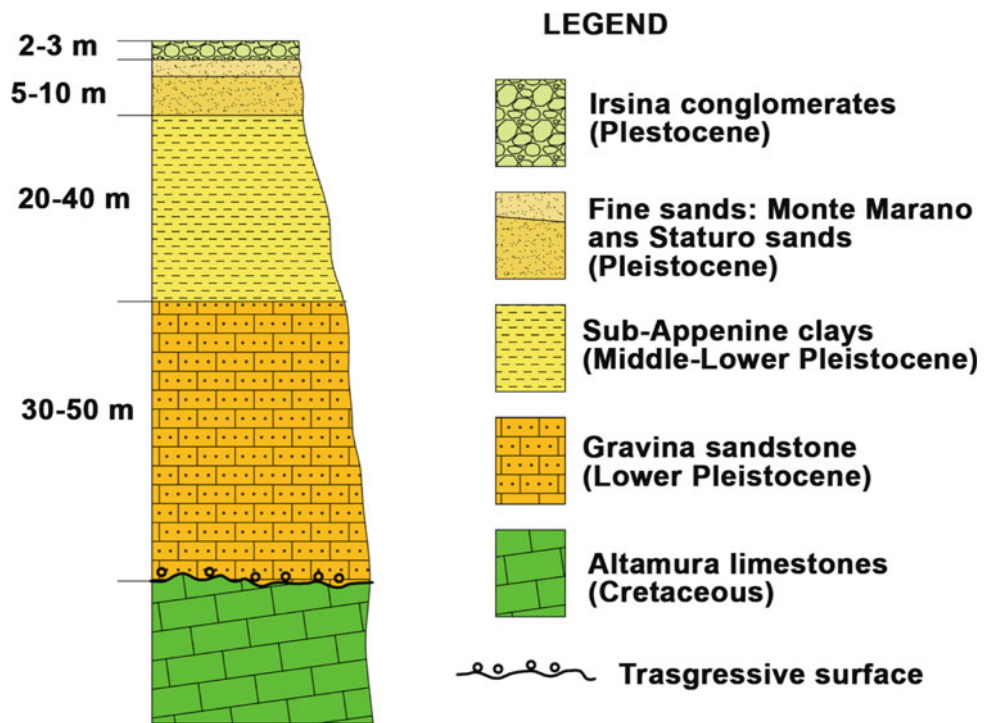
Paradoxically, the weakest levels are easiest to be carved, leaving a more cemented self-supporting and impermeable layer as roof of the grotto. These levels were intensively dug to develop settlements. Sometimes the digging activity was such severe to favor collapses.

The front of several dug settlement suffered of collapse phenomena due to the excavation or to overload. Often new grottoes were dug deeper in the same place, after the removal of the collapsed rock blocks. The collapses of rock masses induced tensile releases, which evolved within the new excavated caves. A lot of them have a series of fractures and discontinuities parallel to the



**Fig. 2** The historical town of Matera on the border of Gravina valley

**Fig. 3** Simplified stratigraphic sequence of Matera area



excavation front giving indications of the tensile release induced by digging with fracturing in macro blocks. Documentary sources point to numerous collapses, always in the same areas (Lionetti and Simeone 2015). These are therefore non-random collapses, related to weakness of sandstone in some areas, or in the presence of structural discontinuities.

An important role in stability is determined also by rocky joints, which even if not easily visible are both mechanical discontinuities, are preferential routes for water infiltration and radical rock degradation. Their presence is due to quaternary uplift and tectonic activity (Cotecchia and Grassi 1975; Lionetti and Simeone 2015) (Fig. 8).

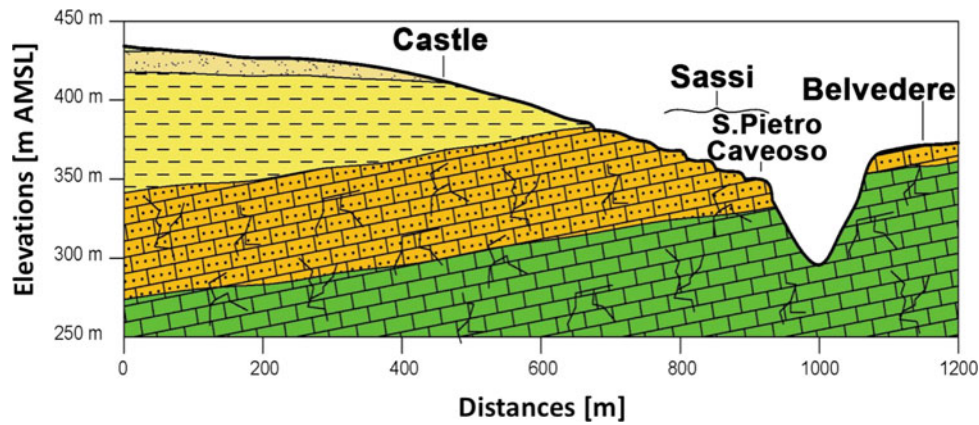


**Fig. 4** Schematic geological cross section according the track of Fig. 1, showing the location of “Sassi” rupestrian settlement

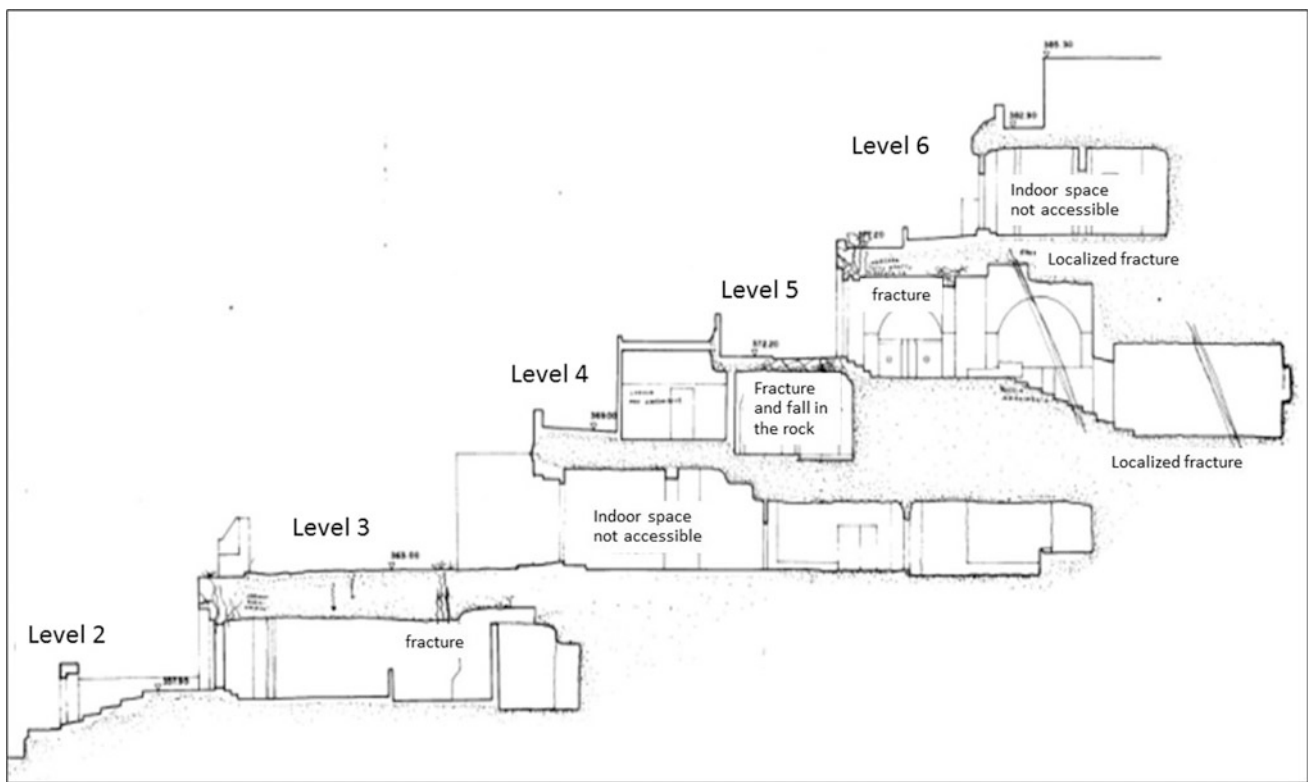


**Fig. 5** Example of cross section of the grottoes dug in “calcarene”

Bio-clastic and cryo-clastic phenomena amplified joints and fracture effects, much more than it can be expected by (Fig. 9). The first is the action of plant roots where cellular turgor may give sever pushing effects while the second is due to the ice effect.

In addition to the irregular distribution of voids within the rock masses also the shape of the underground space has a severe influence on the stability. Simplified simulation of the state of stress in an underground space of 20 m<sup>2</sup>, Fig. 10 shows the tension stress induced in the rock masses are

strongly dependent on the shape of the grotto. When it develop parallel to dug face, they are easily collapsing. In fact, in this case (first in Fig. 10) the maximum tensile stress reaches about 1.85 MPa, that is normally not congruent with sandstone tensile strength. In the case of square form, the maximum stress drops to 0.8 MPa, in the case of elongated shape to 0.52 MPa, compatible with the sandstone tensile strength.

Absence of warning indicators normally characterized the collapse events. Because the strongest level of “calcarene”



**Fig. 6** Decorative element carved in sandstone rock

**Fig. 7** Different characters of Matera “Calcarenite”



has a not high strength (3–4 MPa), but a high stiffness and an elastic modulus of about 4000 MPa (Fig. 11), much higher than that measurable by traditional test of about 500 MPa.

Reinforcing large arches and masonry support structures traditionally were used as safeguard interventions to prevent collapses to limit the unitary stresses, as well as to avoid traction stresses in the sandstone masses. Recently, structural

elements, such as steel nails, have been used, even if sometimes without a great success (Fig. 12).

These kind of consolidation works need to be carried out in a targeted way, only if sandstone are stiff enough. The nails work well, where the sandstone is considerable strong and stiff. Only in that case the use of structural interventions can be effective.



**Fig. 8** Fracture example and collapse due to fracture in Matera “Calcarenite”

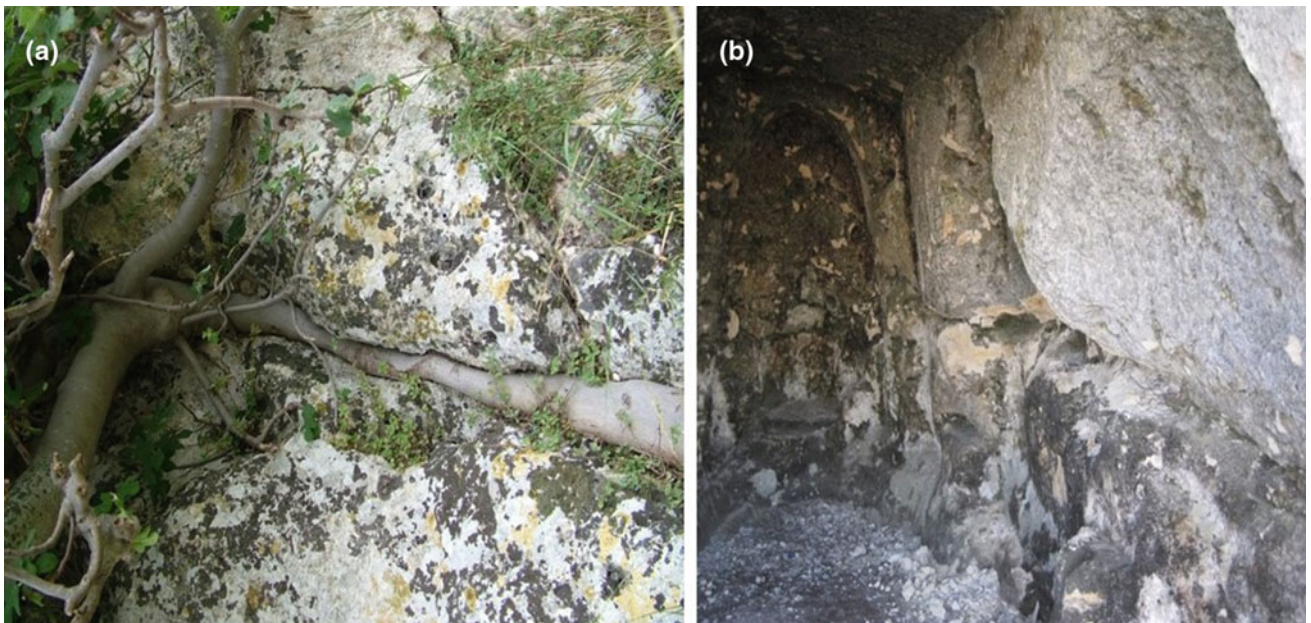


**Fig. 9** Bioclastesis and cryoclastesis damage of Matera sandstone

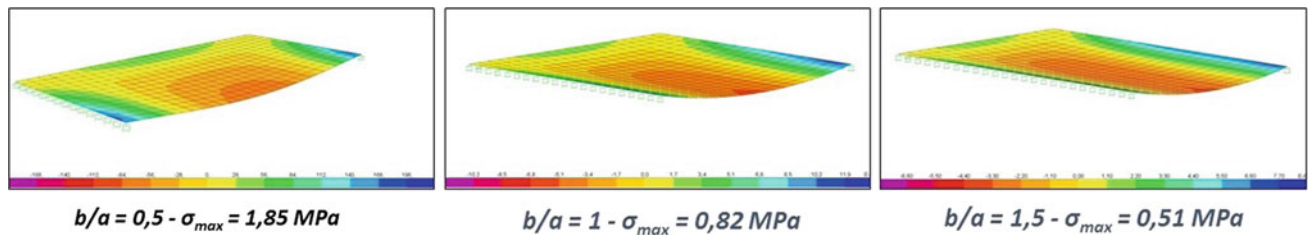


**Fig. 10** Simulation of the state of tensile stress in a dug space as a function of the dimension of the space

**Fig. 11** Compression test on sample of Matera sandstone with a local measurement of deformations for the deformation modulus evaluation

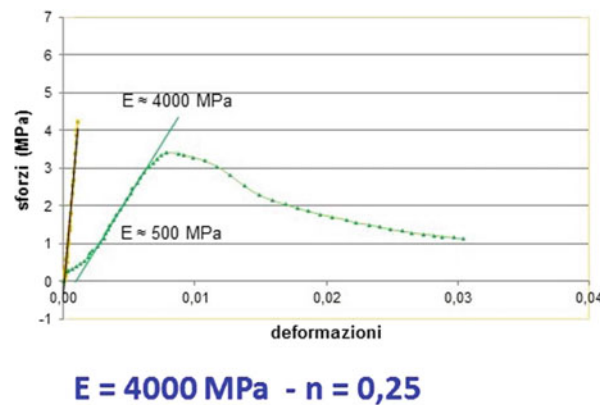


**Fig. 12** Failure of reinforcement with steel elements



### 3 Conclusion

The rupestrian settlements of the ancient historic center of Matera are an interesting example of natural environment used for a human rupestrian settlement. This urban area suffers from of an intrinsic fragility due the geological characteristics, but also to the shape of the underground structure and to the variations of facies of the sandstone. This work briefly presents some of the main fragility causes of this special settlement. It tries to show their

peculiarities and gives an example of problems that could be related to repair work. The work is a preliminary illustration of the several problems that affect these settlements.

**Acknowledgements** This work was partly founded by the Apulian Regional Government as part of the project Future in Research, Data Driven models for groundwater management and the geomorphic analysis of landscape, project number 4A46U38.

The study was carried out in the framework of the project Smart Basilicata in Smart Cities and Communities and Social Innovation (MIUR n.84/Ric 2012, PON 2007–2013).



## References

- Baldassarre, G.: Zonazione geologico tecnica della città di Matera. *Geol. Appl. ed Idrogeol.* **XXV**, 181–194 (1990)
- Cherubini, C., Di Cuià, N., Pagliarulo, R., Ramunni, F.P.: Caratteri petrografici e meccanici delle calcareniti di Matera. *Mem. Soc. Geol. It.* **51**, 761–769 (1996)
- Cotecchia, V., Grassi, D.: Stato di conservazione dei “sassi” di Matera (Basilicata) in rapporto alle condizioni geomorfologiche e geomeccaniche del territorio e alle azioni antropiche. *Geol. Appl. ed Idrogeol.* **X**, 55–105 (1975)
- Grassi, D., Grimaldi, S., Simeone, V.: Geological and geomorphological conditioning in localization of apulian rupestrian settlements. *Geophysical Research Abstract*, vol. 9, 2007 EGU General Assembly 2007, ISSN 1029-7006 (2007)
- Grassi, D., Grimaldi, S., Simeone, V.: On the causes of the instability affecting rupestrian urban centres of Apulia Region (Southern Italy), 32° International Geological Congress Firenze, Paper A32IGC9KF3, Session T16.06—Geoscience for Cultural Heritage—Natural hazard and cultural heritages (2004)
- Lionetti, G., Pelosi, M.: Considerazioni sui complessi rupestri artefatti preellenici della Murgia materana Le Aree Rupestri dell’Italia Centro-Meridionale nell’ambito delle civiltà italiche: Conoscenza, Salvaguardia, Tutela—Atti del IV Convegno internazionale sulla Civiltà Rupestre—Savelletri di Fasano (BR) 26–28 novembre 2009 (2009)
- Lionetti, G., Simeone, V.: Condizionamenti geologici e geomorfologici nella localizzazione, nello sviluppo e nella salvaguardia degli insediamenti rupestri GTA *Geologia Territorio Ambiente—Rivista dell’Ordine dei Geologi di Basilicata*, 25, 23–35 (2015)
- Padula, M., Motta, C., Lionetti, G.: Chiese e asceteri rupestri di Matera. De Luca Editori d’Arte, Roma (1995). ISBN 88-8016-100-8
- Pascale, S., Pastore, V., Sdao, F., Sole, A.: Landslide susceptibility in archaeological and natural historic park of rupestrian churches. In: Margottini, C., Canuti, P., Sassa, K. (eds.) *Landslide Science and Practice, Second World Landslide Forum*, vol. 6, pp. 715–722. Springer-Verlag GmbH, Berlin, Heidelberg (2013). ISBN 9783642313189
- Radina, B.: Saggio e note illustrative di una carta geologico tecnica (tav. 189 III SE “Matera Nord”). *Geol. Appl. ed Idrogeol.* **VIII**, 89–105 (1973)
- Sdao, F., Lioi, D., Pascale, S., Caniani, D., Mancini, I.M.: Landslide susceptibility assessment by using a neuro-fuzzy model: a case study in the Rupestrian heritage rich area of Matera. *Nat. Hazards Earth Syst. Sci. J.* **13**, 395–407 (2013). <https://doi.org/10.5194/nhess-13-1-2013>. ISSN 1561-8633



# Naturally Occurring Asbestos in Argentina: A Compilation of Case Studies

Lescano Leticia, Locati Francisco, Marfil Silvina, Sfragulla Jorge,  
Bonalumi Aldo, and Maiza Pedro

## Abstract

In Argentina, asbestos is associated with meta-mafic or meta-ultramafic igneous rocks, mainly serpentinites (or steatized varieties) and amphibolites, and less commonly with dolomitic rocks (in metamorphic and metasomatic domains). Chrysotile, anthophyllite and tremolite-actinolite were identified as the main asbestiform minerals (in the range of respirable particles). Chrysotile occurs mainly in serpentinites or steatized rocks as well as in amphibolites and other host rocks nearby. It appears filling veins, as slip and cross-fiber, generally associated with fissures or shear zones. Amphibole asbestos, mainly from the tremolite–actinolite series and anthophyllite, commonly occurs together with a non-asbestiform counterpart within the same area and deposits. These minerals have been found in talc ores as well as in vermiculite-rich sectors, or filling fissures in meta-mafic and meta-ultramafic rocks. In this compilation, the results of case studies on mines from the provinces of Córdoba, Mendoza and San Juan (Argentina) are summarized, and

new data from the western sector of the Pie de Palo Complex are included.

## Keywords

Asbestiform minerals • Geological occurrence • Argentina

## 1 Introduction

In a general sense and from a commercial perspective, the term “asbestos” is defined as a group of six minerals (chrysotile, crocidolite, amosite, tremolite, actinolite and anthophyllite) that occur in nature forming bundles of thin and long fibers. They are characterized by having high tensile strength and flexibility, low thermal and electrical conductivity, high absorbance and thermal stability, and resistance to chemicals (Ross et al. 2008). This definition not only has a mineralogical-morphological basis but also alludes to the physicochemical characteristics of the fibers. According to the World Health Organization (WHO 1986) and different regulatory agencies worldwide, respirable asbestos fibers with diameter  $<3 \mu\text{m}$  (and additionally a length  $>5 \mu\text{m}$  and a length to diameter ratio  $\geq 3:1$ ) should be considered hazardous, because they represent the most biologically relevant part of the alveolar fraction. In this compilation, the term “asbestos” is used as a synonym of “asbestiform fibers” for those minerals that can be separated longitudinally into thin and long fibers (excluding cleavage fragments, Gunter 2010) and meet the aforementioned size criteria.

Asbestos generally occurs associated with magnesium-rich (often also iron-rich) rocks affected by metamorphic and/or metasomatic processes. Forming environments typically display shear or evidence for a significant influx of silica-rich hydrothermal fluids (Van Gosen 2007). The rocks that can host asbestos include altered or metamorphosed varieties of ultramafic and mafic rocks (mainly in ophiolitic

L. Leticia (✉) · M. Silvina · M. Pedro  
UNS-CGAMA (CIC de la Prov. de Bs. As-UNS), San Juan 670,  
8000 Bahía Blanca, Argentina  
e-mail: leticia.lescano@uns.edu.ar

M. Silvina  
e-mail: smarfil@uns.edu.ar

M. Pedro  
e-mail: pmaiza@uns.edu.ar

L. Francisco  
CICTERRA (CONICET—UNC), Av. Vélez Sarsfield 1611,  
X5016GCA Córdoba, Argentina  
e-mail: locatifrancisco@gmail.com

S. Jorge · B. Aldo  
Secretaría de Minería (Provincia de Córdoba)—FCEFYN (UNC),  
Av. Vélez Sarsfield 1611, X5016GCA Córdoba, Argentina  
e-mail: sfragulla@gmail.com

B. Aldo  
e-mail: bonalumi.aldo@gmail.com

complexes), dolomitic rocks, iron formations, and alkalic intrusions and carbonatites (e.g., Van Gosen 2007; Vignaroli et al. 2014).

In Argentina most asbestiform minerals are associated with metamorphosed and/or metasomatized mafic and ultramafic igneous rocks, mainly serpentinites and amphibolic rocks, talc and vermiculite deposits as well as with dolomitic rocks (Angelelli et al. 1980; Locati et al. 2014; Lescano et al. 2016a). Their production started in 1920, stimulated by the industrial use of asbestos in postwar years, but they have been banned since 2003 (Rodríguez 2004). However, asbestos research is still important in Argentina because many active mines and future projects can potentially incorporate asbestiform fibers during the exploitation works (e.g., serpentinite, talc, vermiculite and carbonate deposits).

This paper summarizes the results of case studies on mines from the provinces of Córdoba, Mendoza and San Juan (Argentina) where asbestiform minerals were identified. Detailed geologic and mineralogical descriptions of Argentine asbestos are not presented in this article, but the papers that are referenced herein provide the complete information. Furthermore, we present new data of samples from the western sector of the Pie de Palo Complex (San Juan province). Mineral abbreviations after Whitney and Evans (2010) were adopted.

## 2 Geological Occurrence of Asbestos

### 2.1 Asbestos in Meta-Mafic/Ultramafic Rocks

In Argentina mafic and ultramafic igneous rocks are widely distributed in the provinces of Córdoba, Mendoza and San Juan, among others, and have been affected by different metamorphic and/or metasomatic processes (Ramos et al. 2000). These rocks have been mined for decades to extract amphibolite and serpentinite, but also to produce talc, vermiculite and asbestos in minor proportion.

Chrysotile occurs in meta-ultramafic rocks (mainly in serpentinites or steatized rocks) as veins with irregular banding, growing transversely to the fissures (cross-fiber asbestos) and could be interpreted as the product of fluids circulating along fissures (or shear zones) during late metamorphic episodes (Bonalumi and Gigena 1987). In some sectors these veins are also identified in meta-mafic rocks (amphibolites) or in the host rocks (mainly amphibolic/chloritic schists or gneisses). In the province of Córdoba, chrysotile is present in diverse serpentinitic bodies such as those of the mines “Los Guanacos”, “25 de Mayo”, “Árbol Seco”, “La Bélgica”, “Los Congos”, among others (Fig. 1a). The “La Bélgica” mine, one of the most important chrysotile deposits in Argentina (Fig. 1b), was active for about

30 years (Lescano et al. 2015). In the province of San Juan chrysotile veins affecting serpentinite rocks were also documented (e.g., the “Don Leon” mine, Castro de Machuca 1981), while in the province of Mendoza these types of veins with asbestiform chrysotile were identified in serpentinites near the “La Judita” mine (Lescano et al. 2017a).

Amphibole asbestos occurs in meta-ultramafic and meta-mafic rocks, filling veins, and associated with vermiculite and talc-rich zones. In the province of Córdoba veins with fibrous anthophyllite were identified in serpentinites as well as in amphibolites in the “Adita” mine (Lescano et al. 2014) and the “Coco Solo” mine (Angelelli et al. 1980) respectively.

Several vermiculite mines in the province of Córdoba (“Los Guanacos”, “Penachos Blancos”, “La Saltona”, “La Soledad”, “Inés II” and “Rosarito”, among others) were studied to determine the presence of asbestiform minerals. Vermiculite mineralization developed in biotite-rich zones in the contact between igneous bodies (mainly pegmatites) and meta-ultramafic rocks or in fractures, and it is interpreted as the product of reaction between igneous fluids and minerals of the meta-ultramafic rock. Amphibole groups are present in all the vermiculite deposits studied, but only in “Los Guanacos” and “Rosarito” mines (Fig. 1c) asbestiform tremolite was identified (Lescano et al. 2013a, 2017b).

Prismatic and fibrous amphiboles are commonly observed associated with steatized ultramafic bodies or in the contact zone with the host rock in different mines of Argentina. However, only in the “Salamanca” mine in the province of Mendoza scarce asbestiform amphiboles (tremolite-actinolite series) were detected in the contact zone between the steatized body and the host rock (schist) (Lescano et al. 2013b).

### 2.2 Asbestos in Dolomitic Rocks

Pure and impure dolomitic rocks are recognized in different provinces of Argentina, generally not associated with asbestos. In the province of Córdoba they correspond to metamorphic rocks (marbles) that appear as lens or tabular banks with different metamorphic grades associated mainly with gneisses, migmatites, amphibolites, and ultramafic rocks (Sfragulla et al. 1999). In general, minerals of the amphibole group are prismatic or acicular, tremolite being one of the most common accessory minerals in the impure varieties. In the Altautina area, marbles are dolomitic to calc-dolomitic, and they are limited by quartz-biotite gneisses or schists. In the contact zone a metasomatic belt can be recognized, where gneisses/schists are enriched in biotite. In this sector, asbestiform tremolite in veins cross-cutting marble foliation or in discontinuity planes was identified (Locati et al. 2014). In the province of San Juan, the Pie de Palo Complex is composed of gneisses, schists

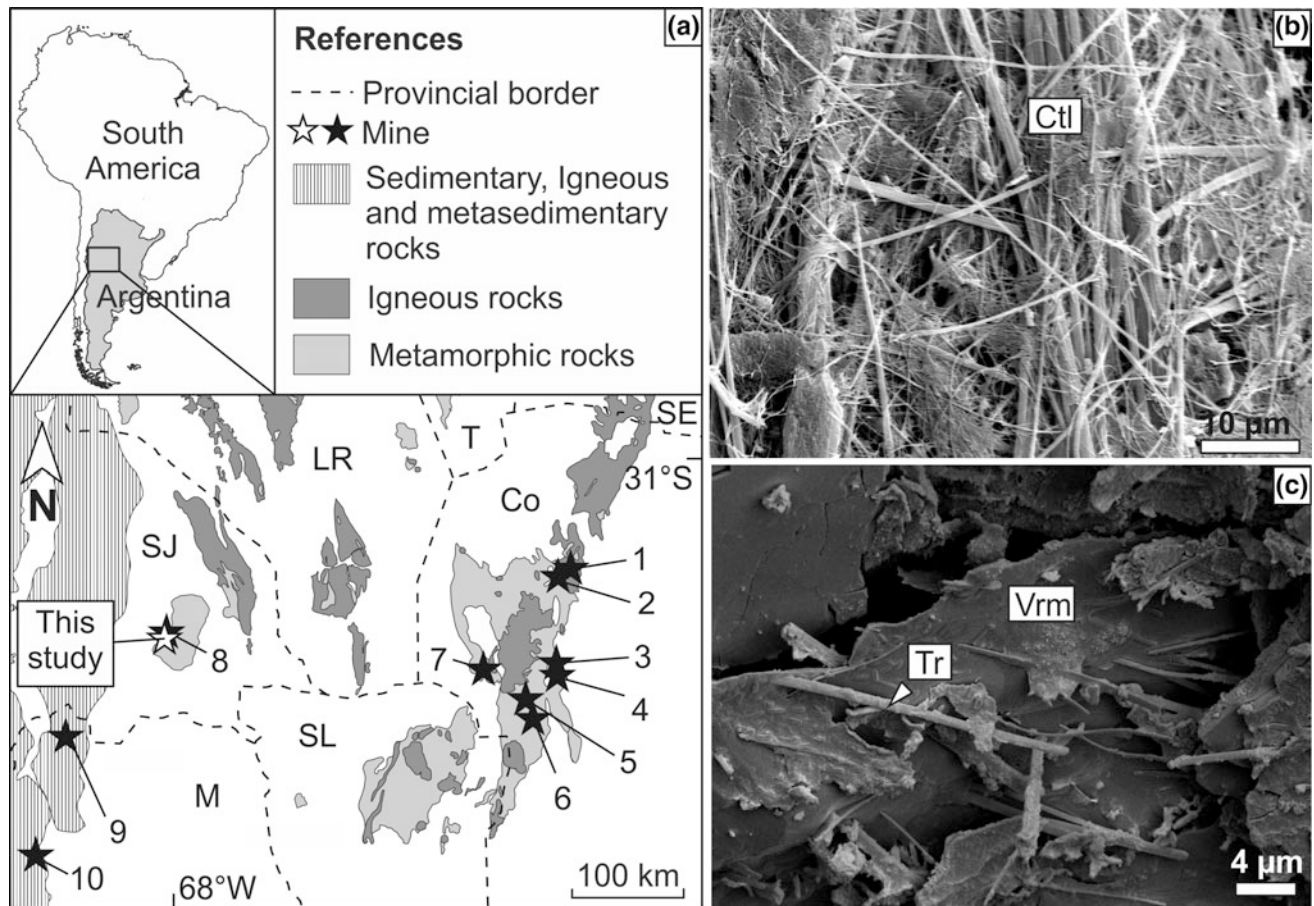


**Fig. 1** a Schematic map of the main geological units of the central-western part of Argentina and the mines cited in the text. M, SJ, Co, T, SL, SE and LR: Mendoza, San Juan, Córdoba, Tucumán, San Luis, Santiago del Estero and La Rioja provinces respectively. Numbers 1–10: Mines (1-“La Saltona”, 2-“Rosarito”, 3-“Adita”, 4-“La Soledad”, 5-“La Bélgica” and “Los Congos”, 6-“Penachos Blancos”,

“Los Guanacos”, “Inés II”, “Árbol Seco”, “Coco Solo” and “25 de mayo”, 7-Altautina area, 8-“Don León”, 9-“La Judita”, 10-“Salamanca”. White star: new samples from Quebrada La Petaca. b Secondary electron image (SEM) of chrysotile from “La Bélgica” mine (Lescano et al. 2015). c Secondary electron image (SEM) of tremolite in vermiculite from “Rosarito” mine (Lescano et al. 2017)

and metamorphosed mafic and ultramafic rocks (serpentinites, meta-gabbros, meta-diorites, amphibolites and mafic schists). In this area hydrothermal fluids produced important talc deposits such as those in the “Don León” mine (Castro de Machuca 1981). In these alteration zones asbestiform actinolite was identified as impurities in dolomite in the Quebrada del Gato sector (Lescano et al. 2016b).

### 3 Asbestiform Minerals from Quebrada La Petaca (San Juan)

In this work two samples (A and B) from Quebrada La Petaca in the western sector of the Pie de Palo Complex (province of San Juan), 1 km SW of the “Don León” mine, were studied (Fig. 1a). Its geological setting is similar to that of Quebrada del Gato (Naipauer et al. 2010).

The mineralogical characterization of samples was performed by polarizing microscopy (Leica DM EP) on thin sections and X-ray diffraction (XRD) on powder samples with a Rigaku D-Max III-C diffractometer (35 kV, 15 mA, Cu K $\alpha$  radiation). The diffraction patterns were recorded between 3° and 60° 2 $\theta$  in steps of 0.04° 2 $\theta$  and 1 s counting time per step. Morphological studies were conducted by scanning electron microscopy (SEM) with a Carl Zeiss EVO ma100 microscope at 20 kV, equipped with an energy dispersive X-ray spectrometer (EDS), on gold-coated samples.

Sample A corresponds to a foliated serpentinite composed of antigorite, magnetite and prismatic tremolite ( $\pm$ chlorite and dolomite) (Fig. 2a, b). In this sample, calcite, quartz and chrysotile veins ( $\sim$ 250  $\mu$ m) crosscutting serpentinite foliation were recognized (Fig. 2c).

Sample B corresponds to a talc-chlorite schist composed of talc, chlorite and dolomite ( $\pm$ antigorite, magnetite and

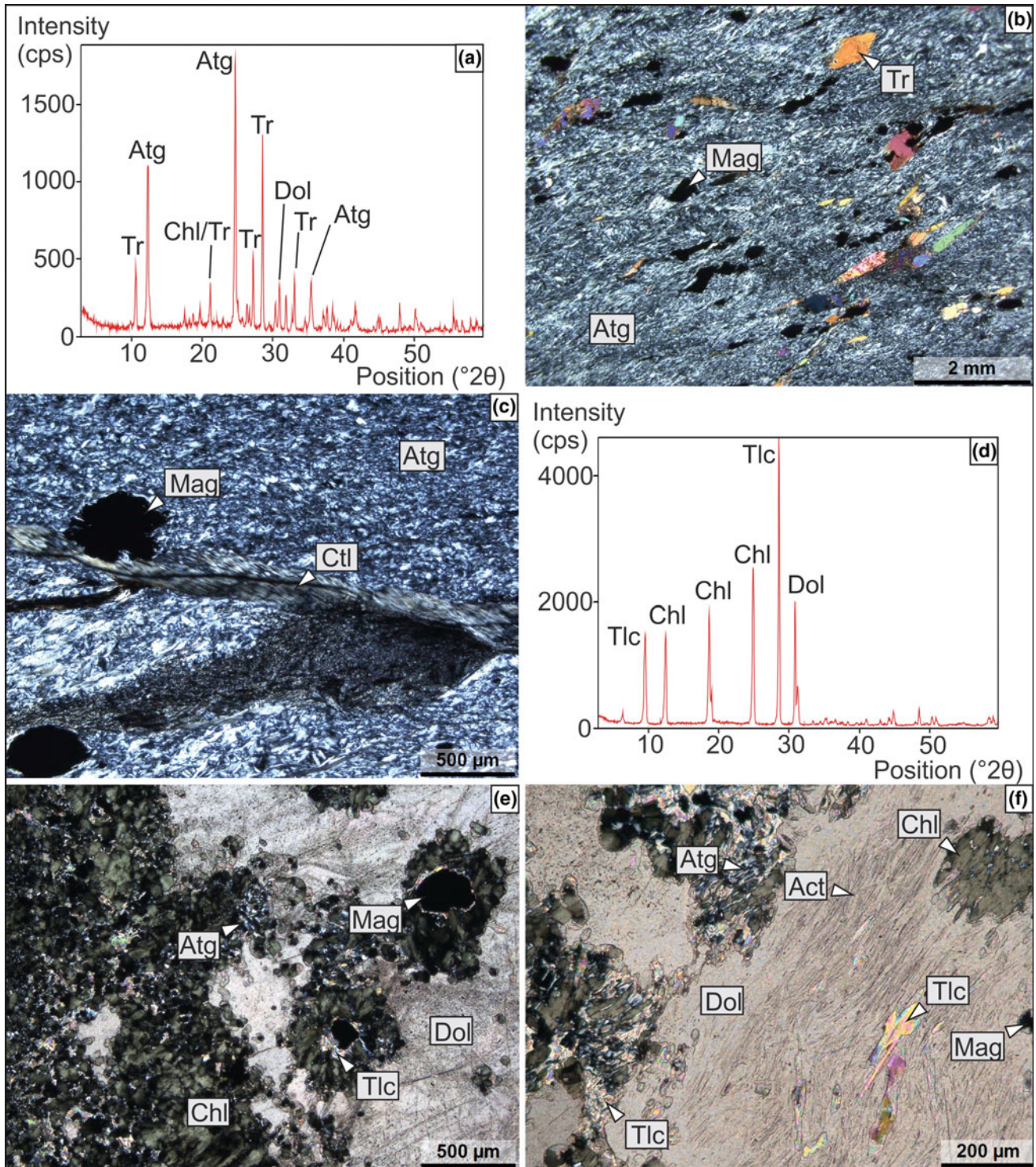


**Fig. 2** a XRD pattern of foliated serpentinite (sample A). Main reflections are marked. b, c Photomicrographs of sample A (crossed nicols). b General texture of the rock. c Detail of a chrysotile vein. d XRD pattern of talc-chlorite schist (sample B). Main reflections are

marked. e, f Photomicrographs of sample B (crossed nicols). e General texture of the rock. f Detail of actinolite fibers and talc sheets included in dolomite

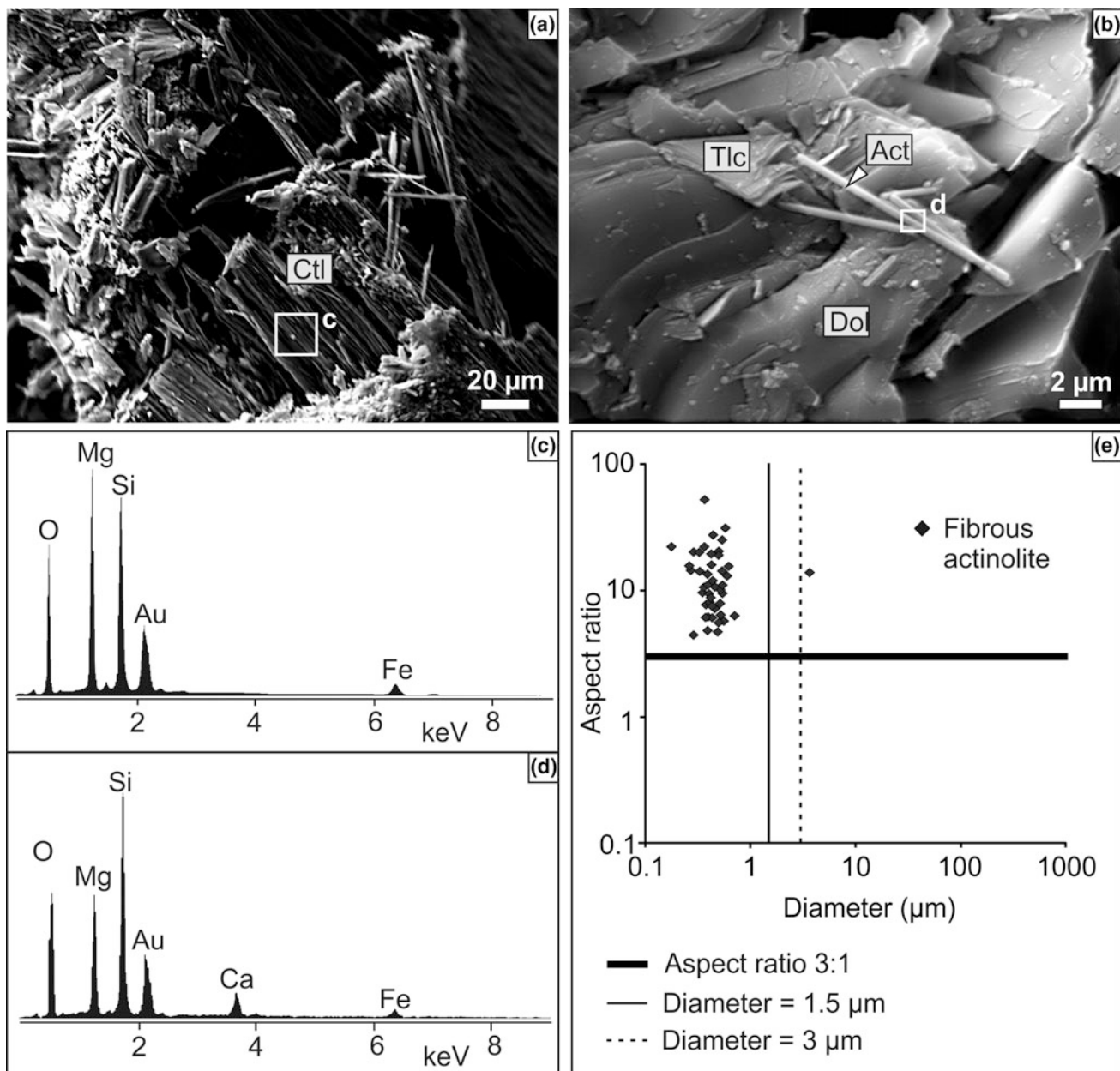


**Fig. 3** **a** Secondary electron image (SEM) of chrysotile fibers from a vein in sample A. Sector “c” corresponds to the area analyzed by EDS. **b** Secondary electron image (SEM) of actinolite fibers associated with talc sheets in dolomite from sample B. Sector “d” corresponds to the

area analyzed by EDS. **c** EDS spectrum of chrysotile in sector “c”. The iron peak is assigned to intermixed iron oxides. **d** EDS spectrum of actinolite in sector “d”. **e** Comparative graph (diameter vs. aspect ratio) of actinolite crystals from sample B

clay minerals) (Fig. 2d, e). Oriented inclusions of talc and very thin fibrous actinolite were observed in dolomite crystals (Fig. 2f).

Fibrous phases in both samples (chrysotile vein and actinolite in dolomite) were studied by SEM-EDS on broken surfaces. Chrysotile appears as bundles of thin, long fibers (Fig. 3a),  $>5 \mu\text{m}$  in length and  $<3 \mu\text{m}$  in diameter, generally associated with iron oxides (Fig. 3c). In general, the main diameters vary between 0.8 and 1.6  $\mu\text{m}$ ; however, the exact

length of the fibers could not be determined. Actinolite appears as thin prismatic fibers associated with folded sheets of talc in the dolomite (Fig. 3b, d). Fifty actinolite crystals were measured in order to analyze their morphology (Fig. 3e). All fibers have an aspect ratio (length to diameter ratio)  $> 3:1$ , and most fibers are  $<1.5 \mu\text{m}$  in diameter (except for one crystal). The length of the fibers varies between 1.3 and 52  $\mu\text{m}$  ( $\sim 42\% > 5 \mu\text{m}$ ). According to these results and the morphological limits set by the WHO (1986),

meta-mafic/ultramafic rocks from Quebrada La Petaca in the western sector of the Pie de Palo Complex may contain asbestiform fibers (chrysotile and actinolite) in the range of respirable fibers.

#### 4 Conclusions

- In Argentina, asbestos is associated with meta-mafic/ultramafic rocks, mainly serpentinites (or steatized varieties) and amphibolites, and less commonly with dolomitic rocks (in metamorphic and metasomatic domains).
- Chrysotile, anthophyllite and tremolite-actinolite were identified as the main asbestiform minerals.
- Amphiboles in talc and vermiculite deposits are present in most of the samples, but their morphology is not always asbestiform.
- In the western sector of the Pie de Palo Complex, meta-mafic/ultramafic rocks with asbestiform chrysotile (in veins) and asbestiform actinolite (as inclusions in dolomite) were recognized.

**Acknowledgements** Financial support was provided by PICT 2011 N° 153 (FONCyT), PUE 2016-CONICET-CICTERRA and SECyT-UNC 05/1708. Authors thank CICTERRA (CONICET-UNC), CIC (province of Buenos Aires) and the Geology Department of the UNS.

#### References

- Angelelli, V., Schalamuk, I., Fernández, R.: Los yacimientos de minerales no metalíferos y rocas de aplicación de la región Centro-Cuyo, vol. XIX, p. 261. Secretaría de Estado de Minería. Anales, Buenos Aires, Argentina (1980)
- Bonalumi, A., Gigena, A.: Relación entre las metamorfitas de alto grado y las rocas básicas y ultrabásicas en el Departamento Calamuchita, Córdoba. *Rev. Asoc. Geol. Argentina* **42**(1–2), 73–81 (1987)
- Castro de Machuca, B.: Génesis de la mina de talco “Don León”, sierra de Pie de Palo, provincia de San Juan VIII. *Congr. Geol. Argentino, San Luis* **IV**, 535–555 (1981)
- Gunter, M.E.: Defining asbestos: differences between the built and natural environments. *Chimia* **64**(10), 747–752 (2010)
- Lescano, L., Marfil, S., Maiza, P., Sfragulla, J., Bonalumi, A.: Amphibole in vermiculite mined in Argentina. Morphology, quantitative and chemical studies on the different phases of production and their environmental impact. *Environ. Earth Sci.* **70**(4), 1809–1821 (2013a)
- Lescano, L., Marfil, S., Maiza, P.: Análisis morfológico de anfíboles en menas de talco de la provincia de Mendoza. *Rev. Asoc. Geol. Argentina* **70**(3), 401–409 (2013b)
- Lescano, L., Bonalumi, A., Maiza, P., Sfragulla, J., Marfil, S.: Asbestiform amphiboles in a serpentinite quarry in operation, province of Córdoba, Argentina, vol. 5. In: IAEG XII Congress, Torino, Italy, pp. 615–618 (2014)
- Lescano, L., Marfil, S., Maiza, P., Sfragulla, J., Bonalumi, A.: Crisotilo en serpentinitas de mina La Bélgica, provincia de Córdoba. *Rev. Asoc. Geol. Argentina* **72**(4), 542–550 (2015)
- Lescano, L., Marfil, S., Sfragulla, J., Bonalumi, A., Locati, F., Maiza, P.: Asbestos in Argentina: mineralogical and morphological characterization. Environmental impact. In: Simmons, D.L. (ed.) *Asbestos: Risk Assessment, Health Implications and Impacts on the Environment*, vol. 8, pp. 145–190. Nova Science Publishers, Hauppauge (2016a)
- Lescano, L., Locati, F., Sfragulla, J., Marfil, S., Bonalumi, A., Maiza, P.: Actinolita de morfología asbestiforme en carbonatos de la Quebrada del Gato, provincia de San Juan. *Acta Geol. Lilloana* **28**(1), 174–176 (2016b)
- Lescano, L., Locati, F., Marfil, S., Sfragulla, J., Bonalumi, A., Maiza, P.: Presencia de minerales asbestiformes en la mina de talco La Judita, Yalguaraz, provincia de Mendoza. In: XX Congr. Geol. Argentino, Tucumán, pp. 53–55 (2017a)
- Lescano, L., Locati, F., Sfragulla, J., Marfil, S., Bonalumi, A., Maiza, P.: Asbestiform and non-asbestiform morphologies in a talc and vermiculite mine from the province of Córdoba (Argentina): a case study. *Environ. Earth Sci.* **76**(18), 1–20 (2017b)
- Locati, F., Lescano, L., Murra, J., Marfil, S., Maiza, P., Baldo, E.: Asbestiform amphiboles in a marble quarry: a case study from the province of Córdoba (Argentina), vol. 5. In: IAEG XII Congress, Torino, Italy, pp. 1281–1284 (2014)
- Naipauer, M., Vujovich, G.I., Cingolani, C.A., McClelland, W.C.: Detrital zircon analysis from the Neoproterozoic-Cambrian sedimentary cover (Cuyania terrane), Sierra de Pie de Palo, Argentina: evidence of a rift and passive margin system? *J. S. Am. Earth Sci.* **29**(2), 306–326 (2010)
- Ramos, V.A., Escayola, M., Mutti, D., Vujovich, G.I. Proterozoic-early paleozoic ophiolites of the Andean basement of southern South America. In: Dilek, Y., Moores, E.M., Elthon, D., Nicolas, A. (eds.) *Ophiolitic and Oceanic Crust: New Insights from Field Studies and the Ocean Drilling Program*, vol. 349, pp. 331–349. Geological Society of America Special Paper (2000)
- Rodríguez, E.J.: Asbestos banned in Argentina. *Int. J. Occup. Environ. Health* **10**(2), 202–208 (2004)
- Ross, M., Langer, A.M., Nord, G.L., Nolan, R.P., Lee, R.J., Van Orden, D., Addison, J.: The mineral nature of asbestos. *Regul. Toxicol. Pharm.* **52**(1), 26–30 (2008)
- Sfragulla, J., Jerez, D., Bonalumi, A.: Mármoles y otras rocas carbonáticas de Córdoba. In: Zappettini, E.O. (ed.) *Recursos Minerales de la República Argentina*, vol. 35, pp. 271–295. SEGEMAR, Buenos Aires (1999)
- Van Gosen, B.: The geology of asbestos in the United States and its practical applications. *Environ. Eng. Geosci.* **13**(1), 55–68 (2007)
- Vignaroli, G., Ballirano, P., Belardi, G., Rossetti, F.: Asbestos fibre identification vs. evaluation of asbestos hazard in ophiolitic rock mélanges, a case study from the Ligurian Alps (Italy). *Environ. Earth Sci.* **72**(9), 3679–3698 (2014)
- Whitney, D.L., Evans, B.W.: Abbreviations for names of rock-forming minerals. *Am. Miner.* **95**, 185–187 (2010)
- World Health Organization (WHO): Asbestos and other natural mineral fibres. In: *International Programme on Chemical Safety*, vol. 53. World Health Organization, Geneva. *Environmental Health Criteria*, 194 pp (1986)

# Author Index

## A

Abe, Ana C.P., 99  
Agyemang, Adu, 91  
Aldo, 169  
Alves, L.E.C., 69

## B

Beauty, Adela, 91  
Bonalumi, 169  
Briaud, Jean-Louis, 1  
Broetto, M.Z., 69  
Burova, V., 33

## C

Caldeira, Laura, 75  
Cripps, J.C., 143  
Czerewko, M.A., 143

## D

da Silva, Paula F., 39  
de Lollo, José Augusto, 99, 107  
Dippenaar, Matthys A., 63  
Doglioni, Angelo, 161

## E

Espindola, Murilo S., 55, 69  
Esquivel, Edmundo Rogério, 27

## F

Francisco, 169

## G

Guerrero, João V.R., 99

## H

Hamel, James V., 121  
Hickel, V.F., 69

## J

Jeremias, Filipe Telmo, 75  
Johnson, W., 153  
Jorge, 169  
Joyner, Andrew, 91

## K

Karfidova, E., 33

## L

Lacertosa, Rosa Maria, 161  
Lescano, Leticia, 169  
Lima, Jacqueline Zanin, 129  
Locati, 169  
Lorandi, Reinaldo, 99, 107  
Luffman, Ingrid, 91

## M

Maiza, 169  
Marques, Jéssica Pelinsom, 27  
Marteli, Alice N., 107  
Marfil, Silvina, 169  
Mirjafari, Yasin, 47  
Mraz, Elena, 21  
Müller, Vitor S., 55, 69

## N

Nandi, Arpita, 91  
Nascimento, Marivaldo S., 55  
Noveletto, Vanessa, 55

## O

Oliveira, Priscilla H.P., 83  
Orense, Rolando P., 47

## P

Pan, Kun, 15  
Paul, Darren, 7



Pedro, [169](#)  
Pizzolo, R. L., [69](#)  
Pombo, Joaquim, [39](#)  
Potten, Martin, [21](#)

**Q**  
Quinta-Ferreira, Mário, [83](#)

**R**  
Raimondi, Isabela Monici, [129](#)  
Ramos, Rute, [75](#)  
Rodrigues, A., [39](#)  
Rodrigues, Valéria Guimarães Silvestre, [27](#), [129](#)

**S**  
Schaeffer, Malcolm F., [135](#)  
Sdao, Francesco, [161](#)  
Sellmeier, Bettina, [21](#)  
Sfragulla, Jorge, [169](#)  
Shakoor, Abdul, [153](#)  
Shidlovskaya, Anna, [1](#)  
Simeone, Vincenzo, [161](#)  
Suemasa, Naoaki, [47](#)

**T**  
Thuro, Kurosch, [21](#)  
Timchenko, Anna, [1](#)

**V**  
van Rooy, J. Louis, [63](#)  
Vilar, Orencio Monje, [27](#)

**W**  
Wilk, Charles M., [113](#)  
Wilkinson, Stephen, [15](#)

**Y**  
Yang, Zhongxuan, [15](#)  
Yeakley, J., [153](#)

**Z**  
Zhao, Chaofa, [15](#)